WATER
WATER
WATER
WATER
WATER
WATER
WATER
WATER
WATER
WATER

1975

Investigation of Vertical Mixing in the Dispersion of Pollutants in Lake Erie

F. M. Galloway, Jr.
Department of Chemical Engineering
The Cleveland State University
Cleveland, Ohio

Office of
Water Research and Technology
United States Department
of the Interior

CONTRACT NO.
A-036-OHIO

FINAL PROJECT REPORT

OWRR PROJECT NO. A-036-OHIO

PROJECT TITLE: INVESTIGATION OF VERTICAL MIXING IN THE DISPERSION OF POLLUTANTS IN LAKE ERIE

Submitted by

F. M. Galloway, Jr., Project Principal Investigator

Department of Chemical Engineering

The Cleveland State University

Cleveland, Ohio 44115

September, 1975

TABLE OF CONTENTS

*M.S. Thesis, Department of Chemical Engineering, The Cleveland State University

**Submitted for publication in Water Resources Research

***Submitted for publication in Journal for Great Lakes Research

1. Introduction

1.1 Background and Motivation

Dispersion models applicable to Lake Erie have been developed to describe the circulation and mixing of conserved and nonconserved pollutants, biological species, etc. Various models deal with areas from the size of harbors or embayments up to basins or entire lakes. Some models assume perfect mixing in the vertical direction and thus include only horizontal convection and diffusion.[1] Others have two or more "layers" in the vertical direction[2,3]. These contain vertical diffusion along with the horizontal terms. The obvious preference for eliminating vertical variations is the simplification and greater efficiency of computer solution that results.

Previous efforts in large lake dispersion modeling raised several questions. These may be stated as follows: (1) When can it safely be assumed that there is complete mixing in the vertical direction so that only horizontal transport need be included in the model? (2) If complete vertical mixing cannot be assumed, what values should be used for a vertical diffusion coefficient? (3) If complete vertical mixing can be assumed, should the resulting horizontal transport model employ modified horizontal diffusion coefficients, and if so how should they be modified? All of these questions relate directly or indirectly to the degree of vertical mixing that occurs and motivated this investigation.

1.2 Goals of the Research Project

The project can be broadly broken up into two parts, a theoretical part and an experimental part. The goals of the theoretical part were to determine under what conditions, for a given vertical diffusion and vertical profile of

horizontal velocity, complete mixing in the vertical direction could be assumed and how the remaining horizontal terms should be modified. These goals pertain to questions (1) and (3) above. The goal of the experimental part was to measure the vertical diffusivity in Lake Erie under various conditions and to attempt to develop a general correlation between vertical diffusivity and other factors characterizing lake conditions. This pertains directly to question (2) above, but also relates to questions (1) and (3).

2. Summary of the Theoretical Study

2.1 Method

The following model equation was solved to obtain the results:

$$\frac{\partial C}{\partial t} + u(z) \frac{\partial C}{\partial x} = \frac{\partial}{\partial z} \left(D_z \frac{\partial C}{\partial z} \right) \qquad (1)$$

where C is concentration, u(z) is horizontal velocity as a function of vertical position, z, D_z is the vertical diffusivity, x is horizontal position and t is the time. This equation contains the basic interaction between horizontal convection and vertical diffusion. Equation (1) was solved numerically for given initial conditions, and for a number of typical velocity profiles, u(z), and diffusivity profiles, $D_z(z)$. From these solutions, C is obtained as a function of t, x and z. The first and second moments of C in the x direction are computed easily from the solution of (1). The square root of the second moment about the mean x, i.e., the standard deviation, σ_{x2}, is of particular interest since it is involved in the fundamental definition of the effective horizontal dispersion coefficient for C, D_x:

$$D_x = \frac{1}{2} \frac{d\sigma_{x2}}{dt} \qquad (2)$$

Thus, from the solution of (1) it can be determined when the vertical variation of C becomes negligible and what the effective rate of horizontal spread of C has become, D_x. It should be noted that D_x results from the combined effect of vertical diffusion and horizontal convection and is in addition to horizontal spread from "horizontal turbulence." D_x in effect substitutes for the vertical direction z.

More detail on the derivation and applicability of the model equation (1) is given in the Introduction of Appendix A4. Details of the numerical solution of equations (1) and (2) are found in Appendix A1, Chapter IV and Appendix A2, Chapter II. Previous work relating to the solution of (1) and (2), the use of moments to find D_x, and the interaction of vertical diffusion and horizontal convection to yield effective horizontal dispersion is discussed in the introduction and background sections of Appendices A1 - A4.

2.2 Results

It was found from the solutions of (1) that for a period after introduction of a "pollutant", vertical variations in C are significant and D_x ($= \frac{1}{2} \frac{d\sigma_x^2}{dt}$) is an increasing function of time. Eventually, however, vertical variations become negligibly small and D_x reaches a constant value in time. These two conditions were found to occur at about the same time in all the computed examples. D_x reaching a constant value therefore appears to be a good criterion for deciding when the vertical direction can be eliminated in a dispersion model. The time, t_1, that it takes D_x to reach a constant can be calculated from

$$t_1 = \frac{H^2}{\alpha_1 \overline{D}_z} \qquad (3)$$

where H is depth, $\overline{D}_z$ is vertical average of the vertical diffusivity and α_1 is a constant for each combination of u(z) and $D_z(z)$ used in (1). (See the appendix of Appendix A3 for a derivation of (3)).

The value of D_x after the vertical direction is eliminated is

$$D_x = C_1 \frac{H^2 U^2_{max}}{\overline{D}_z} \qquad (4)$$

where U_{max} is the change in velocity from surface to bottom and C_1 depends on u(z) and $D_z(z)$. Values of C_1 and α_1 for all the computed examples are given in Table 3, p. 14, of Appendix A4. Examples of the application of these results to dispersion modeling in large lakes are given in Appendix A3, pp. 9-12, and Appendix A4, pp. 15-18. The latter section also shows how the interaction of vertical diffusion and horizontal convection could produce an effective horizontal dispersion coefficient D_x that grows with length scale according to the 4/3 power law that has been used to describe horizontal dispersion in large lakes and oceans. Figure 12 of Appendix A4 compares computed values of $D_x(K_e)$ with those measured in Lake Ontario and attributed to horizontal turbulence. It is clear that the two effects are of the same order of magnitude. In fact, the horizontal dispersion may depend primarily on the phenomenon described here rather than horizontal turbulence in the traditional sense.

Prediction of t_1 and D_x for dispersion in other environmental situations, such as rivers and streams, estuaries, and the atmosphere, can be done by these methods. Some examples are given in Appendix A3, section III.

3. Summary of the Experimental Study

3.1 Method

The vertical diffusivity was measured in two ways. The first way involved releasing a small amount of rhodamine dye in neutrally buoyant solution at the

lake surface. Samples were then taken over the next ten minutes and at depths to ten feet. This provided concentration data so that

$$\sigma_z^2 = \frac{\int_0^\infty Cz^2 dz}{\int_0^\infty C dz} \tag{5}$$

could be evaluated (using a Simpson's rule approximation for the integrals) as a function of time. From this,

$$D_z = 1/2 \quad \frac{d\sigma_z^2}{dt} \tag{6}$$

could be determined. This D_z would represent an average value over the upper five feet or so.

The second way involved releasing a larger amount of rhodamine dye in neutrally buoyant solution at the surface. Measurements were then made over the next thirty minutes and at depths to thirty feet. These data were then used to find optimum values for the parameters in the following model diffusion problem:

$$\frac{\partial C}{\partial t} = \frac{\partial}{\partial t} \left[D_z \frac{\partial C}{\partial z} \right] \tag{7a}$$

$$C(z,0) = Q\, e^{-A_4 z} \tag{7b}$$

$$D_z = A_1 + A_2\, e^{-A_3 z} \tag{7c}$$

C in both these models represents a horizontally averaged concentration at constant z. Thus the variation of D_z with depth could be found from the values of A_2 and A_3. The best values for A_1 to A_4 were found by fitting the numerical solution of (7) to the data using the Marquardt method[4].

The field measurements in both cases were performed in essentially the same way. The entire experiment was designed around the 12 by 75 mm disposable

glass test tube. The reason for this was to make as simple as possible the handling of the several thousand expected individual samples. It had been found that if the sample could be captured in this size tube and identified in the field, it could remain there for its determination of dye concentration in the laboratory.

Considering that the method called for the use of vertical concentration profiles, devices which would support a series of these sample tubes in a vertical line and allow them all to sample simultaneously were designed. The sampling devices that resulted were constructed on an aluminum channel shape. Attached to this channel by means of aluminum rivets were 21 aluminum AA cell battery clamps. These were spaced from 1/2 foot to 2 1/2 feet, depending on the experiment, for a length of 5 to 10 feet and bent in such a way as to support the tube about an inch away from the channel and parallel to it. The clamps had been specially purchased without the electrical terminals and are nearly ideal for supporting this size tube. However, they do have the tendency to scratch the boro-silicate glass and so each tang of the clamp had to be covered with a strip of electrician's plastic insulating tape. This also gave a surer grip and helped prevent the tube sliding along its axis. Also riveted to the channel was a flat spring of shim brass just above each tube clamp. To seal the tube until it should capture its sample an appropriate size vacutainer stopper was fastened to the underside of the flat spring with a thermo plastic glue. A stainless wire was fed through holes drilled in the outer ends of the flat springs and a fisherman's lead split shot was swaged onto the wire just below each flat spring. Lastly, a small 24 volt DC solenoid (ultimately not used) was fastened to the top of the channel by means of an automotive hose clamp and attached to the wire so that when it was actuated,

it would flex all the springs upward and simultaneously "uncork" all the tubes. When the solenoid was deactivated the springs would again cover their respective tubes with their stoppers. As a final refinement, the stoppers were coated with silicon vacuum grease which helped to seal the tubes against inleakage of water before their time to sample and also seemed to help break the surface tension and allow the tube to fill immediately upon opening. Corrosion resistance had been a consideration when choosing the materials of construction for these devices since it was obvious that they would be dunked in the lake many times with little opportunity to dry them off between periods of use.

The sampling devices, sample tubes, concentrated rhodamine solution, stoppers, identification stickers, sample tube transporting boxes and all the equipment associated with the wind and current measurements were carried to the experiment site in a seventeen foot open launch which also towed a canoe. The actual experiment was performed from the canoe while the other boat served as a base of operations. In brief, the dye was released, the patch was sampled, the sample tubes removed from the devices, stoppered and labeled, then carried back to the lab for concentration determination.

The site for a test was selected so as to be certain that dye from previous runs would not be inadvertently picked up in the samples. This generally meant seeking a position a few hundred yards upwind from any previous runs. The canoe, which carried a flask of dye concentrate and the sampling devices which had already been loaded with a quantity of empty tubes, was paddled out to the selected spot. In some experiments the tubes were loaded every six inches, in others they were spaced at one foot or 2 1/2 feet intervals. The dye slug was released from the stern of the canoe while it

drifted downwind so that there was no need to paddle in the immediate vicinity of the dye release.

The release was a simple pouring motion of the flask from a height no more than a few inches above the surface. Care was taken to release the dye in one blob of about 25 ml (1000 ml in the longer time experiments) with as little motion with respect to the surface as possible. The canoe was then allowed to drift down from the patch twenty yards or so before paddling was begun to stabilize it in the wind.

The sampling was timed as closely as possible with a stopwatch with a sweep second hand. In the last seconds before the target time the stern man would bring the bow of the canoe over some part of the patch. The bow man would then lower one of the sampling devices into the patch and take the samples at the desired depth. Then the sampling device would be withdrawn and the canoe was allowed to drift away again. With practice, the stern man could judge the speed of the canoe so that it would be carried into the patch by its momentum, stop and begin to drift back just as the bow man was withdrawing the sampling device. In this way the presence of the canoe disturbed the patch as little as possible.

After the last sampling time the tubes were carried back to the launch to be identified and corked for transport back to the lab. On the launch new tubes could be placed in the sampling devices for another run or wind and current data could be gathered.

The samples were brought back from the experiment site to be measured for dye concentration. This was done by means of a Turner 111 Fluorometer.

The field procedure differed from the proposed method, which was to perform the sampling by an array of samplers of the type described above. The samplers were to have been anchored in a pattern and operated by means of

of the solenoid valves attached to each one which would be activated remotely through wires running to a central power source in the launch. This procedure was found to be not feasible for several reasons. The currents and waves made it very difficult to anchor the samplers in the desired pattern. Premature leakage of the tubes was considerable after the samplers had been in the water for some time. The solenoid valves had difficulty opening the submerged empty tubes against the water pressure. After several attempts, this procedure was abandoned. Running three to five repeats of the experiment using the manual, individual sampler technique from the canoe as described above and then averaging the results is thought to have at least partially compensated for the lack of an array of samplers simultaneously and remotely activated.

The greatest remaining difficulty of the field sampling technique was leakage of some of the tubes as the sampler was being lowered into the water. This was thought to be due to the waves slapping against the shim brass springs which keep the tubes stoppered and also the water drag on these springs as the sampler is being lowered. This leakage necessitated some editing of the data, using the numerical solutions found in Appendices A1 and A2 as a guide. In these solutions it was found that the concentration profile from top to bottom never had more than one relative maximum. If a particular experimental profile deviated from this, appropriate corrections were made. Nevertheless, considerable uncertainty remained in some of the data.

3.2 Results

All field measurements were performed in an area one to two miles out from the light at the east end of the breakwall of the Cleveland harbor. The bottom there is quite flat. The depth is about 40 feet. No significant

temperature variation from top to bottom was measured during any of the experiments. Water temperature was measured with a Weathermeasure Model T621 Remote Temperature Indicator. Surface wind (7 feet above water surface) was measured with an Alnor Type 8500 Thermo-Anemometer. The wind measurements were cross-checked with those taken at Burke Lakefront Airport, which is less than two miles from the measuring site. Water velocity measurements were made with a Thermo-Systems Model 1630 Velocity Transducer calibrated for 0-3 ft/sec. This is a submersible constant temperature hot film anemometer. The probe was mounted on aluminum channel-shaped rods for vertical profiling. Unfortunately, the probe is not very directionally sensitive and the rocking of the boat coupled with the flexibility of the aluminum rods caused the velocity measurements to be extremely unreliable, particularly for purposes of computing velocity gradients.

The measurements made in the summer of 1974 were of the short time (10 minutes) type, designed to measure D_z at or near the surface. The data were treated by means of equations (5) and (6). The results are summarized in Table 1 below.

TABLE 1

Date	Velocity Gradient	Wind	Computed D_z
8/23/75	.8 sec^{-1}	11 mph NW	7.5 cm^2/sec
8/26/75	.3 sec^{-1}	8 mph NW	6.2 cm^2/sec
9/5/75*	no velocity data	9 mph SE to 17 mph NE	18.0 cm^2/sec
9/10/75	.1 sec^{-1}	7 mph SW	3.8 cm^2/sec
9/18/75	no measurable shear	10 mph N	8 cm^2/sec
9/20/75	.1 sec^{-1}	8 mph NE	1.7 cm^2/sec
9/24/75	.1 sec^{-1}	14 mph S	12.1 cm^2/sec

*The experiments on 9/5/75 were done completely within the breakwall of the Cleveland Harbor.

FIGURE 1

Surface D_z Vs. Wind Speed

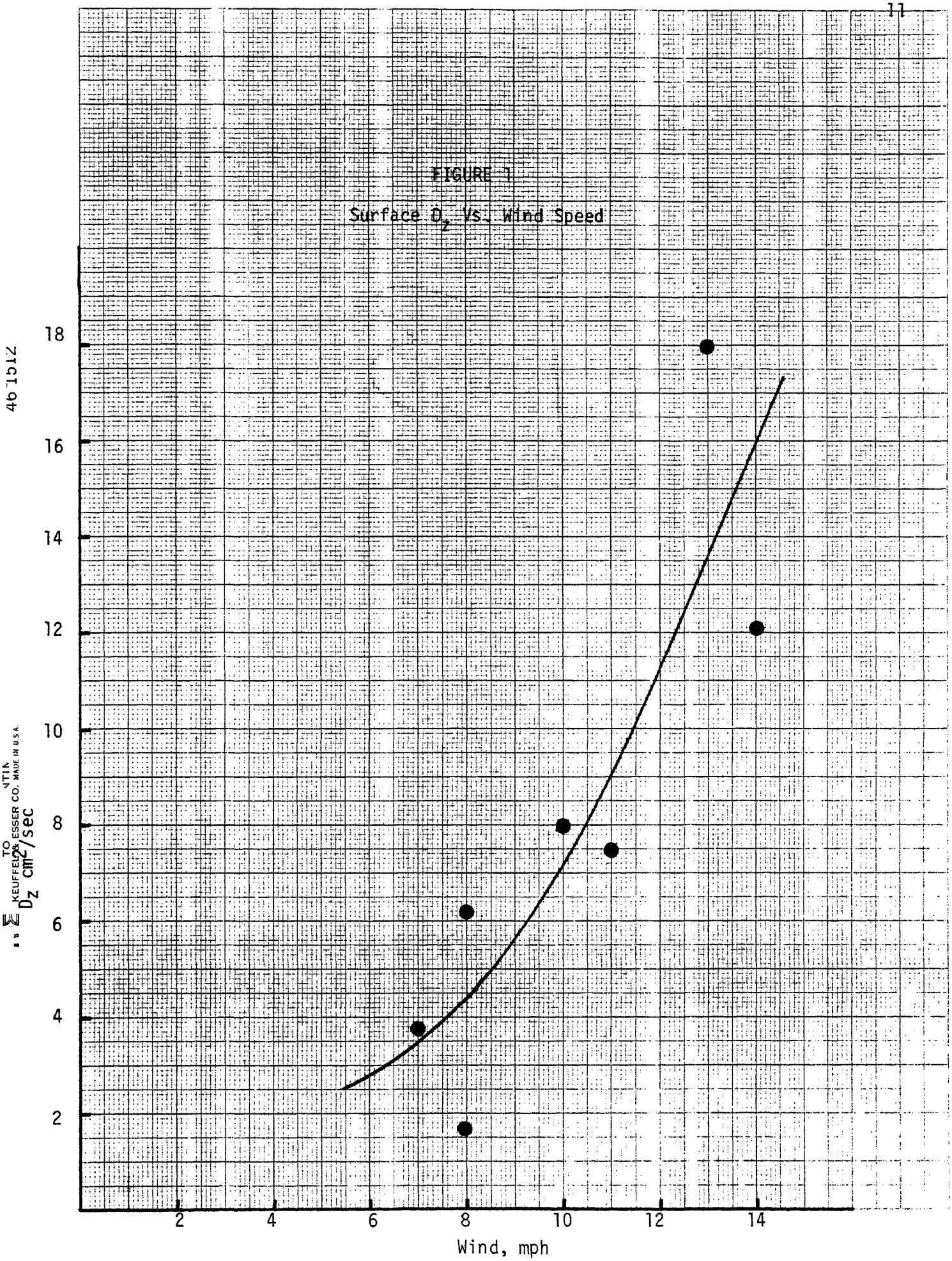

The velocity gradients indicated in Table 1 are average values for the first five-six feet and are extremely unreliable.

From Table 1, there appears to be come correlation between D_z near the surface and the wind speed. Figure 1 is a plot of this relationship. The curve has been roughly drawn through the data points. It is similar to the relation given by Wilson[5] for surface shear stress as a function of wind speed.

The limited amount of field work during the summer of 1975 was designed to shed some light on the possible variation of D_z with depth. The experiments lasted thirty minutes, with samples being taken down to thirty feet. The data were treated by means of the model indicated in equations (7a) - (7c). Unfortunately, the measurements, which were performed on 7/23/75, 7/30/75 and 8/1/75, were made during a period of extremely calm weather. Particularly, the days 7/30/75 and 8/1/75 were during an air pollution alert period for Cleveland due to the lack of wind in the area. Thus, the measured values of D_z were probably much lower than is typical. Also, it is quite possible that the lack of variation of D_z with depth during this period is highly untypical.

The best fit of the data of 7/23/75 produced a D_z of 1.4 cm^2/sec with no vertical variation indicated ($A_3 = 0$ in (7c)). The wind was about 9 mph from the north (data from Burke Airport) although measurements on site gave a value closer to 6 mph. The waves were estimated to be less than one foot.

The data of 7/30/75 produced a D_z of zero. The wind was 7 mph from the south (Burke data) although the on-site measurement was about 2 mph. The lake was extremely calm with only ripples and virtually no waves at all. While the value of zero for D_z is physically unrealistic, it is felt that the

correct value was extremely small, certainly less than 1 cm^2/sec for that day. Qualitative observations support this. Initial introduction of the 1000 ml of dye solution was into the first three feet or so of the water column. After thirty minutes, the dye patch had stretched into a ribbon in the direction of the current. It was estimated to be well over 100 yards long and was only about 15 feet wide. Extreme variations of concentration with depth, usually characteristic of very short dispersion times, were visually apparent even after thirty minutes. There obviously was very little vertical, or horizontal mixing taking place.

The data of 8/1/75 produced D_z = 4.9 cm^2/sec. Again no vertical variation was indicated. The wind was 8 mph from the north, as reported by Burke. Waves were estimated to be less than 1/2 foot. The qualitative observations reported for 7/30/75 above were also true for 8/1/75. The value of D_z = 4.9 cm^2/sec is surprisingly high, and is, therefore, somewhat suspect. The fit of the model to the data for 8/1/75 was the poorest of the three days.

4. Overall Conclusions

The conclusions are presented here first in reference to the motivating questions (1), (2) and (3) given in section 1.1. Question (1) can be answered by computing t_1 from equation (3). This requires a knowledge of total depth, H, the vertically averaged D_z, $\overline{D}_z$, and α_1 for the particular u(z) and $D_z(z)$ that applies. A number of values of α_1 for different u's and D_z's are given in Table 3, p. 14 of Appendix A4.

Question (2) has only been partially answered. The data indicate that the surface D_z is related to the wind, under isothermal conditions, and Figure 1 is a rough indication of what that relationship might be. Unfortunately, the data that has been obtained is not able to shed much light on how D_z varies with depth under essentially isothermal conditions. More experiments of the

longer duration type are required. The method that has been presented here for treating such data appears to be a suitable one.

Question (3) can be answered by computing D_x from equation (4). A knowledge of H, $\overline{D}_z$, and U_{max}, the horizontal velocity variation in the water column, is required, along with the value for C_1. Again, values for C_1 for various u's and D_z's are given in Table 3, p. 14 of Appendix A4.

The measured temporal variation of surface D_z in one location, by a factor of about 10, means that the criterion for vertical averaging and the D_x used in a vertically averaged dispersion model can both vary by an order of magnitude, and quite probably more, at a single location. This is very significant for dispersion modeling strategy in general.

It has been shown that the mechanism of vertical dispersion and horizontal convection can produce effective horizontal dispersion coefficients of the order of magnitude of those that have been observed in dye experiments. It has also been shown that this mechanism can produce a type of 4/3 power law relation between length scale and effective horizontal dispersion coefficient. This suggests that this mechanism may be the controlling one for horizontal mixing, ie., that "horizontal turbulence" is not important. In that event, total horizontal mixing coefficients could be determined from u(z) and $D_z(z)$ data via equation (4) rather than from very large scale dye release experiments as has been done in the past.

REFERENCES

1. Simons, T. J., Proceedings of the Fifteenth Conference on Great Lakes Research, International Association for Great Lakes Research, Ann Arbor, Michigan (1972).

2. Skarupa, K. A., Numerical Solution to a Concentration Gradient in the Western Basin of Lake Erie, M. S. Thesis, The Cleveland State University (1972).

3. Lick, W. and J. Paul, Proceedings of the Seventeenth Conference on Great Lakes Research, International Association for Great Lakes Research, Ann Arbor, Michigan (1974).

4. Marquardt, D. J., Society for Industrial and Applied Mathematics, 11, #2, 431 (1963).

5. Wilson, B. W., Journal of Geophysical Research, 65, #10, 3377 (1960).

APPENDIX A1

NUMERICAL SOLUTION TO A TWO-DIMENSIONAL DISPERSION EQUATION

BY

R. NATARAJAN

Advisor: F. M. Galloway

A thesis submitted to the
Department of Chemical Engineering of
The Cleveland State University
in partial fulfillment of the requirements
for the degree of
Master of Science
August, 1973

NUMERICAL SOLUTION TO A TWO-DIMENSIONAL DISPERSION EQUATION

BY

R. NATARAJAN

Thesis Approved

F.M. Galloway
Thesis Advisor

E.A. Hadlock

Chittaranjan Jain

NUMERICAL SOLUTION TO A TWO-DIMENSIONAL DISPERSION EQUATION

Abstract

by

R. NATARAJAN

Many types of dispersion models are being developed to predict the pollutant concentration in the Great Lakes. A basic question which arises in selecting the model is when the concentration variation in the vertical direction needs to be included. Some dispersion examples were tried in the western basin of Lake Erie and they indicate that the vertical eddy diffusivity D_z may be important in answering this question. Other deciding factors are apparently the vertical profiles of the horizontal velocities and the depth.

All these factors are incorporated in a two-dimensional form of the general transport equation. This equation is numerically solved to get the concentration distribution resulting from an initial narrow Gaussian input. The method was verified by comparing the numerical results for the zero vertical diffusivity case with the solution obtained analytically. Results were obtained for two different velocity profiles and three different dimensionless values of D_z.

The results indicate that, for a given profile, there is significant vertical variation in concentration as long as the effective horizontal dispersion co-efficient D_x^* is increasing. It was found that when D_x^* reaches a constant value, there is very little vertical

variation. The predicted time and space scales for significant vertical variation of concentration, by this approach, appear to correlate well with the computed dispersion examples in the western basin of Lake Erie. The method thus appears to be generally suitable for determining a priori when vertical variation must be considered in a particular dispersion modeling effort.

Since the results are quite sensitive to the D_z values, it appears that D_z should be fairly well defined in order to get accurate prediction of concentration. This necessitates a thorough investigation into the D_z variation in the Great Lakes.

TABLE OF CONTENTS

LIST OF FIGURES

LIST OF TABLES

NOMENCLATURE

a	Parameter in the Gaussian distribution
C	Concentration in equation (2.1); non-dimensionalized concentration elsewhere
$\tilde{C}$	Laplace Transform of C in Chapter III; vertically-averaged concentration elsewhere
D	Non-dimensionalized vertical diffusivity
Dt	Mesh spacing in time
Dx	Mesh spacing in the horizontal direction
DZ	Mesh spacing in the vertical direction
D_x^*	Effective horizontal dispersion co-efficient
D_z	Vertical eddy diffusivity
erf	Error function
H	Depth of lake
m	Laplace transform parameter
s	Laplace transform parameter
t	Time in equation (2.1); non-dimensionalized time elsewhere
u	Velocity in the horizontal direction
x	Co-ordinate in the horizontal direction in equation (2.1); dimensionless co-ordinate elsewhere
$\bar{x}$	Mean of the concentration distribution
z	Co-ordinate in the vertical direction in equation (2.1); dimensionless co-ordinate elsewhere
σ_x^2	Variance of the concentration distribution

Subscript

K Mesh index in the z direction

i Mesh index in the x direction

ref Reference quantity

Superscript

n Mesh index in time

CHAPTER I

INTRODUCTION AND BACKGROUND

1.1 Introduction

The Great Lakes and their connecting channels are used today on a large scale as dumping grounds for refuse of various kinds, the idea being such huge bodies of water could undoubtedly absorb a good deal of domestic and industrial wastes if these mixed readily with the main water masses. Hence the numerical modeling of the dispersion process in the lakes is of considerable importance. The model should be able to predict the flow of pollution in the lake and explain how the naturally-occurring lake currents transport pollutants away from the shores and disperse them over larger water masses.

There are various models which explain the dispersion process in the Great Lakes. The simplest one is the homogeneous one-layer model where the lake is represented by one layer of fluid of constant temperature and density. In this, the horizontal velocity is averaged in the vertical direction. This model is good in predicting dispersion in two-dimensional flow systems with horizontal diffusion. The concentration values predicted may be reasonable approximations to actual values averaged over time periods of several weeks to months and on a regional space scale of over 25 miles.

The multilayer models aim at more detailed predictions of

concentrations on a smaller scale. The time period may be hours to days and space scale may be two to twenty miles. The vertically-averaged velocities in one-layer models are not indicative of the actual velocities to be found in the lake. A three-dimensional flow pattern is taken into consideration in a multilayer model. The model gives the local concentration in the lake resulting due to pollution entering from a particular source.

1.2 Background

One multilayer model which calculates the concentration values at different points in the western basin of Lake Erie as a function of time is due to Skarupa and Galloway (Ref. 9). This model includes detailed three-dimensional velocity profiles in order to calculate accurate pollutant dispersion.

It can be shown that under typical Great Lakes conditions, horizontal eddy diffusion of pollutants is negligible in comparison with the convective terms, while vertical eddy diffusion is of the same order of magnitude as the convective terms in the transport equation (Ref. 9). The values of horizontal eddy diffusivity are very well known and have been calculated by dye-tracer techniques at all scales (Ref. 8). The values of the verical eddy diffusivity are not very well determined. Skarupa used a mean value of 5 cm^2/sec. (Ref. 9).

Figures 1 and 2 show the concentration contours obtained by Skarupa, on the surface and at a depth of 4.56 meters respectively, after a two-day period. The typical value of D_z = 5 cm^2/sec was used. These figures, as well as Figures 3 through 8, were drawn by a plotter

directly from data generated by the computer program. Examining Figures 1 and 2, it can be seen that both sets of contours are quite similar. There is little concentration variation in the vertical direction. The plots show only a small effect of the current reversal on the bottom. The contours generally followed the streamlines of the vertically-averaged horizontal currents. For comparison, a two-dimensional example using the vertically-averaged currents was computed (Ref. 6). Figure 3 shows the concentration contours obtained from the two-dimensional example. For many purposes, they could be considered to be a good approximation to either Figure 1 or 2. The results appeared to indicate that this value of D_z was just large enough to remove most of the vertical variation in concentration created by the vertical variation in horizontal velocity.

To evaluate the effect of vertical diffusivity, two other examples were calculated using D_z = 50 cm^2/sec. and D_z = .5 cm^2/sec.

Figures 4 and 5 show the contours at the two vertical stations after one day, using D_z = 50 cm^2/sec. These examples were computed to only one day because the larger value of D_z imposed a much smaller time step on the calculation. The larger D_z produced contours showing almost no vertical variation. Comparison with the two-dimensional model contours after one day, Figure 6, shows that the three sets, Figures 4, 5, and 6, are virtually identical.

Figures 7 and 8 show the results after 2 days, using D_z = 0.5 cm^2/sec. There is a marked difference between the surface contours and the contours at 4.55 meters. The effect of the vertical structure of the horizontal currents was quite strong. It is evident that

the surface contours are mainly influenced by the surface velocity while the contours at 4.56 meters demonstrate clearly the effect of the reverse flow on the bottom.

The conclusion drawn from these examples is that the local concentration depends heavily on the choice of D_z. Also, it appears that the value of $D_z = 5\ cm^2/sec$ is a transition value between examples where, on one hand, for the larger D_z values a two-dimensional model (one layer model) would be completely satisfactory, and, on the other hand, for smaller D_z values a three-dimensional model is required. The importance of this in terms of possible computing time savings argues for a thorough investigation into D_z variation and its effect on dispersion in the Great Lakes.

CHAPTER II

STATEMENT OF THE PROBLEM

In the previous Chapter, it was outlined how the local value of concentration depends heavily on D_z. The spread of pollution in the horizontal direction depends not only on D_z but also on the vertical variation of horizontal velocity, i.e., the velocity profile. Hence we would like to determine a method for predicting in terms of D_z and the velocity profile when a one-layer model is adequate for concentration prediction.

The problem is approached by solving the two-dimensional diffusion-convection equation:

$$\frac{\partial C}{\partial t} + u(z)\frac{\partial C}{\partial x} = D_z\frac{\partial^2 C}{\partial z^2} \tag{2.1}$$

The x co-ordinate is in the direction of the mean flow, and the z co-ordinate is directed vertically upward from the lake bottom.

Here we are just concerned with the effect of horizontal convection and vertical diffusion on the spread of the pollutant. Horizontal diffusion is ignored as it is found that in the lake it does not generally contribute significantly to the dispersion of the pollutant on the scale we are interested in.

A non-dimensional form of the above equation is derived by defining new variables.

L_{ref} = H = Depth of Lake

$C_{ref} = C_{max}$ = Maximum Concentration Occurring in the Lake

U_{ref} = Maximum Algebraic Difference Between Maximum and Minimum Horizontal Velocity Along a Vertical Line.

Therefore, the non-dimensionalized variables are,

$$x^* = \frac{x}{H}$$

$$z^* = \frac{z}{H} \qquad (0 \leq z^* \leq 1)$$

$$t^* = \frac{t \cdot U_{ref}}{H}$$

$$C^* = \frac{C}{C_{max}}$$

$$u^* = \frac{u}{U_{ref}}$$

$$D^* = \frac{D_z}{U_{ref} \cdot H}$$

By substitution into equation (2.1) it is seen that

$$\frac{\partial C^*}{\partial t^*} + u^* \frac{\partial C^*}{\partial x^*} = D^* \frac{\partial^2 C^*}{\partial z^{*2}} \tag{2.2}$$

We will drop the stars and write (2.2) as

$$\frac{\partial C}{\partial t} + u \frac{\partial C}{\partial x} = D \frac{\partial^2 C}{\partial z^2} \tag{2.3}$$

where the quantities henceforth refer to non-dimensionalized parameters.

The initial distribution of pollutant concentration is

$$C = C(x,z,o) \tag{2.4}$$

and the boundary conditions are

$$\frac{\partial C}{\partial z} = 0 \qquad \text{at } z = 0 \text{ and } z = 1 \tag{2.5}$$

A Gaussian initial distribution is assumed,

$$C(x,z,o) = e^{-\frac{(x-.125)^2}{4a}}$$

where 'a' is a parameter.

Note that the word "distribution" in what follows is used in a loose sense, i.e., it is not normalized.

By picking the variance 'a' very small, this initial condition approximates a delta function input.

The equation (2.3) was solved for various values of D and different velocity profiles.

The spread of the pollutant due to the vertical variation of velocity is evaluated by calculating an effective horizontal dispersion co-efficient D_x^*. The definition of D_x^* will be given in Chapter IV.

Typical D values are as follows:

Western Basin of Lake Erie

$D_z = 5 \text{ cm}^2/\text{sec}$

$H = 900 \text{ cms}$

$U_{ref} = 30 \text{ cms/sec}$

$\therefore D = .000185$

Stratified Lake Where There is a Thermocline

$D_z = 5\ cm^2/sec$

$H = 300$ cms for upper layer

$U_{ref} = 3$ cm/sec

$\therefore\ D = .0055$

The reason for taking a two-dimensional flow and a gaussian initial distribution is as follows.

The pollutant spreads because of the vertical variation in horizontal velocity. The spread also depends on the value of vertical diffusivity. Higher values of vertical diffusivity lead to less horizontal spread and the concentration is more uniform along the vertical direction. A high value of vertical diffusivity increases the mixing in the vertical direction and approximates plug flow.

In a three-dimensional flow, the horizontal movement of a pollutant follows the horizontal streamlines. Here we will consider a special case, namely when the horizontal flow is parallel so that the problem can be looked at in two dimensions. This is considered to be adequate for the purpose of these calculations, i.e., if the one layer model criterion is satisfied for two-dimensional flow, it appears that it will be satisfied for the more general three-dimensional case.

In case of continuous pollutant flow, the concentration varies in the front of the source as it flows into the lake. The concentration will be more or less uniform at the back. Now the concentration variation due to delta input approximates that occurring in the front

of a continuous source.

Hence if the one-layer model criterion is satisfied for a delta input, it will be satisfied for a continuous source.

In summary, the predictions of vertical variation of concentration from our model problem given by equations (2.3-2.5) are expected to be pessimistic in the following sense. Values of D for the model problem which produce negligible vertical variation of concentration will certainly also produce negligible vertical variation for a general three-dimensional case when there is a continuous source. Likewise, the more general case may have negligible vertical variation for even smaller values of D than would be predicted by the model problem.

CHAPTER III

ALTERNATE APPROACHES TO THE PROBLEM

We want to solve the equation

$$\frac{\partial C}{\partial t} + u(z)\frac{\partial C}{\partial x} = D\frac{\partial^2 C}{\partial z^2}$$

with $\frac{\partial C}{\partial z} = 0$ at $z = 0$ and $z = 1$

and $C(x,z,0) = e^{-\frac{(x-.125)^2}{4a}}$

The first velocity profile considered was a linear profile

$$u(z) = z$$

Later on, a velocity profile typical to the lake will be considered.

3.1 Analytical Solution

The possibilities of analytical solution are bad. Different approaches were tried like separation of variables, similarity substitutions, Laplace transform and finite Fourier transform.

All the methods fail. The main difficulty is that 'u' is a function of z.

Because of the failure in obtaining an analytical solution, numerical methods were resorted to.

3.2 Numerical Method

3.2.1 Laplace Transform and Numerical Inversion

Laplace transform is a powerful tool in mathematical analysis and is used in solving this problem numerically. The initial equation is converted to another partial differential equation with a reduced number of variables by taking the Laplace transform of the original equation in the 'x' direction.

Thus we get

$$\frac{\partial \bar{C}}{\partial t} + mu\bar{C} = D\frac{\partial^2 \bar{C}}{\partial z^2}$$

where $\bar{C}(m,z,t)$ = Laplace transform of $C(x,z,t)$.

The value of $C(o,z,o)$ is actually equal to .01 for the value of 'a' which we have chosen. It is approximated to be zero. It reduces as time progresses.

The initial and boundary conditions transform to

$$\frac{\partial \bar{C}}{\partial z} = 0 \text{ at } z = 0 \text{ and } z = 1$$

$$\text{and } \bar{C}(m,z,0) = \sqrt{\pi a}\ e^{am^2}[1-\text{erf}(m\sqrt{a} - \frac{.125}{2\sqrt{a}})]e^{-.125m}$$

Here 'm' is the Laplace transform parameter.

The greatest advantage of this method is that it eliminates the need for finite differencing the convective term $u\frac{\partial C}{\partial x}$. It is this term which has bothered many people and leads to damping and numerical dispersion in many numerical schemes. Also 'x' extends to infinity and this method eliminates finite differencing in an infinite direction.

The resulting partial differential equation is easily solved by scheme

$$\frac{\bar{C}_K^{n+1} - \bar{C}_K^n}{Dt} + mz_K\bar{C} = D \cdot \frac{(\bar{C}_{K+1}^n + \bar{C}_{K-1}^n - 2\bar{C}_K^n)}{DZ^2} \qquad z_K = KDZ$$

$$\bar{C}_K^o = \sqrt{\pi a}\; e^{am^2}[1 - \mathrm{erf}(m\sqrt{a} - \frac{.125}{2\sqrt{a}})]e^{-.125m} \text{ for all } K$$

Here 'K' is the mesh index in the z direction and 'n' is the time index.

$\bar{C}$ is then inverted numerically to get C(x,z,t). The details of the numerical inversion and the method followed are given in the next paragraph.

3.2.2 Numerical Inversion

The method followed here is the one outlined by Richard Bellman (Ref. 1 and 2). Those interested are requested to see these references for greater details.

Starting with the equation

$$\int_0^\infty e^{-st}u(t)dt = F(s) \qquad (3.1)$$

a new variable $x = e^{-t}$ is defined. Then (3.1) becomes

$$\int_0^1 x^{s-1}u(-\log x)dx = F(s) \qquad (3.2)$$

Writing $u(-\log x) = g(x)$ we have

$$\int_0^1 x^{s-1}g(x)dx = F(s) \qquad (3.3)$$

The integral is replaced by a Gaussian quadrature formula so

that (3.3) becomes

$$\sum_{i=1}^{N} x_i^{s-1} g(x_i) w_i = F(s) \tag{3.4}$$

where x_i are the zeroes of the shifted Legendre polynomials and w_i are the weights attached to these values. The weights are parameters introduced to provide additional degrees of freedom so that as few values of $g(x)$ have to be evaluated as possible. Tables of these parameters are tabulated in references 1 and 2.

Next allow the variable 's' to assume N different values, s = 1,2,3,...,N. We then obtain a linear system of N equations in N unknowns.

$$\sum_{i=1}^{N} x_i^{k} g(x_i) w_i = F(k+1) \qquad k=0,1,2,\ldots,N-1 \tag{3.5}$$

where the quantities $g(x_i)$, i=1,2,...,N are the unknowns.

The problem of inverting the Laplace transform has thus been replaced, approximately, by that of solving a system of simultaneous linear algebraic equations.

We want to obtain a formula of the type,

$$g(x_i) = \sum_{k=0}^{N-1} a_{ik} F(k+1) \qquad i=1,2,\ldots,N$$

where the a_{ik} are constants, independent of F(k) determined once and for all, for each N, and tabulated.

Make the change of variables $y_i = w_i g(x_i)$ and $a_k = F(k+1)$ so that (3.5) becomes

$$\sum_{i=1}^{N} x_i^k y_i = a_k \qquad k=0,1,2,\ldots,N-1 \tag{3.6}$$

To solve this system, a classical device is employed. Multiply the k^{th} equation by a parameter q_k, as yet unspecified, and add the corresponding terms in all of the equations.

$$\sum_{i=1}^{N} y_i \left(\sum_{k=0}^{N-1} q_k x_i^k \right) = \sum_{k=0}^{N-1} a_k q_k \tag{3.7}$$

Hence, setting

$$f(x) = \sum_{k=0}^{N-1} q_k x^k$$

(3.7) becomes

$$\sum_{i=1}^{N} y_i f(x_i) = \sum_{k=0}^{N-1} a_k q_k \tag{3.8}$$

where $f(x)$ is a polynomial of degree N-1 to be chosen in some convenient fashion.

Let $f(x) = f_j(x)$ be chosen such that

$$f_j(x_i) = 0 \qquad i \neq j \tag{3.9}$$

$$f_j(x_j) = 1 \tag{3.10}$$

If $f_j(x) = \sum_{k=0}^{N-1} q_{kj} x^k$, then (3.8) reduces to

$$y_j = \sum_{k=0}^{N-1} a_k q_{kj} \tag{3.11}$$

where q_{kj}, $k=0,1,2,\ldots,N-1$ are determined by the conditions

(3.9) and (3.10).

Because of the fact that the x_i are zeroes of the shifted Legendre polynomial P_N^*, we get the explicit relation

$$f_j(x) = \frac{P_N^*(x)}{(x-x_j)P_N^{*1}(x_j)} \quad \text{where } P_N^{*1}(x)=\text{derivative of } P_N^*(x) \tag{3.12}$$

The desired q_{kj} are the co-efficients in this polynomial of degree N-1. Repeating this procedure for each j yields the desired inverse matrix (q_{kj}).

Having obtained the q_{kj} we have a simple procedure for calculating the values $w_i g(x_i)$ from equation (3.11). The required values $g(x_i)$ are then obtained by division. The matrix $(q_{kj}|w_k)$ used to convert F(k+1) directly into $g(x_i)$ is tabulated for N=3,4,...,15 (References 1 and 2).

3.2.3 Instability of Inverse of the Laplace Transform

Bellman clearly indicates that it is unreasonable to expect that any specific method for the inversion of the Laplace transform will work equally well in all cases. The mathematical reason for this is that the Laplace inverse is an unbounded operator. In other words, arbitrarily small changes in F(s) can produce arbitrarily large changes in the value of u(t).

Bellman cites the example of

$$L\{\text{Sin } at\} = \frac{a}{s^2+a^2}$$

For $s \geq 0$, as $a \to \infty$, the right hand side approaches zero uniformly whereas the function

$$u(t) = \text{Sin } at$$

oscillates more and more rapidly between the fixed limits ± 1 as $a \to \infty$.

There are two basic assumptions made in determining the values of u(t) as accurately as possible given the values of F(s) to a prescribed degree of accuracy. First is that an exact determination of F(s) would lead to an exact, and hence, unique determination of u(t); second, that u(t) is sufficiently smooth to permit the approximation methods employed. But it is difficult to recognize a priori by considerating F(s) whether these conditions are met. Hence, there is no guarantee of acceptable results since often quite accurate values of F(s) are required.

This discussion probably explains why the method failed in our case.

3.2.4 Details of the Scheme

Solving the equation at the top of page 12 for $\bar{C}_K^{n+1}$ yields

$$\bar{C}_K^{n+1} = \bar{C}_K^{n} - Dt \cdot m \cdot K \cdot DZ \cdot \bar{C}_K^{n} + \frac{(\bar{C}_{K+1}^{n} + \bar{C}_{K-1}^{n} - 2\bar{C}_K^{n})}{DZ^2} \cdot D \cdot Dt \qquad (3.13)$$

$$\bar{C}_K^{o} = \sqrt{\pi a}\, e^{am^2}[1 - \text{erf}(m\sqrt{a} - \tfrac{.125}{2\sqrt{a}})]e^{-.125m} \text{ for all } K \qquad (3.14)$$

The initial distribution is given by $C = e^{-\frac{(x-.125)^2}{4a}}$. The value of

'a' was chosen such that distribution extended from x = 0 to x = .25. C values are equal to .01 at the above x values. Values less than .01 were essentially taken to be zero.

Starting with the initial value of $\bar{C}$ as given by equation (3.14), successive values of $\bar{C}$ at different times are calculated by marching forward according to equation (3.13).

For getting good accuracy, Dt = .001 and DZ = .01 were taken. Also all the variables were defined in double precision.

Calculations were done for N = 5 and N = 10 for mutual check.

The procedure described for the computational inverse of the Laplace transform provides values of C at the values of x given by

$$x_i = -\log \hat{x}_i \text{ where } \hat{x}_i \text{ are the zeroes of } P_N^*(\hat{x}).$$

Even for N = 15, the maximum value of x is $x = -\log \hat{x} = 5.115$.

Thus the values of x at which we calculate the inverse of $\bar{C}$ seem to be limited by this restriction. However, this was overcome by use of change of time scale as outlined by Bellman (Reference 1).

Hence, we can calculate the C values at any x we want.

3.2.5 Failure of the Method

The method failed as the C values given by N = 5 and N = 10 for the same conditions were different.

Also, for this velocity profile, it can be reasoned qualitatively that C values are symmetric about z = .5 at x=.625 and t = 1. That is, at x=.625 and t = 1, C at z = .6 should be equal to C at z = .4 and so on.

The point of symmetry moves by a distance of .5 in x for every Dt = 1. Hence, C values about z = .5 should also be symmetric at x = 1.125 and t=2.

The symmetry conditions were never satisfied by the values of concentration obtained by this method.

Though the C values seemed to satisfy qualitative considerations, they were not reliable quantitatively. Hence, the method was abandoned.

3.2.5 Probable Reasons for the Failure

Some aspects of the instability of the method were discussed in Section 3.2.3.

While trying to establish this method, it was found that numerical inversion is extremely sensitive to the inverse values of the function. For instance, the example of $C\{e^{-t}\} = \frac{1}{s+1}$ was tried.

The numerical inversion did not give correct answers when the constant '1' in the expression $\frac{1}{s+1}$ was defined in single precision. The method worked only when it was defined in double precision. The co-efficients of the inverse matrix go up to 10^6 for N = 10 and the round-off error is significant for single precision. Even for the simple example, inverse values were needed in double precision.

An accidental experience further indicated the extreme sensitive nature of the method. While working the trial example, one co-efficient from the inverse matrix was taken with a different integer in the eighth place by mistake. The value of the function corresponding to that row of the inverse matrix differred appreciably from

the correct value.

All this indicates that for the numerical inversion to be successful, inverse values are needed with extreme accuracy, say up to 10 places of decimal.

In our case, $\bar{C}$ values are calculated numerically by finite differencing. This restricts the accuracy of the inverse values which we get. At best, the values are accurate to the order of 10^{-4}. But this accuracy is hardly sufficient for numerical inversion.

This probably explains the failure of the method.

3.3 Discussion of Numerical Solution to a Similar Problem

M. B. Fiering and N. Yotsukura (Reference 12) solved this same dispersion equation for flow in an open channel. Initially they used an explicit numerical method but they abandoned it as it failed. Then they developed an implicit scheme. But they clearly state that their scheme cannot accept an initial concentration distribution with a large gradient $\frac{\partial C}{\partial x}$. They assumed that the effect of initial distribution disappeared at distant downstream points and chose an arbitrary initial condition given by

$$C(x,z,0) = \left[\frac{(x-2)^4}{16} - \frac{(x-2)^2}{2} + 1\right]$$

Here $C = 0$ at $x = 0$ and $x = 4$. Hence, the distribution is quite spread out.

We would like to use a distribution with an extremely narrow initial spread. In the next chapter we evolve a numerical scheme for a distribution which initially spreads only till $x=.25$. Such a

distribution has a large $\frac{\partial C}{\partial x}$ and hence, the scheme developed by these authors would fail. This was the reason which motivated us towards developing an alternate scheme.

Also, the method used by these authors is an implicit one and takes considerable computer time. Their explicit method failed. In the next chapter, we have developed a completely explicit method which works even when the initial distribution has a large $\frac{\partial C}{\partial x}$.

Moreover, in this paper, the authors had other interests. They wanted to find out the shape of the distribution at different times. They used the same value of vertical diffusivity D_z in all cases and the same form of velocity distribution.

On the other hand, we are interested in finding out the effect of different values of D_z and different velocity profiles on the initial gaussian distribution and consequently, evaluate D_x^* (defined in Chapter 4) for various cases.

Moreover, the authors have not mentioned anything about the possible numerical dispersion in their scheme arising due to the convective approximation. If the scheme has a low order of accuracy, the pollutant may spread just due to the numerical dispersion in the scheme and in that case, it is difficult to interpret the results. The scheme we have used has a fourth order accuracy in space and a very low numerical dispersion.

CHAPTER IV

METHOD OF SOLUTION

With the failure of the numerical inversion scheme, it became necessary to derive an alternate method for solving the equation. In the new method, we finite difference the entire partial differential equation, including the convective term. It has been already pointed out in the previous chapter that it is the convective term which gives rise to numerical dispersion in many schemes. Hence, we should choose such a scheme that has not only a high order of accuracy but also a low numerical dispersion. It was decided to try the scheme given by J. E. Fromm which satisfies the above requirements (References 4 and 5).

4.1 Development of the Complete Scheme

The diffusion term is finite differenced by a second-order central approximation as used previously.

$$D\frac{\partial^2 C}{\partial z^2} = D \cdot \frac{(C_{K+1}{}^n + C_{K-1}{}^n - 2C_K{}^n)}{DZ^2} \tag{4.1}$$

Here K is the mesh index in the z direction and n is the time index.

It will be shown later that a mesh size of DZ = .1 was found to be adequate. The mesh points we numbered from 2 to 12 so that K = 2 corresponds to z = 0 and K = 12 corresponds to z = 1.

According to the equation (4.1), it then becomes necessary to define C_1 and C_{13}. This is done by using the boundary condition that

$$\frac{\partial C}{\partial z} = 0 \qquad \text{at } z = 0 \text{ and } z = 1$$

If we take a central difference approximation to the derivative, we get the following conditions.

$$C_1 = C_3 \tag{4.2}$$

$$C_{13} = C_{11} \tag{4.3}$$

This is the numerical approximation to the boundary condition. At any time step, the concentration values C_2 through C_{12} for any x are calculated according to the numerical scheme to be outlined below, and C_1, C_{13} are obtained from equations (4.2) and (4.3).

Let us now consider the numerical approximation to

$$\frac{\partial C}{\partial t} + u(z)\frac{\partial C}{\partial x}$$

J. E. Fromm (Reference 5) has developed a fourth-order scheme that may be expressed conservatively as

$$F_{i-\frac{1}{2}} \frac{Dt}{Dx}$$

$$= A_{11}\alpha(C_{i-1}+C_i) + A_{21}\alpha(C_{i-2}+C_{i+1})$$

$$+ A_{12}\alpha^2(C_{i-1}-C_i) + A_{22}\alpha^2(C_{i-2}-C_{i+1})$$

$$+ A_{13}\alpha^3(C_{i-1}+C_i) + A_{23}\alpha^3(C_{i-2}+C_{i+1})$$

$$+ A_{14}\alpha^4(C_{i-1}-C_i) + A_{24}\alpha^4(C_{i-2}-C_{i+1}) \qquad (4.4)$$

where

$$C_i^{n+1} = C_i^n + \frac{Dt}{Dx}(F_{i-\frac{1}{2}}^n - F_{i+\frac{1}{2}}^n)$$

$$\alpha = u(z)\frac{Dt}{Dx}$$

Integers n and i stand for finite time and finite space (x) increments respectively.

The values of the co-efficients are given below.

Co-efficient	Value
A_{11}	7/12
A_{12}	15/24
A_{13}	-1/12
A_{14}	-3/24
A_{21}	-1/12
A_{22}	-1/24
A_{23}	-1/12
A_{24}	-1/24

Equation (4.4) has a lagging phase error and is combined with the following equation which has leading phase error.

$$*F_{i-\frac{1}{2}}\frac{Dt}{Dx}$$

$$= A_{11}(\alpha-1)(C_{i-2}+C_{i-1}) + A_{21}(\alpha-1)(C_{i-3}+C_i)$$

$$+ A_{12}(\alpha-1)^2(C_{i-2}-C_{i-1}) + A_{22}(\alpha-1)^2(C_{i-3}-C_i)$$

$$+ A_{13}(\alpha-1)^3(C_{i-2}+C_{i-1}) + A_{23}(\alpha-1)^3(C_{i-3}+C_i)$$

$$+ A_{14}(\alpha-1)^4(C_{i-2}-C_{i-1}) + A_{24}(\alpha-1)^4(C_{i-3}-C_i) \qquad (4.5)$$

where

$$C_i^{n+1} = C_{i-1}^{n} + \frac{Dt}{Dx}(*F^n_{i-\frac{1}{2}} - *F^n_{i+\frac{1}{2}})$$

A combination of equations (4.4) and (4.5) makes minimization of phase errors possible.

For example, take the simple average such that

$$C_i^{n+1} = \frac{1}{2}(C_{i-1}^{n} + C_i^{n})$$

$$+ \frac{1}{2}\frac{Dt}{Dx}(*F_{i-\frac{1}{2}}^{n} + F_{i-\frac{1}{2}}^{n} - *F_{i+\frac{1}{2}}^{n} - F_{i+\frac{1}{2}}^{n}) \qquad (4.6)$$

Hence, improved phase properties are obtained by directional differences which are combinations of central-space differences of lagging phase errors with upstream differences that have leading phase errors.

For stability, we require that

$$u\frac{Dt}{Dx} < 1$$

The above scheme has fourth-order accuracy in space and second-order accuracy in time (Reference 5).

The initial concentration distribution is given by the equation

$$C(x,z,0) = e^{-\frac{(x-.125)^2}{4a}} \tag{4.7}$$

The value of 'a' is so chosen such that the distribution has a narrow width.

a = .00085 gives

C = .01 at x = 0 and x = .25

Concentration values less than .01 are essentially taken to be zero. Hence, distribution extends from x = 0 to x = .25 with a peak of C = 1 at x = .125.

If we examine the difference scheme, we find that we require the values C_{i-1}, C_{i-2} and C_{i-3}. The mesh points in the x direction are numbered from 4 onwards so that C_4 corresponds to the concentration at x = 0. The initial values of C_1, C_2, C_3 are zero. The spread of the pollutant takes place only in the positive x direction as it is convected only in one direction. Hence, the values C_1, C_2, C_3 are always zero in the scheme.

Hence, the complete numerical scheme is as follows.

$$C_i^{n+1} = \frac{1}{2}(C_{i-1}^{n} + C_i^{n}) + \frac{1}{2}\frac{Dt}{Dx}(*F_{i-\frac{1}{2}}^{n} + F_{i-\frac{1}{2}}^{n} - *F_{i+\frac{1}{2}}^{n} - F_{i+\frac{1}{2}}^{n}) + D \cdot \frac{Dt}{DZ^2} \cdot (C_{K+1}^{n} + C_{K-1}^{n} - 2C_K^{n}) \tag{4.8}$$

The above scheme is explicit and has low numerical dispersion. We start with the initial concentration distribution as given by (4.7).

The concentration values at successive time steps are given by marching forward according to equation (4.8).

4.2 Choice of Grid Size

An optimum grid size was selected based on accuracy, stability, and available computer time. To choose Dx and Dt, experimental runs were made with different combinations of Dx and Dt, maintaining a constant DZ = .1. Once Dx and Dt were selected, DZ was varied and, based on accuracy, an optimum value of DZ was chosen.

The velocity profile considered for determining the grid size was $u(z) = z$. There is an advantage in picking this particular velocity profile. In the absence of an analytical solution, it becomes difficult to evaluate how exactly the grid size affects the accuracy for this scheme. But for this velocity profile, there is a symmetry condition existing in the solution which can be used as a criterion to test the accuracy of the scheme and hence, the grid size.

To start with, the peak is centered at $x = .125$. At time $t = 1$, it can be shown that the C values at $x = .625$ are symmetric about $z = .5$. The point of symmetry moves by a distance of 0.5 in x for every unit rise in t.

The symmetry condition can be tested at various points by having a run up to $t = 1$. Accordingly, the symmetry points are $x = .175$, $x = .225$, etc. at $t = .1$, $t = .2$ respectively. The accuracy of the grid size can be rigorously judged by seeing if the symmetry condition is obeyed at different points. It was found that a coarse grid size gave rise to C values which were not accurate enough to obey the

symmetry condition.

A grid size of Dt = .001 and Dx = .025 was very accurate but it could not be used due to the large computer time required. Grid sizes of Dx = .025, Dt = .005 and Dx = .0125, Dt = .01 were adequate in terms of good accuracy and reasonable computer time. Out of these two, we selected Dx = .0125, Dt = .01. A grid size of Dx = .0125 provides 20 mesh points in the initial spread of the curve. Preliminary runs indicated that the greater the number of mesh points in the initial spread, the better is the accuracy.

After choosing Dx, Dt, a run was made with DZ = .05. It essentially gave the same results as DZ = .1. Hence, the final grid size selected was Dx = .0125, Dt = .01 and DZ = .1.

Also this grid size satisfied the mass conservation very accurately. Theoretically, the amount of mass due to the initial distribution is equal to .103. It was found that this scheme maintained pollutant mass within a difference of .01% of the initial value. This shows the conservative nature of the scheme chosen and the accuracy of the grid size.

4.3 Reduction of Numerical Results

The results of the numerical computation can be best represented in terms of moments of the distribution. Let $\bar{C}$ be the vertically averaged concentration at a given x. At any time t, we define the following parameters.

$$\bar{x} = \frac{\int_{-\infty}^{\infty} \bar{C}(x)x\,dx}{\int_{-\infty}^{\infty} \bar{C}(x)\,dx} \tag{4.9}$$

$$\sigma_x^2 = \frac{\int_{-\infty}^{\infty} \bar{C}(x)(x-\bar{x})^2\,dx}{\int_{-\infty}^{\infty} \bar{C}(x)\,dx} \tag{4.10}$$

It can be proved that (4.10) reduces to the following equation.

$$\sigma_x^2 = \frac{\int_{-\infty}^{\infty} \bar{C}(x)x^2\,dx}{\int_{-\infty}^{\infty} \bar{C}(x)\,dx} - \bar{x}^2 \tag{4.11}$$

The longitudinal dispersion co-efficient is defined as (Reference 3)

$$D_x^* = \frac{1}{2}\frac{d\sigma_x^2}{dt}\Big|_t \qquad \text{at any time t.} \tag{4.12}$$

Here D_x^* is non-dimensionalized. The dimensional D_x can be obtained from

$$D_x = D_x^* \cdot H \cdot U_{ref}$$

D_x^* is obtained from the graph of σ_x^2 vs. t.

Now D_x^* represents the spread of the pollutant due to the vertical variation of horizontal velocity.

Calculation of the above quantities was also included in the program.

4.4 Main Features of the Program

To start with, we use a grid size of Dt = .01, Dx = .0125 and DZ = .1. We set the initial concentration distribution according to equation (4.7). The values of concentration at successive times are computed according to the difference scheme. In order to calculate D_x^* it is necessary to carry on the computation for a significant length of time. As time increases, the dispersion progresses to a greater distance in the x direction. As values of Dt, Dx are small, a large amount of computer time is required if we maintain constant Dt, Dx. Hence, a method was devised for increasing Dt, Dx as the computation proceeds without impairing accuracy. The computer time is reduced greatly as a result. The value of DZ was maintained constant at all times.

The computation was carried out until t = 1 using the initial values of Dt, Dx. The initial distribution which is narrow spreads in the x direction due to convection. At t = 1, we check the spread in the x direction. We determine the x mesh points at which C values at z = 0 are equal to .01. Let n_1 be the mesh point at which C is greater than or equal to .01. Let n_2 be the mesh point at which C is less than or equal to .01. The mesh point n_1 corresponds to the beginning of the distribution and n_2 corresponds to the end. The initial distribution which was confined between x = 0 and x = .25 (4 and 24 are the corresponding mesh points) has now spread and is confined between the points n_1 and n_2. The new grid size is computed from the formula

$$Dx_{new} = I \cdot Dx_{old} \tag{4.13}$$

where I = integer part of $\frac{n_2 - n_1}{20}$

This method assures that there are still 20 mesh points within the width of the distribution even with the new grid size.

The value of Dt is increased by the same formula. This procedure is repeated at t = 2, t = 3 and so on and helps to reduce the computer time to an appreciable extent.

Sometimes the value of I in (4.13) is equal to 1. This means that the spread is not sufficiently large. The computation is carried out with the old grid size until another large time step and the whole procedure is repeated.

When the grid size is changed, the old concentration array is re-assigned in accordance with the new grid points. There are many other features which were included in the program to save computer time. Those are considered minor and are not reported here.

The calculation of the different integrals required in connection with mass conservation, $\bar{x}$ values and σ_x^2 was done by the Simpson's rule.

4.5 Crank-Nicholson Scheme

The calculations were done for 3 values of D namely, .01, .1, and 1.0. The expression for the truncation error involves D. In other words, the higher the value of D the greater is the truncation error.

The method for increasing Dt and Dx simultaneously worked very

well with D = .01. To check the accuracy, the program was repeated by increasing only Dx and maintaining Dt constant at .01. The results agreed quite closely with the previous run. This means that increasing Dt simultaneously does not introduce an appreciable error in the results. As a consequence, we are able to carry on the computation for a greater extent in time than by using a fixed Dt of .01.

For D = .1, it was not possible to increase Dt to a great extent because of the factors outlined below.

In the absence of the convection term, the scheme is stable if and only if $D\frac{Dt}{DZ^2} \leq \frac{1}{2}$. Hence, a higher value of D provides an upper limit to the value of Dt that can be used.

It is difficult to analyze mathematically how the convection term affects the stability condition for this scheme. But it can be intuitively said that a higher value of D makes it necessary to use a lower value of Dt for stability.

Hence, for D = .1, we resorted to the Crank-Nicholson scheme so that we may use a higher value of Dt. The Crank-Nicholson scheme uses a better approximation to the diffusion term and is discussed below.

In the absence of the convection term, i.e., for the diffusion equation, the Crank-Nicholson scheme is unconditionally stable for all values of Dt (Reference 10). As stated before, it is difficult to analyze how the convection term affects the stability criterion. But we hoped that it will enable us to use a higher value of Dt than before.

The numerical approximation to the convection term remains the same as before as outlined by J. E. Fromm. For the diffusion term,

we used a simple central difference approximation. In the Crank-Nicholson scheme, the diffusion term is represented by a simple average of the central difference at the current time step and the central difference at the next time step. Thus

$$\frac{\partial^2 C}{\partial z^2} = \frac{1}{2}\left[\frac{(C_{K+1}^{\,n} + C_{K-1}^{\,n} - 2C_K^{\,n})}{DZ^2} + \frac{(C_{K+1}^{\,n+1} + C_{K-1}^{\,n+1} - 2C_K^{\,n+1})}{DZ^2}\right] \tag{4.14}$$

It can be proved that this representation makes the diffusion equation unconditionally stable (Reference 10). Since differencing at a higher time step is involved, the method is implicit in z.

For simplicity, the application of the Crank-Nicholson scheme will be outlined considering the diffusion equation. Its application to our equation follows on identical lines.

Thus, the Crank-Nicholson scheme for

$$\frac{\partial C}{\partial t} = D\frac{\partial^2 C}{\partial z^2} \quad \text{is}$$

$$\frac{(C_K^{\,n+1} - C_K^{\,n})}{Dt} = \frac{D}{2}\left[\frac{(C_{K+1}^{\,n} + C_{K-1}^{\,n} - 2C_K^{\,n})}{DZ^2} + \frac{(C_{K+1}^{\,n+1} + C_{K-1}^{\,n+1} - 2C_K^{\,n+1})}{DZ^2}\right] \tag{4.15}$$

Rearranging, (4.15) becomes

$$- \frac{D}{2} \cdot \frac{Dt}{DZ^2} \cdot C_{K+1}^{n+1} + (1 + D \cdot \frac{Dt}{DZ^2}) C_K^{n+1} - \frac{D}{2} \cdot \frac{Dt}{DZ^2}$$

$$\cdot C_{K-1}^{n+1} = \frac{D}{2} \cdot \frac{Dt}{DZ^2} C_{K+1}^{n} + (1 - D \cdot \frac{Dt}{DZ^2}) C_K^{n} + \frac{D}{2} \cdot \frac{Dt}{DZ^2}$$

$$\cdot C_{K-1}^{n} \qquad (4.16)$$

This gives rise to a tri-diagonal matrix and is solved by the matrix factorization technique as given in Varga (Reference 11). It is necessary to factorize the matrix just once and store the coefficients. Then C values at different K and n are calculated by a simple algorithm.

For D = .1, the Crank-Nicholson scheme made it possible to use a higher value of Dt for stability. But unfortunately, this did not prove very helpful. As indicated before, the truncation error depends on the value of D. We repeated the run with a constant Dt = .01. The C values for this run differed from the previous run when Dt was increased.

Hence, though the Crank-Nicholson enable us to use a higher value of Dt, it is not of much use since accuracy is affected. We could have retained the original scheme for computation.

But this experience served a very useful purpose. The C values were calculated by two different schemes and they tallied very well. It reinforces the effectiveness and success of the overall scheme. It was found that Crank-Nicholson scheme took more or less than the same computer time as the explicit method.

For D = 1, the original scheme cannot be used even with Dt = .01 as it violates the stability condition. There is no choice but to use Crank-Nicholson method. Our previous experience with Crank-Nicholson for D = .1 proved quite useful.

Since the truncation error depends on D and D = 1 is quite large, calculations were repeated with Dt = .005 to check for accuracy. This run gave essentially the same C values as Dt = .01. This again indicates the success of the overall scheme.

All the computations were done both for the linear velocity profile and lake velocity profile. Details about the lake profile will be given in Section 4.7.

4.6 Evaluation of Effective Horizontal Dispersion Co-Efficient for Zero Vertical Diffusivity

A final conclusive check on the accuracy of the numerical scheme was made by calculating an analytical expression for D_x^*. For this purpose, we considered the hypothetical case of D = 0 for the linear profile. The results will be derived for two different initial distributions -- the Gaussian distribution which we have considered so far and a rectangular distribution having properties similar to the Gaussian distribution.

Our Gaussian distribution is

$$C = f(x) = e^{-\frac{(x-.125)^2}{4a}} \qquad \text{for } 0 \le x \le .25$$

$$C = 0 \qquad \text{otherwise.}$$

The rectangular distribution considered is

$C = f(x) = 1$ for $0 \leq x \leq .25$

$C = 0$ otherwise.

We have considered two different distributions because qualitatively it can be reasoned that D_x^* should have the same dependence on t for the two distributions. This is indeed indicated by the analytical results which are identical for the two cases.

4.6.1 Analytical Solution

For D = 0, the differential equation is

$$\frac{\partial C}{\partial t} + u\frac{\partial C}{\partial z} = 0$$

with $u = z$

It can be verified that $C = f(x - z \cdot t)$ is a solution of this differential solution.

4.6.2 Rectangular Distribution

The initial condition is

$C = f(x) = 1$ for $0 \leq x \leq .25$

$\therefore$ $C = f(x - zt) = 1$ for $0 \leq x - zt \leq .25$

To calculate the vertically-averaged concentration $\bar{C}$, we have to integrate C in the z direction. The lower (z_ℓ) and the upper (z_u) limits for z are found as follows.

If we consider $x - zt \geq 0$,

we get $z \leq \frac{x}{t}$

If we consider $x - zt \leq .25$,

we get $z \geq \frac{x-.25}{t}$

Hence in general,

$$z_\ell = \frac{x - .25}{t}$$

$$z_u = \frac{x}{t}$$

The above expressions hold good for all positive and negative values of x and z.

Since in our case, x is positive only and z is restricted between 0 and 1, we have to consider three different cases.

Range (i) $\quad 0 \leq x \leq .25$

Here z_ℓ becomes negative and this is not admissible.

Hence, the limits are

$$z_\ell = 0$$

$$z_u = \frac{x}{t}$$

Range (ii) $\quad .25 \leq x \leq t$

This gives positive values for z_ℓ and z_u

$$\therefore z_\ell = \frac{x - .25}{t}$$

$$z_u = \frac{x}{t}$$

Range (iii) $\quad x > t$

Here z_u becomes greater than 1 and this is not admissible.

$$\therefore \quad z_\ell = \frac{x - .25}{t}$$

$$z_u = 1$$

Hence, we have to take into account three different ranges of x to calculate $\bar{C}$.

For the linear profile C = 0 for $x > t + .25$. Hence, at any time, C has a finite value for $0 \leq x \leq t + .25$.

Range (i) $\quad \bar{C} = \int_{z_\ell}^{z_u} f(x-zt)dz$

$$= \int_{z_\ell}^{z_u} 1 \, dz$$

$$= \frac{x}{t}$$

Range (ii) $\quad \bar{C} = \frac{.25}{t}$

Range (iii) $\quad \bar{C} = \frac{t + .25 - x}{t}$ where $t \leq x \leq t + .25$

Thus we see that $\bar{C}$ is independent of x for range (ii). For ranges (i) and (iii), $\bar{C}$ is dependent on x and $\bar{C} = 0$ at $x = 0$ and $x = t + .25$.

Initial amount of mass = .25. Now mass at any time is given by

$$\int_{-\infty}^{\infty} \bar{C}dx = \int_{0}^{t+.25} \bar{C}dx = .25$$

where the appropriate values of $\bar{C}$ should be taken in the three different ranges. Hence, the solution satisfies mass conservation.

Calculation of $\bar{x}$

$$\bar{x} = \frac{\int_{0}^{t+.25} \bar{C}x dx}{.25}$$

$$= \frac{t}{2} + \frac{1}{8} \tag{4.17}$$

The details have been left out.

Calculation of σ_x^2

$$\sigma_x^2 = \frac{\int_{0}^{t+.25} x^2 \bar{C}dx}{.25} - \bar{x}^2$$

$$= \frac{t^2}{12} + \frac{1}{192} \tag{4.18}$$

Again the details have been left out.

It can be easily seen that, at $t = 0$

$$\bar{C} = 1 \qquad \text{for } 0 \leq x \leq .25$$

$$\tilde{x} = \frac{\int_{0}^{.25} \bar{C}dx}{.25} = \frac{1}{8} \tag{4.19}$$

$$\sigma_x^2 = \frac{\int_{0}^{.25} (x-\tilde{x})^2 \bar{C}dx}{.25} = \frac{1}{192} \tag{4.20}$$

If we put t = 0 in (4.17) and (4.18), $\bar{x}$ and σ_x^2 reduce to (4.19) and (4.20) respectively.

Thus, we get an interesting result.

$$\sigma_x^2 \propto t^2$$

$$\therefore \quad D_x^* \propto t$$

Hence, D_x^* increases continuously with time.

4.6.3 Gaussian Distribution

The derivation for this distribution follows on similar lines but is more complicated. The details are given in Appendix I.

Range (i) $\quad 0 \leq x \leq .25$

$$\bar{C} = \frac{\sqrt{a\pi}}{t}\left[\operatorname{erf}\left(\frac{.125}{2\sqrt{a}}\right) + \operatorname{erf}\left(\frac{x-.125}{2\sqrt{a}}\right)\right]$$

Range (ii) $\quad .25 \leq x \leq t$

$$\bar{C} = \frac{\sqrt{a\pi}}{t}\left[\operatorname{erf}\left(\frac{.125}{2\sqrt{a}}\right) + \operatorname{erf}\left(\frac{.125}{2\sqrt{a}}\right)\right]$$

Range (iii) $\quad t \leq x \leq t + .25$

$$\bar{C} = \frac{\sqrt{a\pi}}{t}\left[\operatorname{erf}\left(\frac{t+.125-x}{2\sqrt{a}}\right) + \operatorname{erf}\left(\frac{.125}{2\sqrt{a}}\right)\right]$$

Here also $\bar{C}$ behaves in the same way as in the rectangular distribution. For range (ii), $\bar{C}$ is independent of x whereas for ranges (i) and (iii), $\bar{C}$ is dependent on x. Also $\bar{C} = 0$ at $x = 0$ and $x = t+.25$.

$\bar{x}$ and σ_x^2 are given by

$$\bar{x} = \frac{t}{2} + \frac{1}{8} \tag{4.21}$$

$$\sigma_x^2 = \frac{t^2}{12} + \text{initial variance (at } t = 0)$$

$$= \frac{t^2}{12} + .0017 \tag{4.22}$$

$$\therefore \quad D_x^* \propto t$$

Hence, the results are identical with those of the rectangular distribution.

Hence theoretically, we have derived that D_x^* increases linearly with time for the case $D = 0$. If the numerical scheme gives results in agreement with theoretical calculations, then it indeed verifies the accuracy of the scheme. This is found to be true and is discussed in Section 5.1.

4.7 Velocity Profile for the Lake

The actual velocity profile for the lake is three dimensional and depends on various factors. We are considering a two-dimensional flow and are interested in investigating how the horizontal convection and vertical diffusion affect the spread of the pollutant. Hence, we should select such a velocity profile which has the same qualitative properties as that of the lake. Gedney (Reference 7) has considered the case of the constant depth basin when the wind is uniform with no inflow or outflow. For this case, the flow is found to be independent

of the x,y coordinates. He has plotted the horizontal velocity distribution at different levels below the water surface for various ratios of lake depth to friction thickness. We take the plot corresponding to a ratio of 1, as Lake Erie has this typical value. He has represented the velocity vectors at different depths by points and the magnitude can be obtained by connecting the origin of the coordinate system with points indicated on the curve. The points correspond to levels of ·1H, ·2H, etc. Since we are considering a two-dimensional flow, we just take the magnitude of the velocity vectors and we get the following values.

Values of z	Values of u(z)
1.0	.777
0.9	.452
0.8	.227
0.7	-.066
0.6	-.111
0.5	-.161
0.4	-.201
0.3	-.223
0.2	-.178
0.1	-.111
0	0

The above values have been calculated after non-dimensionalizing each of the velocity values by U_{ref} which represents the algebraic difference between the maximum and minimum values.

This profile has the same qualitative properties as that of the lake. It has a reverse flow at the bottom and as a result, the

pollutant is convected in both x directions. Because of this, it is necessary to carry on the computation in both positive and negative x directions. We avoid this by adding a constant quantity corresponding to the maximum negative velocity to the velocity value at each point so that the maximum negative velocity is reduced to zero and the rest are all positive.

Here the maximum negative velocity is $U_0 = -.223$ at $z = .3$. This is added to each velocity value so that $u = 1$ at $z = 1$, $u = .223$ at $z = 0$ and $u = 0$ at $z = .3$. The rest of the values transform in like fashion.

Due to this profile, the pollutant is convected in only one direction and consequently, the computation has to be carried on in only one direction.

It might appear as if our problem has been changed by this transformation but it is not.

Our original differential equation is

$$\frac{\partial C}{\partial t} + u\frac{\partial C}{\partial x} = D\frac{\partial^2 C}{\partial z^2} \tag{4.23}$$

Consider the change of variable

$$x = \hat{x} - U_0 t$$

where U_0 = maximum negative velocity.

(4.23) transforms to

$$\frac{\partial C}{\partial t} + (u + U_0)\frac{\partial C}{\partial \hat{x}} = D\frac{\partial^2 C}{\partial z^2} \tag{4.24}$$

Now $u + U_0 = v(z)$ is our resultant velocity profile.

Solving (4.24) numerically gives $C(\hat{x},z,t)$. To get $C(x,z,t)$ we use the computer results of (4.24) and shift to the left by $U_0 t$.

At $t = 0$,

$$x = \hat{x}$$

Thus the initial condition in terms of x or $\hat{x}$ is the same.

But the above transformation does affect the $\bar{x}$ values, since $\bar{x}$ for original profile = $\bar{x}$ for resultant profile - $U_0 t$ (4.25)

If we examine the expression for σ_x^2, we can deduce that its value does not change. This is because there is a quantity $(x-\bar{x})^2$ occurring in the integral and this value does not change due to the transformation because $U_0 t$ is subtracted from both the quantities.

4.8 A Short Note on Linear Profile

As a matter of fact, the linear profile

$$u(z) = z$$

can be viewed as a profile resulting by adding $U_0 = .5$ to the following profile

$$u = z - .5 \tag{4.26}$$

For this profile,

$u = .5$ at $z = 1$

$u = 0$ at $z = .5$

$u = -.5$ at $z = 0$

It can be considered as an extremely crude approximation to the lake profile.

Hence, the results obtained for u = z are equally applicable to this profile.

CHAPTER V

RESULTS AND DISCUSSION

5.1 Evaluation of D_x^* for the case D = 0

In Section 4.6, we derived an analytical expression for $\bar{x}$ and σ_x^2 for the case D = 0 considering the gaussian distribution. Table 5.1 summarizes the values of $\bar{x}$ and σ_x^2 as calculated from the analytical expressions given by equations (4.21) and (4.22) respectively. Table 5.2 gives the results obtained by the numerical scheme. Comparison of the two tables clearly indicates that the numerical scheme gives excellent results in agreement with theoretical calculations. Even at t = 5, the error in $\bar{x}$ is .16% and the error in σ_x^2 is .1%.

For D = 0, the vertical variation in concentration is very steep as indicated by the analytical solution. As an example, at t = 1 and x = 1.125, C = 0 for z = 0 through z = .8, C = .0528 at z = .9 and C = 1 at z = 1. At t = 1 and x = .75, C = 0 for z = 0 through z = .5, C = .832 at z = .6, C = .191 at z = .7 and C = 0 for z = .8 through z = 1. With such a wide variation in concentration with z, any numerical integration procedure will have some error associated with it. The error arises mainly because there are only 11 grid points in the z direction. A comparison of the C values calculated by the scheme with the analytical values indicated that DZ = .1 gave sufficiently accurate C values. The maximum error in C values was about 2%. But DZ = .1 leads to a higher error in the $\bar{C}$ values due to the numerical integration. The average error was 10 - 15% and this may be

positive or negative. But surprisingly when $\bar{C}$ was integrated in the x direction for calculating $\bar{x}$ and σ_x^2, the errors seemed to average out. The overall error in $\bar{x}$ and σ_x^2 was quite low as indicated before. For finite D values, the diffusion tends to reduce the vertical variation in concentration. This is illustrated by the graphs later. As a matter of fact, for D = 1.0, there is very little variation in concentration. Under these conditions the error in vertical integration to get $\bar{C}$ will be much less than D = 0. The fact that the scheme gave such accurate values of $\bar{x}$ and σ_x^2 for D = 0 means that one can expect σ_x^2 values obtained for finite D values to be at least as accurate. This represents a conclusive check on the accuracy of the scheme used here.

5.2 Spatial Distribution of Concentration for the Linear Profile

The concentration at any time is a function of both x and z. To find out how C varies with x, we plot the C values at z = .5 versus x.

Figures 9.1 to 9.4 give the concentration distribution for the linear profile at different times. In comparing the figures, care should be taken since the scales for the co-ordinate axes change from figure to figure.

If we examine the figures, we see that D = .01 has a higher peak than D = 0.1 and D = 1.0 at t = 1. As time progresses, its peak reduces until at t = 7, it has the lowest peak. It should be noted that peaks for all the three D values occur at the same x value. This is due to the fact that the velocity profile is linear. For D = .01, the concentration distribution is narrow at t = 1 but spreads as time

increases. At t = 7, its spread is slightly more than that of D = 0.1. The distribution for D = 0.1 is spread out at all times. For D = 1.0, the pollutant moves along x more or less like a slug as the increase in spread is not much.

5.3 Spatial Distribution of Concentration for the Lake Profile

Figures 10.1 through 10.4 give the concentration distribution for the lake profile at different times. We observe the same qualitative properties as that of the linear profile with minor differences. Because the velocity profile is not symmetric, the peaks for the different values of D are centered at different x values. As with the linear profile, D = .01 has the highest peak at t = 1 which reduces as time progresses. At t = 6, its peak is less than that of D = 1.0 but is still higher than that of D = 0.1. The distribution for D = 0.1 is very skewed unlike the linear profile. It has a long tail at the downstream end which increases as time progresses. D = .01 has a narrow distribution at t = 1 but becomes more and more skewed as time proceeds. For D = 1.0, the pollutant moves like a slug as evidenced also in the linear profile. For all the three D values, the pollutant spread for the lake profile is less than that of the linear profile. This is quantitatively confirmed by the Dx* values to be reported later.

5.4 Vertical Distribution of Concentration for the Linear Profile

To determine the vertical variation in concentration, plots are made of C versus z at a given x. For each D value, plots are made at three different x values namely x_ℓ, x_r and x_m. Now x_m corresponds to

the maximum concentration in the spatial distribution graph. x_ℓ and x_r lie on either side of x_m and correspond to the concentration when it is about half the peak value. This ensures that the vertical variation in concentration is obtained at different points along the horizontal spread of the pollutant.

Figures 11.1 through 11.9 give the vertical variation in concentration at different times, for the linear profile. Now the peak value of concentration occurs at the same x value (x_m) for all the three D values. x_ℓ and x_r correspond to about half the peak concentration for D = 1.0.

Figures 11.2 and 11.3 correspond to the values x_ℓ and x_r respectively for t = 1. It should be noted that x_ℓ and x_r are symmetrically placed with respect to x_m. The figures are symmetric in the sense that

$$C \text{ for } z = 0 \text{ at } x_\ell = C \text{ for } z = 1 \text{ at } x_r$$

$$C \text{ for } z = .1 \text{ at } x_\ell = C \text{ for } z = .9 \text{ at } x_r$$

and so on. For the linear profile, this property can be argued from qualitative considerations in a manner similar to the deduction of the previous symmetry condition. (See Sections 3.2.5 and 4.2) The fact that the numerical scheme gives results verifying this is another indication of the reliability of the scheme. For other t values, plots are made only at x_ℓ and x_m.

Referring to the figures 11.1 through 11.9 we can see that for D = 1.0, there is practically no variation in concentration in the

vertical direction at x_m for all t values. At x_ℓ, there is slight variation for all t values. For D = 0.1, there is relatively more variation in concentration. The variation becomes less as time progresses. At t = 4 and t = 7, there is very little variation. For D = .01, there is wide variation in concentration at all times.

5.5 Vertical Distribution of Concentration for the Lake Profile

Figures 12.1 to 12.12 give the vertical distribution of concentration for the lake profile. Here x_ℓ, x_m and x_r are different for each D value since the peaks occur at different x values. This necessitates a separate plot for each D. Since the velocity profile is not symmetric, graphs are drawn at all the three x values.

We observe the same qualitative properties as that of the linear profile. For D = 1.0, there is very little variation at all times. For D = 0.1, there is relatively more variation which reduces as time progresses. At t = 4 and t = 6, the variation is slight. For D = .01, the variation is quite large at all times.

5.6 Regression Analysis

To evaluate the results accurately for quantities like D_x^* and to get a mathematical relationship between the variables, a regression analysis was made for each set of results reported in Tables 5.3 through 5.8. The analysis yields an ANOVA (Analysis of Variance) table in each case but that will not be given here. Only the essential details from it will be reported.

The following quantities are reported in each case.

F = Ratio of "Mean Sum of Squares Due to Regression" to "Mean Sum of Squares About Regression."

M = Mean Sum of Squares About Regression.

S = Total Number of Observations.

The results were analyzed by a simple linear regression package program. To begin with, the program tries to fit a first-order model to the values. It calculates the ANOVA table for this model and based on this, determines if the model is adequate. If not, a second-order model is tried and again the ANOVA table is calculated. This is done until the most satisfactory model is determined.

5.7 D_x^* Values for the Linear Profile

Tables 5.3 through 5.5 give the values of σ_x^2 for the linear profile for the three D values. Figures 13.1 through 13.3 represent the plot of these values.

5.7.1 Analysis for D = .01

Figure 13.1 clearly indicates that σ_x^2 does not increase linearly with t. According to Aris, for any velocity profile and a finite D value, D_x^* reaches an asymptotic constant value (Reference 13). This means that, after a long time, $\frac{d\sigma_x^2}{dt}$ becomes a constant or σ_x^2 increases linearly with time. However, we would like to know the dependence of σ_x^2 on t at intermediate times. We can assume a relationship between σ_x^2 and t to be given by

$$\sigma_x^2 = Kt^n + .0017 \qquad (5.1)$$

where K,n are constants to be determined.

This is exactly similar to the theoretical relation between σ_x^2 and t which was derived for the case D = 0.

At time t = 0, $\frac{\partial C}{\partial z} = 0$

Hence initially, convection is the dominating factor in the spread of the pollutant. After sometime, vertical diffusion also becomes important. For D = 0, it was proved that $\sigma_x^2 \propto t^2$. Hence the index n in equation (5.1) is close to 2 in the initial stages of dispersion and reaches an asymptotic value of 1.

The calculations were done until t = 16. Since n changes continuously with time, the time period of t = 0 to t = 16 was subdivided into three smaller ranges. Throughout each subrange, equation (5.1) was assumed to hold good,and average values of n and K were calculated by regression analysis.

From t = 1 to t = 5: n = 1.92 K = .086

From t = 6 to t = 9: n = 1.78 K = .102

From t = 10 to t = 16:n = 1.67 K = .136

The limiting value of D_x^* for the linear profile is given by Saffman (Reference 14)

$$D_x^* = \frac{1}{120D} \qquad (5.2)$$

Thus D_x^* is inversely proportional to D.

For D = .01, $D_x^* = .833$

At t = 16, taking n = 1.67 and K = .136, we get

$$D_x^* = \frac{1}{2}Knt^{n-1}$$

$$= .725$$

Hence even at t = 16, D_x^* has not reached the ultimate value.

The dimensional D_x corresponding to this D_x^* value in the western basin of Lake Erie is

$$D_x = D_x^* \cdot U_{ref} \cdot H$$

$$= 1.96 \times 10^4 \text{ cm}^2/\text{sec.}$$

This value of D_x is of the same order of magnitude as the value reported by Murthy for horizontal eddy diffusivity in Lake Ontario for about a two-mile scale which is equal to 5×10^4 cm^2/sec. (Reference 8).

The time required to reach the steady state value by D_x^* is important and its significance will be discussed in Chapter VI. Aris has used an analytical approach to describe the dispersion of a solute in a tube of circular section in terms of moments of distribution (Reference 13). He has given the unsteady state equation for D_x^*, but only solved this equation for the asymptotic value of D_x^*. By considering the nature of the unsteady state terms in his equation, it can be seen that the time required to reach the steady state value is inversely proportional to D. This fact will be used to base some of our conclusions in Chapter VI.

5.7.2 Analysis for D = 0.1

Figure 13.2 indicates that the graph of σ_x^2 versus t is a straight line after t = 3.

Regression analysis of a linear model for the values from t = 3 to t = 8 gave the following results.

F = 44590

M = .00001

S = 6

The high value of F indicates that the linear relationship is extremely good.

From the analysis, slope = .172

$$D_x^* = \frac{1}{2}\frac{d\sigma_x^2}{dt}$$

$$= .086$$

This compares closely with the theoretical value of $D_x^* = .0833$ from equation (5.2).

From t = 0 to t = 3, the graph of σ_x^2 versus t is not linear. Since the curve is concave upwared in this range, D_x^* increases with time until t = 3 after which it reaches a constant value of .086.

5.7.3 Analysis for D = 1.0

Figure 13.3 represents the graph of σ_x^2 versus t. Initial runs indicated that σ_x^2 increases linearly with t within a very short time (after t = .5).

Results of Regression Analysis

F = 13039

M = .0000014

S = 8

Again, the high value of F indicates that the linear relationship is extremely good.

From the analysis, slope = .0182

$$\therefore D_x^* = .0091$$

The theoretical value of $D_x^* = .00833$ from equation (5.2).

The higher value of D_x^* given by the scheme is most likely due to the fact that the truncation error from the diffusion approximation becomes large for D = 1.0.

Hence, summarizing,

For D = .01, $\sigma_x^2 \propto t^n$ where n decreases with time.

D_x^* increases with time at least until t = 16.

For D = 0.1, $\sigma_x^2 \propto t$ after t = 3.

D_x^* initially increases with time and then becomes a constant with a value equal to .086.

For D = 1.0, $\sigma_x^2 \propto t$

D_x^* is a constant with a value equal to .0091.

Now D_x^* is a measure of the horizontal spread of the pollutant.

The horizontal spread decreases with increasing value of D. This is a quantitative confirmation of the results from the figures discussed earlier.

5.8 D_x^* Values for the Lake Profile

Tables 5.6 through 5.8 give the σ_x^2 values for the lake profile for the three D values. Figures 14.1 through 14.3 represent the plot of these values.

We can easily see that both σ_x^2 and D_x^* have the same qualitative dependence on t as the linear profile.

5.8.1 Analysis for D = .01

Figure 14.1 indicates that σ_x^2 does not increase linearly with t. Again, we can assume a relationship between σ_x^2 and t to be given by equation (5.1). The calculations were done until t = 14. As in the case of the linear profile, the time period from t = 0 to 14 was subdivided into three ranges and average values of n and K for each range were calculated by regression analysis.

From t = 1 to t = 4: n = 1.85 K = .066

From t = 5 to t = 8: n = 1.69 K = .084

From t = 9 to t = 14: n = 1.57 K = .106

At t = 16, taking n = 1.57 and K = .106, we get

$$D_x^* = .61$$

5.8.2 Analysis for D = 0.1

Figure 14.2 shows that σ_x^2 increases linearly with t after t = 3.

Regression Analysis Results for the Values Between t = 3 and t = 8

F = 30789

M = .00005

S = 6

Slope = .094

$\therefore D_x^* = .047$

From t = 0 to t = 3, the curve is concave upward. Hence D_x^* increases with time until t = 3.

5.8.3 Analysis for D = 1.0

Initial runs indicated that σ_x^2 increases linearly with t after t = .4.

Regression Analysis Results

F = 49368

M = almost 0

S = 8

Slope = .01

$\therefore D_x^* = .005$

Hence, the following table compares D_x^* values for the linear

and lake profiles.

D_x^* Values

	Linear Profile	Lake Profile
D = 0.1	.086	.047
D = 1.0	.0091	.005
D = .01 (at t = 16)	.725	.610

Hence, the spread of the pollutant is less for the lake profile but the qualitative effect of the different values of D on D_x^* is similar for both the profiles.

5.9 Computer Time

Table 5.9 gives the computer time for the different runs on IBM computer 370/145. Runs 1 and 2 were made for the same value of D = .01. In run 1, both Dt and Dx were increased simultaneously. In run 2, Dt was kept constant at .01 while Dx was increased. In run 1, Dt increased by a factor of 2 so that σ_x^2 values were obtained at t = 1, t = 2 and so on up to t = 16. Hence, run 2 was necessitated to calculate σ_x^2 at other intermediate times. We had indicated in Section 4.5 that increasing Dt affects the accuracy of σ_x^2 values except for D = .01. This was another reason for making run 2 so that we could check the σ_x^2 values at t = 4 and t = 8 obtained by both the runs. They were essentially the same. The same considerations apply to runs 5 and 6. In run 5, Dt does not always increase by a factor of 2 as in run 1. Hence, t_{final} is equal to 14.

In the remaining runs, Dt was kept constant at .01 to ensure the accuracy of σ_x^2 values. In runs 1 and 5, a higher value of t_{final} is reached in a much shorter time as Dt is also increased.

For D = 0.1 and D = 1.0, the computation was carried out only until t = 8 as D_x^* reaches a constant value by that time.

From the table, one can see that the lake profile takes a longer computer time than the linear profile. This is because the horizontal spread of the pollutant is less for the lake profile than the linear profile. Consequently, Dx does not increase as much as the linear profile. (See Section 4.4) The smaller value of Dx leads to a higher computer time.

5.10 Discussion

The gross behavior of the pollutant spread remains the same with minor differences for both the linear and lake profiles. The lake profile makes the concentration distribution somewhat skewed depending on the value of D. But there is a quantitative difference in the spread of the pollutant for the two cases. Lake profile leads to less horizontal spread than the linear profile for all values of D. Also the horizontal spread decreases with increasing value of D for both the profiles. These are illustrated both by the figures and the D_x^* values. This is to be expected based on analytical results given by Saffman for channel flow with linear profile (Reference 14). His equation given by (5.2) shows that the asymptotic value of D_x^* decreases as D increases.

For both the profiles, different values of D have similar effect

on the behavior of D_x^*. D = 1.0 gives a constant D_x^*. For this value of D, there is very little variation in concentration in the vertical direction. For D = 0.1, D_x^* increases initially and then becomes a constant. Likewise, initially there is more concentration variation in the vertical direction which decreases as time progresses. D = .01 leads to a value of D_x^* which continuously increases with time until t = 16. The concentration variation in the vertical direction is quite large at all these times.

Hence, we see an interesting relationship between D_x^* and the concentration variation in the vertical direction regardless of the shape of the velocity profile. When D_x^* is constant, there is a small variation in concentration. On the other hand, as long as D_x^* is increasing, there is a wide variation in concentration.

CHAPTER VI

CONCLUSIONS

It is found that the shape of the velocity profile has little qualitative effect on the horizontal spread of the pollutant. Quantitatively the lake profile leads to less horizontal spread than the linear profile.

There seems to be a definite relation between the value of D (dimensionless D_z) and the length of time during which D_x^* keeps on increasing. For D = 1.0, D_x^* reaches a constant value within a very short time, i.e., after t = .5. For D = 0.1, D_x^* becomes a constant after t = 3. Both of these D_x^* values are much smaller than that for D = .01 at t = 16. For D = .01, D_x^* increases at a rate faster than $t^{.5}$ for both the linear and lake profiles even at t = 16. For a given velocity profile, it is probably impossible in general to obtain an analytic expression for D_x^* as a function of t. However, it is known that for any velocity profile and a finite D value that D_x^* reaches an asymptotic constant value (Reference 13). In any case, for D = .01, D_x (dimensional D_x^*) at t = 16 has already approximately reached the value of horizontal eddy diffusivity for a two-mile scale reported by C. R. Murthy (Reference 8).

There seems to be an interesting relationship between D_x^* increasing and the vertical variation in concentration. When D_x^* is constant, the numerical results indicate a relatively small vertical variation in concentration. On the other hand, as long as D_x^*

increases, there is a significant vertical variation in concentration.

Thus it appears that this approach may be very useful in deciding when a three-dimensional model should be used for dispersion modeling and when a two-dimensional model is adequate. When the vertical variation is relatively small (which is pointed out above, seems to correlate well with D_x^* having reached a constant value), a two-dimensional model can be used with good accuracy with D_x^* predicted by this method. A two-dimensional model will cut down the computer time significantly. In the Great Lakes, D_x^* could increase the rate of horizontal dispersion, due only to the horizontal turbulence, in the current direction. On the other hand, as long as D_x^* is increasing which corresponds to the case when there is a relatively large vertical variation, a three-dimensional model should be used for reasonable accuracy.

The results for the dispersion of pollutant in the western basin of Lake Erie discussed earlier and given by figures 1 to 8 appear to qualitatively fit this general conclusion. This can be viewed as follows. For D = .01 (corresponding to D_z = 270 cm^2/sec. in the western basin of Lake Erie), D_x^* variation with time continued up to t = 16 and it could be conjectured that it would persist up to t equal to perhaps 20-30. This dimensionless time corresponds to a length scale of 30H since the maximum dimensionless velocity is 1. Hence, for length scales greater than about 30H the vertical variation would not be significant. The western basin results were calculated using a mesh size of 2 miles and contours at the longest times of calculation extended about 10 miles from the source. It was found that not until D_z was decreased to 0.5 cm^2/sec. did a significant

vertical variation in concentration appear. Very qualitatively extrapolating the time of D_x^* variation from the above results, it is not unreasonable to expect this time to be of the order of 1000 when D = 2×10^{-4} (corresponding approximately to D_z = 5 cm^2/sec. in the western basin). For the reference quantities used in the western basin examples, this dimensionless time corresponds to a length scale on the order of 5 miles. For D_z = 5 cm^2/sec. the western basin examples begin to show some vertical variation in concentration. If D is as small as 2×10^{-5} or D_z approximately equal to 0.5 cm^2/sec., a period of variation for D_x^* on the order of 10,000 might be expected. This would correspond, in the western basin example to a length scale of 50 miles within which significant vertical dependency of concentration could be expected. As noted above, this indeed proved to be the case in the western basin examples using D_z = 0.5 cm^2/sec.

To make these results more generally applicable in the Great Lakes, more examples should be tried using different velocity profiles u(z) and different values of D_z for specific Great Lake situations. Instead of taking a constant D_z it will be a good idea to take D_z as a function of z as it is found that D_z changes with depth in the Great Lakes. Based on the relative insensitivity of the results to the shape of the velocity profile u(z), probably no more than 5 or so velocity profiles would be needed to characterize a great majority of the situations commonly found in the Great Lakes.

Since the results are quite sensitive to the D_z values, it appears that D_z (as a function of z) should be fairly well defined in order to get accurate prediction of concentration. An accurate

dispersion model will have to incorporate at least the gross features of the variation of D_z from one locality to the next. To handle this in a practical way would require D_z as a function of local velocity gradients, temperature gradients, depth, etc. This requires more information about the variation of D_z than has so far been reported.

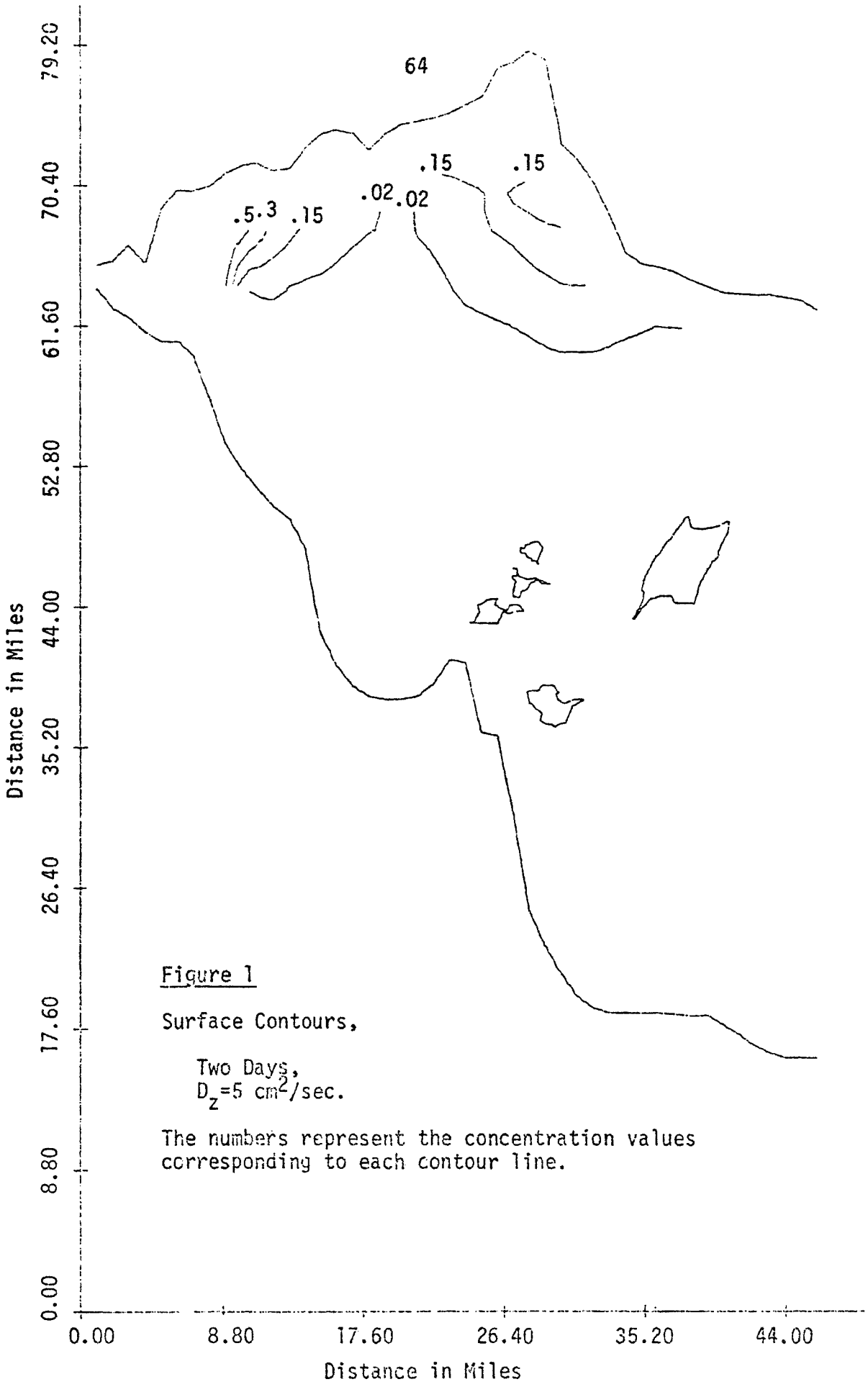

Figure 1

Surface Contours,

Two Days,
D_z=5 cm^2/sec.

The numbers represent the concentration values corresponding to each contour line.

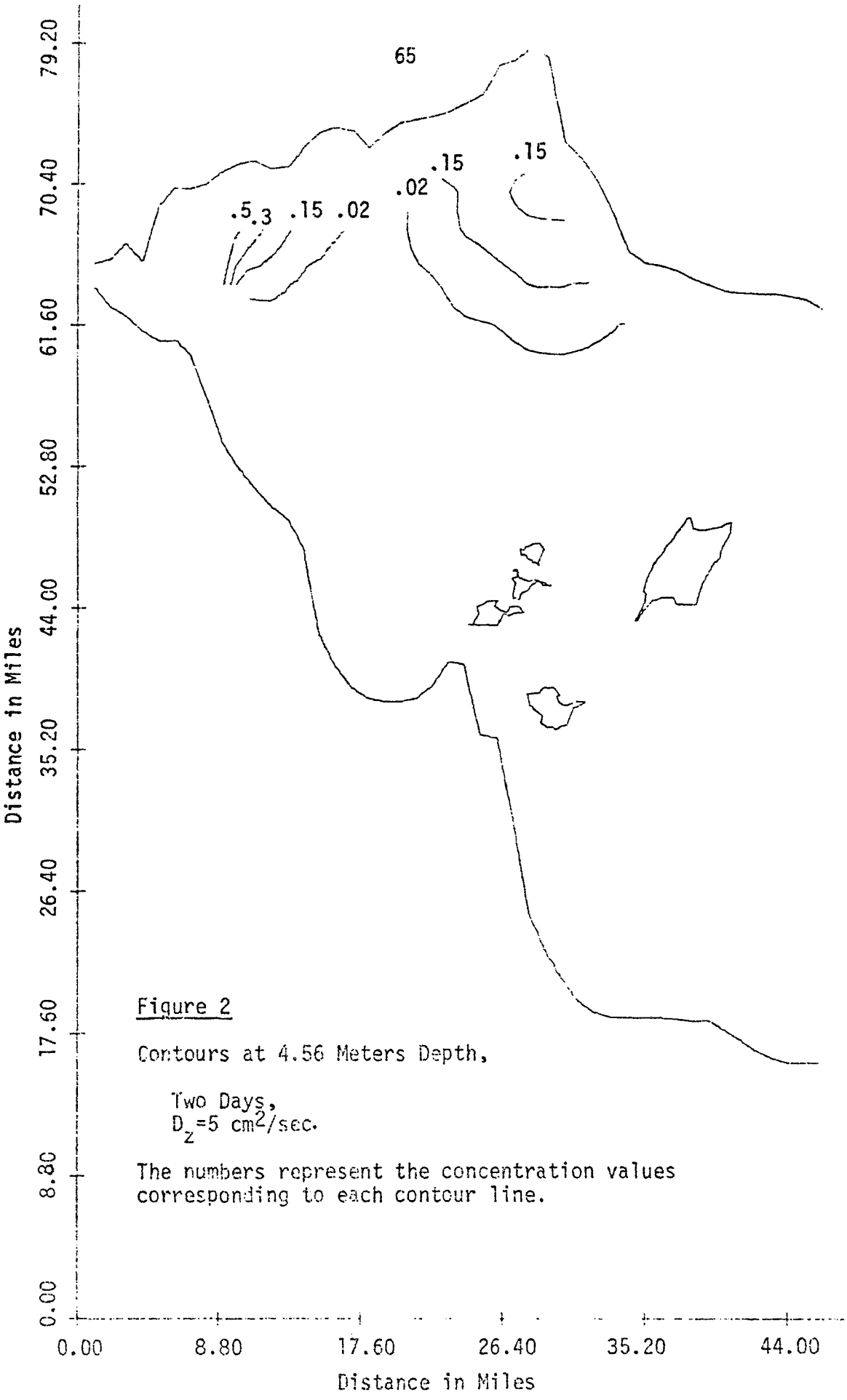

Figure 2

Contours at 4.56 Meters Depth,

Two Days,
D_z=5 cm^2/sec.

The numbers represent the concentration values corresponding to each contour line.

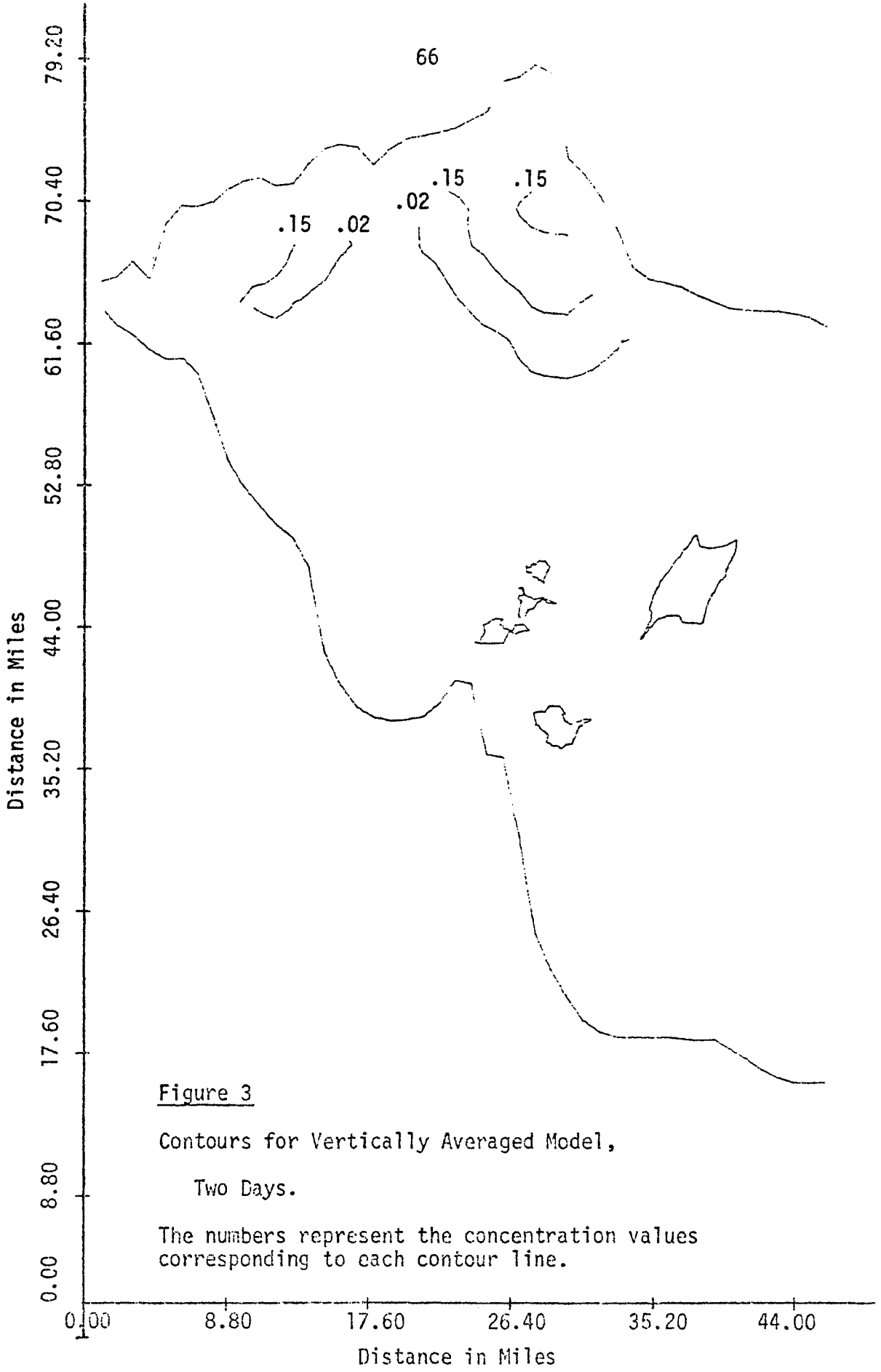

Figure 3

Contours for Vertically Averaged Model,

Two Days.

The numbers represent the concentration values corresponding to each contour line.

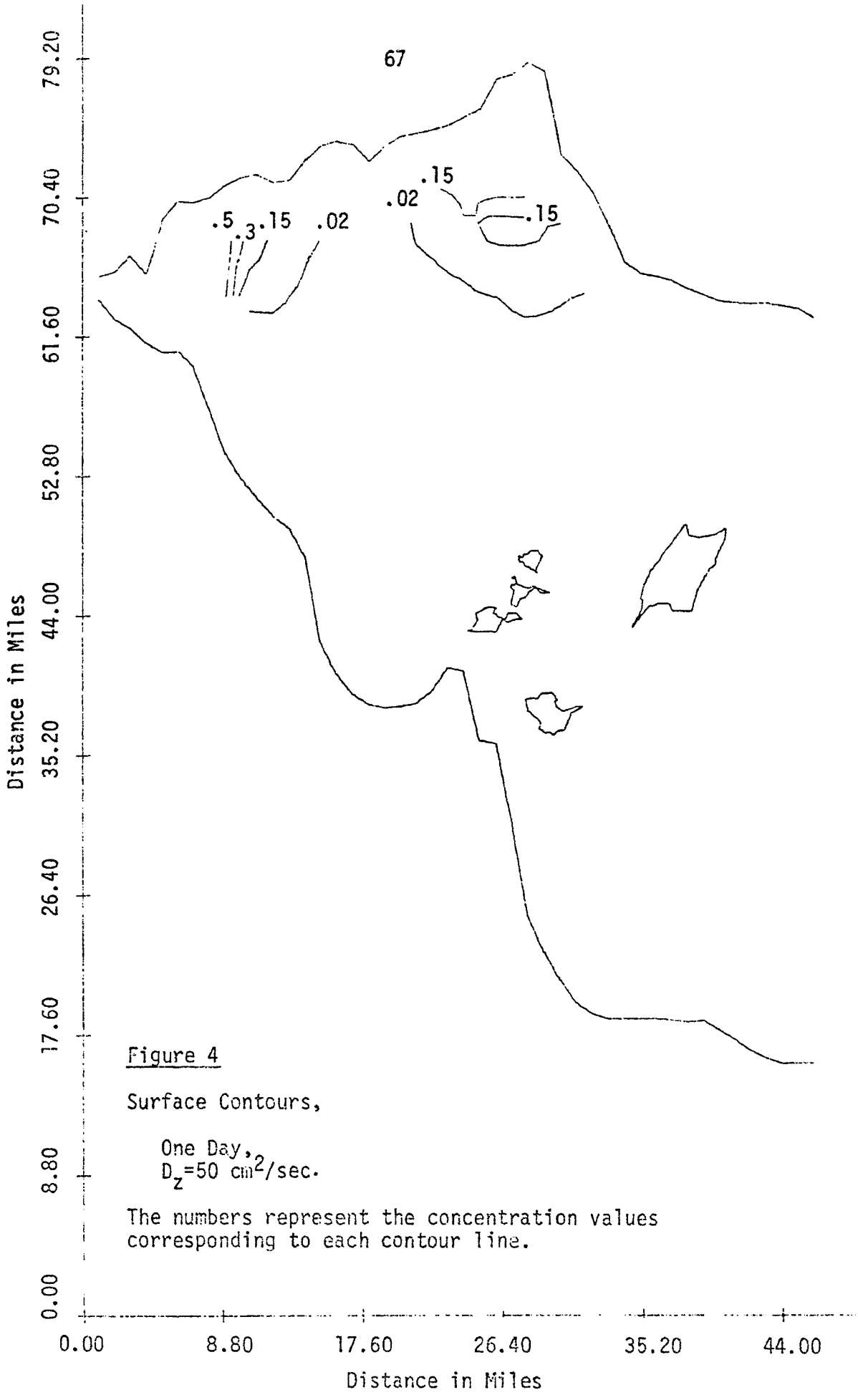

Figure 4

Surface Contours,

One Day,
D_z=50 cm^2/sec.

The numbers represent the concentration values corresponding to each contour line.

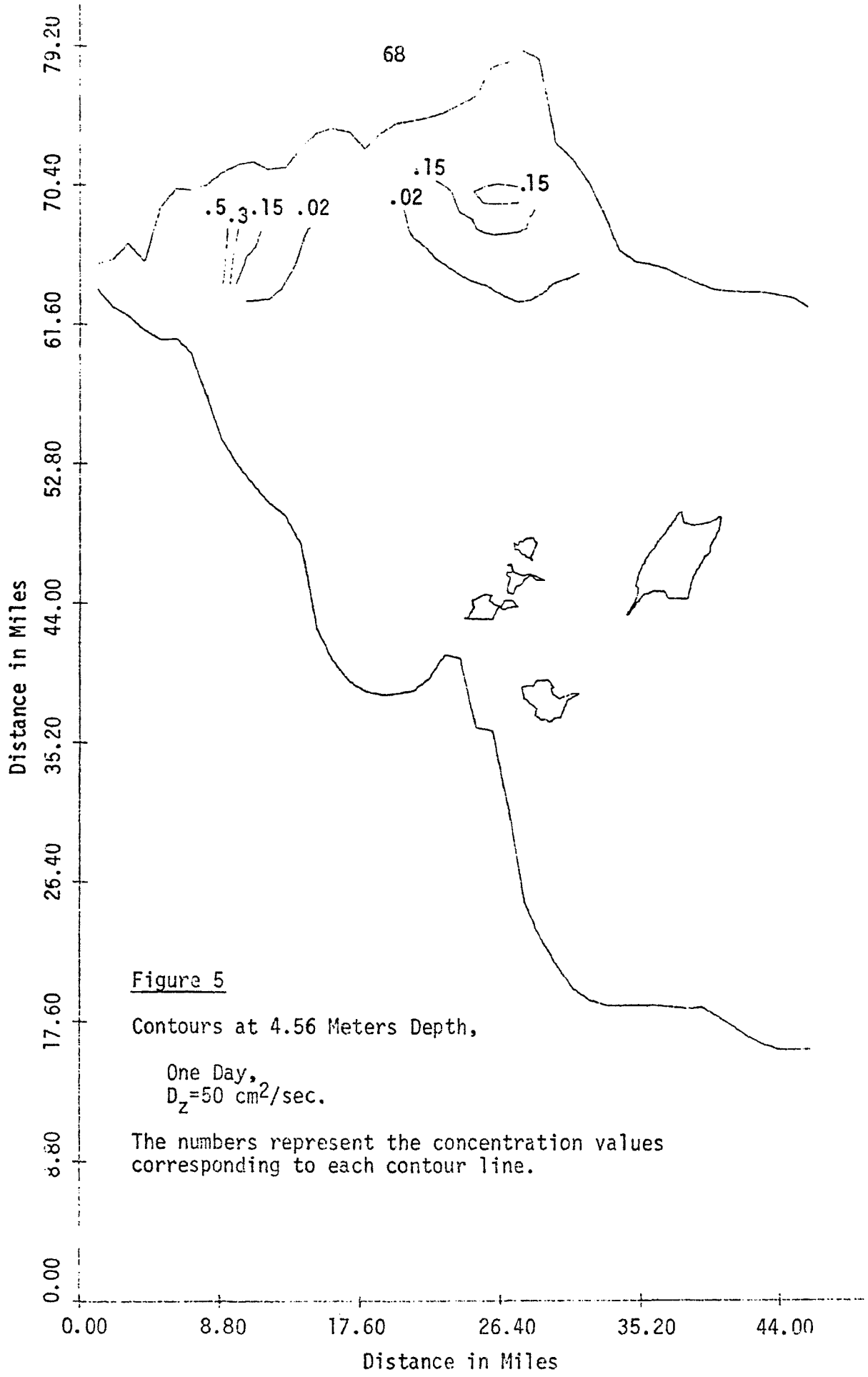

Figure 5

Contours at 4.56 Meters Depth,

One Day,
D_z=50 cm^2/sec.

The numbers represent the concentration values corresponding to each contour line.

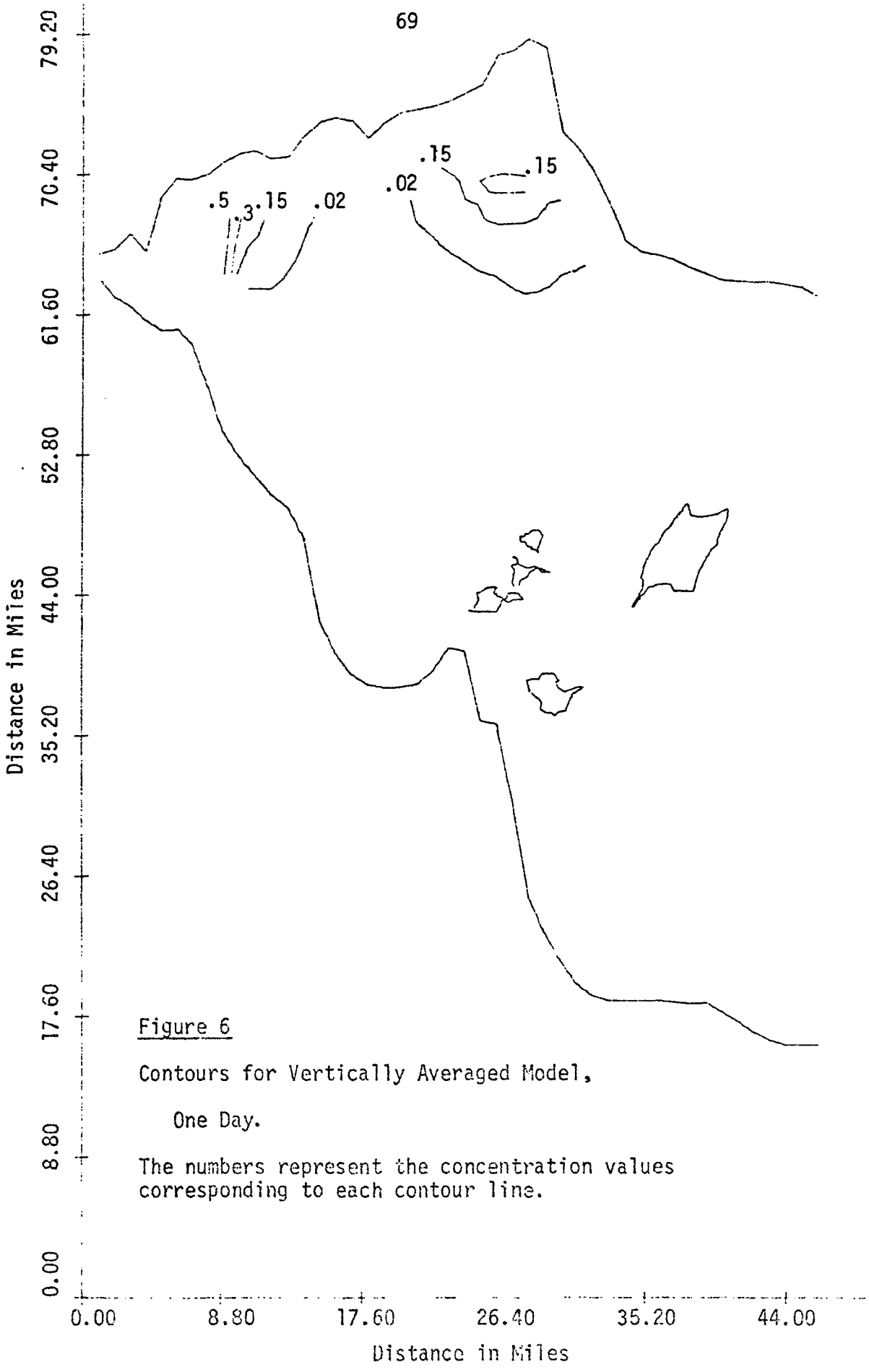

Figure 6

Contours for Vertically Averaged Model,

One Day.

The numbers represent the concentration values corresponding to each contour line.

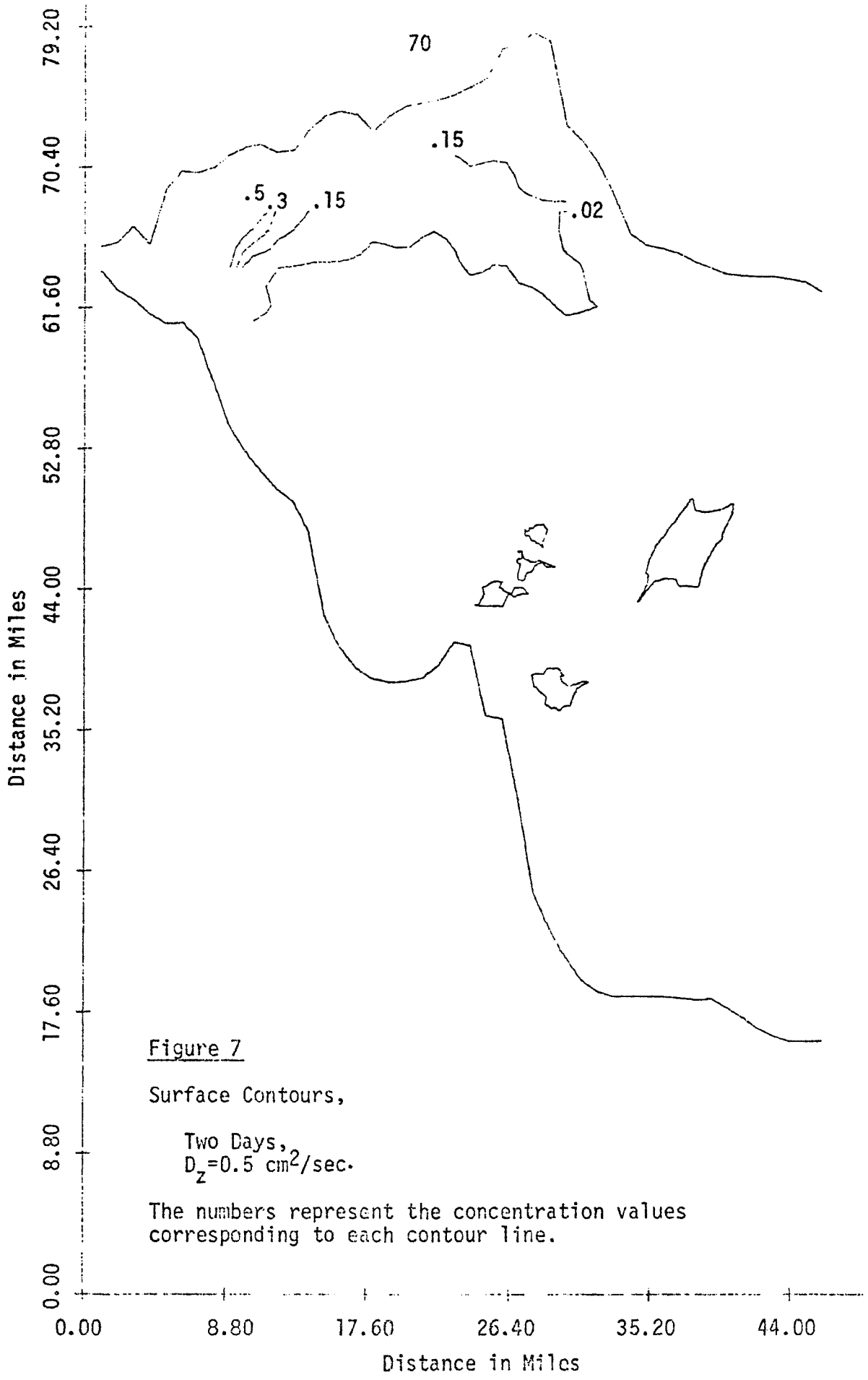

Figure 7

Surface Contours,

Two Days,
D_z=0.5 cm^2/sec.

The numbers represent the concentration values corresponding to each contour line.

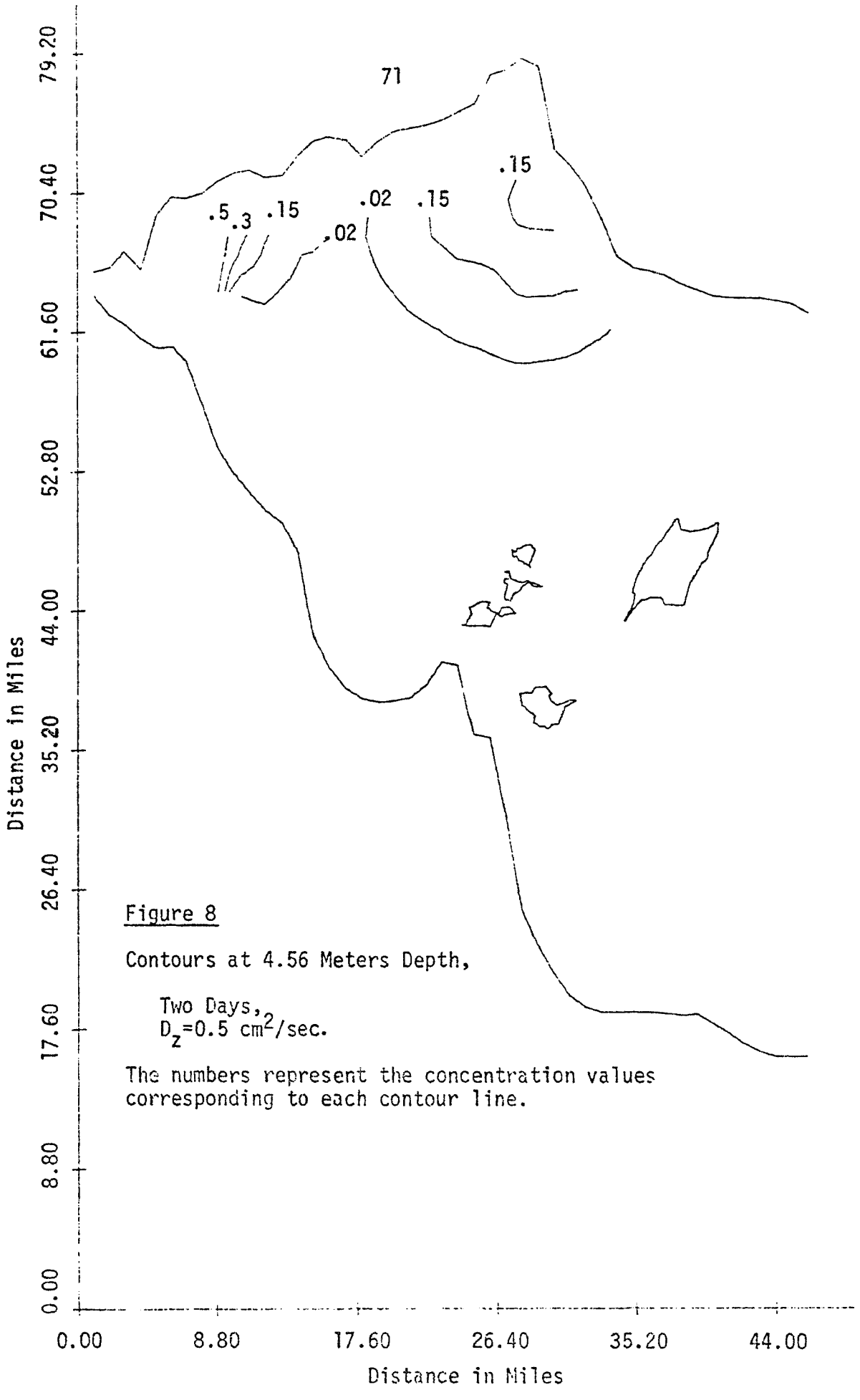

Figure 8

Contours at 4.56 Meters Depth,

Two Days,
D_z=0.5 cm^2/sec.

The numbers represent the concentration values corresponding to each contour line.

Figure 9.1: Concentration vs. Horizontal Distance for the LINEAR Profile at Time t=1. Plots made at z=.5

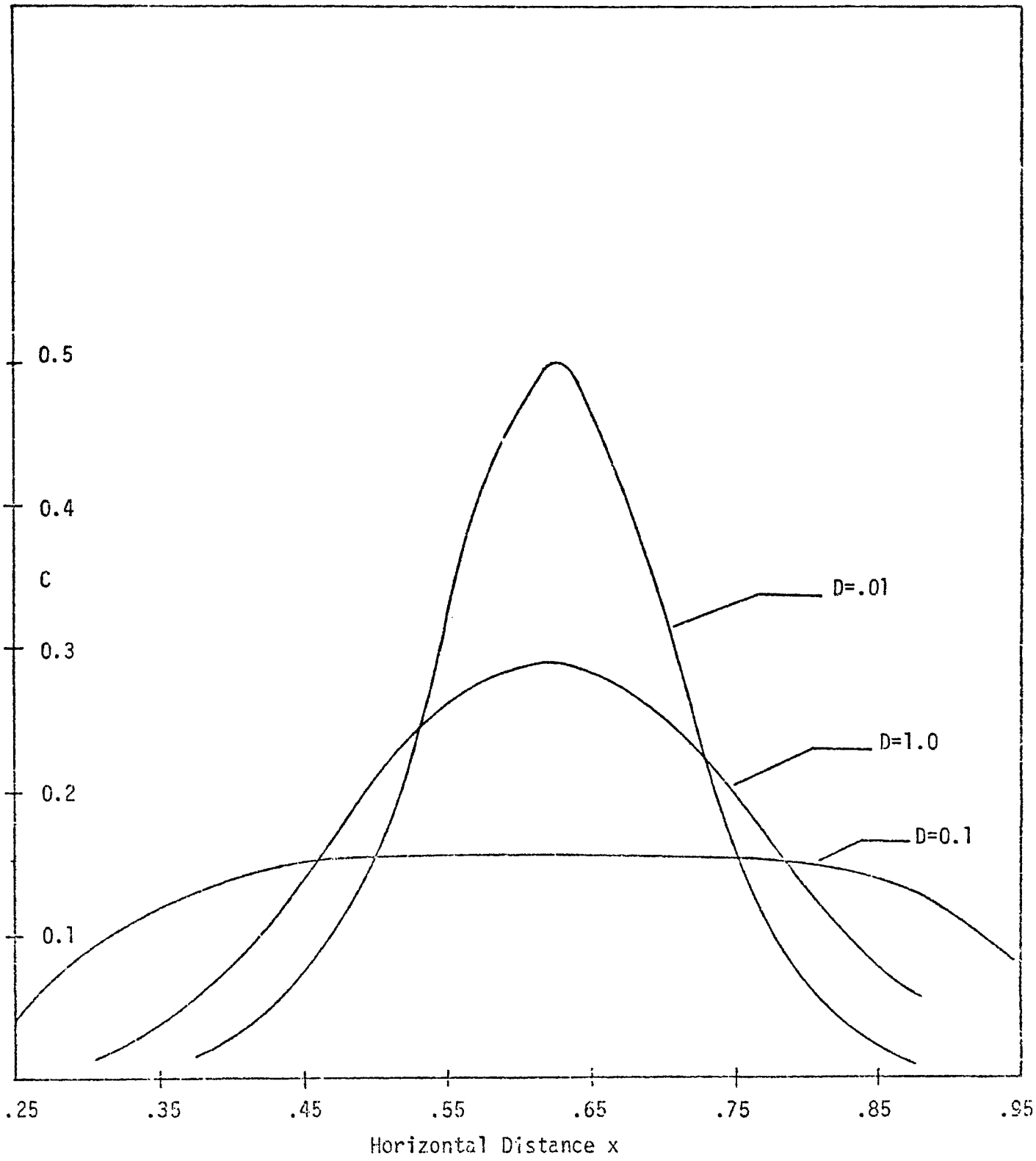

Figure 9.2: Concentration vs. Horizontal Distance for the LINEAR Profile at Time t=2. Plots made at z=.5

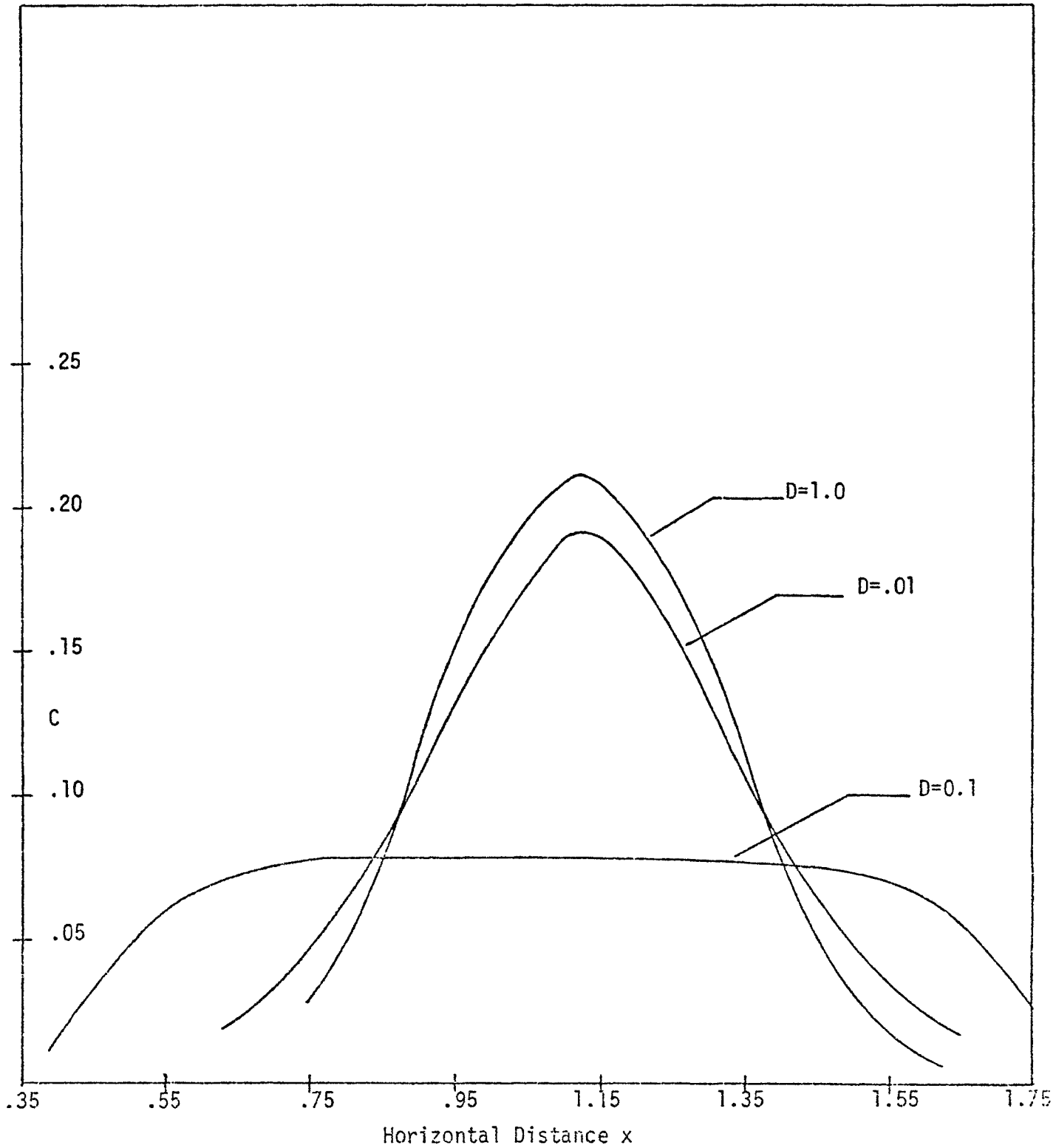

Figure 9.3: Concentration vs. Horizontal Distance for the LINEAR Profile at Time t=4. Plots made at z=.5

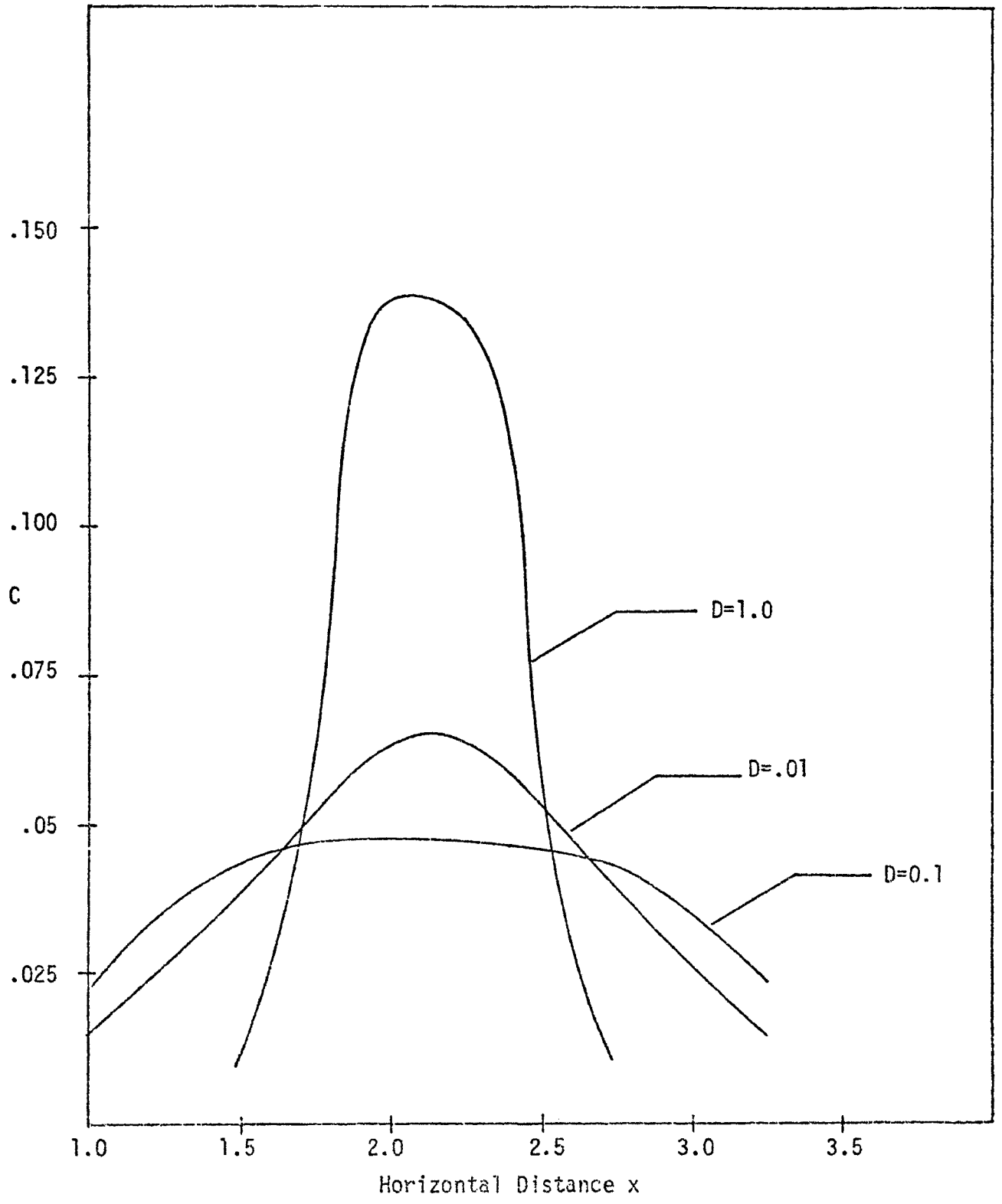

Figure 9.4: Concentration vs. Horizontal Distance for the LINEAR Profile at Time t=7. Plots made at z=.5

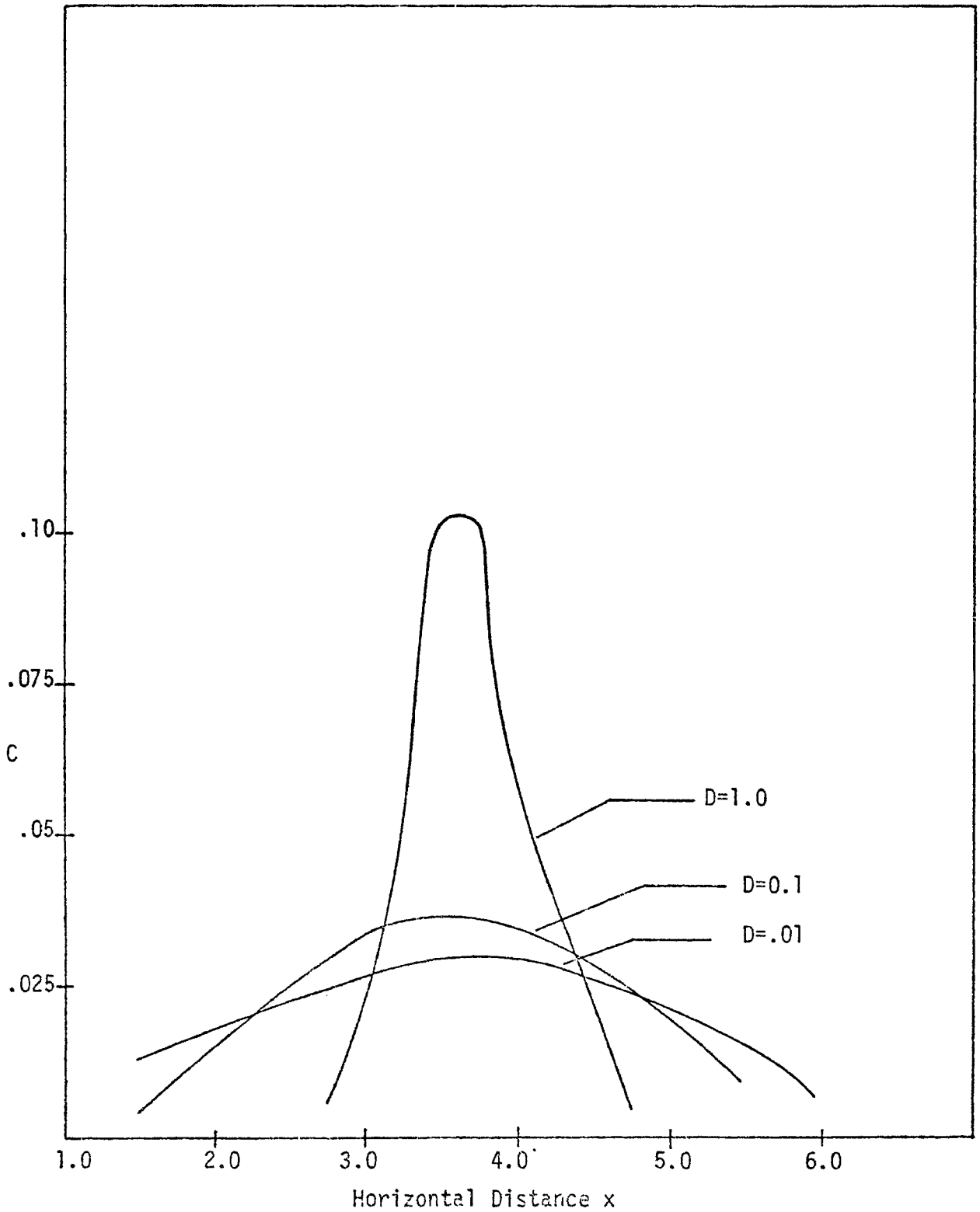

Figure 10.1: Concentration vs. Horizontal Distance for the LAKE Profile at Time t=1

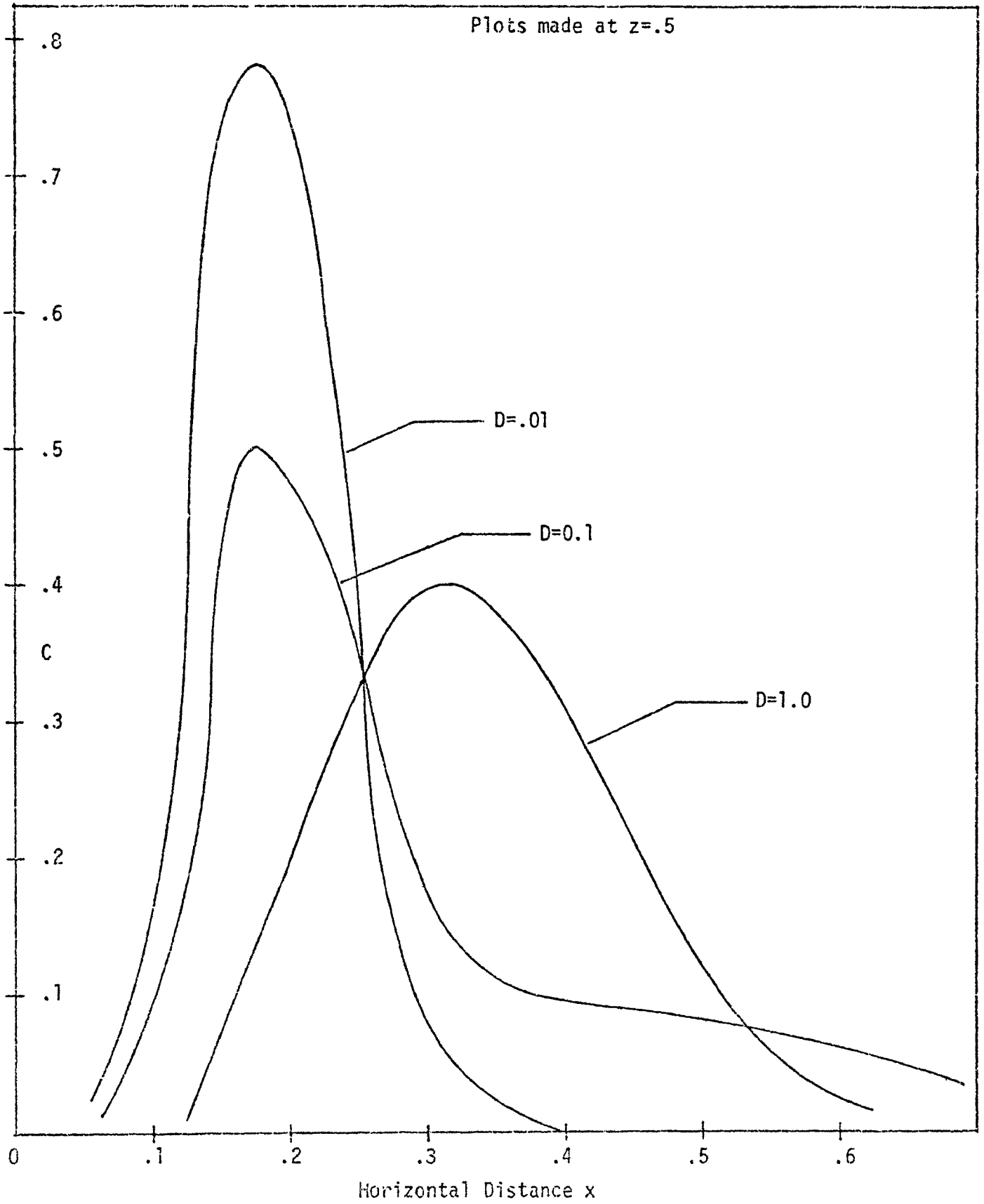

Figure 10.2: Concentration vs. Horizontal Distance for the LAKE Profile at Time t=2

Plots made at z=.5

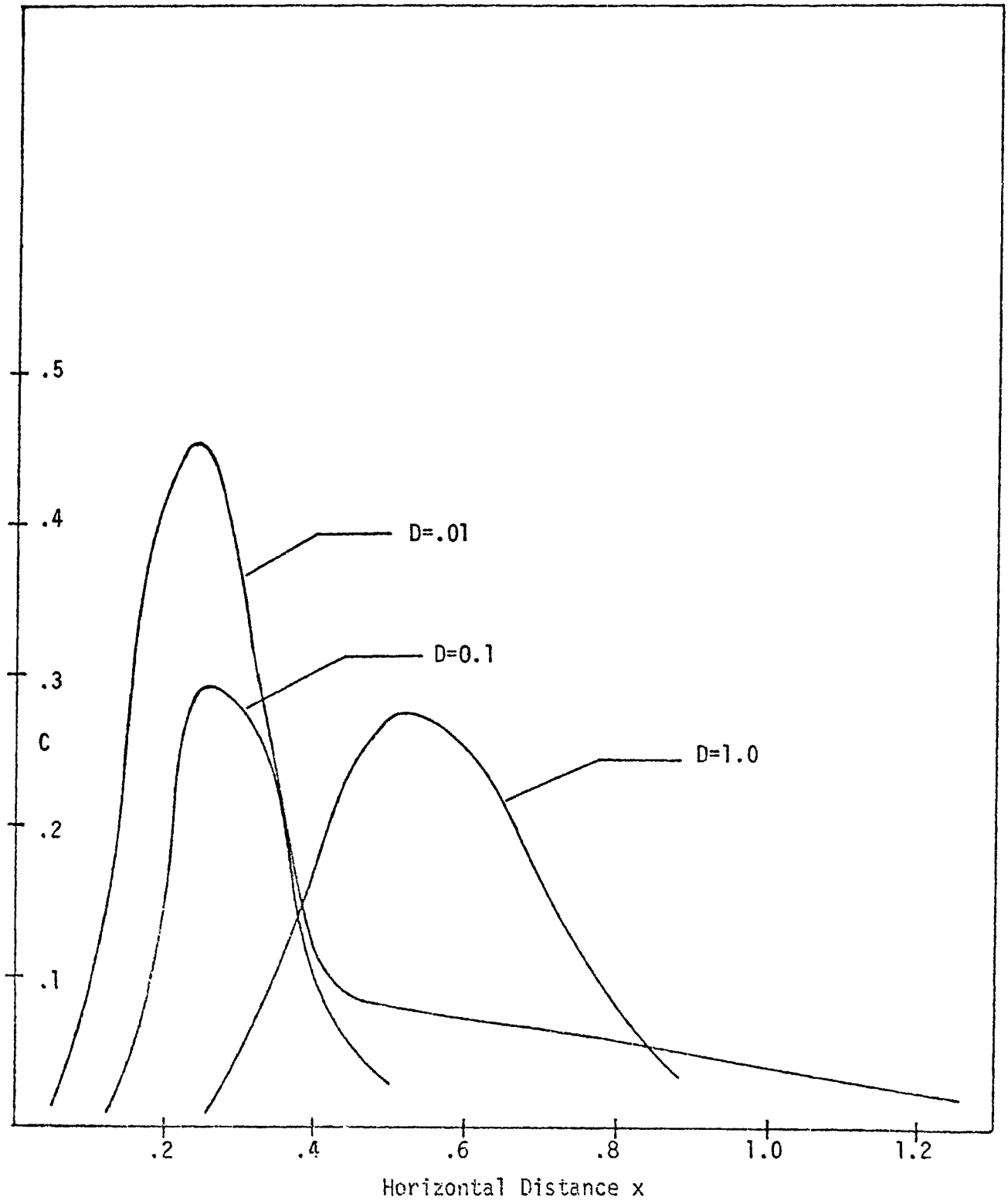

Figure 10.3: Concentration vs. Horizontal Distance for the LAKE Profile at Time t=4

Plots made at z=.5

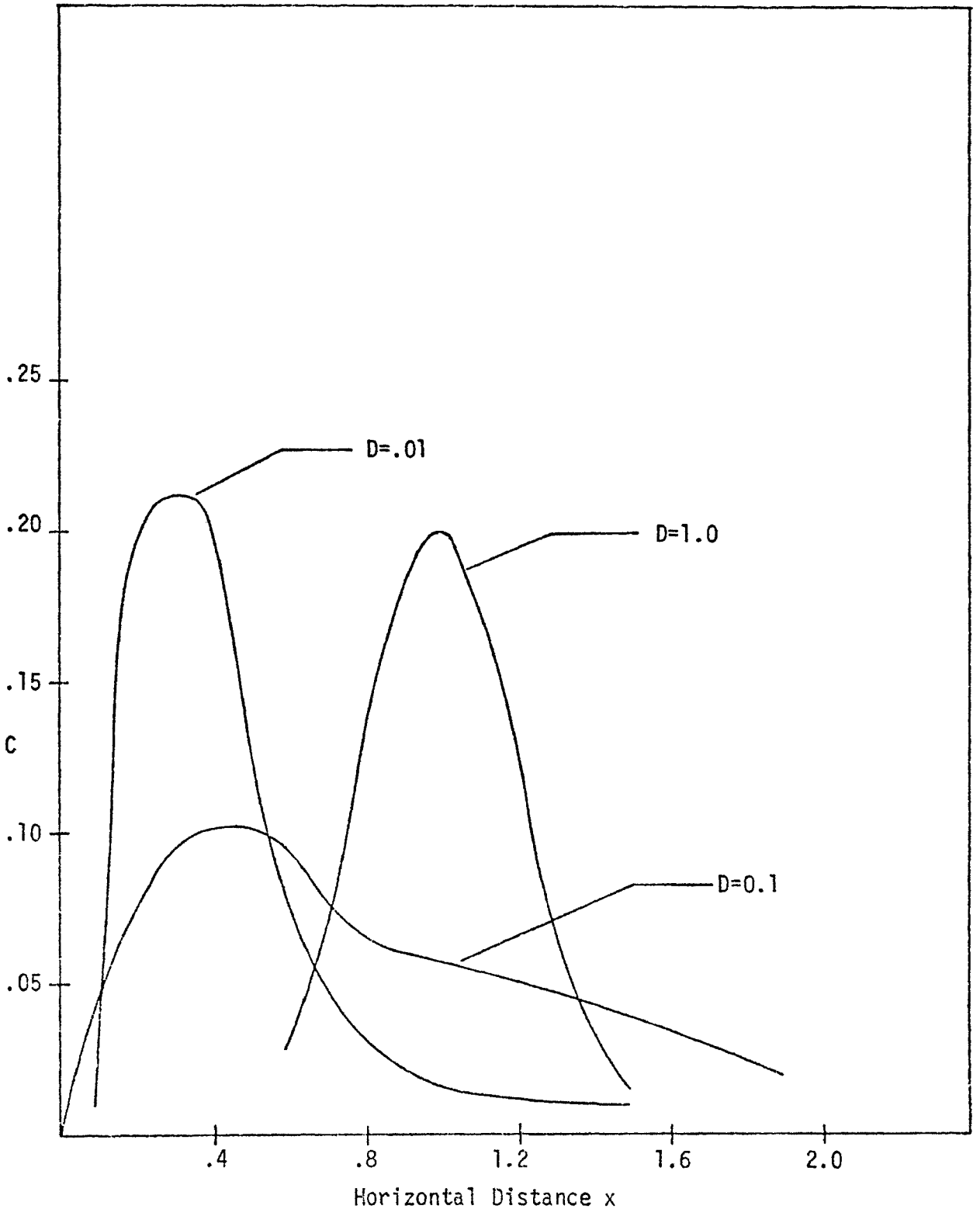

Figure 10.4: Concentration vs. Horizontal Distance for the LAKE Profile at Time t=6

Plots made at z=.5

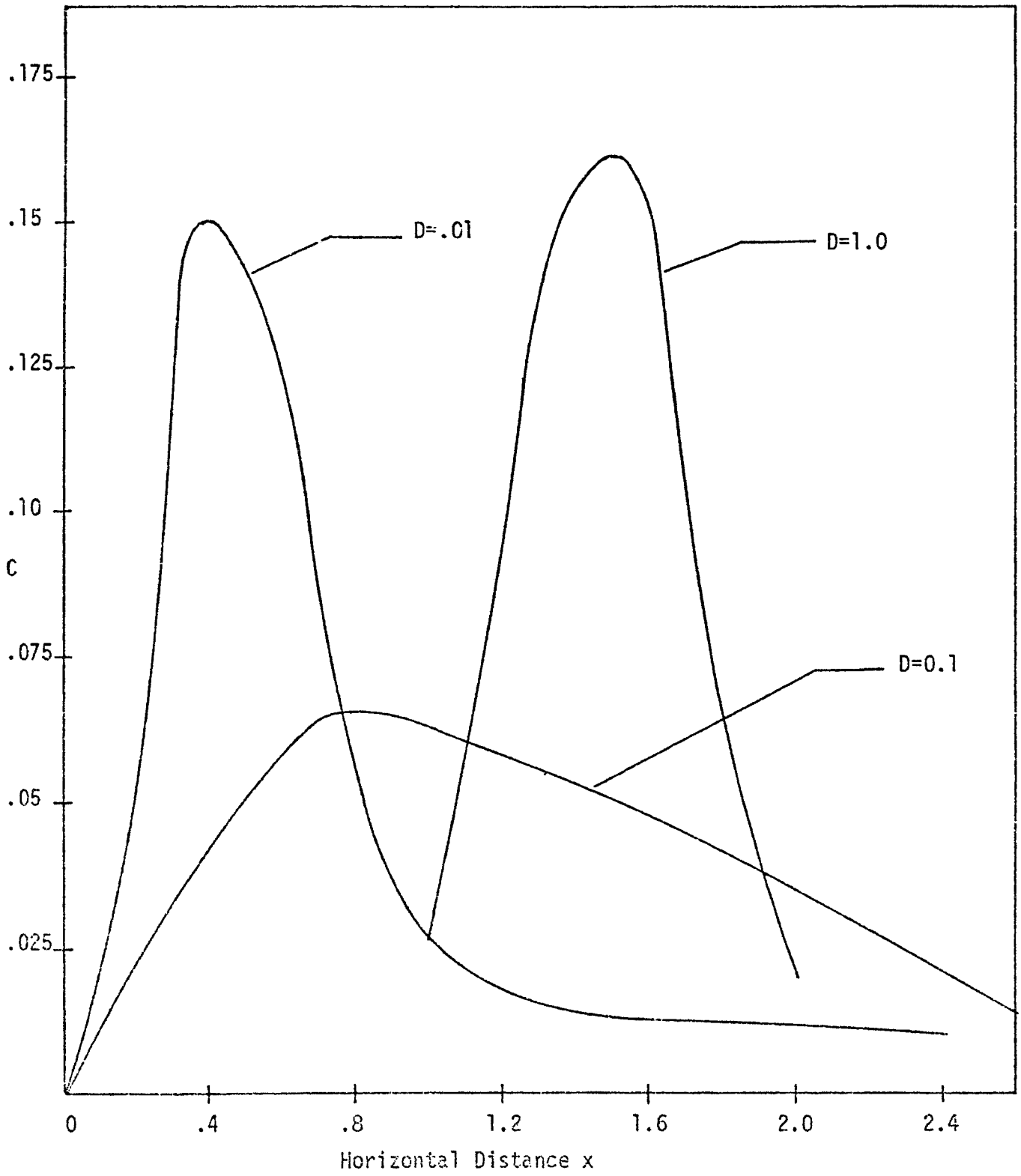

Figure II.1: Concentration vs. Vertical Distance for the LINEAR Profile at Time t=1

Plots made at x_m=.625

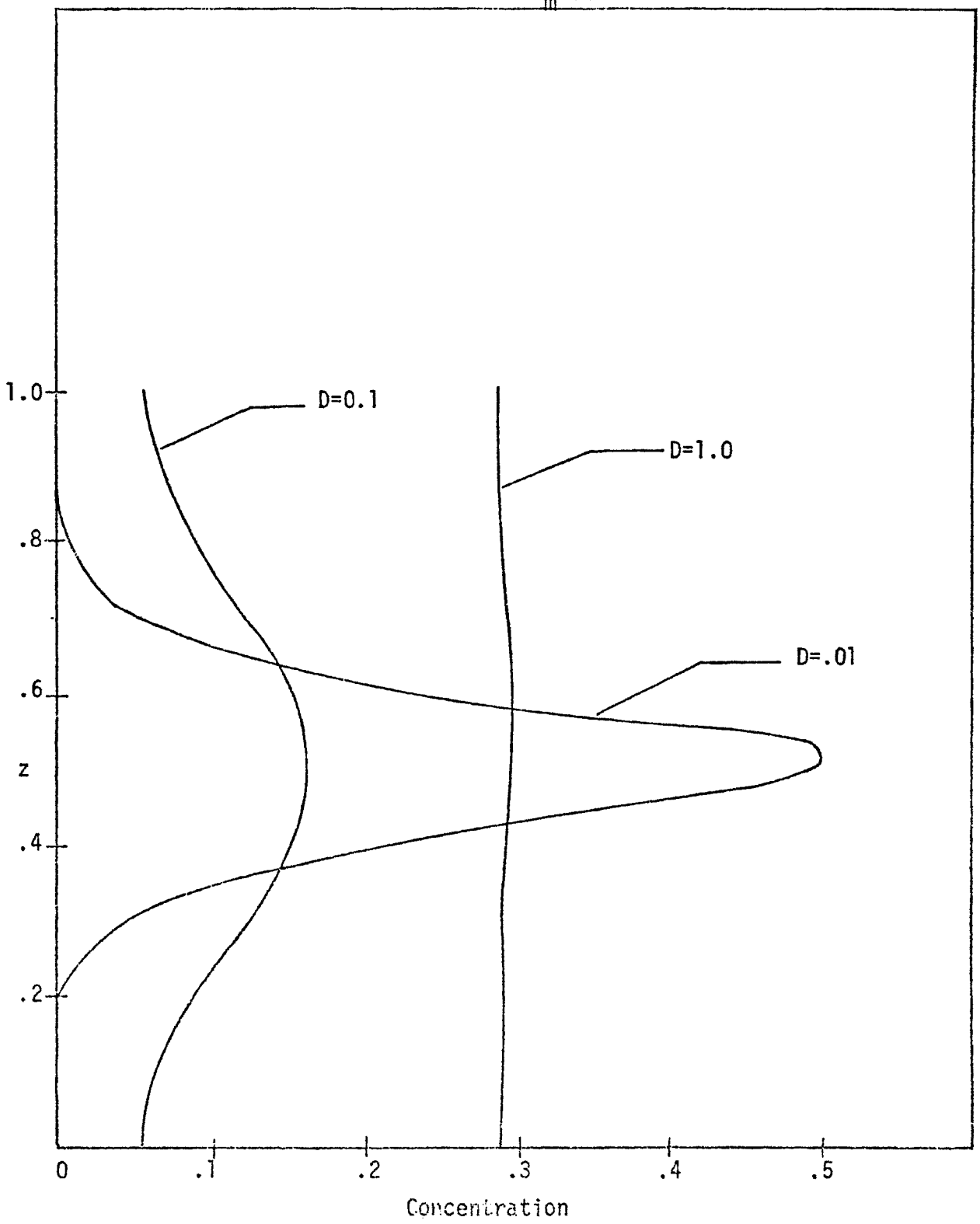

Figure 11.2: Concentration vs. Vertical Distance for the LINEAR Profile at Time t=1. Plots made at x_ℓ=.5.

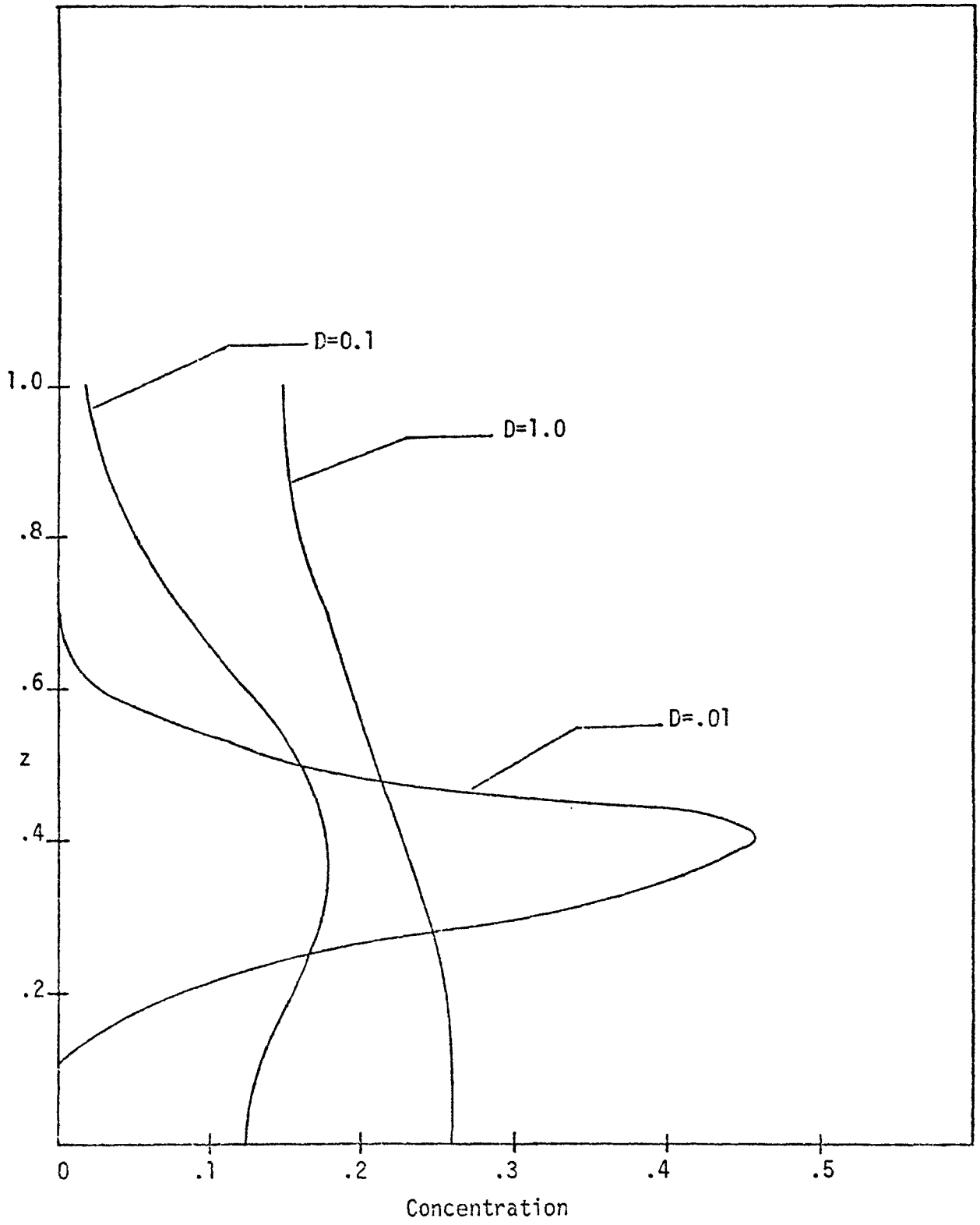

Figure 11.3: Concentration vs. Vertical Distance for the LINEAR Profile at Time t=1. Plots made at x_r=.75

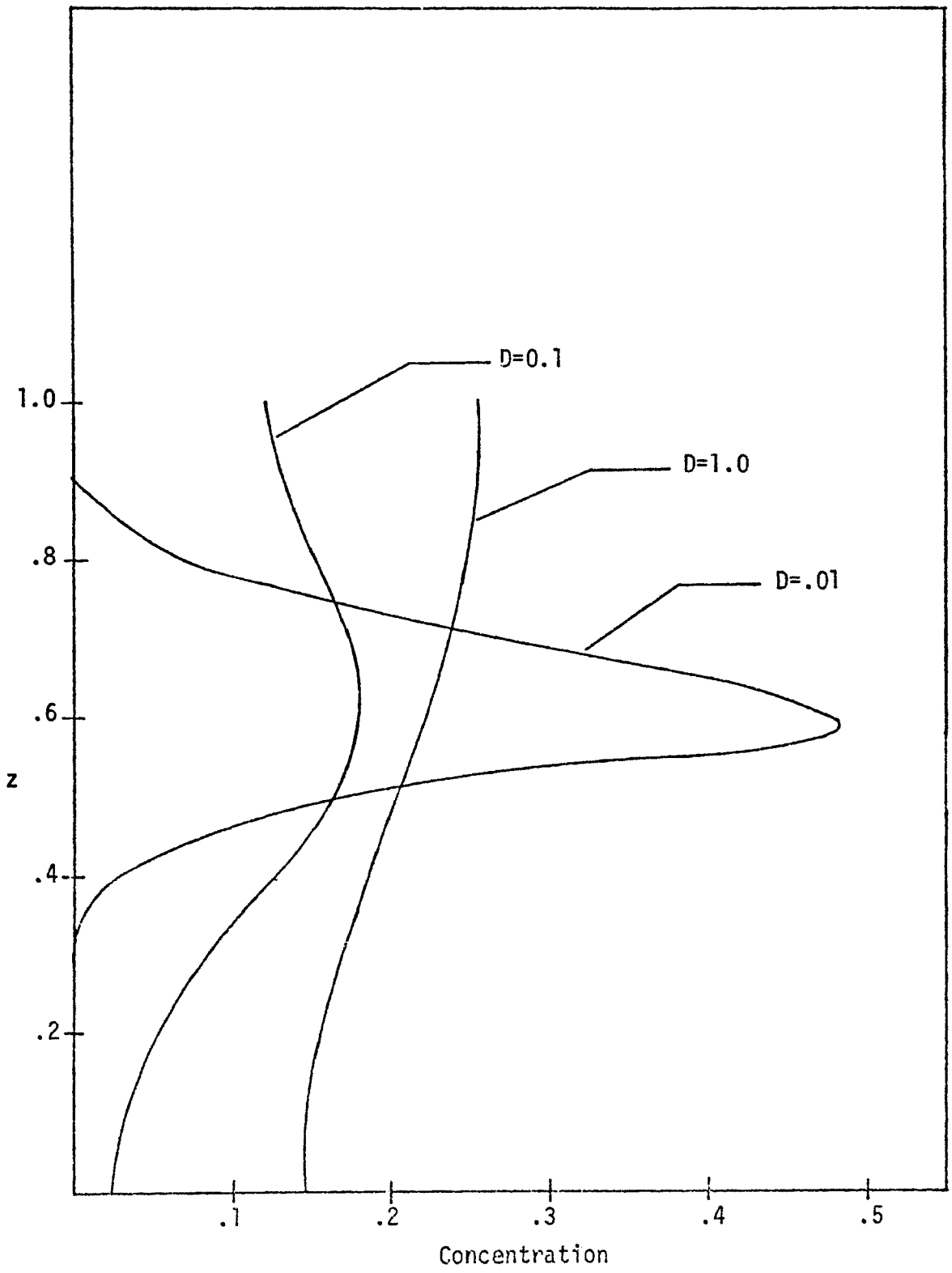

Figure 11.4: Concentration vs. Vertical Distance for the LINEAR Profile at Time t=2. Plots made at x_m=1.125

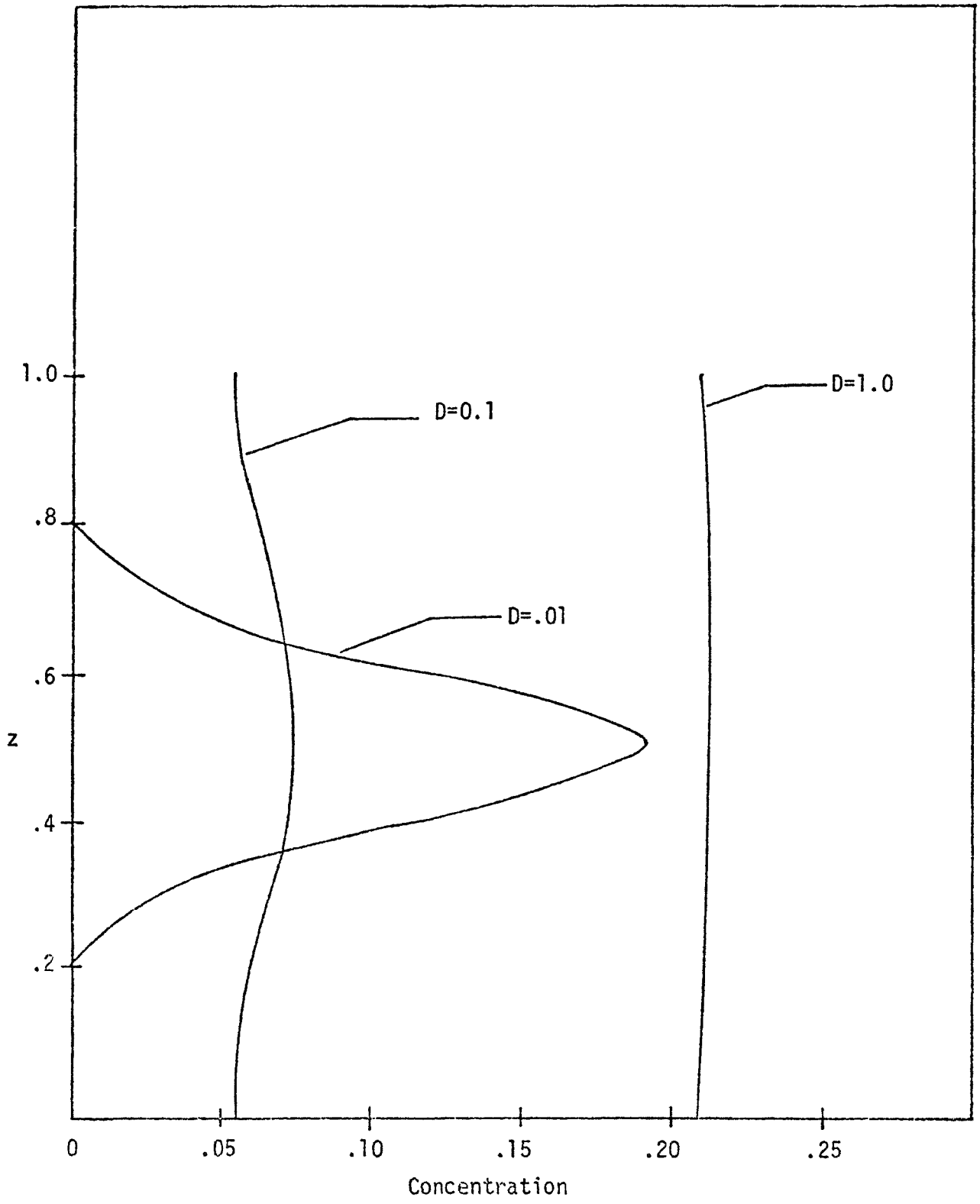

Figure 11.5: Concentration vs. Vertical Distance for the LINEAR Profile at Time t=2. Plots made at x_ℓ=.875

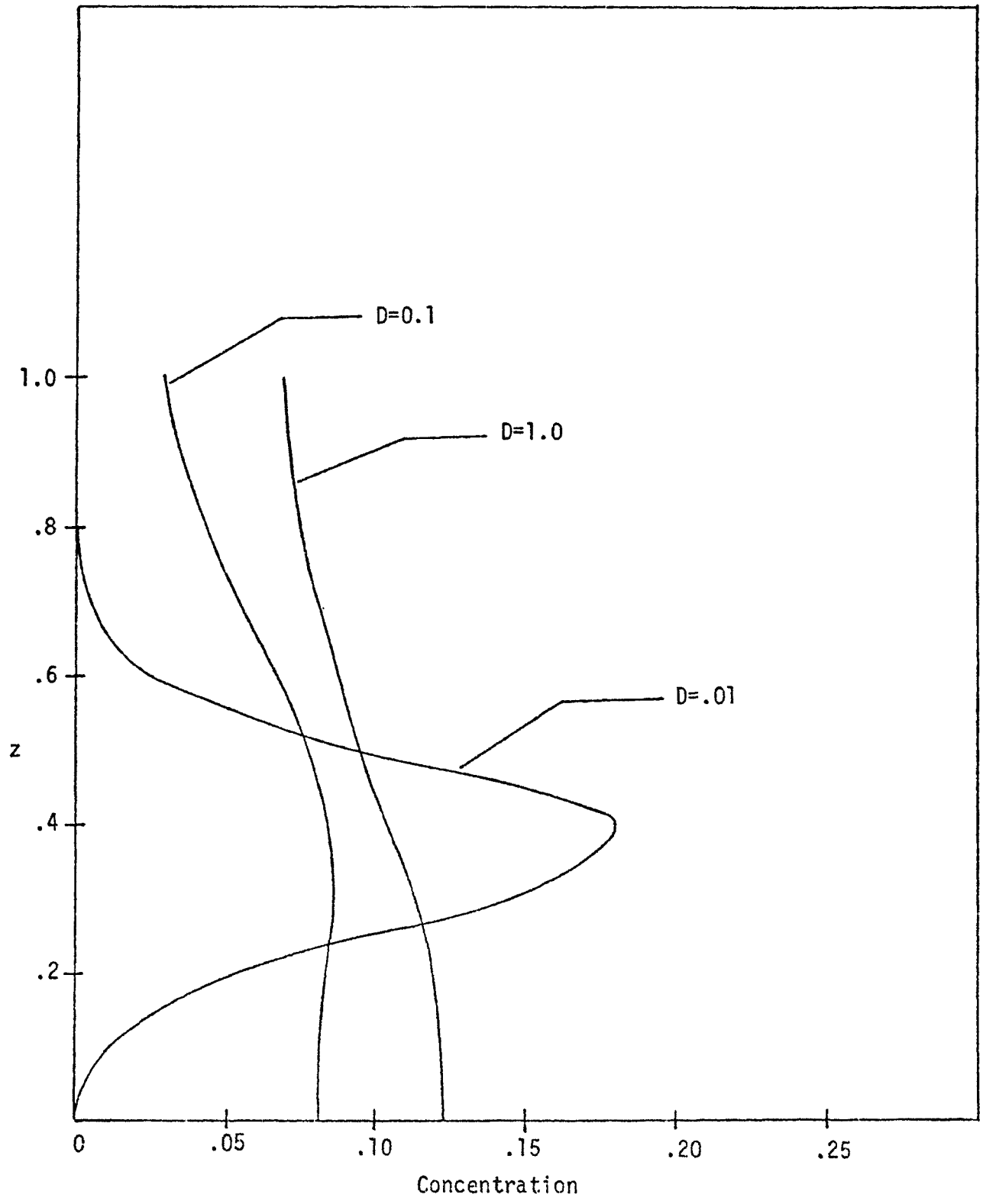

Figure 11.6: Concentration vs. Vertical Distance for the LINEAR Profile at Time t=4. Plots made at x_m=2.25

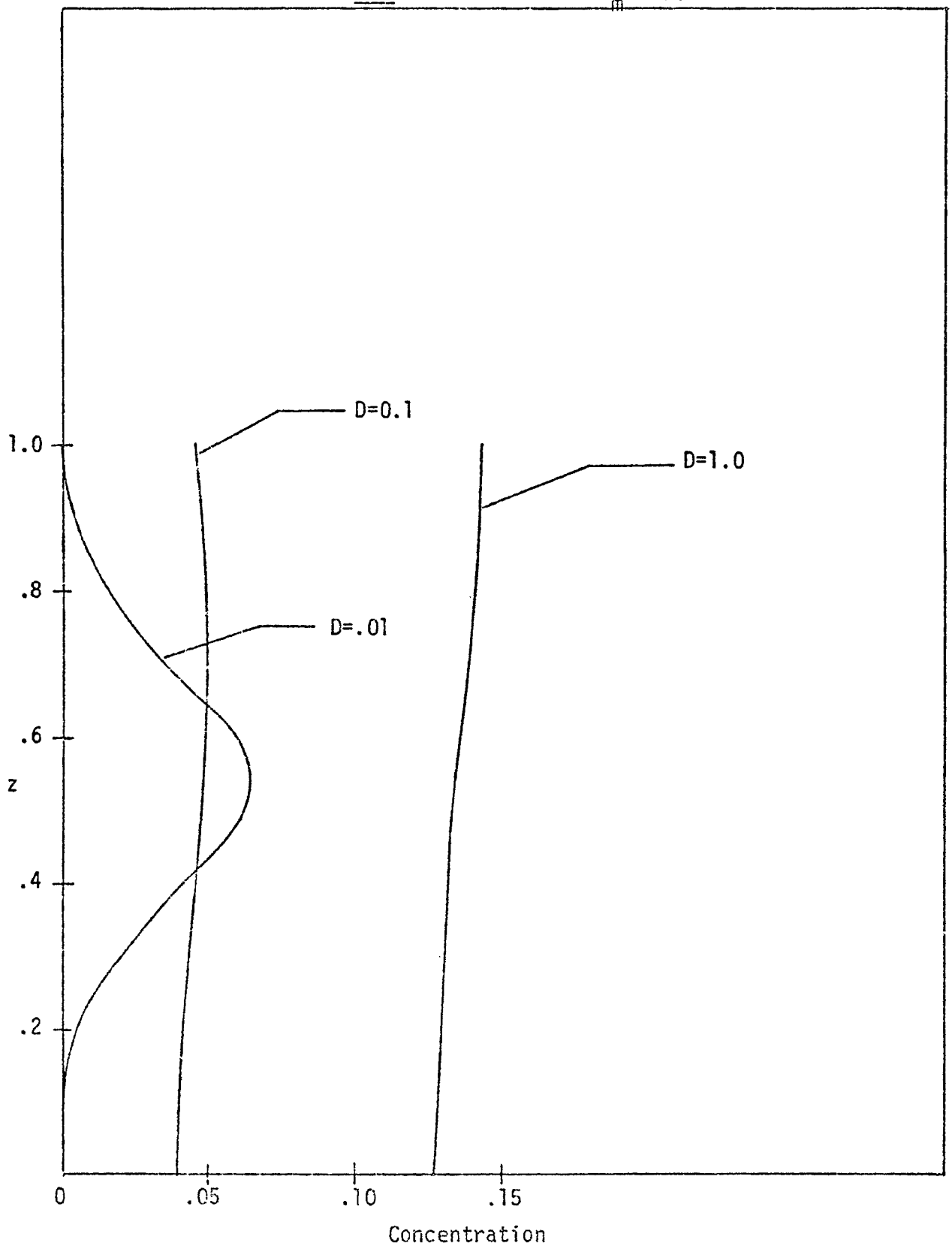

Figure 11.7: Concentration vs. Vertical Distance for the LINEAR Profile at Time t=4. Plots made at x_ℓ=1.75

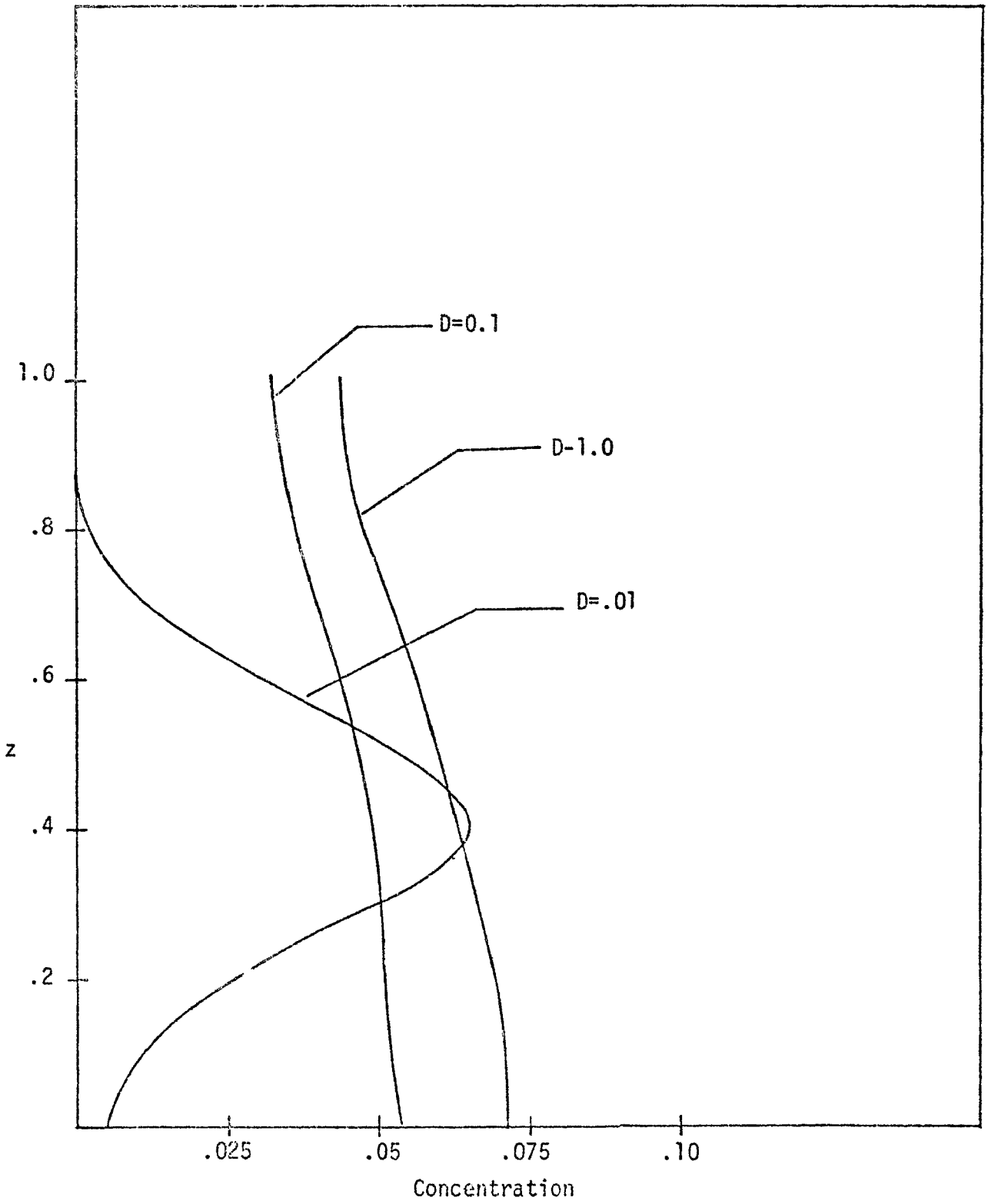

Figure 11.8: Concentration vs. Vertical Distance for the LINEAR Profile at Time t=7. Plots made at x_m=3.5

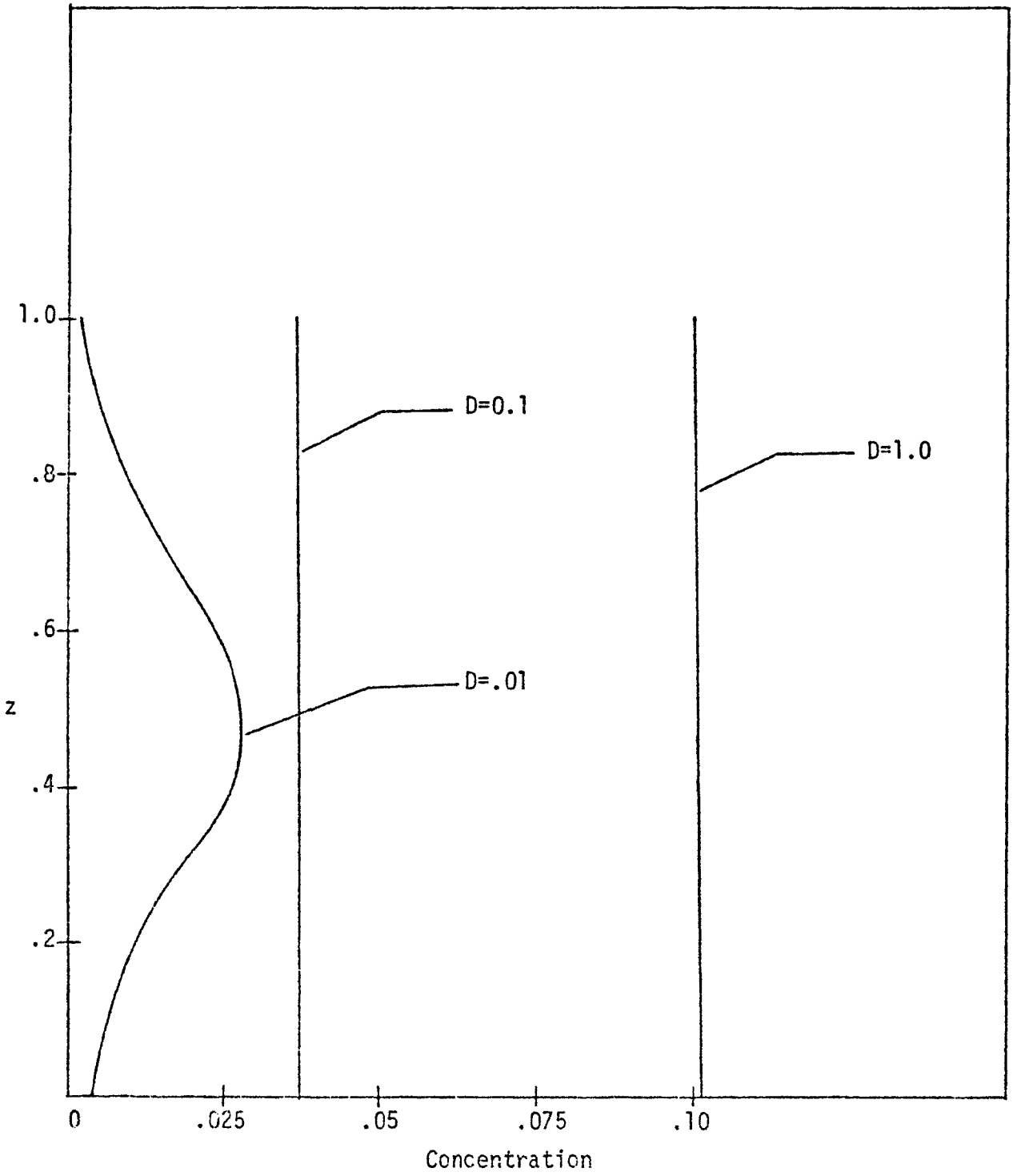

Figure 11.9: Concentration vs. Vertical Distance for the LINEAR Profile at Time t=7. Plots made at x_ℓ=3.0

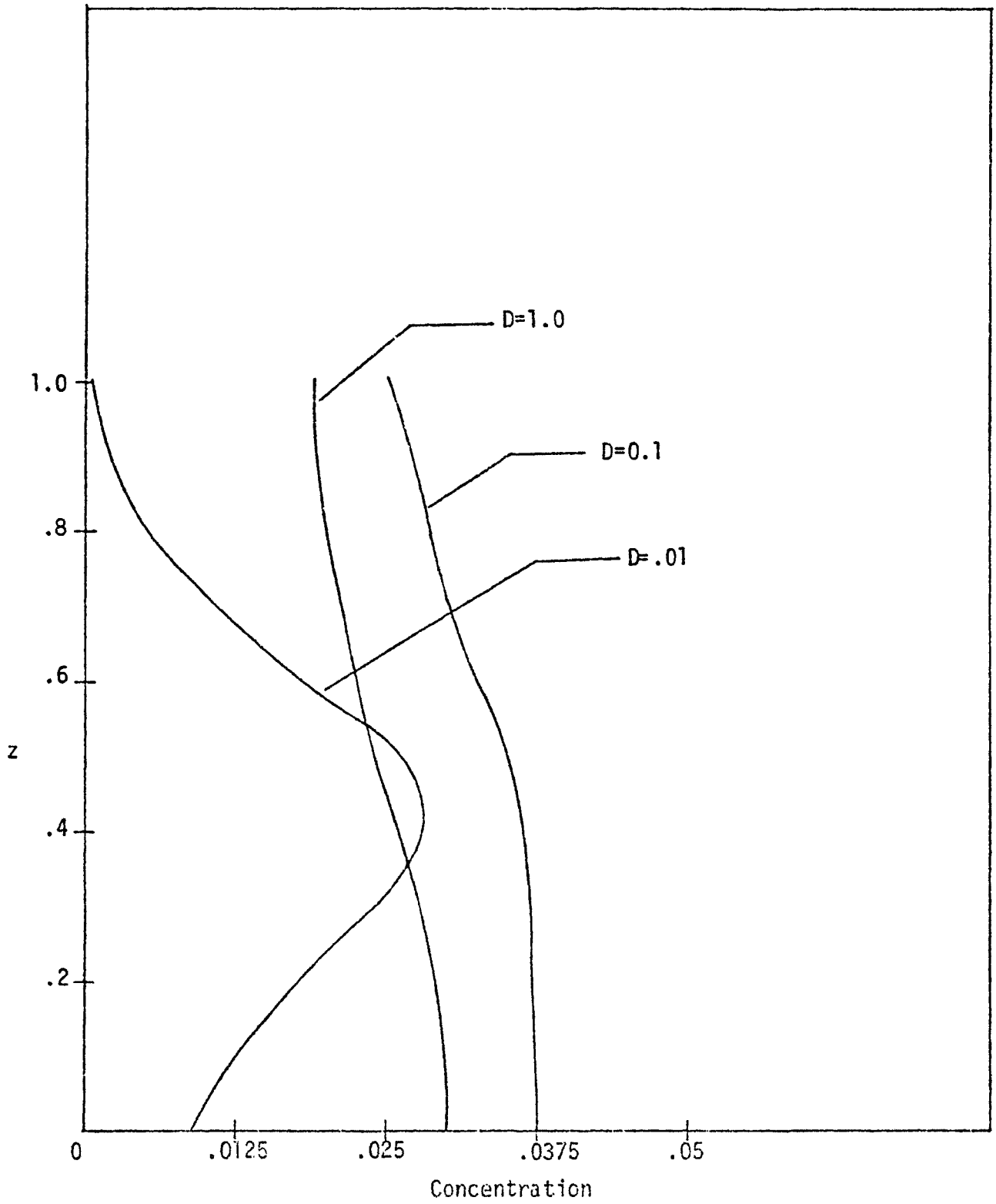

Figure 12.1: Concentration vs. Vertical Distance for the LAKE Profile at Time t=1. Plots made for D=.01

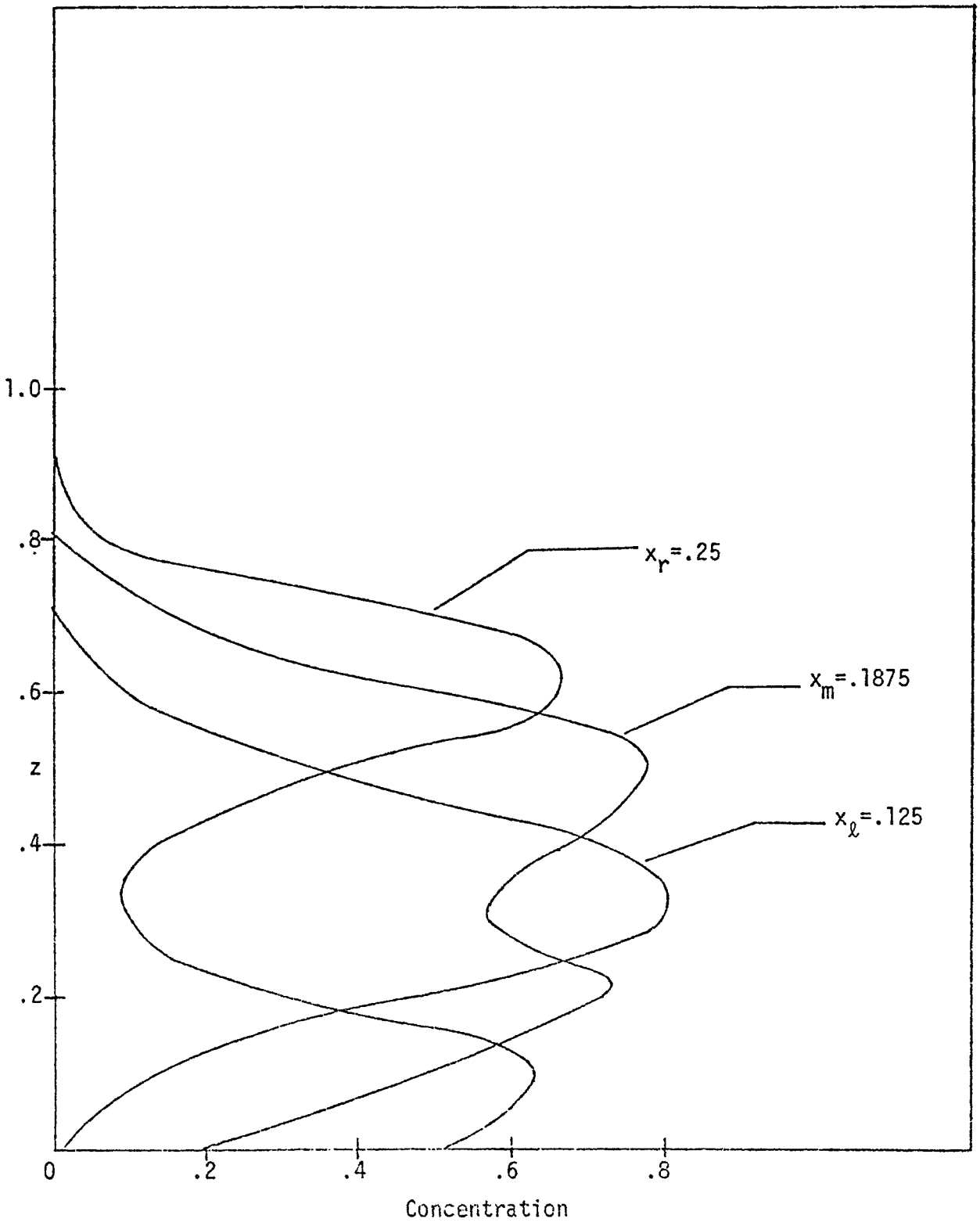

Figure 12.2: Concentration vs. Vertical Distance for the LAKE Profile at Time t=2. Plots made for D=.01

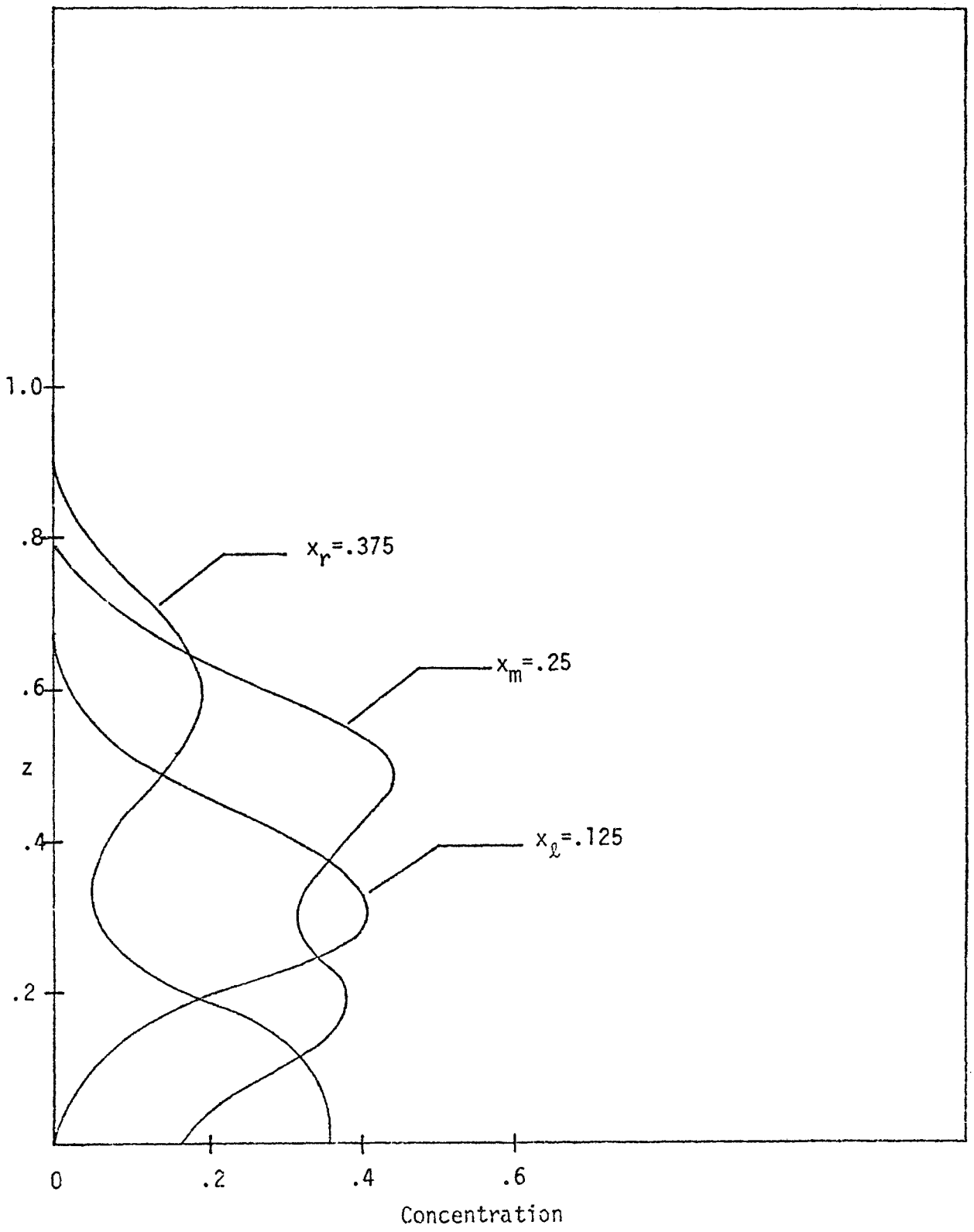

Figure 12.3: Concentration vs. Vertical Distance for the LAKE Profile at Time t=4. Plots made for D=.01

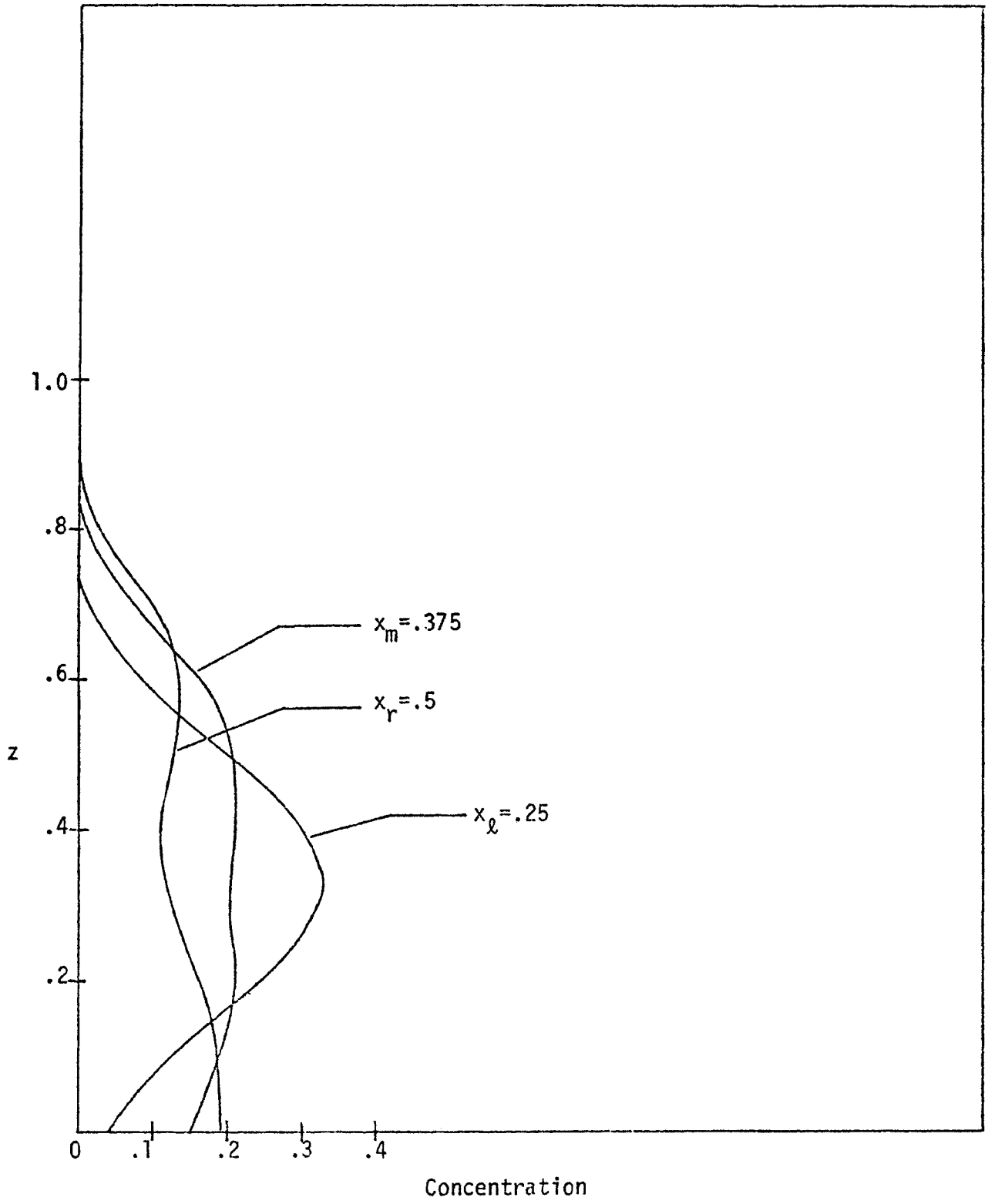

Figure 12.4: Concentration vs. Vertical Distance for the LAKE Profile at Time t=6. Plots made for D=.01

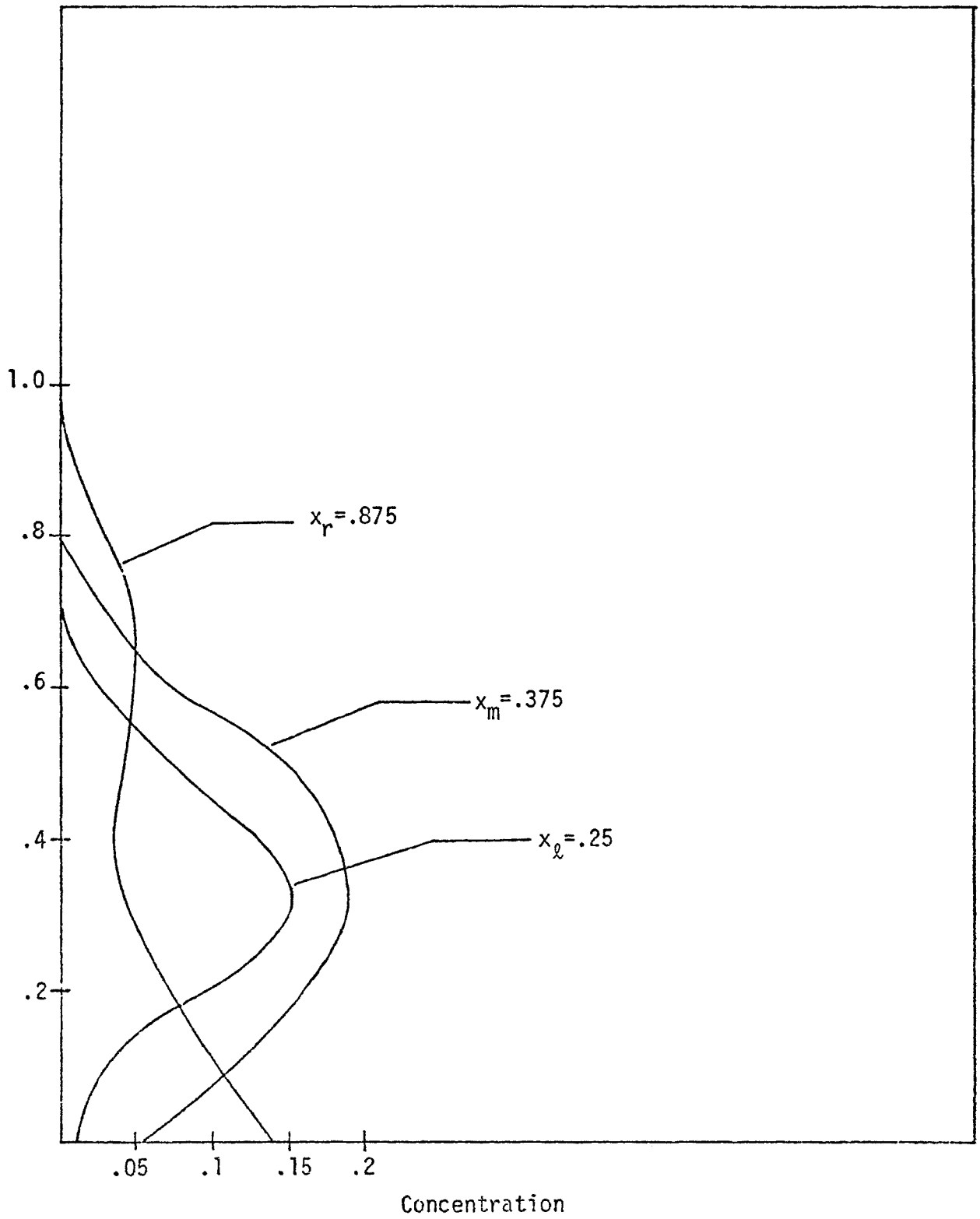

Figure 12.5: Concentration vs. Vertical Distance for the LAKE Profile at Time t=1. Plots made for D=0.1

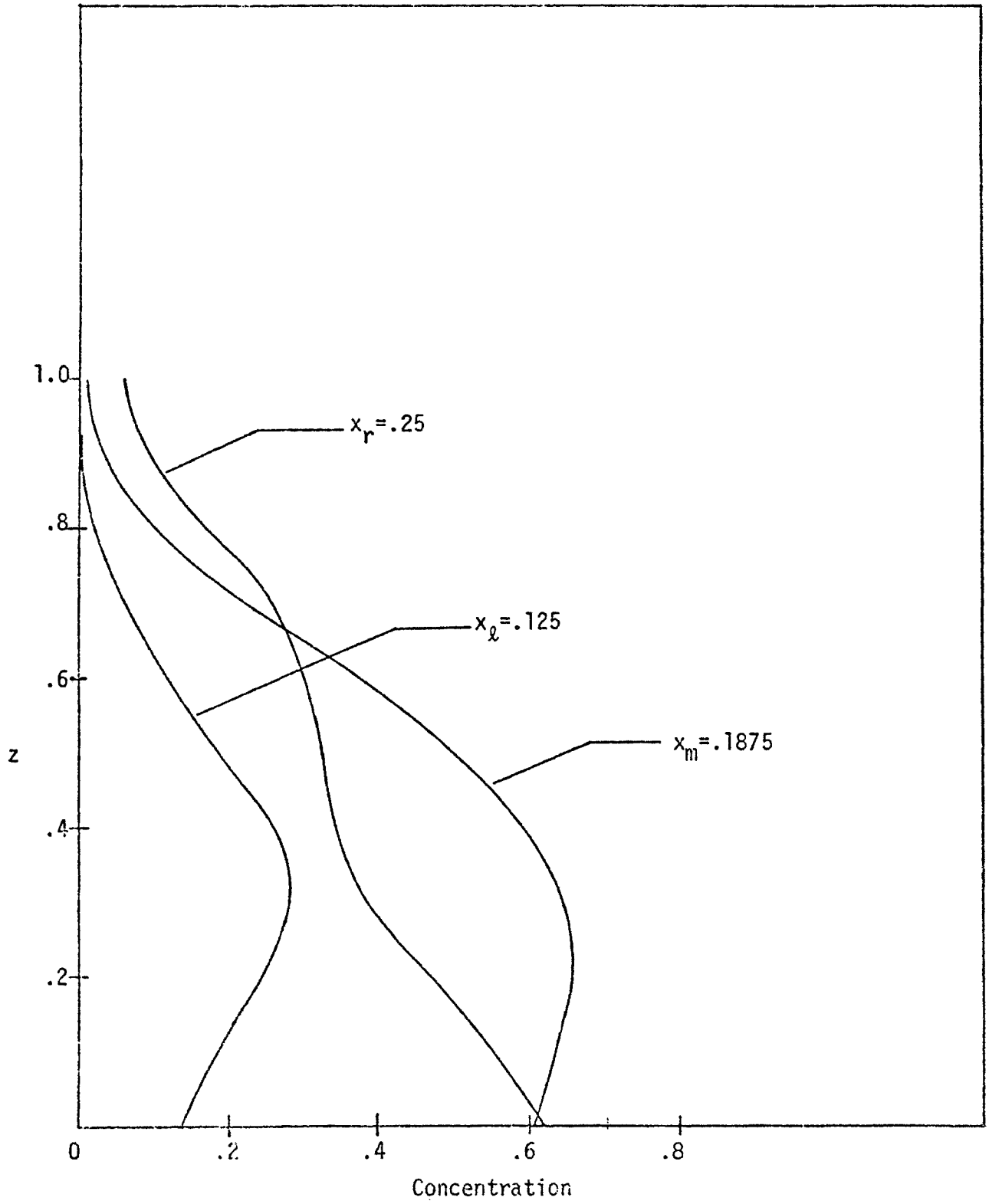

Figure 12.6: Concentration vs. Vertical Distance for the LAKE Profile at Time t=2. Plots made for D=0.1

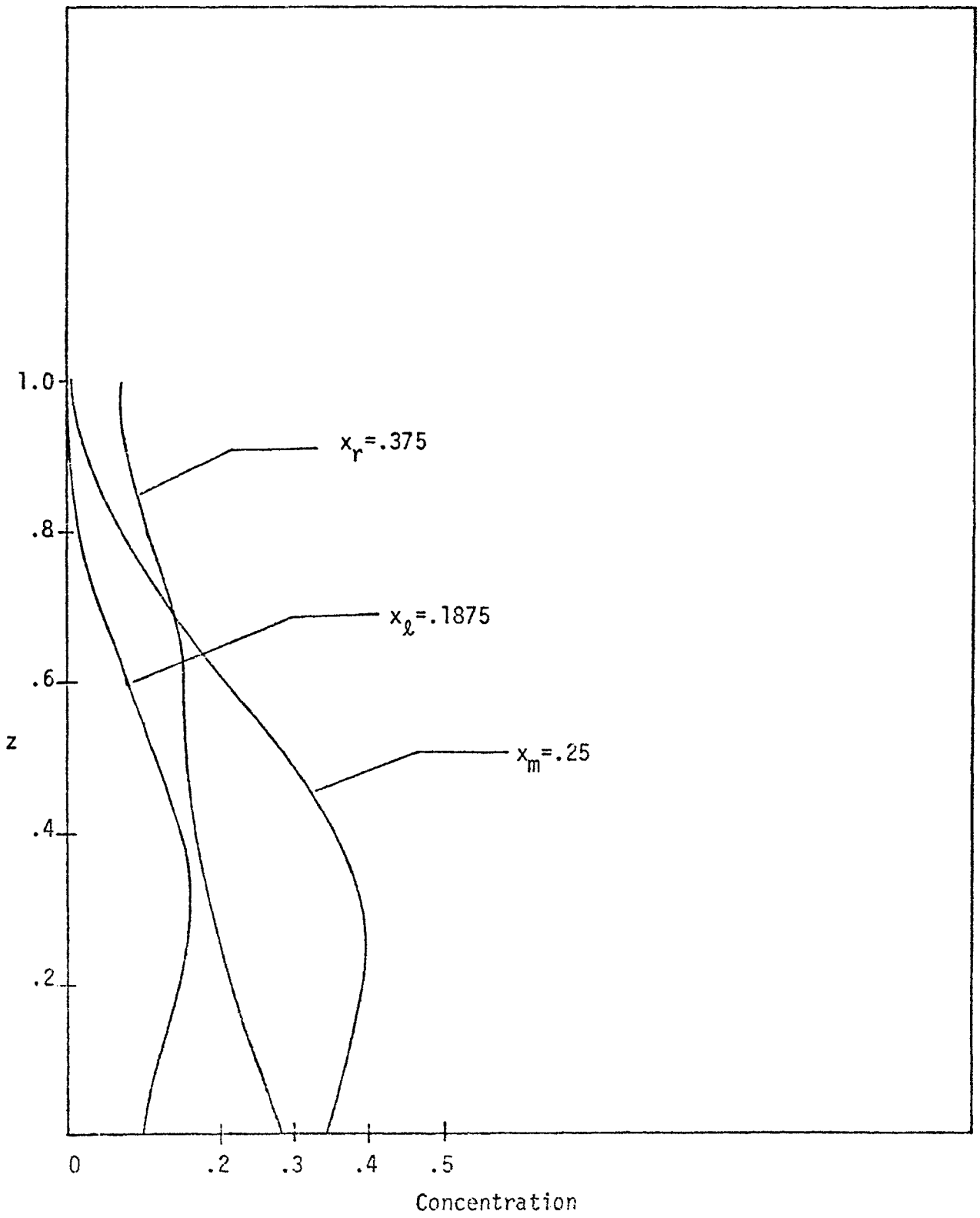

Figure 12.7: Concentration vs. Vertical Distance for the LAKE Profile at Time t=4. Plots made for D=0.1

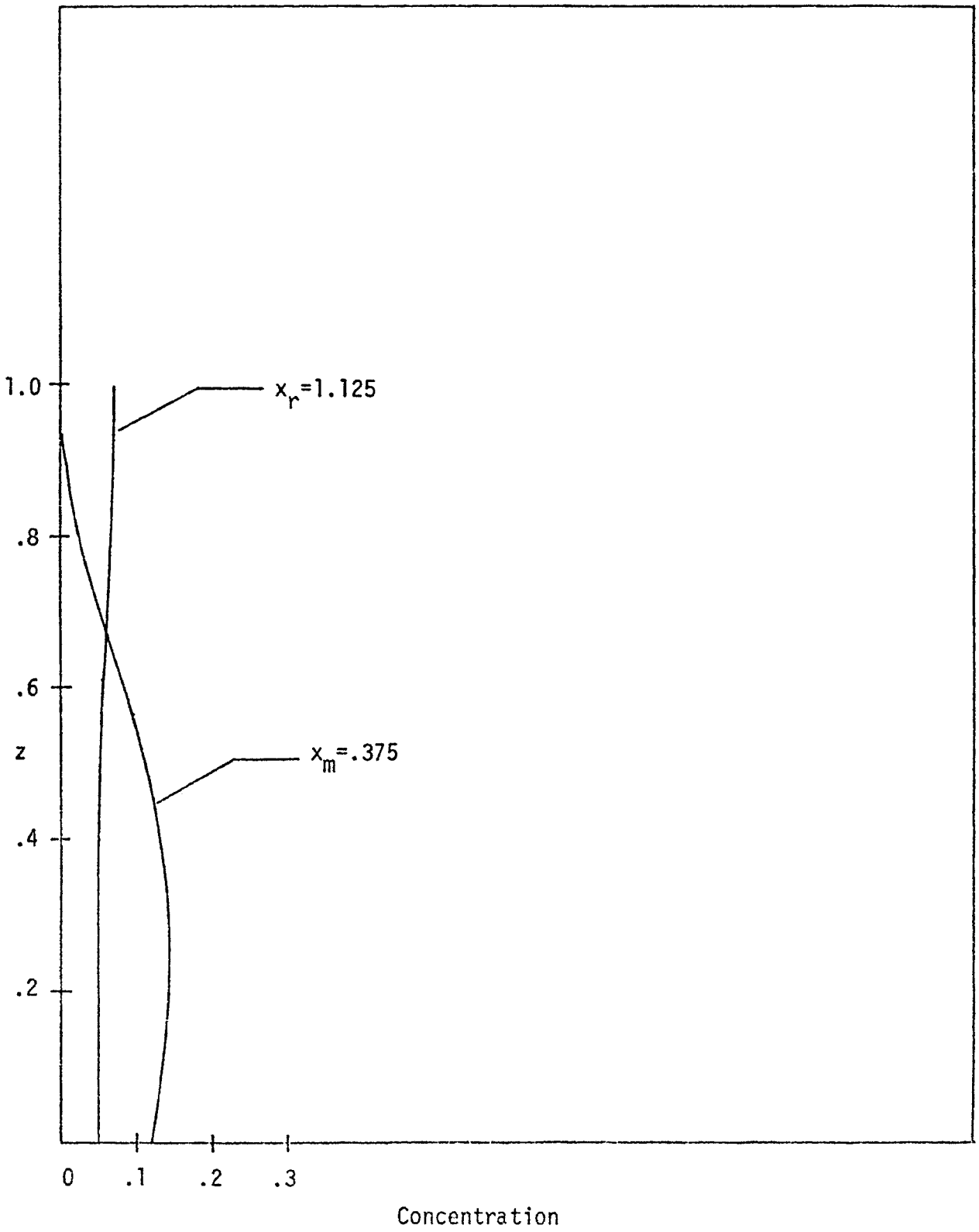

Figure 12.8: Concentration vs. Vertical Distance for the LAKE Profile at Time t=6. Plots made for D=0.1

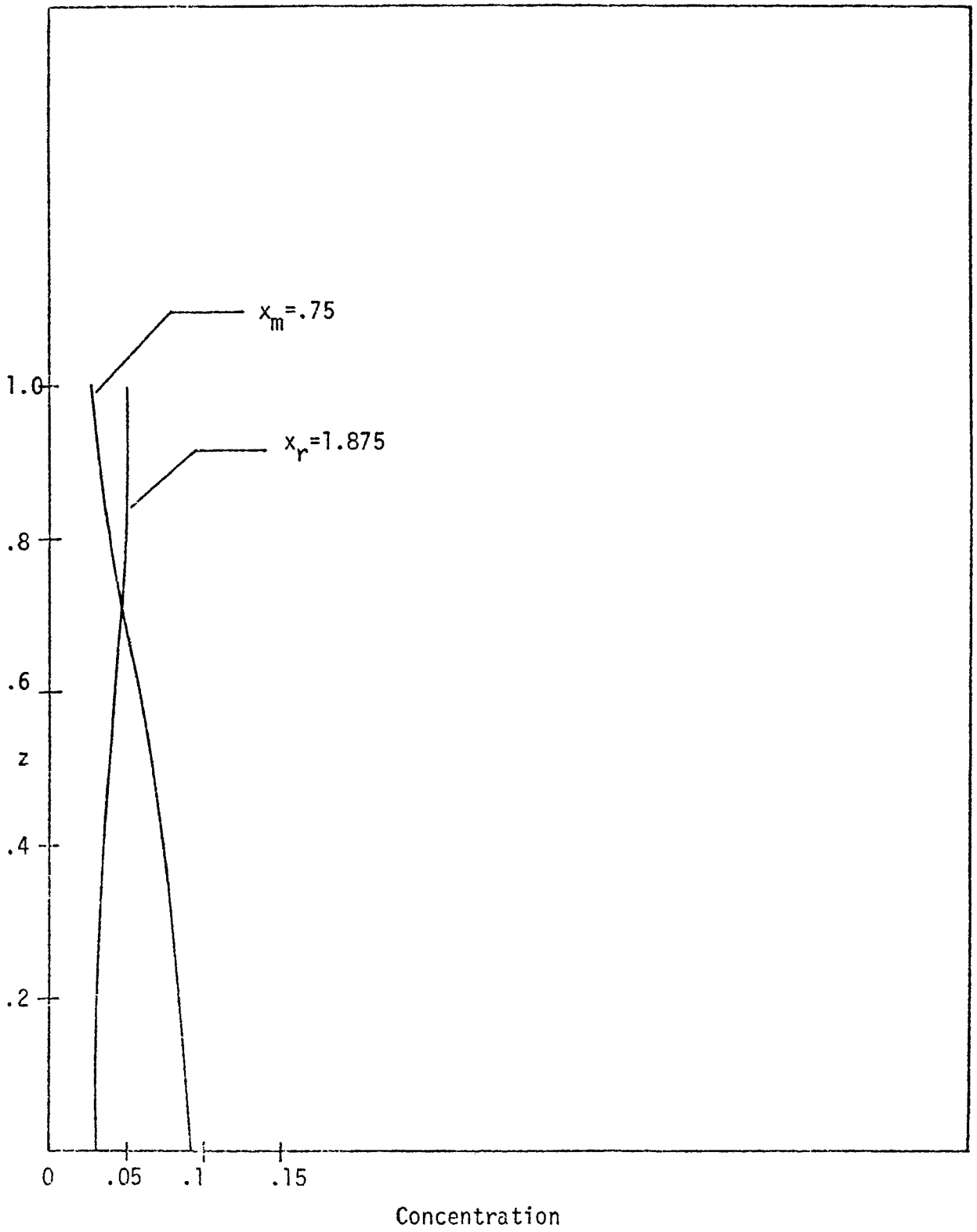

Figure 12.9: Concentration vs. Vertical Distance for the LAKE Profile at Time t=1. Plots made for D=1.0

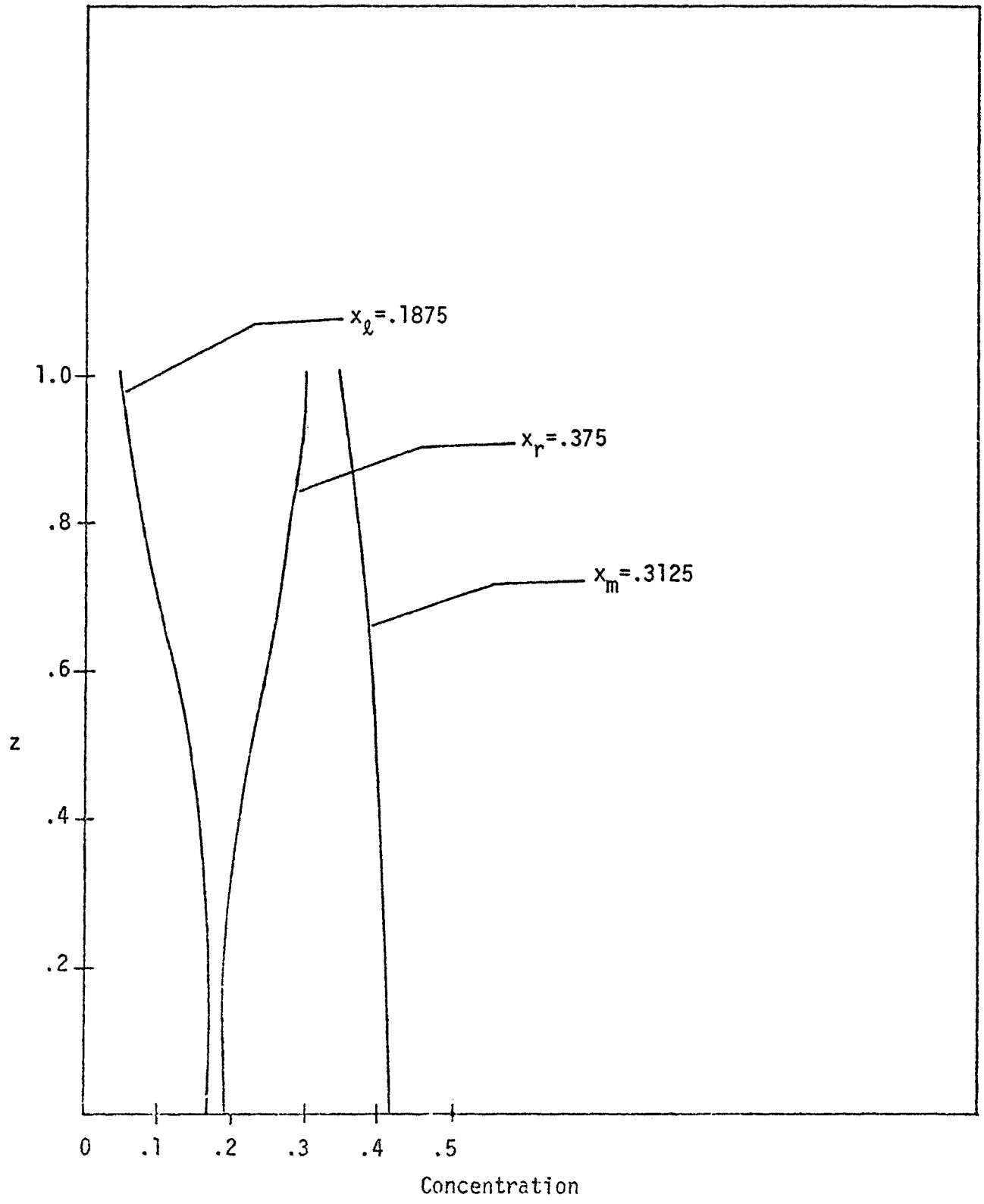

Figure 12.10: Concentration vs. Vertical Distance for the LAKE Profile at Time t=2. Plots made for D=1.0

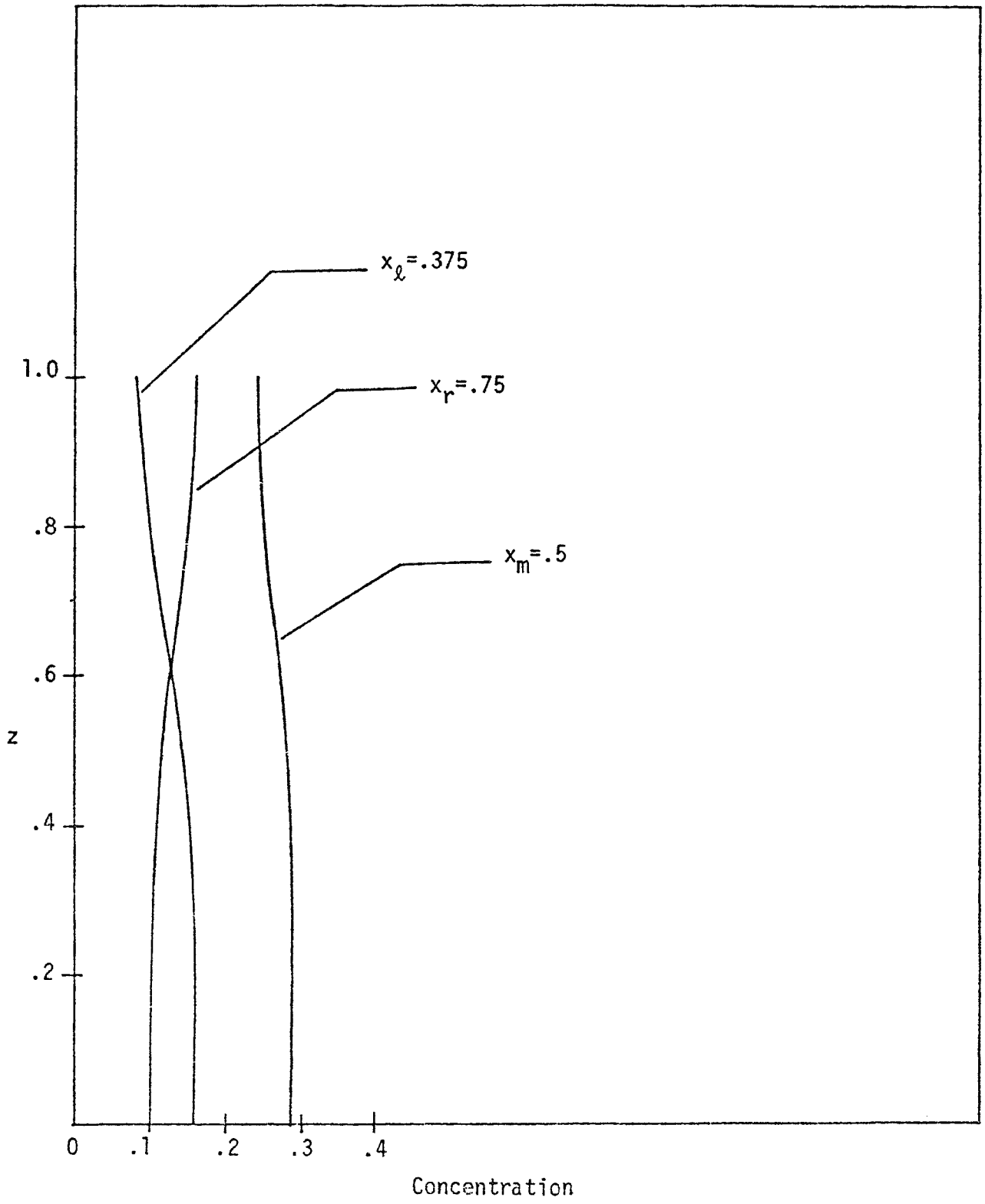

Figure 12.11: Concentration vs. Vertical Distance for the LAKE Profile at Time t=4. Plots made for D=1.0

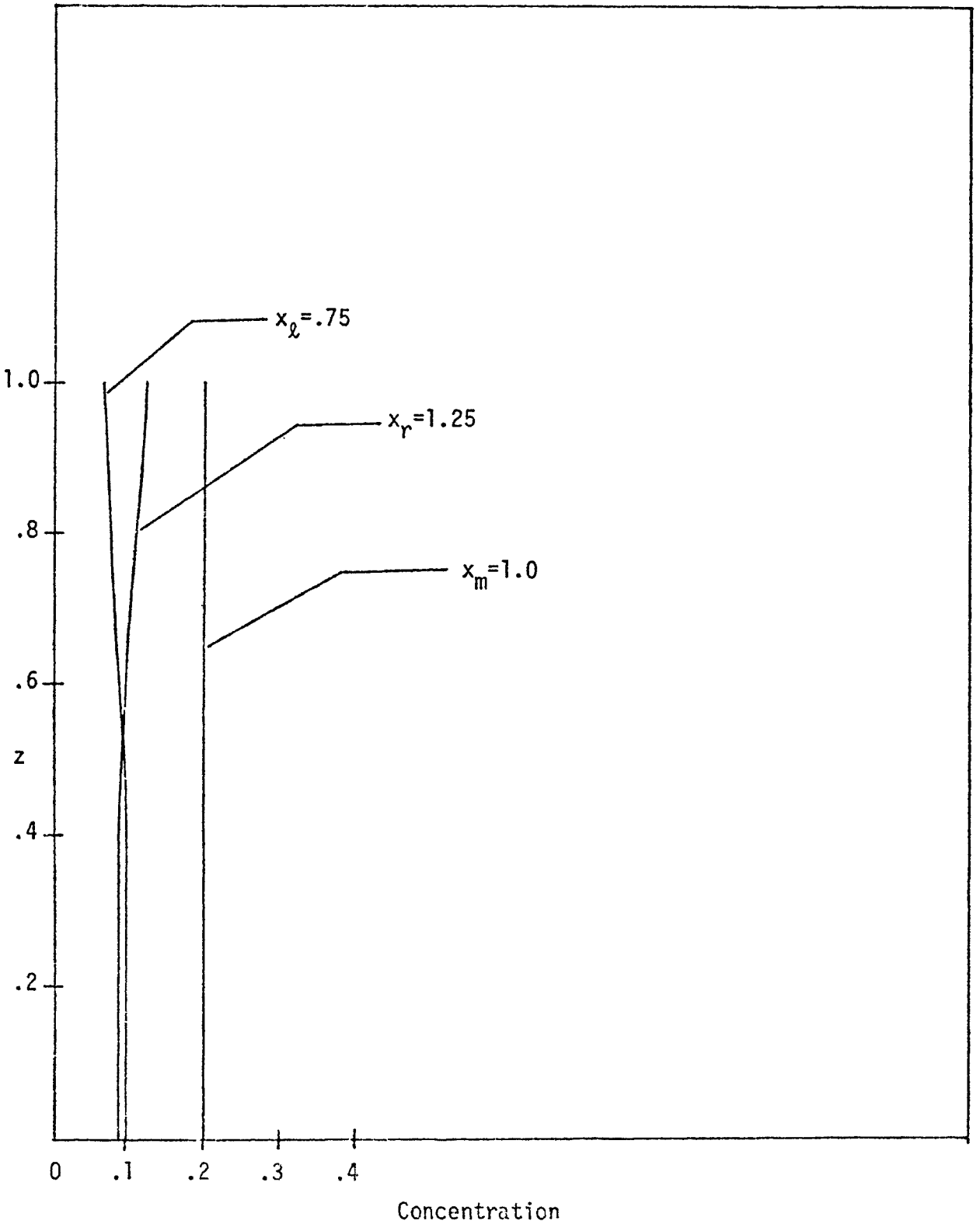

Figure 12.12: Concentration vs. Vertical Distance for the LAKE Profile at Time t=6. Plots made for D=1.0

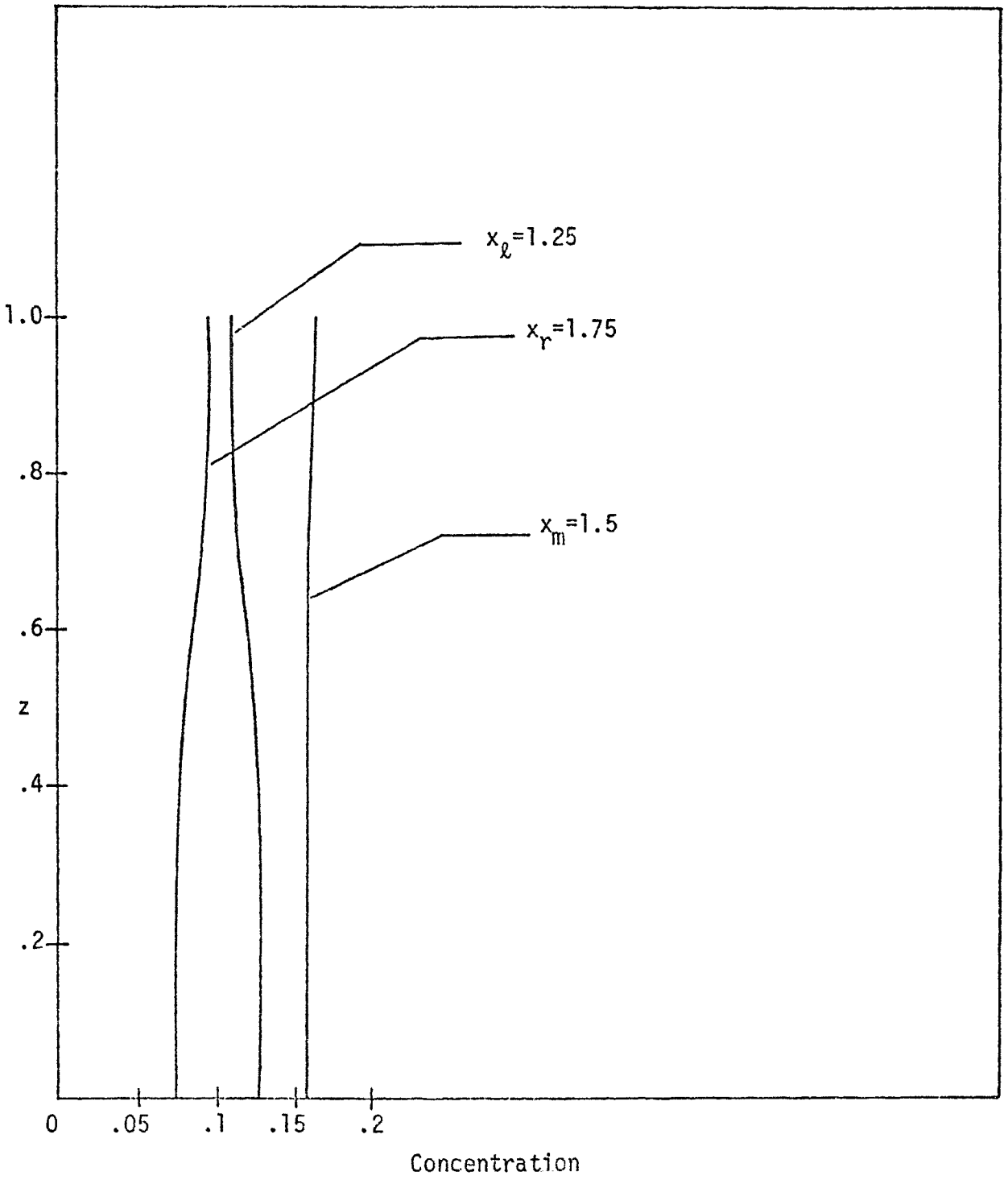

Figure 13.1: σ_x^2 vs. Time for the LINEAR Profile for D=.01

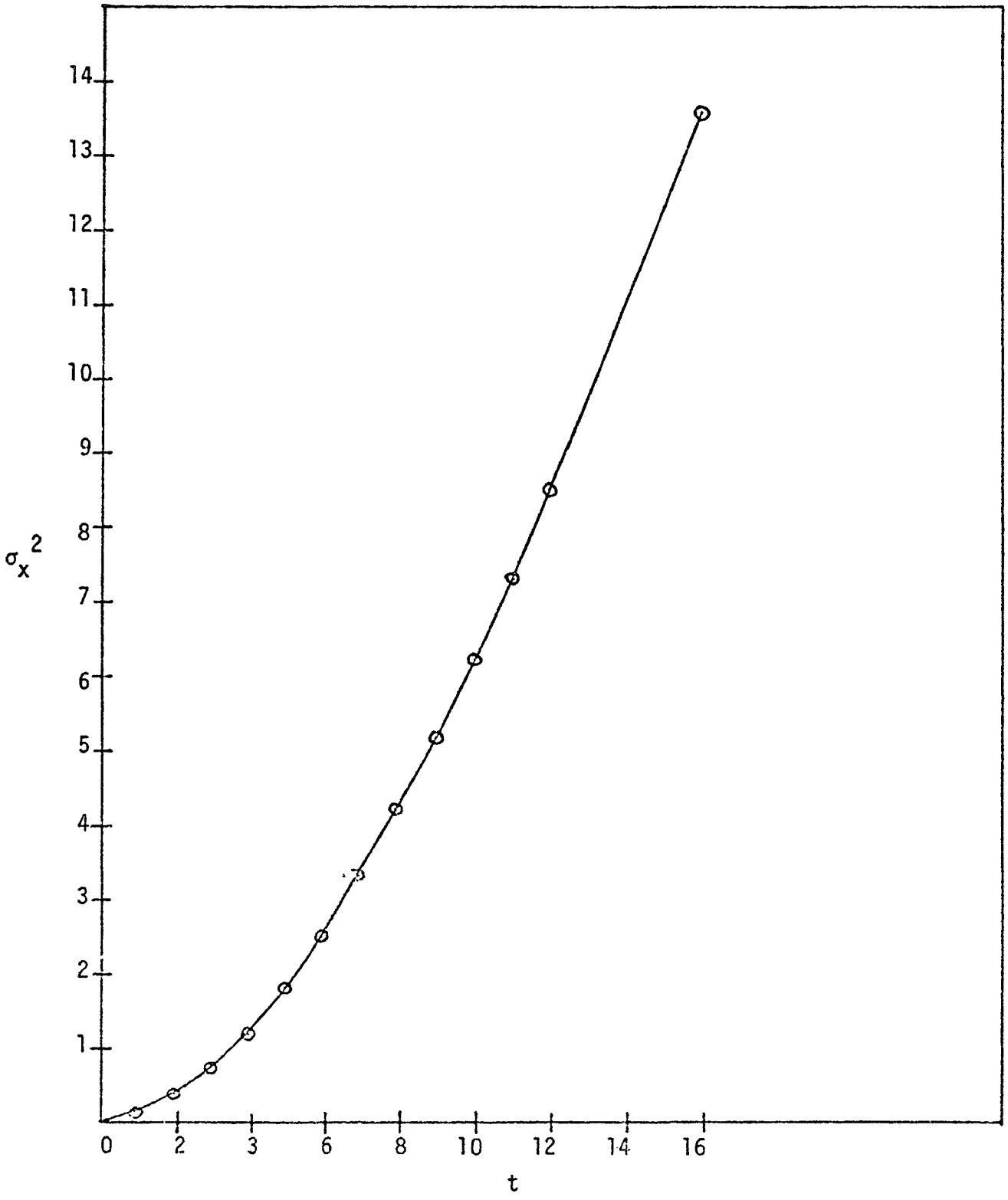

Figure 13.2: σ_x^2 vs. Time for the LINEAR Profile for D=0.1

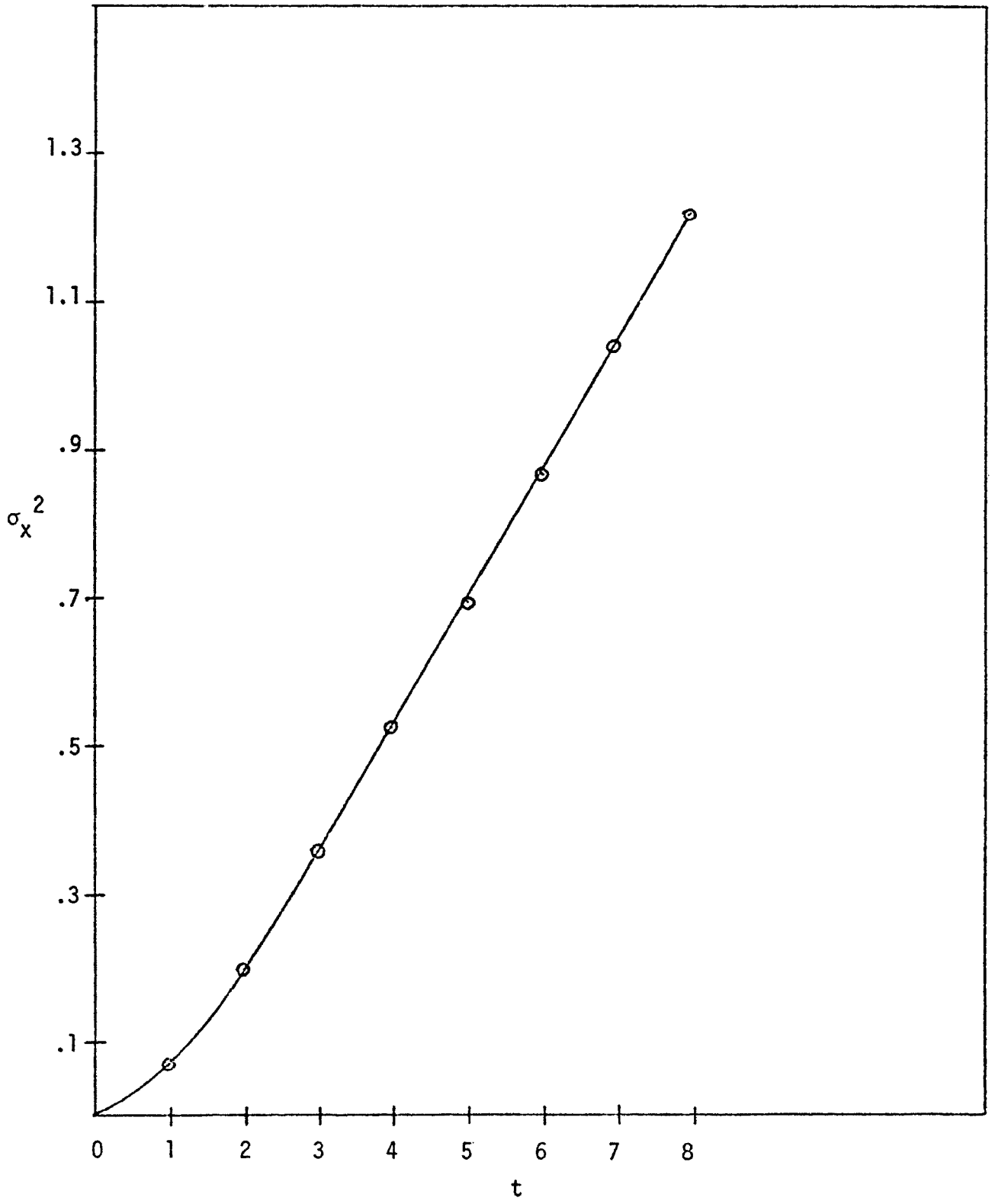

Figure 13.3: σ_x^2 vs. Time for the LINEAR Profile for D=1.0

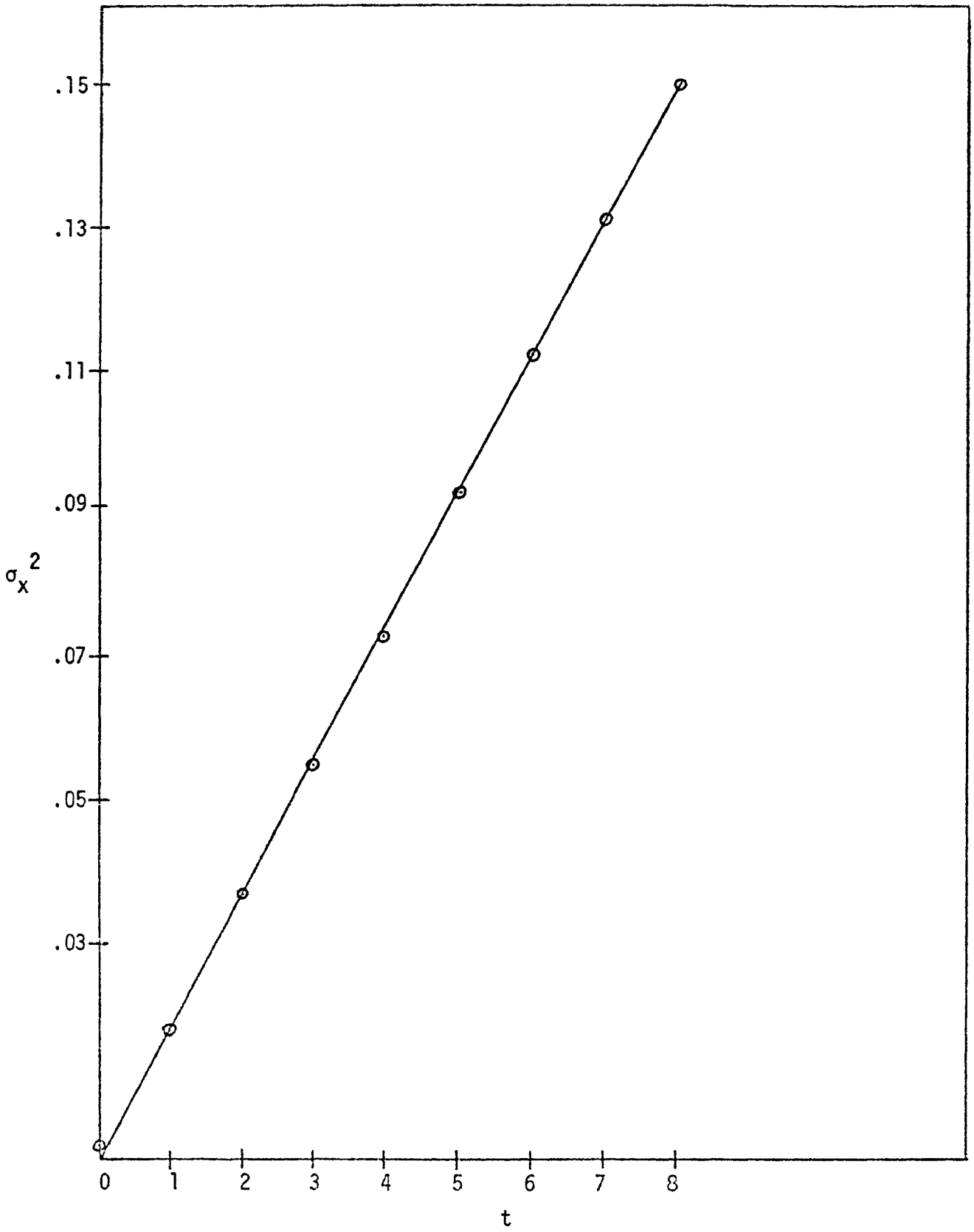

Figure 14.1: σ_x^2 vs. Time for the LAKE Profile for D=.01

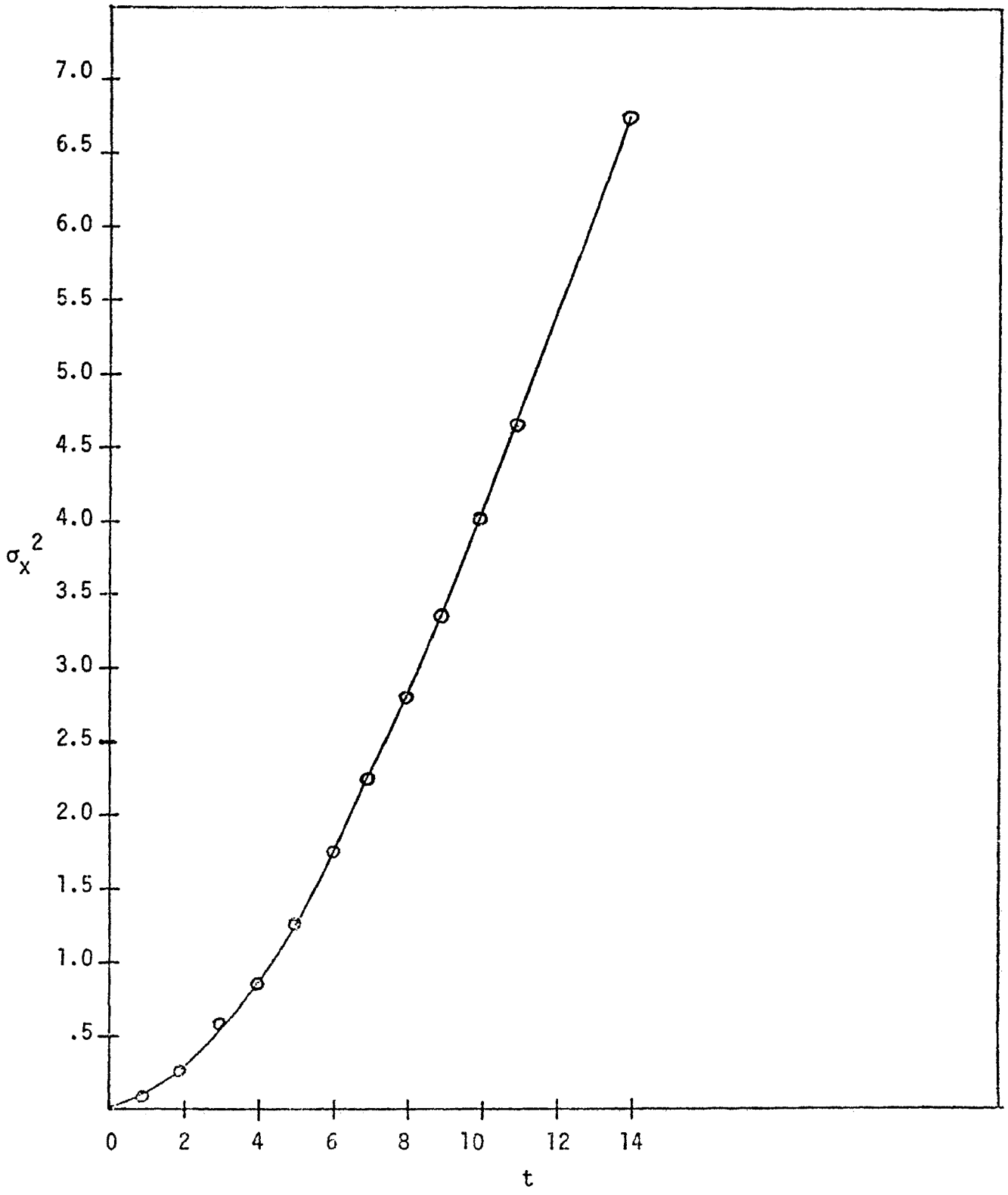

Figure 14.2: σ_x^2 vs. Time for the LAKE Profile for D=0.1

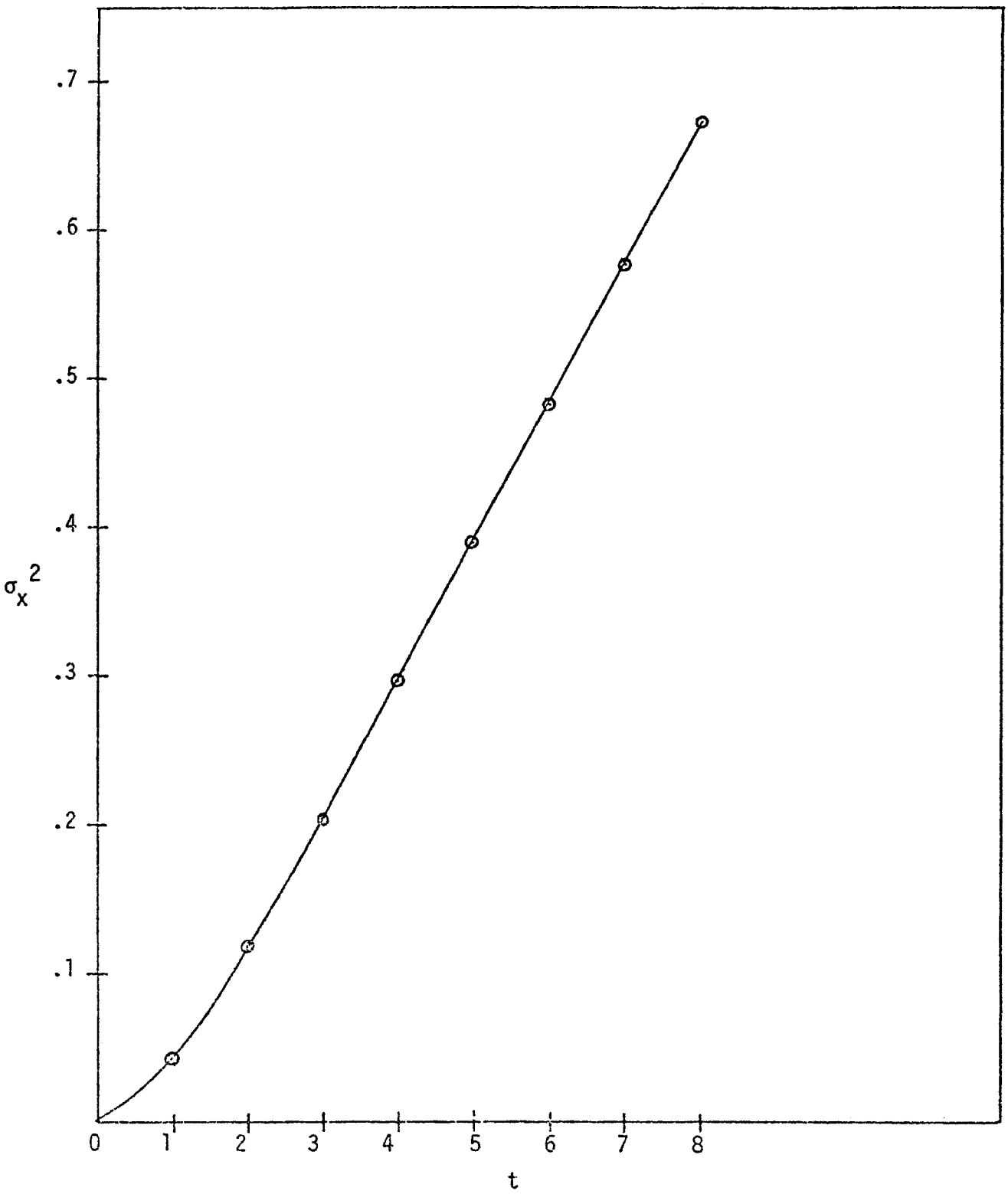

Figure 14.3: σ_x^2 vs. Time for the LAKE Profile for D=1.0

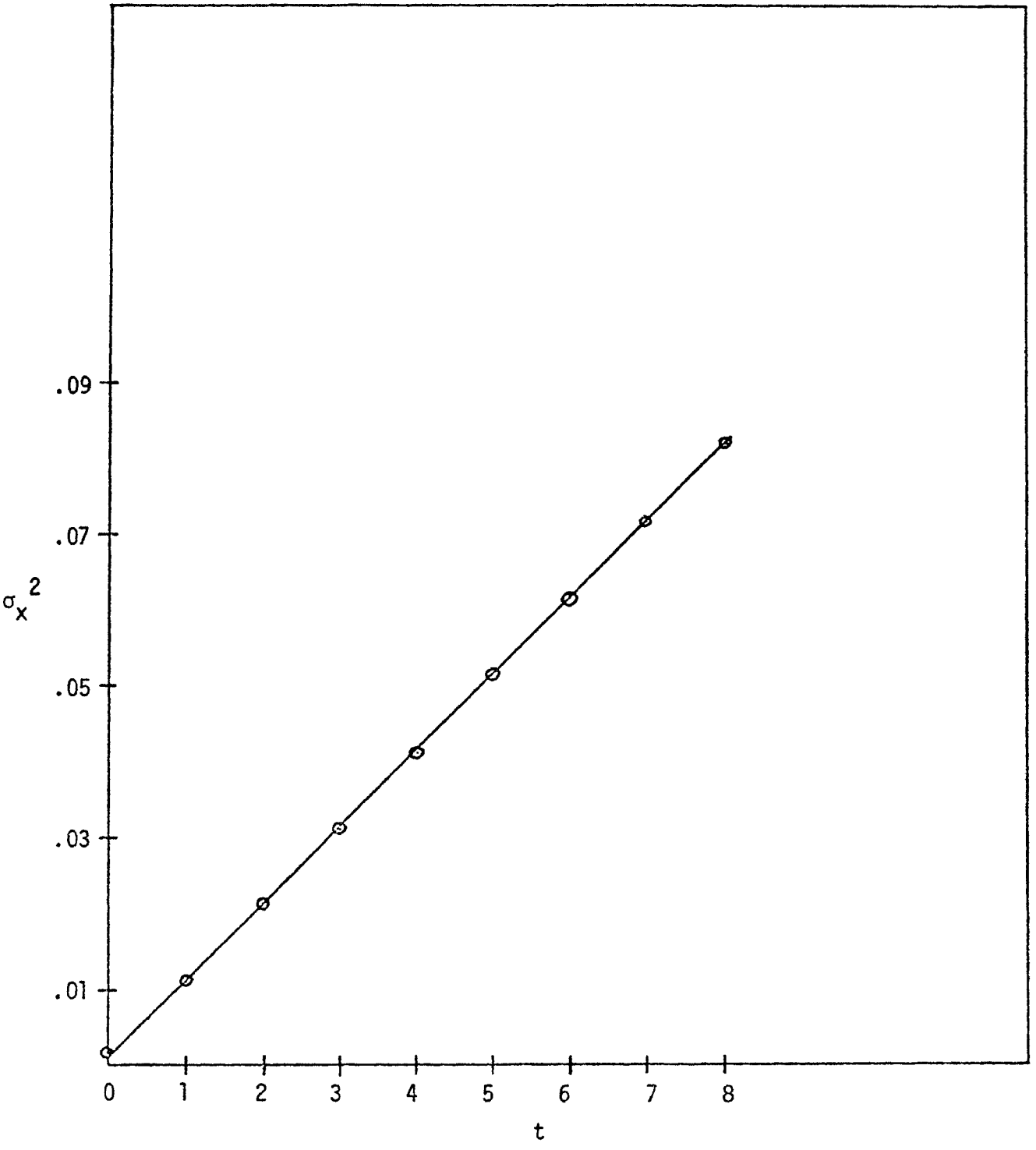

TABLE 5.1

Linear Profile

Theoretical Values of $\bar{x}$ and σ_x^2 for D=0

Time	$\bar{x}$	σ_x^2
t=1	0.625	0.08503
t=2	1.125	0.33503
t=3	1.625	0.75170
t=4	2.125	1.33503
t=5	2.625	2.08503

TABLE 5.2

Linear Profile

Values of $\bar{x}$ and σ_x^2 for D=0

as Obtained by the Numerical Scheme

Time	$\bar{x}$	σ_x^2
t=1	0.62421	0.08491
t=2	1.12354	0.33458
t=3	1.62286	0.75069
t=4	2.12210	1.33323
t=5	2.62135	2.08215

TABLE 5.3

Linear Profile

Values of σ_x^2 for D=.01

Time	σ_x^2
t=1	0.0835
t=2	0.3183
t=3	0.6910
t=4	1.1890
t=5	1.8000
t=6	2.5150
t=7	3.3200
t=8	4.2150
t=9	5.1850
t=10	6.2200
t=11	7.3220
t=12	8.4800
t=16	13.6400

TABLE 5.4

Linear Profile

Values of σ_x^2 for D=0.1

Time	σ_x^2
t=1	0.0644
t=2	0.1955
t=3	0.3530
t=4	0.5200
t=5	0.6910
t=6	0.8640
t=7	1.0380
t=8	1.2150

TABLE 5.5

Linear Profile

Values of σ_x^2 for D=1.0

Time	σ_x^2
t=1	0.0179
t=2	0.0362
t=3	0.0546
t=4	0.0725
t=5	0.0924
t=6	0.1120
t=7	0.1310
t=8	0.1500

TABLE 5.6

Lake Profile

Values of σ_x^2 for D=.01

Time	σ_x^2
t=1	0.0670
t=2	0.2445
t=3	0.5122
t=4	0.8500
t=5	1.2610
t=6	1.7220
t=7	2.2300
t=8	2.7810
t=9	3.3690
t=10	4.0020
t=11	4.6410
t=14	6.7600

TABLE 5.7

Lake Profile

Values of σ_x^2 for D=0.1

Time	σ_x^2
t=1	0.0422
t=2	0.1173
t=3	0.2040
t=4	0.2950
t=5	0.3880
t=6	0.4810
t=7	0.5750
t=8	0.6730

TABLE 5.8

Lake Profile

Values of σ_x^2 for D=1.0

Time	σ_x^2
t=1	0.0109
t=2	0.0209
t=3	0.0310
t=4	0.0412
t=5	0.0513
t=6	0.0610
t=7	0.0718
t=8	0.0821

TABLE 5.9

Computer Time

Run No.	Profile	D Value	Mode	Dx Value in the Final Iteration	t_{final}	Computer Time in Minutes
1	Linear	.01	A	.1	16	70
2	Linear	.01	B	.1	12	120
3	Linear	0.1	B	.1	8	80
4	Linear	1.0	B	.05	8	90
5	Lake	.01	A	.05	14	90
6	Lake	.01	B	.05	11	160
7	Lake	0.1	B	.075	8	90
8	Lake	1.0	B	.05	8	100

A -- Both Dt, Dx increased simultaneously

B -- Only Dx increased; Dt constant at .01

BIBLIOGRAPHY

1. Bellman, R. E. and others, Numerical Inversion of Laplace Transform, American Elsevier Publishing Company, Inc., New York, 1966.

2. Bellman, R. E. and others, Invariant Imbedding and Time-Dependent Transport Processes, American Elsevier Publishing Company, Inc., New York, 1964.

3. Frenkiel, F. N., "Turbulent Diffusion," Advances in Applied Mechanics, Vol. III, Edited by R. von Mises and Theodor von Karman, Academic Press Inc., New York, New York, 1953.

4. Fromm, J. E., "A Method for Reducing Dispersion in Convective Difference Schemes," Journal of Computational Physics, 3, pp. 176-189 (1968).

5. Fromm, J. F., "Practical Investigation of Convective Difference Approximations of Reduced Dispersion," The Physics of Fluids Supplement II, pp. 3-12 (1969).

6. Galloway, F. M., Paper presented at the Sixteenth Conference on Great Lakes Research, Huron, Ohio, April 16-18, 1973.

7. Gedney, R. T., "Numerical Calculations of the Wind-Driven Currents in Lake Erie," NASA TM X-52985, pp. 75 and 125, March 1971.

8. Murthy, C. R., "An Experimental Study of Horizontal Diffusion in Lake Ontario," 13th Conference on Great Lakes Research, Buffalo, New York, March 31-April 3, 1970.

9. Skarupa, K. A., "Numerical Solution to a Concentration Gradient in the Western Basin of Lake Erie," M.S. Thesis, Cleveland State University, June 1972.

10. Smith, G. D., Numerical Solution of Partial Differential Equations, Oxford University Press, p. 24 (1965).

11. Varga, R.S., Matrix Iterative Analysis, Prentice-Hall, Inc., Englewood Cliffs, New Jersey, p. 195 (1962).

12. Yotsukura, N. and Fiering, M. B., "Numerical Solution to a Dispersion Equation," Journal of the Hydraulics Division, ASCE, HY5, pp. 83-104 (1964).

13. Aris, R., "On the Dispersion of a Solute in a Fluid Flowing Through a Tube," Proceedings of the Royal Society of London, Vol. 235 (Series A), p. 67 (1956).

14. Saffman, P. G., "The Effect of Wind Shear on Horizontal Spread from an Instantaneous Ground Source," Royal Meteorological Society Quarterly Journal, Vol. 88, p. 382 (1962).

APPENDIX I

DERIVATION OF $\bar{x}$ AND σ_x^2 FOR THE GAUSSIAN DISTRIBUTION

The solution of

$$\frac{\partial C}{\partial t} + z\frac{\partial C}{\partial x} = 0 \quad \text{is}$$

$$C = f(x - zt)$$

Now initially,

$$C = f(x) = e^{-\frac{(x-.125)^2}{4a}} \qquad \text{for } 0 \leq x \leq .25$$

$$C = 0 \text{ otherwise}$$

$$C = e^{-\frac{(x-zt-.125)^2}{4a}} \qquad \text{for } 0 \leq x - zt \leq .25$$

For convenience, the following notation is used for the different quantities.

$$d = \frac{.125}{2\sqrt{a}}$$

$$m = \frac{x - .125}{2\sqrt{a}}$$

$$g = \frac{t + .125 - x}{2\sqrt{a}}$$

$$B = \text{erf}(d)$$

$$\ell = \frac{zt + .125 - x}{2\sqrt{a}}$$

The initial amount of mass is given by

$$M = \int_0^{.25} e^{-\frac{(x-.125)^2}{4a}} dx = 2\sqrt{a\pi} \cdot \text{erf}(d)$$

For finding $\bar{C}$, we have to consider three ranges of x as indicated in Section 4.6.2.

Range (i) $0 \le x \le .25$

$$z_\ell = 0$$

$$z_u = \frac{x}{t}$$

$$\bar{C} = \int_{z_\ell}^{z_u} e^{-\frac{(x-zt-.125)^2}{4a}} dz$$

$$= \frac{2\sqrt{a}}{t} \int_{-m}^{d} e^{-\ell^2} d\ell$$

$$= \frac{\sqrt{a\pi}}{t} [\text{erf}(d) + \text{erf}(m)]$$

$$= \frac{\sqrt{a\pi}}{t} [\text{erf}(\frac{.125}{2\sqrt{a}}) + \text{erf}(\frac{x-.125}{2\sqrt{a}})] \qquad (1)$$

Range (ii) $.25 \le x \le t$

$$z_\ell = \frac{x-.25}{t}$$

$$z_u = \frac{x}{t}$$

$$\bar{C} = \int_{z_\ell}^{z_u} e^{-\frac{(x-zt-.125)^2}{4a}} dz$$

$$= \frac{2\sqrt{a}}{t} \int_{-d}^{d} e^{-\ell^2} d\ell$$

$$= \frac{2\sqrt{a\pi}}{t}[\text{erf}(d)]$$

$$= \frac{\sqrt{a\pi}}{t}[\text{erf}(\frac{.125}{2\sqrt{a}}) + \text{erf}(\frac{.125}{2\sqrt{a}})] \qquad (2)$$

At x = .25, (1) and (2) are equal.

Range (iii) $\quad t \leq x \leq t + .25$

$$z_\ell = \frac{x-.25}{t}$$

$$z_u = 1$$

$$\bar{C} = \int_{z_\ell}^{z_u} e^{-\frac{(x-zt-.125)^2}{4a}} dz$$

$$= \frac{2\sqrt{a}}{t} \int_{-d}^{g} e^{-\ell^2} d\ell$$

$$= \frac{\sqrt{a\pi}}{t}[\text{erf}(g) + \text{erf}(d)]$$

$$= \frac{\sqrt{a\pi}}{t}[\text{erf}(\frac{t+.125-x}{2\sqrt{a}}) + \text{erf}(\frac{.125}{2\sqrt{a}})] \qquad (3)$$

At x = t, (2) and (3) are equal.

MASS CONSERVATION

Mass at any time is given by

$$M = \int_0^{t+.25} \bar{C}dx$$

Range (i)

$$\text{Contribution to } M = \int_0^{.25} \bar{C}dx$$

$$= \frac{\sqrt{a\pi}}{t} \int_0^{.25} \text{erf}(d)dx + \frac{\sqrt{a\pi}}{t} \int_0^{.25} \text{erf}(m)dx$$

$$\text{Now } \int_0^{.25} \text{erf}(m)dx$$

$$= \int_0^{.25} \text{erf}\left(\frac{x-.125}{2\sqrt{a}}\right)dx$$

$$= 2\sqrt{a} \int_{-d}^{d} \text{erf}(m)dm$$

$$= 0 \quad \text{since erf}(m) \text{ is an odd function.}$$

$$\therefore \text{Contribution to } M = \frac{\sqrt{a\pi}}{t} \cdot [\text{erf}(d)] \cdot (0.25)$$

Range (ii)

$$\text{Contribution to } M = \frac{2\sqrt{a\pi}}{t} \int_{.25}^{t} \text{erf}(d)dx$$

$$= \frac{2\sqrt{a\pi}}{t} \cdot [\text{erf}(d)] \cdot (t - .25) \qquad (5)$$

Range (iii)

$$\text{Contribution to } M = \frac{\sqrt{a\pi}}{t}\int_t^{t+.25} \text{erf}(d)dx + \frac{\sqrt{a\pi}}{t}\int_t^{t+.25} \text{erf}(g)dx$$

Now $\int_t^{t+.25} \text{erf}(g)dx$

$$= \int_t^{t+.25} \text{erf}\left(\frac{t+.125-x}{2\sqrt{a}}\right)dx$$

$$= 2\sqrt{a}\int_d^{-d} \text{erf}(g)dg$$

$$= 0$$

$$\therefore \text{Contribution to } M = \frac{\sqrt{a\pi}}{t} \cdot [\text{erf}(d)] \cdot (0.25) \qquad (6)$$

Adding (4), (5) and (6), we get

$$M = 2\sqrt{a\pi} \cdot \text{erf}(d)$$

Hence, mass conservation is satisfied.

CALCULATION OF $\bar{x}$

$$\bar{x} = \frac{\int_o^{t+.25} \bar{C}xdx}{M}$$

Range (i)

Contribution to $\bar{x}$

$$= \frac{1}{2tB}\int_o^{.25} x\text{erf}(d)dx + \frac{1}{2tB}\int_o^{.25} x\text{erf}(m)dx$$

The second integral is

$$= 2\sqrt{a} \cdot (0.125) \int_{-d}^{d} \text{erf}(m)dm + 4a \int_{-d}^{d} \text{merf}(m)dm$$

The first term is zero and the second cancels with an exactly opposite term contributed by range (iii).

$$\therefore \text{ Contribution to } \bar{x} = \frac{1}{64t} \tag{7}$$

Range (ii)

$$\text{Contribution to } \bar{x} = \frac{1}{tB} \int_{.25}^{t} x\,\text{erf}(d)dx$$

$$= \frac{t}{2} - \frac{1}{32t} \tag{8}$$

Range (iii)

Contribution to $\bar{x}$

$$= \frac{1}{2t} \int_{t}^{t+.25} xdx + \frac{1}{2tB} \int_{t}^{t+.25} x\,\text{erf}(g)dx$$

Now second integral is

$$= 2\sqrt{a} \cdot (t + .125) \int_{-d}^{d} \text{erf}(g)dg - 4a \int_{-d}^{d} \text{gerf}(g)dg$$

The first term is zero and the second term concels with the opposite term from range (i)

$$\therefore \text{ Contribution to } \bar{x} = \frac{1}{8} + \frac{1}{64t} \tag{9}$$

Adding (7), (8) and (9), we get

$$\bar{x} = \frac{t}{2} + \frac{1}{8} \tag{10}$$

We can calculate $\bar{x}$ at $t = 0$

At $t = 0$

$$\bar{C} = e^{-\frac{(x-.125)^2}{4a}}$$

$$\bar{x} = \frac{\int_0^{.25} e^{-\frac{(x-.125)^2}{4a}} dx}{M}$$

$$= \frac{2\sqrt{a}}{8M} \int_{-d}^{d} e^{-m^2} dm + \frac{4a}{M} \int_{-d}^{d} m e^{-m^2} dm$$

The second term is zero

$$\therefore \bar{x} = \frac{2\sqrt{a\pi}\ \mathrm{erf}(d)}{8M}$$

$$= \frac{1}{8}$$

Putting $t = 0$ in (10) gives $\bar{x} = \frac{1}{8}$ which is indeed so.

CALCULATION OF σ_x^2

Range (i)

Contribution to σ_x^2

$$= \frac{1}{2t} \int_0^{.25} (x-\bar{x})^2 dx + \frac{1}{2tB} \int_0^{.25} (x-\bar{x})^2 \mathrm{erf}(m) dx$$

Now $\int_0^{.25} (x-\bar{x})^2 \mathrm{erf}(m) dx$

$$= 2\sqrt{a}\int_{-d}^{d}(2\sqrt{a}\cdot m - \frac{t}{2})^2 \mathrm{erf}(m)dm$$

This will be combined with a similar term from range (iii).

Contribution by the other integral to σ_x^2

$$= \frac{1}{2t}\int_{o}^{.25}(x-\bar{x})^2 dx \qquad (11)$$

Range (ii)

$$\text{Contribution to } \sigma_x^2 = \frac{1}{t}\int_{.25}^{t}(x-\bar{x})^2 dx \qquad (12)$$

Range (iii)

$$\text{Contribution to } \sigma_x^2 = \frac{1}{2t}\int_{t}^{t+.25}(x-\bar{x})^2 dx + \frac{1}{2tB}\int_{t}^{t+.25}(x-\bar{x})^2 \mathrm{erf}(g)dx$$

Now $\int_{t}^{t+.25}(x-\bar{x})^2 \mathrm{erf}(g)dg$

$$= 2\sqrt{a}\int_{-d}^{d}(\frac{t}{2} - 2\sqrt{a}\cdot g)^2 \mathrm{erf}(g)dg$$

This will be combined with a similar term from range (i).

Contribution by the other integral to σ_x^2

$$= \frac{1}{2t}\int_{t}^{t+.25}(x-\bar{x})^2 dx \qquad (13)$$

Combining (11), (12) and (13) we get

$$\text{Contribution to } \sigma_x^2 = \frac{1}{2t}\int_{o}^{t+.25}(x-\bar{x})^2 dx + \frac{1}{2t}\int_{.25}^{t}(x-\bar{x})^2 dx$$

$$= \frac{t^2}{12} + \frac{1}{64} \qquad (14)$$

Combining the leftover terms from range (i) and (iii), we get

$$\frac{2\sqrt{a}}{tB} \cdot \int_{-d}^{d} \left(\frac{t}{2} - 2\sqrt{a} \cdot m\right)^2 \operatorname{erf}(m)\,dm$$

where 'm' here is the variable of integration.

Now $\int_{-d}^{d} \operatorname{erf}(m)\,dm = 0$

and $\int_{-d}^{d} m^2 \operatorname{erf}(m)\,dm = 0$

since both are odd functions.

Hence, the only term left from the integral is

$$-\frac{4a}{B} \int_{-d}^{d} m \operatorname{erf}(m)\,dm$$

Let $I = \int_{-d}^{d} m \operatorname{erf}(m)\,dm$

Integrating by parts, taking 1 as the second part, we get

$$I = \left[m^2 \operatorname{erf}(m)\right]_{-d}^{d} - \int_{-d}^{d} m \operatorname{erf}(m)\,dm - \frac{2}{\sqrt{\pi}} \int_{-d}^{d} m^2 e^{-m^2}\,dm$$

$$\therefore \quad I = d^2 \operatorname{erf}(d) - \frac{1}{\sqrt{\pi}} \int_{-d}^{d} m^2 e^{-m^2}\,dm$$

$$\therefore \quad -\frac{4a}{B} I = -\frac{1}{64} + \frac{4a}{\sqrt{\pi} \cdot B} \int_{-d}^{d} m^2 e^{-m^2}\,dm \qquad (15)$$

Combining (14) and (15), we get

$$\sigma_x^2 = \frac{t^2}{12} + \frac{4a}{\sqrt{\pi} B} \int_{-d}^{d} m^2 e^{-m^2}\,dm$$

Now it can be shown that

$$\frac{4a}{\sqrt{\pi}\cdot B}\int_{-d}^{d} m^2 e^{-m^2}\,dm$$

$$= \frac{1}{2\sqrt{a\pi}B}\int_{0}^{.25}(x-.125)^2 e^{-\frac{(x-.125)^2}{4a}}\,dx$$

= initial variance of the distribution

Without much error, the initial variance can be taken as equal to the variance of the same gaussian distribution extending from $-\infty$ to ∞. In that case,

the initial variance = $2a = .0017$

$$\therefore \sigma_x^2 = \frac{t^2}{12} + .0017 \qquad (16)$$

NUMERICAL VERIFICATION

The analytical solution is

$$C = e^{-\frac{(x-zt-.125)^2}{4a}}$$

The expressions for $\bar{C}$ are given by equations (1), (2) and (3) respectively for the three ranges of x.

They were verified by numerically integrating the above expression for C in the z direction. For this purpose DZ was taken as .01 and Simpson's rule was used. The analytical expressions check with the numerical values.

Similarly, $\bar{x}$ and σ_x^2 were calculated by numerically integrating

$\tilde{C}$ as given by equations (1), (2) and (3) in the x direction. They check with the values of $\bar{x}$ and σ_x^2 given by equations (10) and (16) respectively.

Thus, the analytical derivation was numerically verified.

APPENDIX A2

CRITERIA FOR THE USE OF VERTICAL AVERAGING IN GREAT LAKES DISPERSION MODELS

Shailesh Vakil

Bachelor of Chemical Engineering

University of Mississippi

June, 1970

Submitted in partial fulfillment of requirements for the degree

MASTER OF SCIENCE IN CHEMICAL ENGINEERING

at

THE CLEVELAND STATE UNIVERSITY

June, 1975

This thesis has been approved

for the Department of Chemical Engineering

and the College of Graduate Studies by

_____

Thesis Advisor

_____

(Department/Date)

_____

_____

(Department/Date)

_____

_____

(Department/Date)

ACKNOWLEDGEMENT

I wish to express my sincere gratitude to Dr. F. M. Galloway for his valuable guidance to make this work possible and also to the Computer Center for their help and time.

I also appreciate Dr. L. T. Novak and Dr. R. H. Pao for their efforts in reviewing this work.

ABSTRACT

A basic question, in developing a dispersion model, is when a two dimensional model is an adequate approximation for a three dimensional model. The use of a two dimensional model instead of a three dimensional model results in considerable savings of computer time.

A model problem involving horizontal convection and vertical diffusion is solved on the computer to establish a criteria to choose between two and three dimensional dispersion models for large lakes. Different combinations of vertical profiles of velocity and diffusivity were used. The arrival of the horizontal direction variance of the concentration distribution to a linear time dependence was found to be a suitable criterion for the use of vertical averaging.

Effective horizontal dispersion coefficients (K_e) for use after vertical averaging were computed from the results of the model problem and also from a formula given by Csanady. Both the methods gave good agreement of the values of K_e.

It is shown that the time to reach the condition for vertical averaging correlates as $t_1 = h^2/(\alpha_1 \overline{D}_z)$, while the effective dispersion coefficient is given by $K_e = (C_1 h^2 U^2)/\overline{D}_z$, where h is depth, $\overline{D}_z$ is average vertical diffusivity, U is a characteristic velocity and α_1 and C_1 depend on profiles used. Over the range of profiles studied, α_1 varied by a factor less than 1.5 and C_1 by a factor less than 3.0.

The method and results presented have wide application in dispersion modeling for large lakes pertaining to the choice of a two or three dimensional model and an effective horizontal dispersion coefficient for the vertically averaged cases.

TABLE OF CONTENTS

LIST OF TABLES

LIST OF FIGURES

NOMENCLATURE

a	Parameter in the Gaussian distribution
C	Concentration; dimensional in equation (2.1), dimensionless elsewhere
C_1	Evaluated from dimensionless form of equations 2.19 and 2.20 with $\overline{D}_z = 1.0$
D(z)	Vertical diffusivity profile
D, D_z	Non-dimensionalized vertical diffusivity
Dt	Mesh spacing in time
Dx	Mesh spacing in the horizontal direction
Dz	Mesh spacing in the vertical direction
D_x^*	Effective horizontal dispersion coefficient, dimensionless
H,h	Depth of lake
k	A number dependent upon the geometry of the cross-section
K_e	Effective horizontal dispersion coefficient - dimensional
L	Reference length
q	Total amount of material released
t	Time; dimensional in equation (2.1), dimensionless elsewhere
u	Velocity in horizontal direction; dimensional in equation (2.1), dimensionless elsewhere
U_{max}	Reference velocity taken to be magnitude of the difference between maximum and minimum velocities across the layer

X	Co-ordinate in the horizontal direction; dimensional in equation (2.1), dimensionless elsewhere
$\overline{x}$	Mean x coordinate of the concentration distribution
z	Co-ordinate in vertical direction; dimensional in equation (2.1), dimensionless elsewhere

Greek Letters

α_1	Smallest eigenvalue of Strum-Liouville problem defined in Appendix II, dimensionless

Subscript

K	Mesh index in the z direction
i	Mesh index in the x direction
n	Mesh index in time
ref	Reference quantity

CHAPTER 1

INTRODUCTION AND BACKGROUND

1.1 Introduction

Large bodies of water such as estuaries, lakes, rivers, and seas are widely used for dumping a great quantity of industrial and domestic wastes. It is assumed that pollutants are dispersed by naturally occurring currents and horizontal mixing. Hence, the numerical modeling to show how these pollutants are carried away from the place of dumping and dispersed over larger masses is of great importance.

In recent years investigations have been done on dispersion in lakes, rivers, and seas. The main concern in this thesis is the dispersion processes of the Great Lakes. The problem is not only concerning factors causing dispersion and mixing in lakes, but also how effectively these factors work both individually and interactionally. One of the possibilities of interaction is between the factors of vertical diffusion and the shear of the horizontal velocity profile. This is the main area of investigation in this thesis.

In the general case, the transport of a dissolved, conserved pollutant in a large lake is described by

$$\frac{\partial C}{\partial t} + u \frac{\partial C}{\partial x} = \frac{\partial}{\partial z}\left(D_z \frac{\partial C}{\partial z}\right) + D_x \frac{\partial^2 C}{\partial x^2} \qquad (1.1)$$

where z is the vertical coordinate, x is a horizontal coordinate, u is

the horizontal velocity, D_z is vertical eddy diffusivity and D_x is horizontal eddy diffusivity. A second horizontal direction y does not appear explicitly in equation (1.1) since it is assumed that x is a local coordinate in the direction of the main horizontal currents and that the flow is nearly parallel. Thus convection in the y direction perpendicular to x is assumed to be negligible. Diffusion in y direction is eliminated if the concentration, C, is considered to be averaged in the y direction. Thus the transport equation involves three space dimensions. The numerical solution of a three space dimensional equation is very costly in terms of computer time. It is therefore, desirable to reduce equation (1.1) to two space dimension dependency by a vertical averaging procedure, if this can be done without significant loss of accuracy in the solution. Formally, equation (1.1) can be vertically averaged as

$$\frac{1}{h}\int_0^h \left[\frac{\partial C}{\partial t} + u\frac{\partial C}{\partial x} = \frac{\partial}{\partial z}\left(D_z\frac{\partial C}{\partial z}\right) + D_x\frac{\partial^2 C}{\partial x}\right] dz \qquad (1.2)$$

which yields

$$\frac{\partial \bar{C}}{\partial t} + \bar{u}\frac{\partial \bar{C}}{\partial x} + \frac{1}{h}\int_0^h u'\frac{\partial C'}{\partial x}\,dz = D_x\frac{\partial^2 \bar{C}}{\partial x^2} \qquad (1.3)$$

where the "bar" indicates a vertically averaged quantity and $u' = u-\bar{u}$ and $C' = C - \bar{C}$. The first term on the right hand side of equation (1.2) vanishes by use of the boundary conditions, $D_z\frac{\partial C}{\partial z} = 0$ at $z = 0, h$. Following the practice used in turbulent flow problems, the third term on the left hand side is represented as

$$\frac{1}{h}\int_0^h u' \frac{\partial C'}{\partial x}\, dz = u' \overline{\frac{\partial C'}{\partial x}} = -K_e \frac{\partial^2 \overline{C}}{\partial x^2} \qquad (1.4)$$

where K_e is an effective horizontal dispersion coefficient which is supposed to account for vertical effects. Thus, equation (1.1) becomes

$$\frac{\partial \overline{C}}{\partial t} + \overline{u}\,\frac{\partial \overline{C}}{\partial x} = (D_x + K_e)\frac{\partial^2 \overline{C}}{\partial x^2} \qquad (1.5)$$

and the vertical averaging has reduced the dimensionality by one. Equation (1.5) can obviously be solved much more efficiently by computer.

The above development has practical utility for dispersion modeling in large lakes only if K_e can be determined. The main concern of this investigation is to predict when a time-dependent K_e can be used in equation (1.5) and also to estimate the value of K_e. The question of when does K_e become time-dependent is answered in terms of a criterion for the use of vertical averaging that depends on the interaction of u and D_z. It is also shown how K_e can then be calculated as a function of u and D_z.

The bases for the investigation are numerical solutions of equation (1.1) without the term $D_x \frac{\partial^2 C}{\partial x^2}$. The results mentioned above are derived from these solutions. The elimination of the horizontal diffusivity term is justified on the basis of the analysis by Aris (Ref. 1). He showed that the two mechanisms for horizontal spreading, namely that due to the interaction of u and D_z, work independently. Thus once K_e is obtained it can simply be added to D_x to get the combined effect as shown in equation (1.5). The work of Aris is further discussed in section 1.2.

1.2 Background

Pioneer study of the interaction between horizontal velocity and vertical diffusivity and their combined effect on dispersion was done by Taylor (Ref. 11). He illuminated theoretically and experimentally, for a laminar flow in a circular tube, basic concepts involved in the interaction between vertical diffusion and horizontal convection. Two phases of transport were identified. The first, extending from the point of introduction of the solute to some distance downstream, is characterized by significant cross-plane variations in concentration of solute and an increasing rate of dispersion in the downstream direction of the solute cloud taken as a whole. Small variations in cross-plane concentration, after a sufficient time, identifies the second phase. He reasoned mathematically and demonstrated experimentally that the cross-plane averaged concentration in this second phase approaches a Gaussian distribution in the downstream direction. Further spread in this phase can be explained by an effective downstream diffusion coefficient which depends on the cross-plane shear of the downstream velocity, and the cross-plane diffusion coefficient. Thus he showed that cross-plane averaging is a theoretically sound treatment of dispersion problems, provided that the solute cloud has entered the second phase of transport. We should be aware here that our work concerns the detailed description of the first phase of transport and a prediction of the beginning of the second phase as well as the effective downstream diffusion coefficient for the second phase.

Aris (Ref. 1) extended Taylor's concept of mathematical analysis to tubes of arbitrary cross-section. Taylor's result for the effective

diffusion coefficient contained some restriction on the parameters. Aris extended his work to more general geometry by introducing the method based on the moments of the concentration distribution. His work showed that the rate of growth of variance in the axial direction is proportional to the sum of the molecular diffusion coefficient D, and the Taylor diffusion coefficient $K_e = ka^2U^2/D$, where U is the mean velocity and a is a dimension characteristic of the cross-section of the tube. By showing that K_e is a constant after a long enough time, he demonstrated that a finite distribution of solute tends to become normally distributed. We can also obtain an effective downstream dispersion coefficient for the general case from Aris' results by solving a non-homogeneous second order partial differential equation with variable coefficients. Aris' introduction of the moment method has proven very useful in the application of Taylor's concept to environmental situations.

Elder (Ref. 4) applied Taylor's analysis to obtain the effective horizontal dispersion coefficient for open channel flow. Saffman (Ref. 10) extended Taylor's and Aris' concepts to atmospheric dispersion. Thackston and Krenkel (Ref. 12) and Fischer (Ref. 5) worked on streams applying the same technique. Bowden (Ref. 2) stretched the idea to sea for horizontal mixing due to shearing current. Most of this work is very well summarized by Csanady (Ref. 3).

Taylor's and Aris' analyses show that the effective horizontal diffusion coefficient, D_x^*, always approaches a constant value as t approaches infinity for any positive, finite $D_z(Z)$. Csanady presents a method to determine D_x^* without solving the diffusion equation in detail. His method provides a good check on the final value of D_x^*.

His method can be used at a long enough time t after releasing a point or line source. At this time, the cloud distributes itself vertically uniformly over the mixed layer, and its further drift and diffusion proceed only along the horizontal direction. We will be using Csanady's approach as a check.

One model including interaction of vertical diffusion and horizontal convection, which calculates the concentration as a function of time and space was developed by Natarajan (Ref. 9). Calculations were presented for two different velocity profiles with three different constant values of vertical diffusivity. Natarajan's model can be justified since it can be shown that horizontal eddy diffusion is negligible in comparison with horizontal convection. However, vertical eddy diffusion is of the same order of magnitude as horizontal convection in the Great Lakes. Values of horizontal eddy diffusivity have been investigated extensively (Ref. 7, 8), but values of vertical eddy diffusion are not very well known. Natarajan used mean values of 0.01, 0.1, and 1.0 for the dimensionless vertical diffusivity. He took two velocity profiles into consideration for all three values of vertical diffusivity. One profile was the linear profile, and the other was the "lake profile."

It is evident from his results that the shape of the velocity profile has little qualitative effect on the horizontal spread, and quantitatively the lake profile leads to less horizontal spread than the linear profile. For both the velocity profiles, where values of vertical diffusivity of 1.0 and 0.1 were used, the vertical variation in concentration became very small. The effective horizontal dispersion

coefficient reached an asymptotic constant value. For a vertical diffusivity value of 0.01, even at a large dimensionless time (t = 16), the value of effective horizontal dispersion coefficient is increasing. A significant vertical variation in concentration also exists. Thus, it is evident that as long as the effective horizontal dispersion coefficient is increasing, there is a significant vertical variation in concentration and when it reaches a constant value, the vertical variation becomes small.

He concluded that when the vertical variation is relatively small a two dimensional model can be used with good accuracy, which will cut down computer time significantly. On the other hand, when there is a large vertical variation, a three dimensional model should be used for reasonable accuracy.

This work extends Natarajan's investigation to include seven different combinations of velocity and diffusivity profiles. A criterion is established for vertical averaging and the results are correlated in terms of two dimensionless parameters, α_1 and C_1, and are easily applied to a wide range of conditions typical of the Great Lakes.

CHAPTER II

METHOD OF SOLUTION

2.1 Finite Difference Approximations

As it was described in the previous chapter, the problem is to consider the effect of vertical diffusivity and shear of horizontal velocity. A variable vertical diffusivity was taken into consideration instead of an average constant for the value of vertical diffusivity. We will approach the problem by solving the two dimensional diffusion-convection equation:

$$\frac{\partial C}{\partial t} + u(z) \frac{\partial C}{\partial x} = \frac{\partial}{\partial z} \left(D(z) \frac{\partial C}{\partial z} \right) \qquad (2.1)$$

The x-coordinate is in the direction of the mean flow and the z-coordinate is directed vertically upward from the bottom.

Horizontal diffusion is ignored as it does not provide great changes in the dispersion process. The convection term produces larger effects in the horizontal direction than the horizontal diffusion term.

By defining new variables, we will derive a non-dimensional form of the above equation:

H_{ref} = H = Depth of Lake

C_{ref} = C_{max} = Maximum Concentration Occurring in Lake

u_{ref} = Maximum Algebraic Difference Between Maximum and Minimum Horizontal Velocity Along a Vertical Line

Now we can define non-dimensionalized variables:

$$x^* = \frac{x}{H}$$

$$z^* = \frac{z}{H} \quad (0 \leq z^* \leq 1)$$

$$t^* = \frac{t\, u_{ref}}{H}$$

$$C^* = \frac{C}{C_{max}}$$

$$u^* = \frac{u}{u_{ref}}$$

$$D_z^* = \frac{D_z}{u_{ref} H}$$

By substitution into equation 2.1 we get:

$$\frac{\partial C^*}{\partial t^*} + u^* \frac{\partial C^*}{\partial x^*} = \frac{\partial}{\partial z^*} \left(D_z^* \frac{\partial C^*}{\partial z^*}\right) \tag{2.2}$$

We will omit * here and consider it as

$$\frac{\partial C}{\partial t} + u \frac{\partial C}{\partial x} = \frac{\partial}{\partial z} \left(D_z \frac{\partial C}{\partial z}\right) \tag{2.3}$$

where these quantities henceforth will be considered as non-dimensional variables. The initial pollutant concentration is $C = C(x,z,0)$.
The boundary conditions are

$$D_z \frac{\partial C}{\partial z} = 0 \quad \text{at } z = 0 \text{ and } z = 1.$$

A guassian initial distribution is assumed

$$C(x,z,0) = e^{-\frac{(x-.125)^2}{4a}}$$

where 'a' is a parameter.

By picking the variance 'a' very small, this initial condition approximates a delta function input.

Equation 2.3 was solved for various diffusivity and velocity profiles. The spread of pollutant due to the vertical variation of velocity is evaluated by calculating an effective horizontal dispersion coefficient D_x^*. Definition and evaluation of D_x^* will be discussed later.

A finite-difference method is now developed to solve equation 2.3 with the given initial and boundary conditions. First we will study the diffusion term $\frac{\partial}{\partial z}\left(D_z \frac{\partial C}{\partial z}\right)$. This term is replaced by a first order forward difference approximation

$$\frac{\partial}{\partial z}\left(D_z \frac{\partial C}{\partial z}\right) \simeq \frac{D_{K+\frac{1}{2}} \left.\frac{\partial C}{\partial z}\right|_{K+\frac{1}{2}} - D_{K-\frac{1}{2}} \left.\frac{\partial C}{\partial z}\right|_{K-\frac{1}{2}}}{DZ}$$

$$\simeq \frac{D_{K+\frac{1}{2}} \left[C^n_{K+1} - C^n_K\right] - D_{K-\frac{1}{2}} \left[C^n_K - D^n_{K-1}\right]}{DZ^2} \qquad (2.4)$$

Here K is the mesh index in the z direction, n is the time index, and DZ is the mesh spacing in the z direction. In the z direction, the mesh points are numbered from 2 to 12 so that K = 2 corresponds to z = 0 and K = 12 corresponds to z = 1. It is evident from equation 2.4 that C_1 and C_{13} need to be defined. The boundary conditions $D_z \frac{\partial C}{\partial z} = 0$ at z = 0 and z = 1, will provide this information.

Considering expansion of the derivative in Taylor series up to the second order terms, the following conditions for C_1 and C_{13} are found:

$$C_1 = \frac{D_3}{D_1} \quad (C_3 - C_2) \quad + \quad C_2 \tag{2.5}$$

$$C_{13} = - \frac{D_{21}}{D_{23}} \quad (C_{12} - C_{11}) \quad + \quad C_{12} \tag{2.6}$$

Mesh points for the diffusivity profile in the z direction were numbered from 2 to 22, in order to get values of diffusivity at K + 1/2 and K - 1/2 points. Values of D_1 and D_{23} were chosen by extrapolation of the diffusivity profile.

Numerical approximation to the terms:

$$\frac{\partial C}{\partial t} \quad + \quad u \quad \frac{\partial C}{\partial x}$$

is given by Natarajan (Ref. 9). He has followed Fromm's (Ref. 6) fourth order scheme for the numerical approximation to the convective term. We are going to use the same method here for our purpose. Final form of the numerical approximation to these terms is

$$C_i^{n+1} \quad = \quad 1/2 \ (C_{i-1}^n \quad + \quad C_i^n \ ) \quad + \quad 1/2 \ \frac{DT}{DX} \quad (*F_{i-1/2}^n \quad + \quad F_{i-1/2}^n \ -$$

$$*F_{i+1/2}^n \quad - \quad F_{i+1/2}^n \ ) \tag{2.7}$$

The F's are a function of C and u at various mesh points (See Ref. 6). This scheme has fourth-order accuracy in space and second order accuracy in time.

The initial concentration distribution is given by the equation

$$C(x,z,0) \quad = \quad e^{-} \quad \frac{(x \ - \ .125)^2}{4a}$$

The value of 'a' is so chosen such that the distribution has a narrow width. a = 0.00085 gives C = 0.01 at x = 0.0 and x = 0.25. Concentration values less than 0.01 are essentially taken to be zero. Hence,

the initial distribution extends from x = 0 to x = 0.25 with a peak of C = 1 at x = 0.125.

The complete numerical approximation of the differential equation is as follows:

$$C_i^{n+1} = 1/2(C_{i-1}^n + C_i^n) + 1/2 \frac{Dt}{Dx} (*F_{i-1/2}^n + F_{i-1/2}^n - *F_{i+1/2}^n - F_{i+1/2}^n) + \frac{Dt}{Dz^2} [D_{2K-1}^{**} (C_{K+1} - C_K) - D_{2K-3} (C_K - C_{K-1})] \quad (2.8)$$

Natarajan worked out the whole scheme for constant diffusivity. Here the only change we have is the variable vertical diffusivity. With the modifications shown above, the whole scheme basically follows the same pattern as Natarajan's (Ref. 9) scheme for constant vertical diffusivity.

2.2 Choice of Grid Size

Choice of grid sizes was quite important in some cases. Five different sets of grid sizes were used. In all of them, DX was constant. The DX used by Natarajan for the constant diffusivity case was suitable also in the examples where vertical diffusivity varied. Only once was it necessary to change DZ. For the combination of the lake velocity profile with the lake diffusivity profile, a value of DZ = 0.05 was used instead of 0.1 for good accuracy. A great change in the grid size of Dt was necessary for various combinations of velocity and diffusivity profiles. Five different sets of grid sizes were used for computations for different velocity and diffusivity profiles. They are:

Dt	DX	DZ	Velocity Profile	Diffusivity Profile
.01	.0125	.1	Linear	Constant
.01	.0125	.1	Lake	Constant
.01	.0125	.1	Linear	Log
.005	.0125	.1	Log	Constant
.005	.0125	.05	Lake	Lake
.002	.0125	.1	Log	Lake
.001	.0125	.1	Linear	Lake

Thus, as can be seen from the values of Dt, it became necessary to use very small values of Dt in some cases, thus requiring large amounts of computer time. In each example, the largest values of Dt, DX and DZ that would allow good accuracy were used. Only the above sets were adequate to use for particular combinations of diffusivity and velocity profiles.

2.3 Reduction of Numerical Results

The results of numerical computation can be best represented in terms of moments of the distribution. Let $\overline{C}$ be the vertically averaged concentration at a given x. At any time t, we define the following parameters

$$\overline{X} = \frac{\int_{-\infty}^{\infty} \overline{C}\,(x)\; x\; dx}{\int_{-\infty}^{\infty} \overline{C}\;(x)\; dx} \tag{2.9}$$

$$\sigma x^2 = \frac{\int_{-\infty}^{\infty} \overline{C}\,(x)\;(x - \overline{x}\,)^2\; dx}{\int_{-\infty}^{\infty} \overline{C}\,(x)\; dx} \tag{2.10}$$

It can be proven that equation 2.10 reduces to the following equation:

$$\sigma x^2 = \frac{\int_{-\infty}^{\infty} \bar{C}(x)\, X^2\, dx}{\int_{-\infty}^{\infty} \bar{C}(x)\, dx} - \bar{x}^2 \qquad (2.11)$$

The longitudinal dispersion coefficient is defined as

$$D^*_x = 1/2 \left.\frac{d\sigma x^2}{dt}\right|_t \quad \text{at any time t.} \qquad (2.12)$$

D^*_x represents the spread of pollutant due to the interaction of the vertical variation of horizontal velocity and the vertical diffusion. The integrals in equations (2.9) to (2.11) are evaluated by Trapezoidal and Simpson's rule integrations using the C distribution from the solution of equation (2.8).

2.4 Velocity and Diffusivity Profiles

2.4.1 Velocity Profiles

The linear velocity profile and the lake velocity profile are discussed by Natarajan (Ref. 9), so we will not discuss them here. Along with the linear and the lake velocity profiles, we have also considered one more profile which is described by the equation

$$u(z) = 1.0 + 0.217 \ln(z) \qquad (2.13)$$

between z = 0.1 and z = 1.0. It is assumed that the velocity profile from z = 0 to z = 0.1 will be linear and follow the equation

$$u(z) = 5z \qquad (2.14)$$

In this profile, it can be seen that at z = 0, u(z) = 0 and at z = 1, u(z) = 1.0.

2.4.2 Diffusivity Profiles

Two more vertical diffusivity profiles were taken into consideration

besides the constant diffusivity value. They are namely the log diffusivity profile and the lake diffusivity profile.

The log diffusivity profile was derived by Reynold's analogy applied to the log velocity profile. The form of the diffusivity profile is described by Yotsukura and Fiering (Ref. 13). They took in consideration the Reynold's analogy and obtained the following equation: $k = y(1-y)/2.5$, where k = vertical diffusivity and y = distance in vertical direction.

We have assumed the same form of equation and have arrived at the following equation:

$$D(z) = 0.6\ z\ (1-z) \qquad (2.15)$$

where the constant has been picked to make the vertically averaged $\overline{D}_z = 0.1$. Since D(z) = 0 for any z cannot be used, for reasons to be discussed later, it is evident from the equation (2.15) that we need to define values of diffusivity at z = 0 and z = 1. Two alternatives were considered. It was assumed that the value of diffusivity below z = 0.03 and above z = 0.97 is constant. The constants used are the values obtained from equation (2.15) for a dimensionless height of 0.03 and 0.97. It can be seen from the equation that values of D(z) at z = 0.03 and z = 0.97 are the same. Another alternative had the same kind of consideration, but the values of diffusivity were considered constant below z = 0.1 and above z = 0.9, using the constant value from Equation (2.15) for z = 0.1 and z = 0.9. These diffusivity profiles were considered only with the linear velocity profile.

The lake diffusivity profile was so named as the lake velocity profile was taken into consideration to derive this particular diffusivity profile. As there was a reverse flow in the actual lake velocity profile, to have the velocity non-negative, Natarajan added the maximum negative velocity to the values of velocity for all the points in the z direction. By doing this, a zero velocity at z = 0.3 (the point where maximum negative velocity occurs) is obtained. This lake diffusivity profile was considered to vary from points z = 0.3 to z = 1.0 and to be constant everywhere below z = 0.3. Between z = 0 and z = 0.3 the value of diffusivity is a constant 0.05, and above z = 0.3 the diffusivity profile follows the equation:

$$D(z) = 0.05 + 0.2041\ (z - 0.3) \qquad (2.16)$$

This profile was used with all three velocity profiles.

It should be pointed out that both these diffusivity profiles, when averaged in the z direction, give the average value of $\overline{D}_z = 0.1$.

2.5 An Alternate Method for Calculating D_x^*

As was discussed in the background section, a second computer program was written for the solution of the equations given by Csanady (Ref. 3). Results from the numerical method applied to equation (2.1) describe the first phase of transport. Values of σ_x^2 as a function of time can be obtained from these results. The effective horizontal dispersion coefficient D_x^* can be calculated from the values of σ_x^2. Beginning of the second phase of transport was described as when the effective horizontal dispersion coefficient reaches a constant value. This method will provide another means for calculating the effective horizontal dispersion coefficient for the second phase of

transport. Knowing this value for the effective horizontal dispersion coefficient makes it possible to determine from the results of the previous program when the system is entering the second phase of transport.

The method for this program was derived from the series of equations given in Csanady (Ref. 3) for shear-augmented diffusion in a channel. He also followed the solution with moments of the distribution. The first moment was described as,

$$\theta_{1,o}\ (z,t) = q/h\ [ut + \phi\ (z)] \tag{2.17}$$

where $\theta_{1,o}$ is the first moment of the distribution, q is the total amount of material released, h is height and t is a dimensionless time. $\phi(z)$ as shown by Csanady, is obtained from

$$\phi(z) = \int_{z_1}^{z} \frac{dz}{D(z)}\ (\bar{u}-u)\ dz \tag{2.18}$$

with the lower limit z_1 defined so as to give,

$$\int_0^{1.0} \phi(z)\ dz = 0.0 \tag{2.19}$$

where $\bar{u} = \int_0^{1.0} u\ (z)\ dz.$

The effective horizontal dispersion coefficient D_x^* is defined as,

$$D_x^* = \int_0^{1.0} u(z)\ \phi\ (z)\ dz \tag{2.20}$$

Equations (2.18), (2.19) and (2.20) are solved for D_x^*. First, in order to get $\phi\ (z)$ equations (2.18) and (2.19) must be solved. Once $\phi\ (z)$ is obtained, equation (2.20) can be solved for D_x^*.

For illustrative purposes, consider a mesh size of Dz = 0.1.

$\bar{u}$ was obtained using the Trapezoidal rule as

$$\bar{u} = \int_0^{1.0} u(z)\, dz = \sum_{K=2}^{12} \frac{Dz}{2.0} [u(K+1) + u(K)]$$

Here K=2 corresponds to z = 0 and K = 12 corresponds to z = 1. Equation (2.18) was evaluated at each point in the z direction and a set of equations for $\phi(z)$ was obtained with z_1 as an unknown parameter. Let us call

$$I(0.1) = \frac{\Delta z}{2.0} [2\bar{u} - u(0.1) - u(0.0)] \simeq \int_0^{0.1} (\bar{u} - u)\, dz.$$

Similarly,

$$I(0.2) = \frac{\Delta z}{2.0} [2\bar{u} - u(0.1) - u(0.2)] + I(0.1) \simeq \int_0^{0.2} (\bar{u} - u) dz.$$

Thus, a set of equations are obtained such as:

$$I(0.0) = 0.0$$

$$I(0.1) = \frac{\Delta z}{2.0} [2\bar{u} - u(0.1) - u(0.0)]$$

$$I(0.2) = \frac{\Delta z}{2.0} [2\bar{u} - u(0.2) - u(0.1)] + I(0.1) \quad \text{And, so on to}$$

$$I(1.0) = \frac{Dz}{2.0} [2\bar{u} - u(1.0) - u(0.9)] + I(0.9)$$

Now

$$\phi(z) = \int_{z_1}^{z} \frac{I(z)}{D(z)}\, dz$$

Picking a value of $z_1 = 0.5$, then

$$\phi(0.0) = \int_{0.5}^{0.0} \frac{I(z)}{D(z)}\, dz$$

This integral can be written as

$$\phi(0.0) = -\int_{0.0}^{0.1} \frac{I(z)}{D(z)}\, dz - \int_{0.1}^{0.2} \frac{I(z)}{D(z)}\, dz \ldots - \int_{0.4}^{0.5} \frac{I(z)}{D(z)}\, dz$$

Thus, a set of equations from $\phi(0)$, ϕ (.1), ϕ (.3) ... to ϕ (1.0) is obtained. This set of equations is then integrated in the z direction from 0 to 1 and compared with 0.0 to see if equation (2.19) is satisfied. If it is not equal to zero a new value of z_1 is picked using a Newton-Raphson method and calculations are carried on until the value of the integral equals zero. Once z_1 is obtained, then equation (2.20) is evaluated with the set of ϕ (z) equations.

In all calculations the Trapezoidal rule was used for evaluation of the integrals. In actual calculations a grid size of Dz = 0.005 was used. Different grid sizes were tried, but this one was the largest which gave very accurate results.

Appendix 1 shows the analytical solution for D_x^* for the log diffusivity profile and the linear velocity profile. Appendix 3 shows the listing of the computer program for the method discussed in this section.

CHAPTER III

RESULTS AND DISCUSSION

Results will be presented in turn for each velocity profile with different diffusivity profiles. Mainly, each velocity profile was combined with a constant $D_z = 0.1$ and the lake diffusivity profile. Since all diffusivity profiles give $\overline{D}_z = 0.1$, it will be possible to compare the effect of constant D_z vs. variable D_z when both have the same average value. Only the linear velocity profile was combined with the log diffusivity profiles. In Figures 6.1 through 7.4, numerals I, II and III correspond to the constant, the lake and the log diffusivity profiles respectively.

3.1 Horizontal Distribution of Concentration for the Linear Velocity Profile

There are four different situations to be considered, the linear profile with constant diffusivity, the two log diffusivity profiles and the lake diffusivity profile.

Concentration at any time is a function of z and x. Here in this section, the major interest is to study the variation of C with x so the C values will be plotted in the x direction at $z = 0.5$.

Figures 6.1 to 6.4 give the concentration distribution for the linear velocity profile at different times. Because of the large amount of computer time required for the linear velocity profile, with

the lake diffusivity profile, there were no results obtained for that example beyond dimensionless time = 5. Figure 6.5 represents the concentration values in the x direction for constant diffusivity and the log diffusivity profile at t = 8.

Examining Figures 6.1 to 6.5, it is noticeable that there is only one curve shown for the log diffusivity profiles derived from two different sets of end values. The reason for this is that both the sets have given identical results. Thus, they coincide with each other on the graph.

Figures 6.1 to 6.4 show concentration values in the x direction for the linear velocity profile with constant diffusivity, the log diffusivity profile and the lake diffusivity profile. Examination of Figure 6.1 shows that the lake diffusivity profile gives the highest peak, then the log diffusivity profile, and finally the constant value of diffusivity gives the lowest peak. Figures 6.2, 6.3 and 6.4 give the concentration distribution in the x direction at time 2, 4 and 5. Examination of these figures shows that the pollutant starts spreading out. Note that there is a change of scale in the x direction. As time progresses, for all the three diffusivity profiles, the skewness starts to smooth out and the concentration distribution approaches the normal distribution. At t = 1 there is a narrow distribution while at t = 5 it has spread out with lower peak. Examining Figure 6.5 it can be seen that pollutant has spread out well in the x direction. Again, this confirms the approach to a normal distribution.

3.2 Horizontal Distribution of the Log Velocity Profile

Figures 7.1 through 7.4 show the concentration distribution in the

x-direction at different times. Here also the lake diffusivity profile gives the higher peak in the x-direction for all time units. As time progresses, pollutants start to distribute over the x-direction. Concentration peaks are lower at large time. There is no change in scale in concentration scale but there is a change in the x-direction scale as pollutants move along. We observe the same kind of behavior as for the linear profile. One thing that is important to notice is that there is less spread of pollutants here than for the linear velocity profile. The peak concentration value at time $t = 1$ is 0.45 for the lake diffusivity profile and 0.37 for a constant diffusivity, while for the linear velocity profile at $t = 1$ the peak concentration value is 0.195 for the lake diffusivity profile and 0.164 for constant diffusivity. Thus, there is a considerable difference in spread. Moreover, it is noticeable from Figures 7.1 through 7.4 that as time progresses, the concentration distribution approaches a normal distribution. It is also evident that the lake diffusivity profile takes longer time than constant diffusivity to approach a normal distribution.

3.3 Horizontal Distribution of Concentration for the Lake Velocity Profile

Concentration values in the horizontal direction are plotted at different times for constant diffusivity and the lake diffusivity profile. Figures 8.1 through 8.4 show the distribution at times 1, 2, 4 and 6. Here it is interesting to note that the lake diffusivity profile no longer has the highest peak. Now the constant diffusivity

gives the highest peak. Again for the lake velocity profile it is true in Figures 8.1 through 8.4 that there is a narrow distribution followed by a long tail at the upstream end. This is quite opposite from the log velocity profile (Figures 7.1 through 7.4) where there is a long tail at the downstream end followed by a narrow distribution at the upstream end. Once again as time progresses, for both the diffusivity profiles, the concentration profile is losing its skewness and gradually approaches the normal distribution.

3.4 Vertical Concentration Distribution for the Linear Velocity Profile

Vertical concentration distribution was demonstrated by a series of graphs made of concentration versus z at a given x. x was picked from the horizontal concentration distribution graphs. It is the x location where maximum concentration occurred at a given time. At this value of x (called x_m) concentration was plotted against z. Figures 6.6 through 6.10 show the vertical variation in concentration for the linear velocity profile combined with the constant, log and lake diffusivity profiles at different times. Vertical concentration profiles were plotted at the same times as for the horizontal distribution plots. Examining these figures it is evident that as time progresses the vertical variation in concentration becomes smaller, eventually leaving a straight line in the vertical direction. It is also evident from the graphs that the constant diffusivity and the log diffusivity profiles give the same type of results as they follow very closely to each other at all times except t = 2. The lake diffusivity

profile starts with large variation in the vertical direction and moves toward small variations. However, the vertical variation is always greater compared to the other diffusivity profiles. There is some variation in the z direction even at time t = 5 for the lake diffusivity profile. Besides this particular combination also required large computer time. Because of large consumption of computer time it was not possible to get results beyond t = 5 for this combination. There are only two curves (practically straight lines) in Figure 6.10 for constant diffusivity and the log diffusivity profile. There is no more vertical variation at this particular time. The pollutant has spread over the z direction uniformly. Except at t = 2, the maximum value of concentration occurs at the same x for constant diffusivity and the log diffusivity profile.

3.5 Vertical Concentration Distribution for the Log Velocity Profile

Figures 7.5 through 7.8 show the vertical variation in concentration for the log velocity profile with constant diffusivity and the lake diffusivity profile at different times. Each plot represents the concentration distribution in the z direction at x_m as in Section 3.4

Examining Figures 7.5 through 7.8 it is observed that as time progresses variation in the vertical direction decreases and for constant diffusivity it shows practically no variation at t = 6. There is still a little variation in the vertical direction for the lake diffusivity profile. Thus, pollutant has spread uniformly in the z direction for constant diffusivity, while for the lake diffusivity profile there is still some more time required for uniform spread.

3.6 Vertical Concentration Distribution for the Lake Velocity Profile

Figures 8.5 through 8.8 represent the vertical concentration distribution of the lake velocity profile with constant diffusivity and the lake diffusivity profile at different times. It is evident from these figures that they follow the same kind of pattern as the log velocity profile and show small variation in vertical direction as time progresses. Plots were made at time 1, 2, 4, and 6. Figure 8.8 shows that there is still a little variation in the z direction for constant diffusivity, while the lake diffusivity profile gives almost a straight line. This behavior is quite opposite from the one observed for the linear and the log velocity profiles. Here the lake diffusivity profile gives uniform distribution in the z direction, while for constant diffusivity there is still some variation even at time t = 6.

3.7 Combined Effects of Velocity and Diffusivity Profiles

It is interesting to learn the combined effects of velocity and diffusivity profiles from Figures 6.1 through 8.4. The lake velocity profile combined with the lake diffusivity profile sets a good example to study. In cases with the linear and the log velocity profiles combined with the lake diffusivity profile gave high peaks (Figures 6.1 through 6.4 and 7.1 through 7.4) in the horizontal direction while for the lake velocity profile combined with constant diffusivity gave a high peak (Figures 8.1 through 8.4). In the vertical direction it is true for the linear and the log velocity profiles that for constant diffusivity after t = 4 there is no variation in the z direction, but for the lake diffusivity profile there is still some variation (Figures

6.9 and 7.8). The lake velocity profile produces the opposite results where there is no concentration variation in the z direction at larger time for the lake diffusivity profile, but for constant diffusivity there is still some variation in the z direction (Figure 8.8). It does show here that the particular combination of velocity and diffusivity profiles has great importance on the overall spread.

3.8 D_x^* Values for the Linear Profile

Tables 3.1 to 3.3 give the values of σx^2 for the linear profile for constant diffusivity, the log diffusivity profile and the lake diffusivity profile. Figures 9.1 through 9.3 represent the graphical view of the same.

Examining Figure 9.1 one can see that σx^2 does not vary linearly with time. According to Aris, for any velocity profile and a finite D_z value, D_x^* reaches an asymptotic constant value. This means that after a long time σx^2 varies linearly with time and $\frac{d\sigma x^2}{dt}$ becomes a constant. By definition

$$D_x^* = \frac{1}{2} \frac{d\sigma_x^2}{dt}$$

Values of D_x^* will be obtained from the slope of Figures 9.1 through 9.3. These values were matched with the values from another program which was written for the series of equations from Csanady.

From Figure 9.1 it is evident that σx^2 varies linearly with time after t=3. We can get the slope of the line which will give the value of $\frac{d\sigma_x^2}{dt}$. Dividing this value by 2 will give the value of D_x^*.

From Figure 9.1, the slope = 0.172 and therefore

$$D_x^* = 1/2\ (0.172) = 0.086$$

This represents the D_x^* value for the linear velocity profile and constant diffusivity.

Figure 9.2 represents the values of σx^2 plotted against t for the linear velocity profile and the log diffusivity profile.

The slope = 0.1443 and

$$D_x^* = 1/2\ (0.1443) = 0.0722$$

Similarly, Figure 9.3 represents the graph of σx^2 versus t for the linear velocity profile and the lake diffusivity profile.

The slope = 0.2036 and

$$D_x^* = 1/2\ (0.2036) = 0.1018$$

3.9 D_x^* Values for the Log Velocity Profile

As described in the previous chapter D_x^* values have been calculated for the log velocity profile combined with constant diffusivity and the lake diffusivity profile.

Tables 3.4 and 3.5 represent the values of σx^2 for the log velocity profile combined with the constant diffusivity and the lake diffusivity profile. Figures 9.4 and 9.5 represent the graphs of σx^2 versus t for the same.

Figure 9.4 represents the σx^2 values at different t for the log velocity profile with constant diffusivity. We can say that σx^2 varies linearly with time after t = 3.

D_x^* Values

Diffusivity Profile	Linear Profile	Log Profile	Lake Profile
Constant	0.086	0.0387	0.047
Log	0.0722	--	--
Lake	0.1018	0.0543	0.0483

3.11 D_x^* Values from Check Program

A computer program was written for values of D_x^* by evaluating the series of equations from Csanady. This was discussed in the second chapter. The following values of D_x^* for different velocity profiles were obtained with different diffusivity profiles.

D_x^* Values

Diffusivity Profile	Linear Profile	Log Profile	Lake Profile
Constant	0.0833	0.0368	0.0536
Log	0.0691	--	--
Lake	0.1000	0.0524	0.0487

These values of D_x^* for different combinations match well with the calculated values of D_x^* from the main program. The small differences between these two values can probably be accounted for by the numerical error in the main program. The following accuracy criteria are a good explanation for the numerical error.

Fromm's scheme for the approximation of the convective term has fourth order accuracy in space and second order accuracy in time. The

approximation for the diffusion term is only first order in time and second order in space. The boundary condition approximation is also second order in space. Use of Simpson and Trapezoidal rules also adds some criteria for numerical error. It is difficult to evaluate the combined effect of the above accuracy criteria, but the numerical error for one step is of the order $O(DZ^2 + Dt) = O(0.1^2 + 0.01)$ $O(0.01)$. The difference between the two calculated values of D_x^* is well within this error. At this point it is also appropriate to present some explanation of stability criteria.

For stability it is required that $u \frac{\Delta t}{\Delta x} < 1$ for the convection term. Also, the scheme for the approximation of the diffusivity term requires the following criterion for stability,

$$D \frac{Dt}{DZ^2} < \frac{1}{2}$$

It is difficult to analyze mathematically the stability condition for the total scheme. The diffusion approximation requires a smaller Dt than the convective criterion. In any event examining grid sizes in the table on page 13 in the previous chapter there has been no violation of any of these stability criteria. Dt was always less than the requirement of the individual criterion. In some cases, Dt had to be much smaller than the individual criterion allow. This is thought to be due to a complex interaction between the convective and diffusive terms.

3.12 Correlation of K_e and t_1

It is shown in Appendix II that based on equation (A2:1), the approach of $\frac{d\sigma_x^2}{dt}$ to a constant value is exponential with exponent

$-\alpha_1 \overline{D}_z^* t$, where α_1 is generally the smallest eigenvalue in a certain Sturm-Liouville problem, and $\overline{D}_z^*$ is the mean non-dimensional cross-plane diffusion. Dimensional time, t_1, to reach phase II transport thus scales as

$$t_1 = \frac{h^2}{\alpha_1 \overline{D}_z}$$

where $\overline{D}_z$ in this equation is the mean dimensional diffusivity. When phase II is reached, the z direction can be replaced by an effective dispersion coefficient in the x direction, D_x^*. This, by definition, is

$$D_x^* = 1/2 \frac{d\sigma^2}{dt}$$

and can be evaluated from the solution for C in equation 2.3. A more direct approach is to compute D_x^* by the method given by Csanady (Ref. 3). The method is described in the previous chapter. If equations (2.19) and (2.20) are non-dimensionalized it can be seen that

$$K_e = C_1 \frac{h^2 u_{max}^2}{\overline{D}_z}$$

where C_1 is determined from the equation (2.20) with $\overline{D}_z^* = 1.0$.

As all the values of C_1 are known from the previous section, K_e can be evaluated for each case.

For example, the value of C_1 for the linear velocity profile and constant diffusivity can be calculated as follows. The value of D_x^* from the slope of Figure 9.1 is 0.086. This is sufficiently close to the more accurate value of 0.0833 obtained analytically and also by the dimensionless form of equation (2.19) and (2.20). Now

$$K_e = C_1 \frac{h^2 u_{max}^2}{\overline{D}_z}$$

and

$$C_1 = D_x^* \times 0.1$$

The factor 0.1 must be included because the value of $D_x^* = 0.0833$ was obtained using $\overline{D}_z^* = 0.1$ instead of 1. Therefore,

$$C_1 = 0.0833 \times 0.1 = 0.00833$$

Figure 6.8 indicates that by t = 4, the vertical concentration variations have become quite small. Figure 9.1 shows that by t = 4, σx^2 has approached an approximate linear growth rate. Thus,

$$\alpha_1 \overline{D}_z = 1/4$$

and

$$\alpha_1 = 2.5 \text{ since } \overline{D}_z^* = 0.1$$

Therefore,

$$t_1 = \frac{h^2}{2.5 \times \overline{D}_z}$$

Values of C_1 and α_1 can be obtained for each combination of velocity and diffusivity profile. Table 3.8 summarizes these values of C_1 and α_1. More will be said about α_1 and C_1 in the discussion section.

3.13 Computer Time

A large amount of computer time was used for the lake diffusivity profile with either of the velocity profiles. The linear velocity profile combined with constant value of diffusivity used 90 minutes of computer time until time = 14. Also the linear velocity profile with the log diffusivity profile used 90 minutes of computer time to

give results until time = 12. Dt was kept constant and so was DZ. The value of DX was changing with time. About 380 minutes of computer time were used to get results until time = 5 for the linear velocity profile with the lake diffusivity profile. A small Dt had to be used in order to get the satisfactory results at different times. Use of a larger Dt value made the system unstable. A value of Dt = 0.001 was used.

The log velocity profile was the one which used the largest computer time in all three velocity profiles. Even with constant diffusivity a time step Dt = 0.005 had to be used. The required computer time was 200 minutes to get the results until time t = 8. The log velocity profile with the combination of the lake diffusivity profile used the largest computer time, 618 minutes, to give the results until t = 6. Dt = 0.002 was used. Dt could never be made larger than .002, otherwise the system became unstable. This shows that this particular combination has some peculiar combined effect which required the use of the smallest time step.

The lake diffusivity profile along with constant diffusivity used 120 minutes of computer time to give us the results until t = 12. Here the larger time step Dt = 0.01 was used. The lake velocity profile combined with the lake diffusivity profile used 120 minutes of computer time and gave results until t = 6. Here also we were able to use larger Dt than the log velocity combined with the lake diffusivity profile. Here we used Dt = .005.

Table 3.9 summarizes the computer time for each velocity profile and the use of grid sizes for particular computer runs.

3.14 Discussion

It is evident from the results that in all the three velocity profiles the spreading of pollutant follows the same path. As time increases the narrow distribution starts to spread out. The log and the lake velocity profiles make the concentration distribution somewhat shewed. The log velocity profile gives a skewed distribution in the downstream direction, while the lake velocity profile gives a skewed distribution with a long tail in the upstream direction. The linear velocity profile combined with constant diffusivity and the log diffusivity profile gives a symmetric distribution while with the lake diffusivity profile a skewed concentration distribution toward the upstream end is obtained.

There is a quantitative difference in the spread of the pollutant for all the three cases. The linear velocity profile has the largest spread in the horizontal direction, compared with the log and the lake velocity profiles.

The linear and the log velocity profiles give more variation in the vertical direction using the lake diffusivity profile than is obtained using the constant diffusivity. A similar effect on the behavior of D_x^* is also observed. D_x^* values are larger using the lake diffusivity profile than those obtained using the constant diffusivity for both the linear and the log velocity profiles. The lake velocity profile behaves opposite to the linear and the log velocity profiles. The lake velocity profile gives more vertical variation of concentration using constant diffusivity than is obtained using the lake diffusivity profile. The D_x^* value using the lake diffusivity profile is less than the D_x^* obtained using the constant diffusivity.

These examples demonstrate that the vertical variation of concentration and the value obtained for D_x^* can significantly depend upon the combination of velocity and diffusivity profiles.

Correlation of K_e and t_1 with α_1 and C_1 also establishes an interesting situation for consideration. In table 3.8 it can be seen that the values of α_1 and C_1 fall in a narrow range. α_1 varies only by a factor of 1.5 and C_1 varies by a factor less than 3.0. Thus t_1 and K_e can be well estimated from these results for a wide range of cases of practical interest. Typical values of height, U_{max} and $\overline{D}_z$ in the western basin of Lake Erie are 900 cm., 30 cm/sec and 5 cm^2/sec respectively. K_e can be calculated as follows from the values of α_1 and C_1 related to the lake velocity and diffusivity profiles:

$$K_e = C_1 \frac{h^2 U^2_{max}}{\overline{D}_z}$$

$$K_e = 0.0049 \frac{(900)^2 (30)^2}{5}$$

$$K_e = 7.14 \times 10^5 \ cm^2/sec$$

This value of K_e can be compared to the values calculated by Murthy (Ref. 8) from his dye release experiments in Lake Ontario. To find the comparable value of K_e from his results, a reference length is required. This can be calculated as follows:

$$t_1 = \frac{h^2}{\alpha_1 \overline{D}_z}$$

$$t_1 = \frac{(900)^2 \ cm^2}{2.0x5 \ cm^2/sec} = 81000 \text{ sec}$$

and

$$L = t_1 \times U_{max}$$

$$L = 81{,}000 \times 30$$

$$L = 2.43 \times 10^6 \text{ cm}$$

From Figure 10.1, the extrapolated value of K_e for this reference length is $6.5 \times 10^5 \frac{cm^2}{sec}$.

Other values of K_e and L corresponding to 100, 200, 300, 500, and 700 cm depths can similarly be calculated (C_1, α_1, $\bar{D}_z$, and U_{max} remain the same as in the above example of 900 cm depth). A series of such points is presented in Figure 10.1 along with Murthy's experimental points and a line given by Murthy representing his data in terms of the "4/3 - power law" for diffusion. It can be seen that Murthy's data is reasonably well predicted by these results. The maximum value of h, corresponding to the computed point that gives the largest value of K_e shown on Figure 10.1, is 9 meters which is less than the depth of the thermocline which Murthy measured at about 10-20 meters.

This suggests that horizontal spreading due to vertical shear in the horizontal velocity coupled with vertical diffusion is at least as important as that due to horizontal turbulence. The effect of horizontal velocity gradients in elongating dye patches in his experiments was noted by Murthy. It should be emphasized that the points displayed in Figure 10.1 were computed using typical values of $\bar{D}_z$ and U_{max}, and do not necessarily correspond to the conditions of Murthy's experiment.

CHAPTER IV

CONCLUSIONS

The following conclusions are drawn from this study of the combined effect of the velocity and the diffusivity profiles.

It is found that the shape of the velocity profile has little qualitative effect on the horizontal spread of the pollutant. As time progresses, approach to the normal distribution is noticed in all cases studied. Quantitatively the lake velocity profile leads to the slowest rate of horizontal spread.

As time progresses, it is also found, in the vertical direction, that vertical variation becomes small and finally the vertical distribution of concentration becomes uniform. D_x^* is increasing and finally reaches a constant value. Vertical variation in concentration becoming relatively small and D_x^* reaching a constant value are well correlated. Thus, the use of D_x^* reaching a constant value is a good criterion for using vertical averaging, which leads to a two dimensional model, without significant loss of accuracy. D_x^* for use in a two dimensional model can be predicted by this method.

One of the important relationships which has been established is the correlation of the dimensionless results with α_1 and C_1. α_1 is related to the time when D_x^* reaches a constant value. C_1 is related to the constant value of D_x^*. α_1 and C_1 can then be used to obtain t_1 and K_e. t_1 the time for phase I transport, scales as,

$$t_1 = \frac{h^2}{\alpha_1 \overline{D}_z}$$

and K_e, the effective horizontal dispersion coefficient, scales as

$$K_e = \frac{C_1 h^2 U^2_{max}}{\overline{D}_z}$$

α_1, and thus the time for phase I transport mainly depends on $D_z(z)$ and is only weakly affected by u(z) (described in Appendix II). Thus, t_1, time to reach phase II, generally does not depend on the details of the velocity profile. Some situations, such as existence of a thermocline, are not covered by the results given here, since this would represent a vastly different D_z profile from any of the examples. However, in all the cases studied α_1 and C_1 varied within a small range. α_1 varied within a factor of 1.5 and C_1 varied by a factor less than 3.0. Thus, results obtained here can be used to predict t_1 and K_e for a wide range of reasonable velocity and diffusivity profiles. For velocity and diffusivity profiles that are very different from the ones studied here α_1 and C_1 can be calculated by the method used here and new values of t_1 and K_e can be obtained from the above identities.

It was seen in Figure 10.1 that K_e as calculated in this investigation compares favorably with measured horizontal diffusivities in Lake Ontario. The importance of the vertical shear of the horizontal velocity combined with vertical diffusion on horizontal spreading appears to be at least the same as the effect of horizontal turbulence. More information is necessary to decide the dominating factor. It is suggested that an experiment should be performed studying the effects

of both of these phenomena at the same time. Results from this experiment will be helpful to decide the dominating factor.

TABLE 3.1

Linear Velocity Profile

Values of σ_x^2 for Constant Diffusivity

TIME	σ_x^2
t = 1	0.0640
t = 2	0.1945
t = 3	0.3507
t = 4	0.5165
t = 5	0.6860
t = 6	0.8569
t = 7	1.0283
t = 8	1.2000
t = 9	1.3717
t = 10	1.5435
t = 11	1.7153
t = 12	1.8871
t = 13	2.0590
t = 14	2.2309

TABLE 3.2

Linear Velocity Profile

Values of σ_x^2 for Log Diffusivity Profile

TIME	σ_x^2
t = 1	0.0601
t = 2	0.1791
t = 3	0.3155
t = 4	0.4574
t = 5	0.6011
t = 6	0.7452
t = 7	0.8895
t = 8	1.0339
t = 9	1.1782
t = 10	1.3226
t = 11	1.4670
t = 12	1.6113

TABLE 3.3

Linear Velocity Profile

Values of σ_x^2 for Lake Diffusivity Profile

TIME	σ_x^2
t = 1	0.0660
t = 2	0.2083
t = 3	0.4827
t = 4	0.6820
t = 5	0.7838

TABLE 3.4

Log Velocity Profile

Values of σ_x^2 for Constant Diffusivity

Time	σ_x^2
t = 1	0.0318
t = 2	0.0918
t = 3	0.1628
t = 4	0.2379
t = 5	0.3145
t = 6	0.3916
t = 7	0.4691

TABLE 3.5

Log Velocity Profile

Values of σ_x^2 for Lake Diffusivity Profile

TIME	σ_x^2
t = 1	0.0366
t = 2	0.1124
t = 3	0.2068
t = 4	0.3097
t = 5	0.4166
t = 6	0.5253

TABLE 3.6

Lake Velocity Profile

Values of σ_x^2 for Constant Diffusivity

TIME	σ_x^2
t = 1	0.0419
t = 2	0.1168
t = 3	0.2033
t = 4	0.2942
t = 5	0.3868
t = 6	0.4800
t = 7	0.5733
t = 8	0.6684
t = 9	0.7604
t = 10	0.8540
t = 11	0.9476
t = 12	1.0412

TABLE 3.7

Lake Velocity Profile

Values of σ_x^2 for Lake Diffusivity Profile

TIME	σ_x^2
t = 1	0.0429
t = 2	0.1155
t = 3	0.2021
t = 4	0.2946
t = 5	0.3902
t = 6	0.4869

TABLE 3.8

Velocity Profile	Diffusivity Profile	α_1	C_1
Linear	Constant	2.5	0.00833
Linear	Log	2.5	0.00691
Linear	Lake	2.0	0.0100
Log	Constant	2.0	0.00368
Log	Lake	1.7	0.00524
Lake	Constant	1.7	0.00536
Lake	Lake	2.0	0.00487

TABLE 3.9

Run No.	Velocity Profile	Diffusivity Profile	Dx	Dt	Dz	t_{final}	Computer time in Minutes
1	Linear	Constant	0.0125	0.1	0.1	14	83
2	Linear	Log	0.0125	0.1	0.1	12	90
3	Linear	Lake	0.0125	0.1	0.1	5	351
4	Log	Constant	0.0125	0.005	0.1	7	191
5	Log	Lake	0.0125	0.005	0.05	6	620
6	Lake	Constant	0.0125	0.002	0.1	12	120
7	Lake	Lake	0.0125	0.001	0.1	6	198

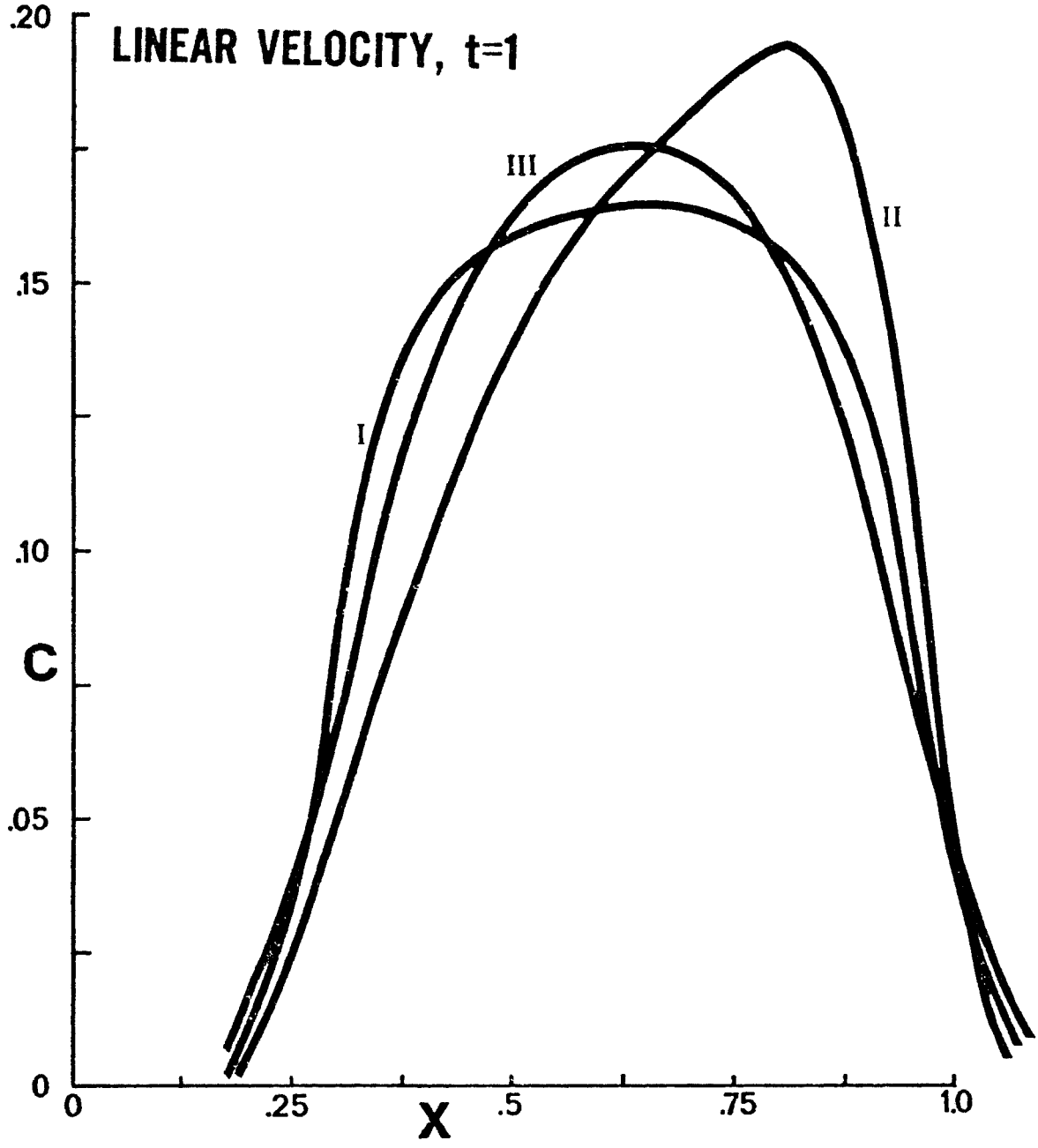

FIGURE 6.1

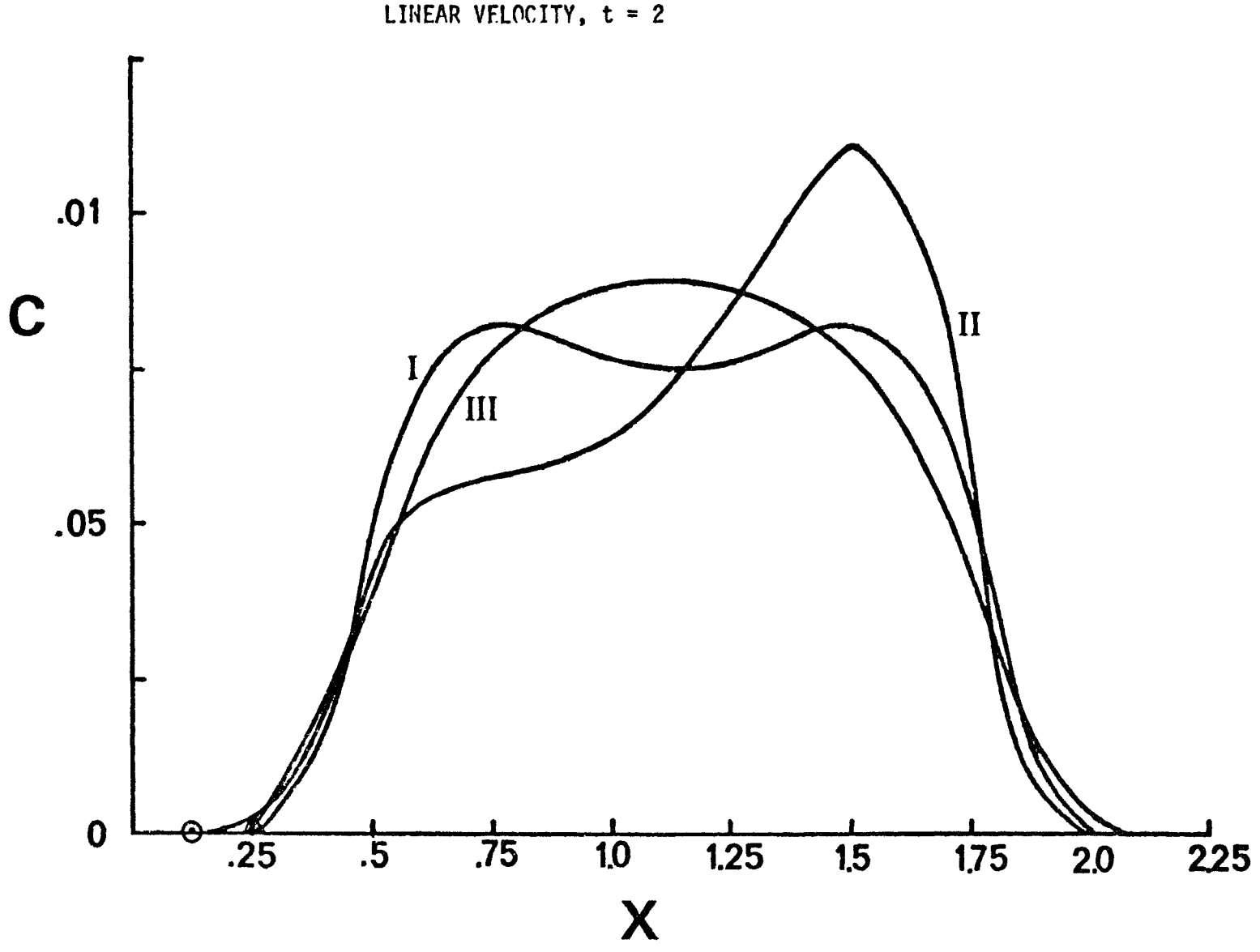

FIGURE 6.2

LINEAR VELOCITY, t = 4

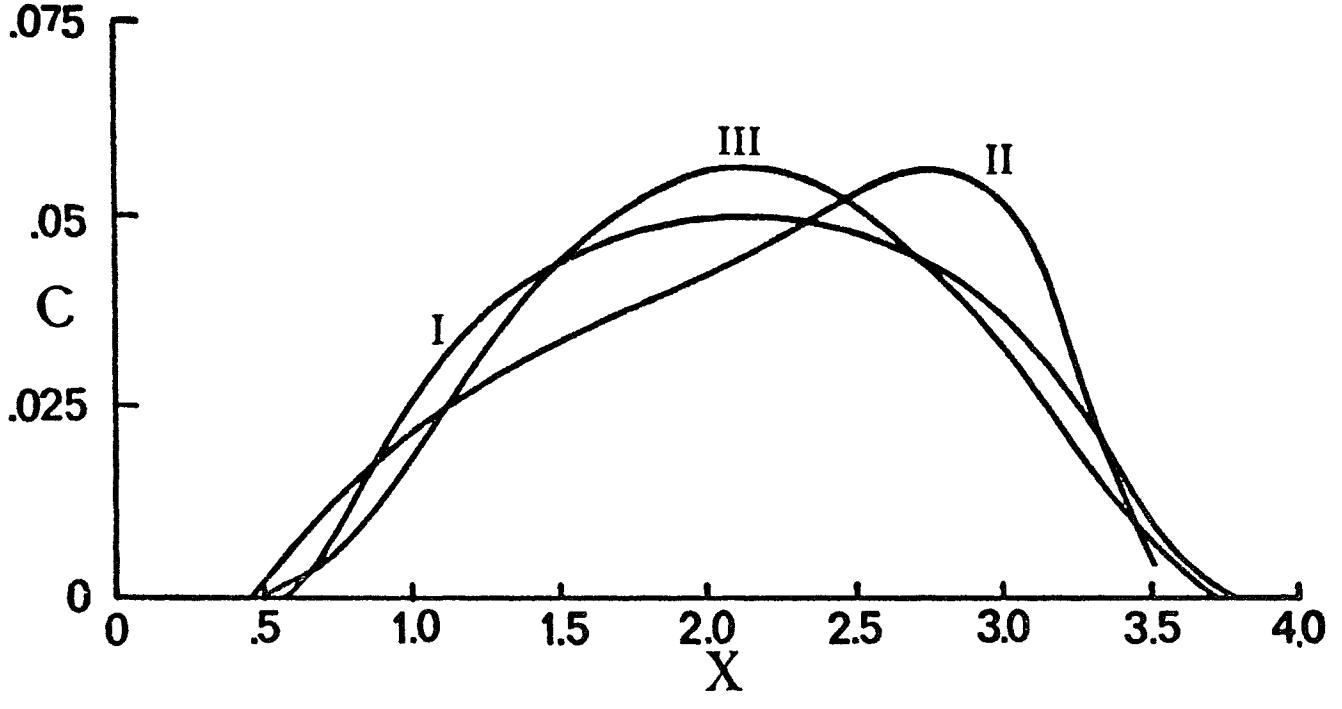

FIGURE 6.3

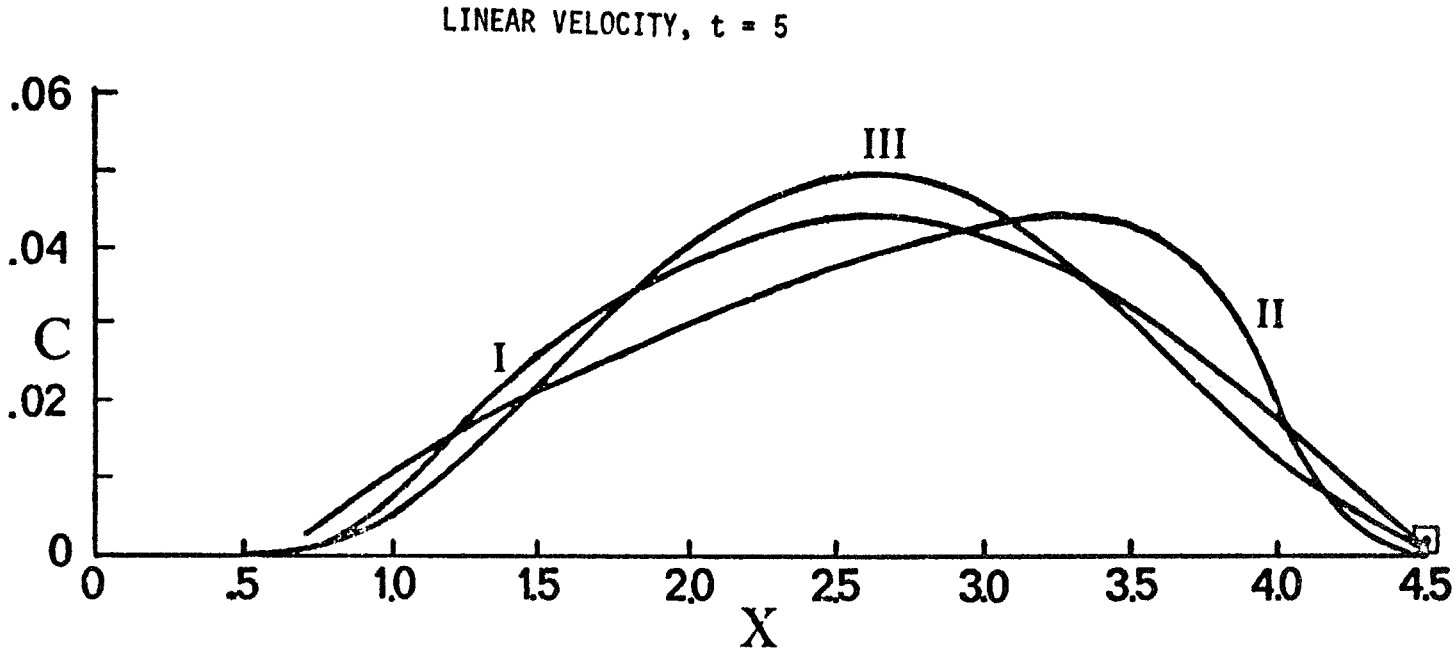

FIGURE 6.4

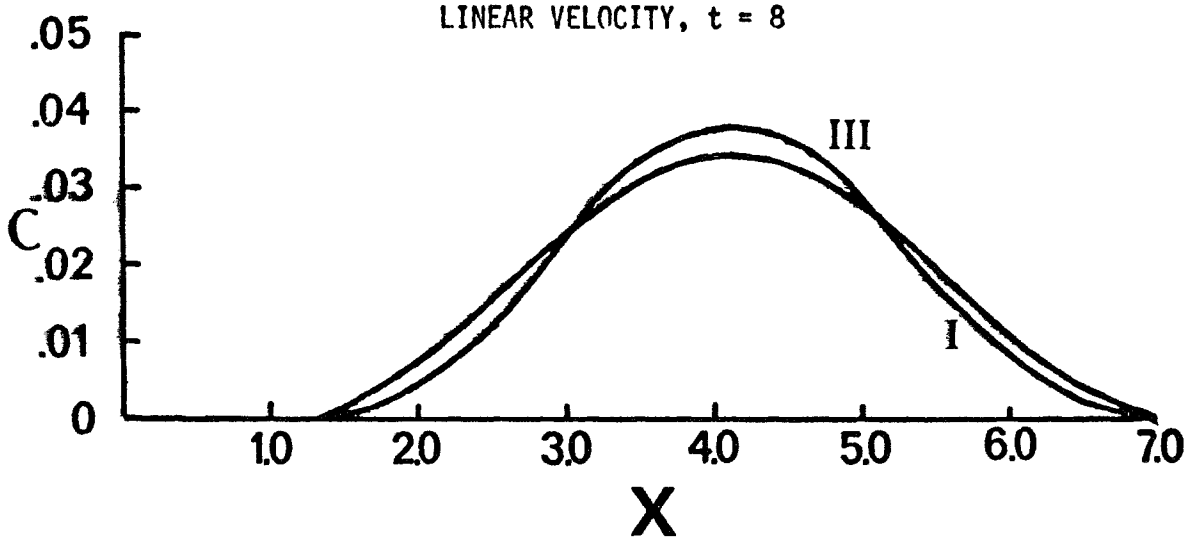

FIGURE 6.5

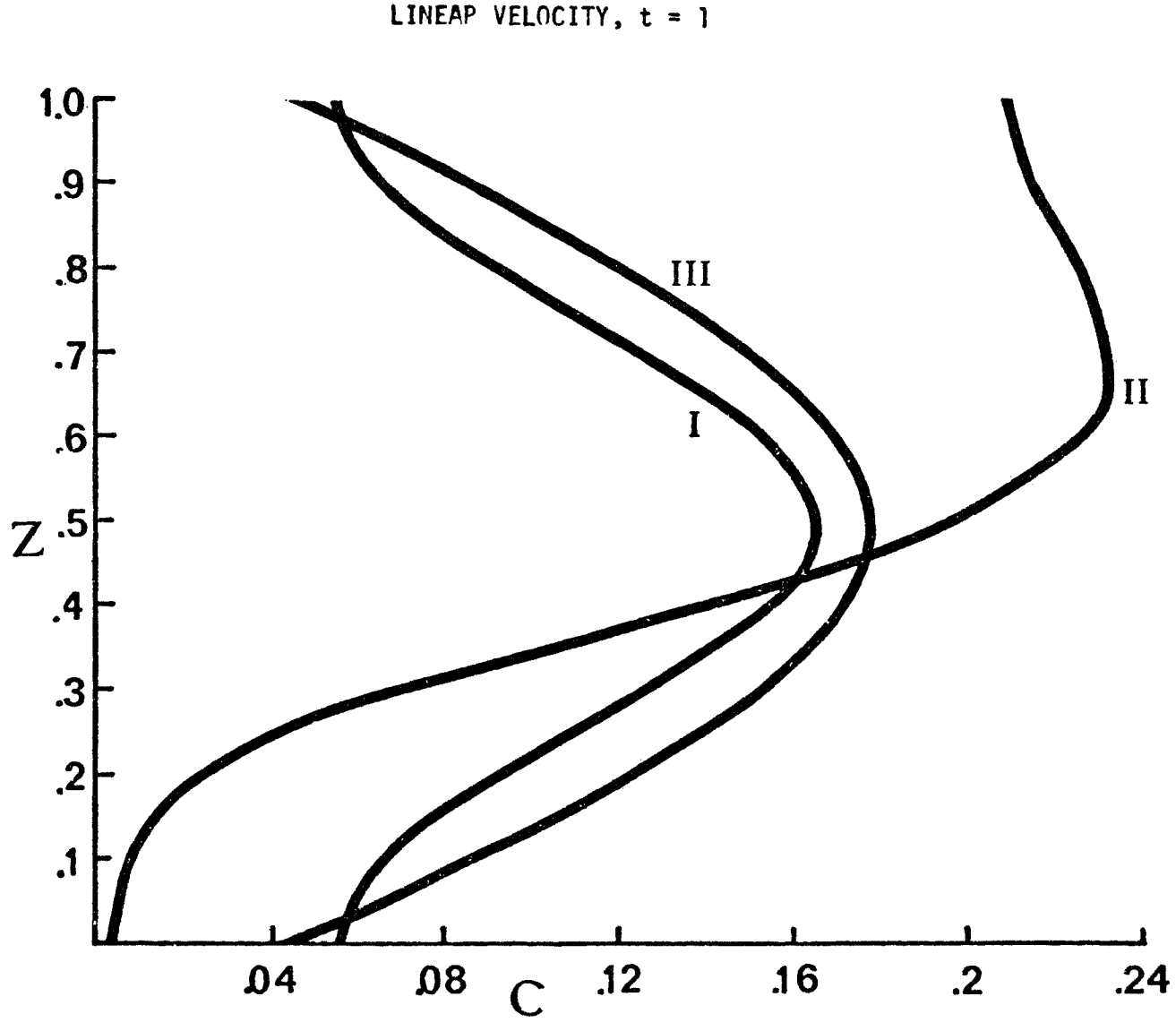

FIGUPE 6.6

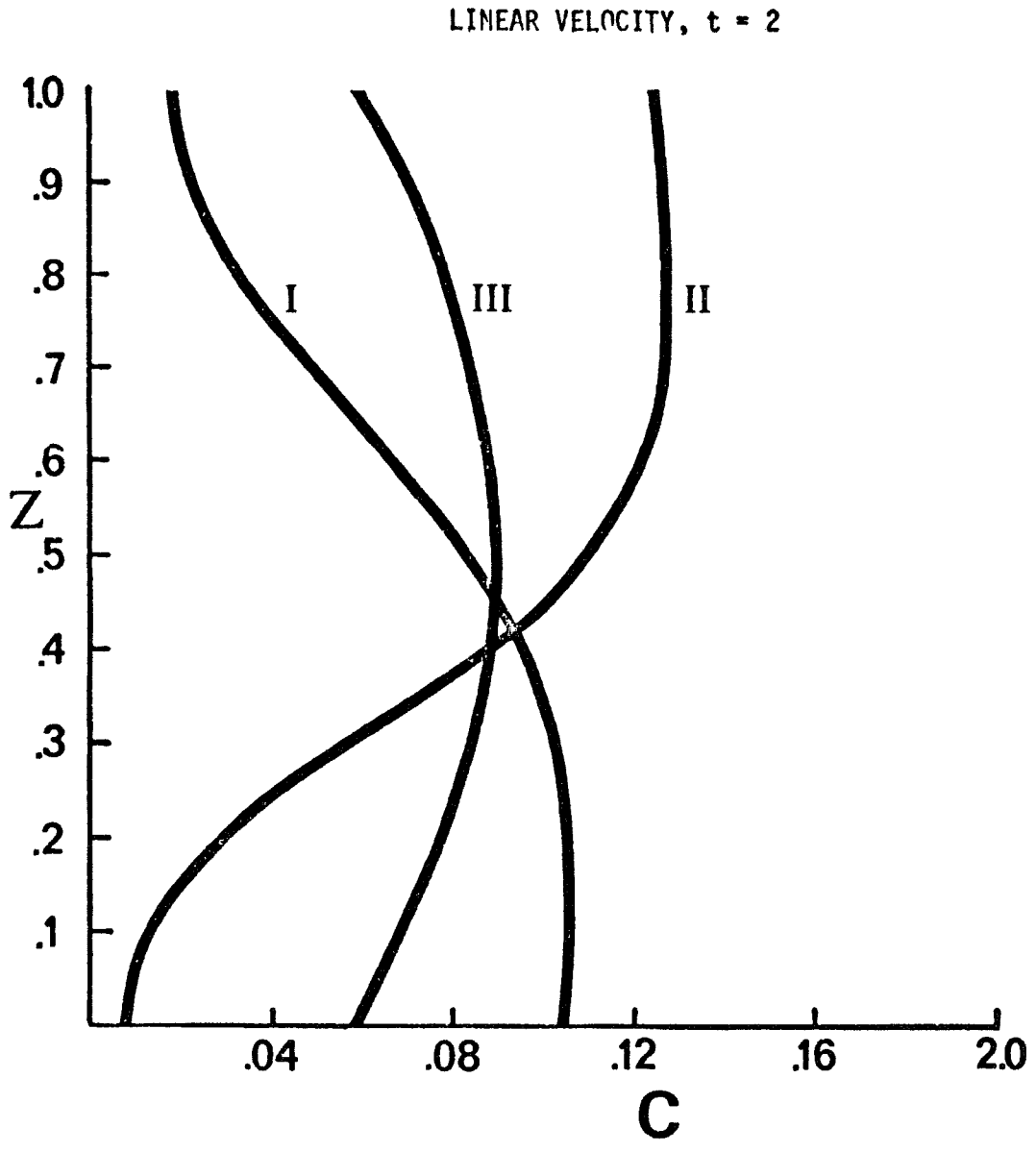

FIGURE 6.7

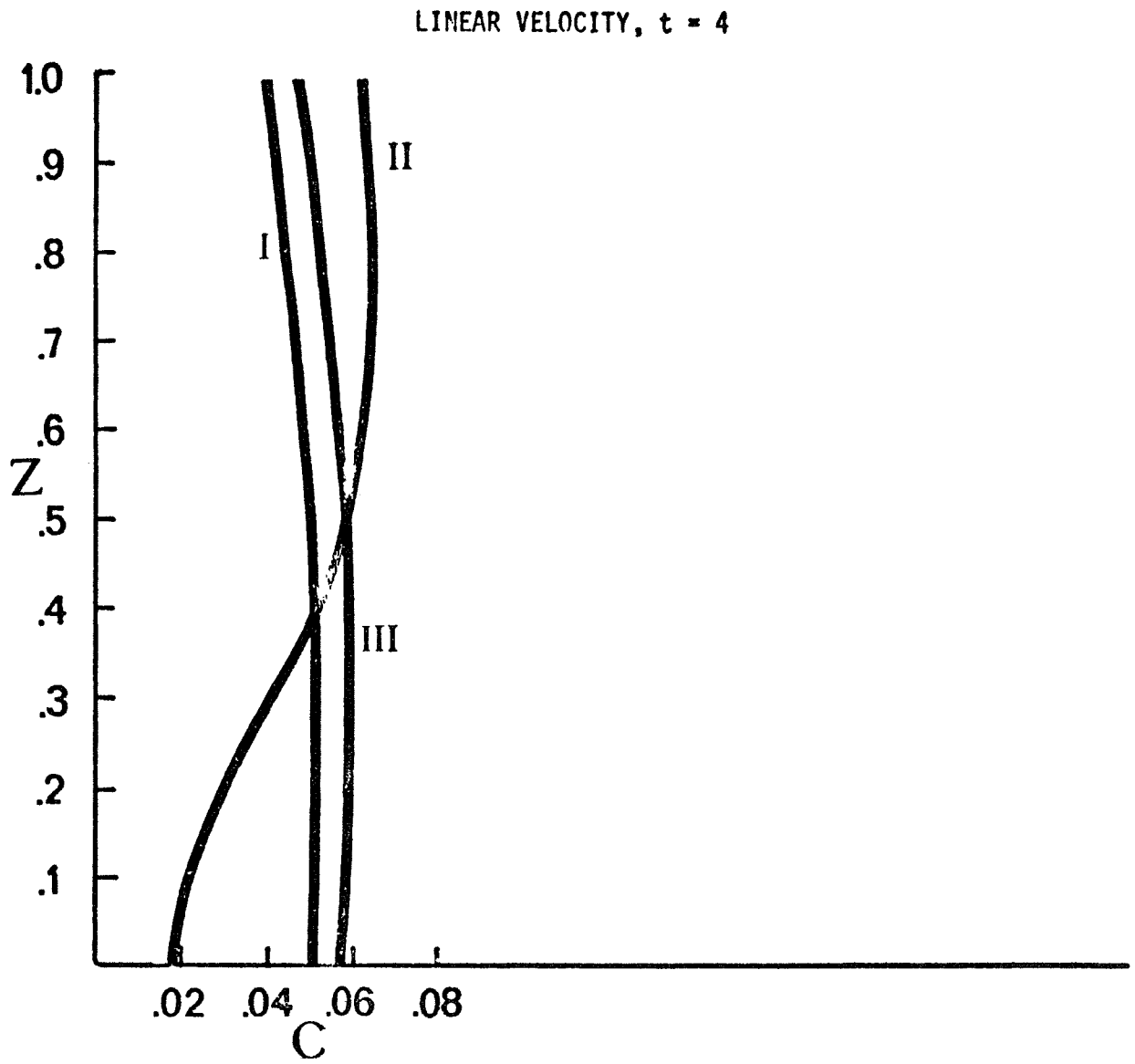

FIGURE 6.8

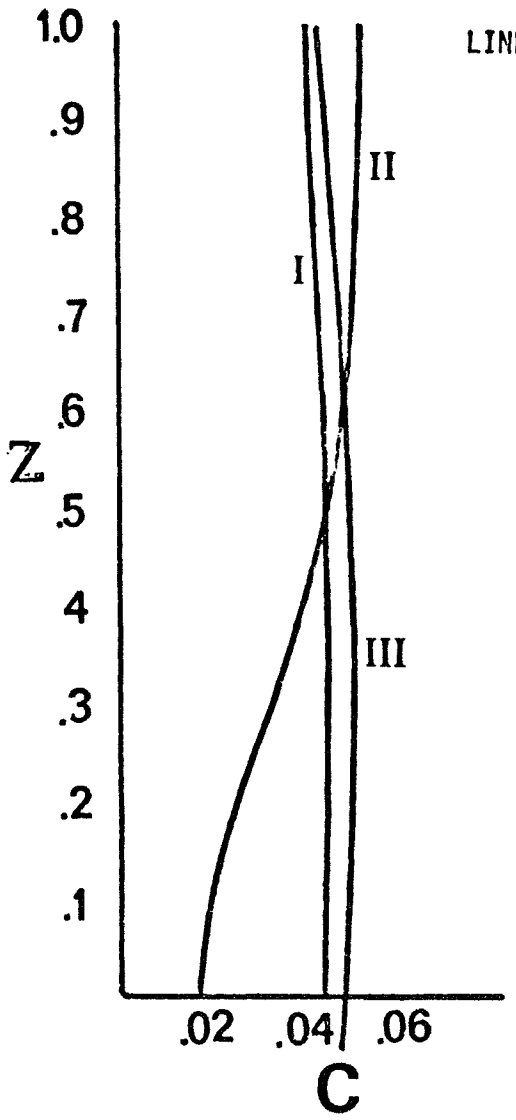

FIGURE 6.9

LINEAR VELOCITY, t = 8

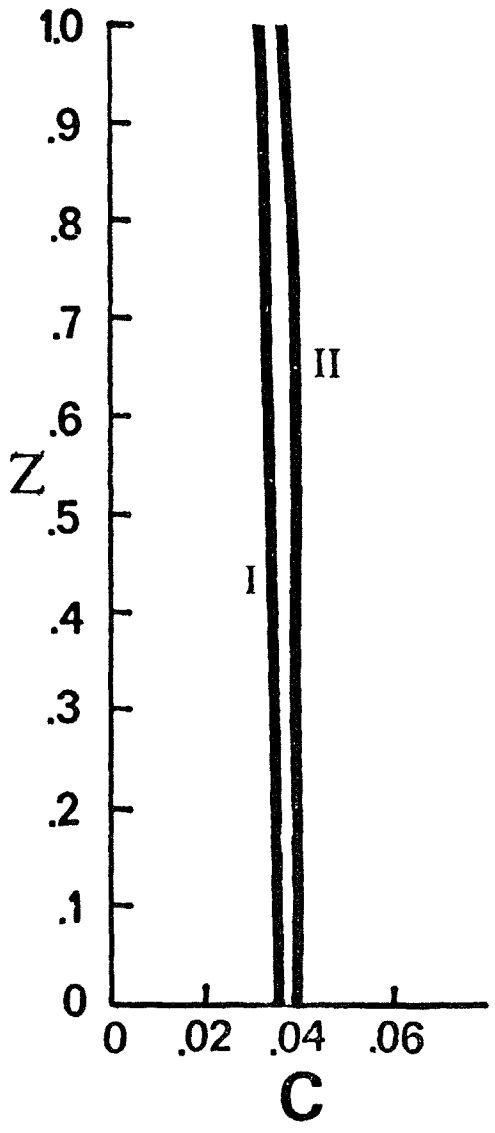

FIGURE 6.10

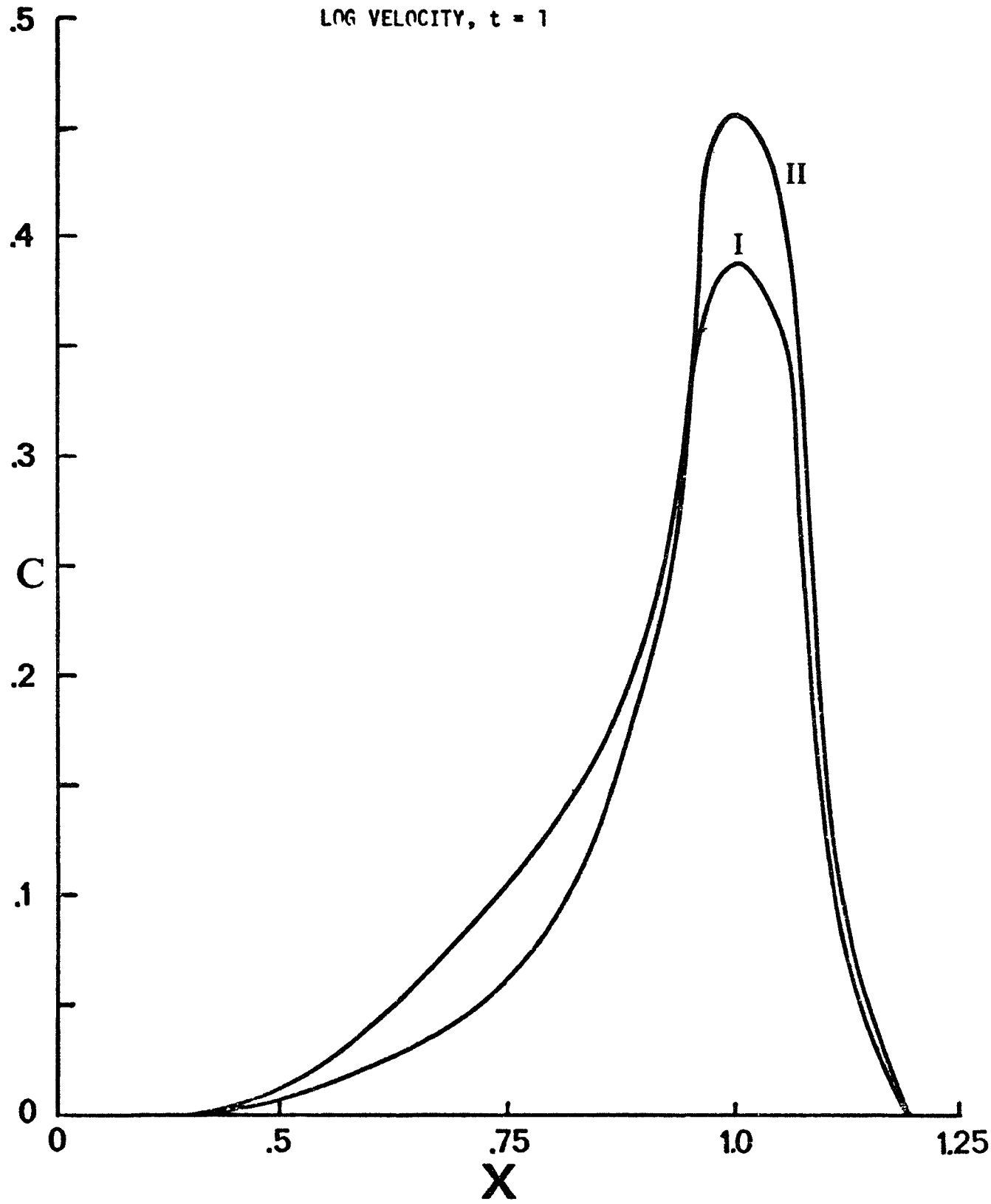

FIGURE 7.1

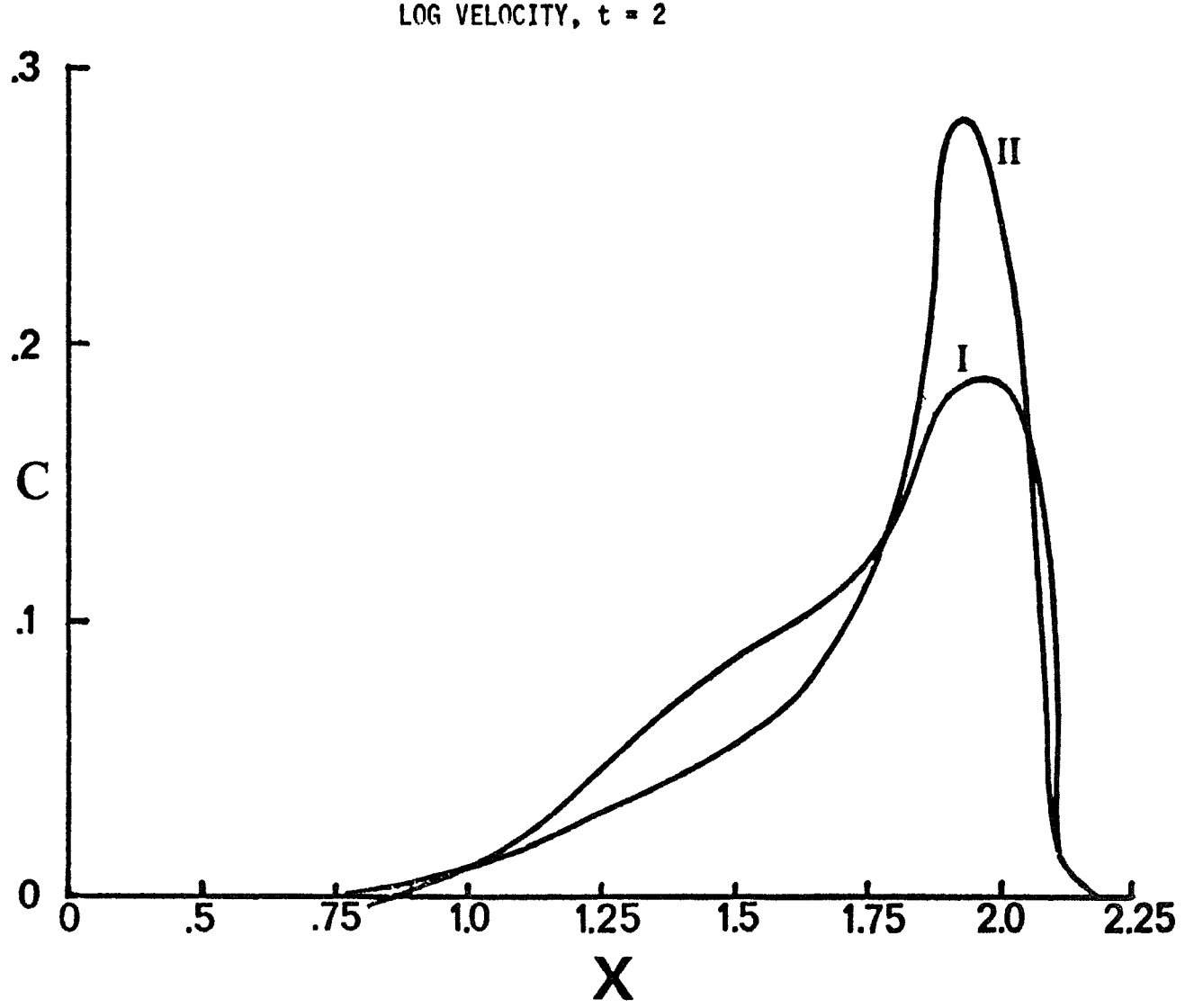

FIGURE 7.2

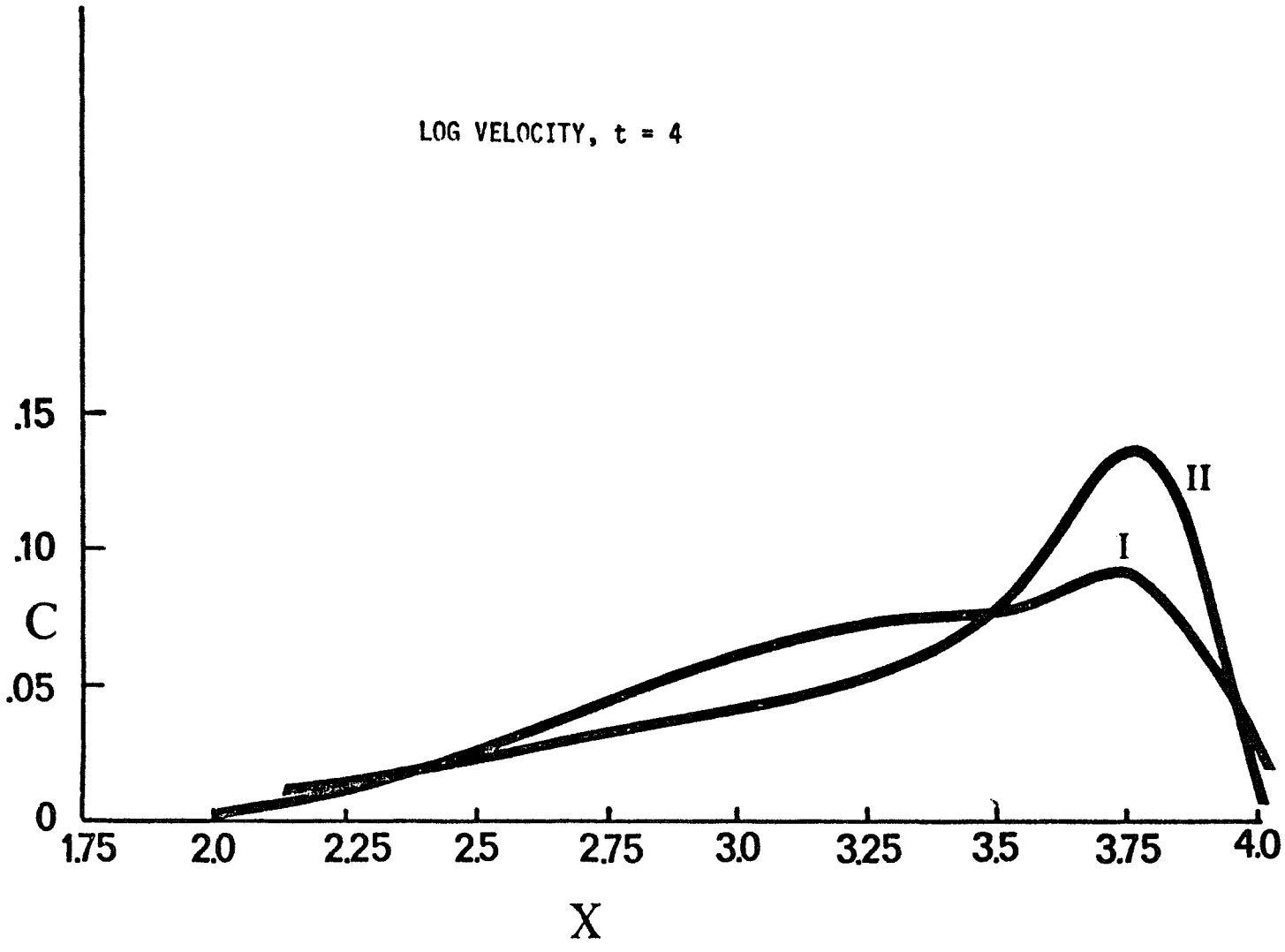
LOG VELOCITY, t = 4
.15
.10
C
.05
0
1.75
2.0
2.25
2.5
2.75
3.0
3.25
3.5
3.75
4.0
X
I
II

FIGURE 7.3

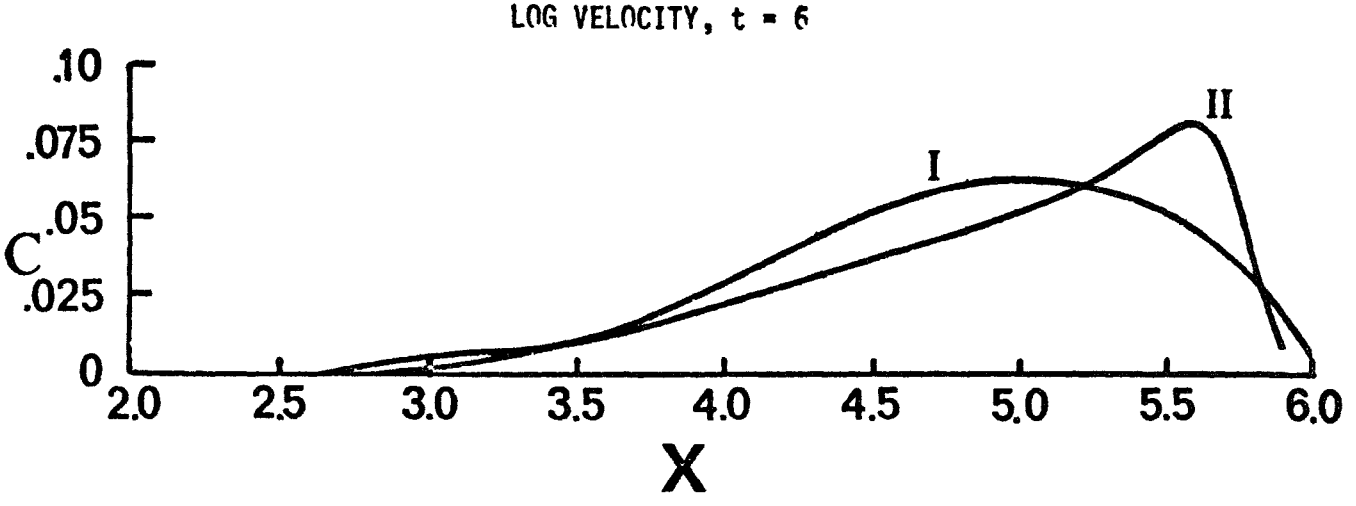

FIGURE 7.4

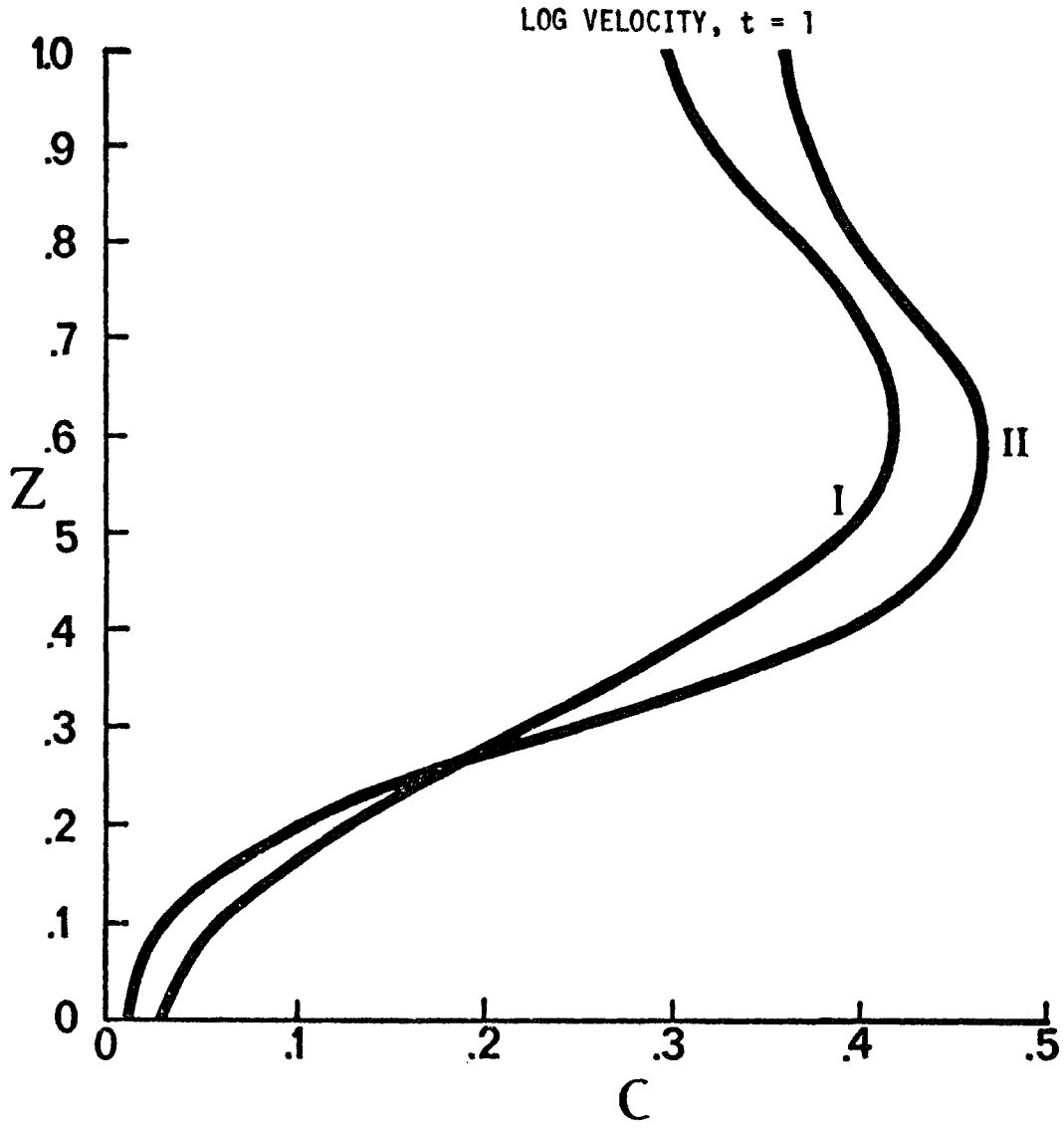

FIGURE 7.5

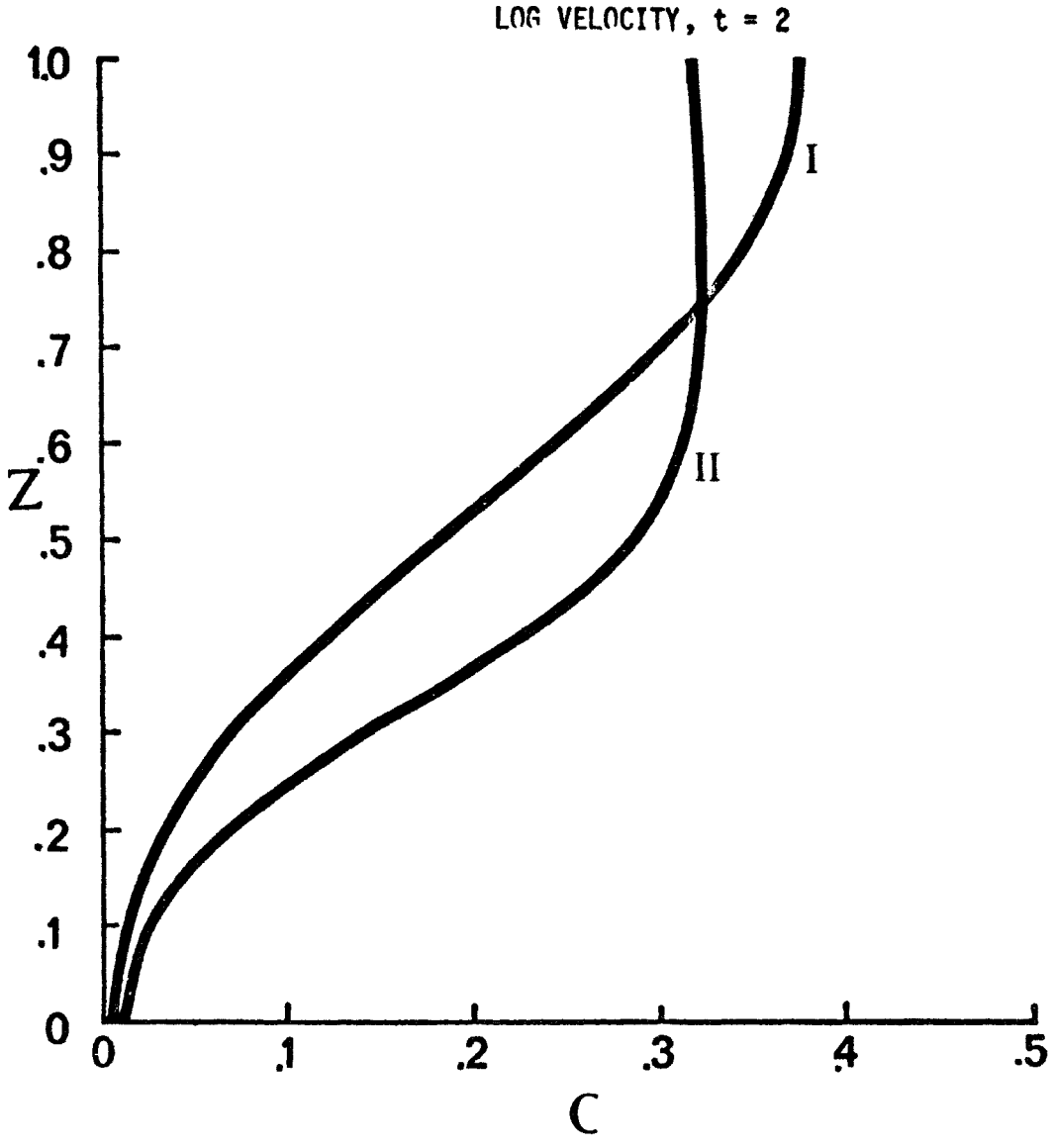

FIGURE 7.6

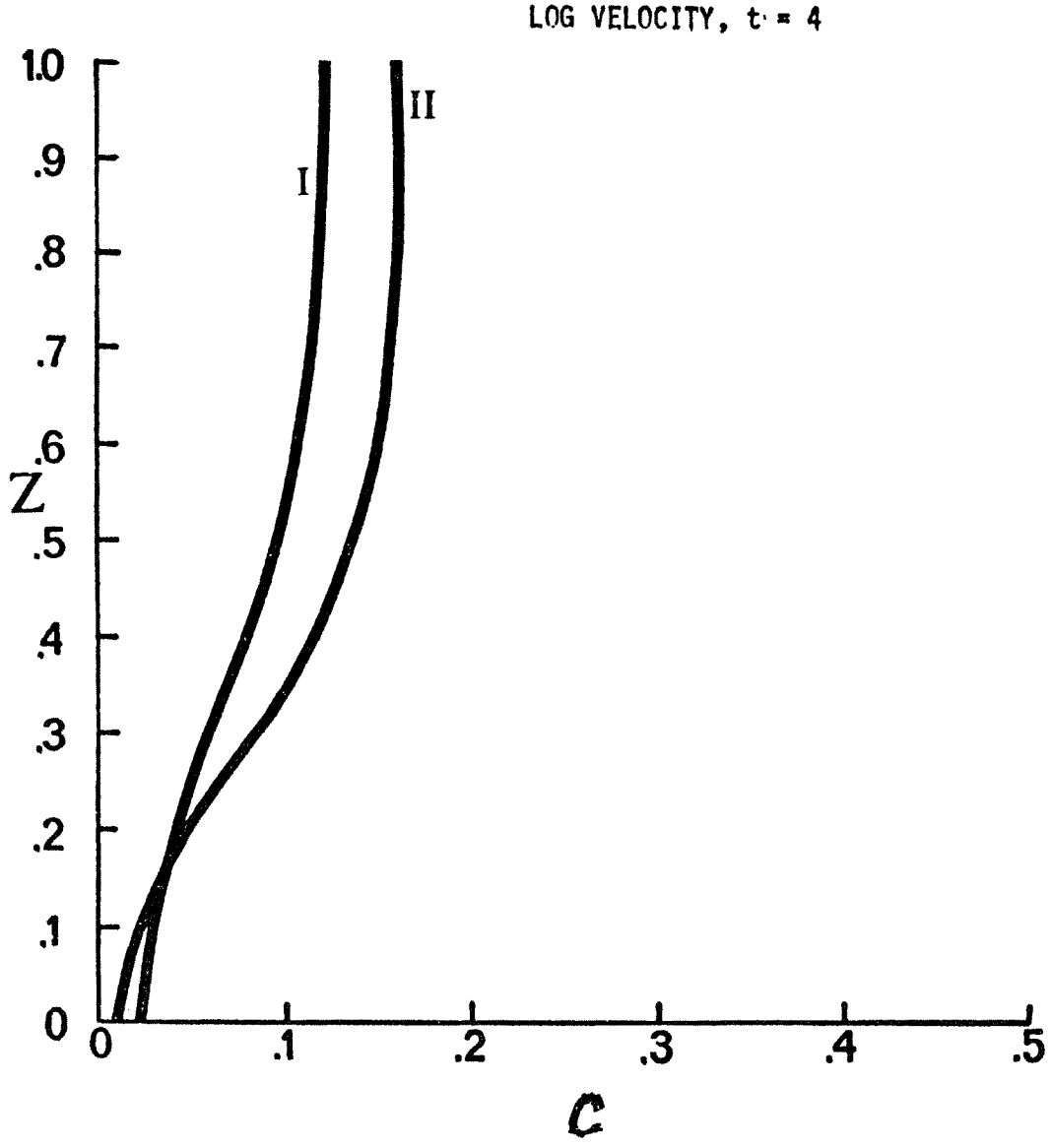

FIGURE 7.7

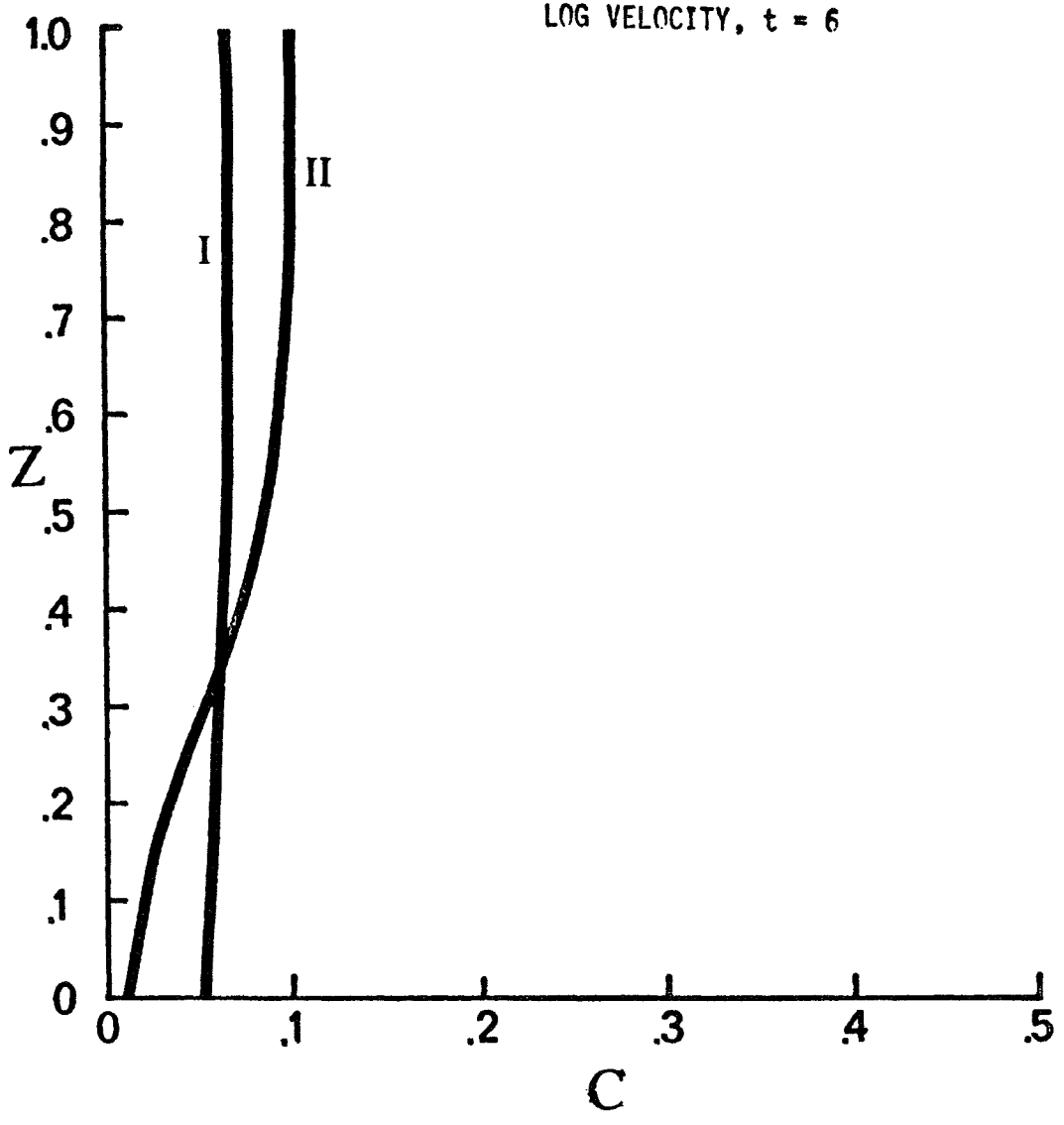

FIGURE 7.8

LAKE VELOCITY, t = 1

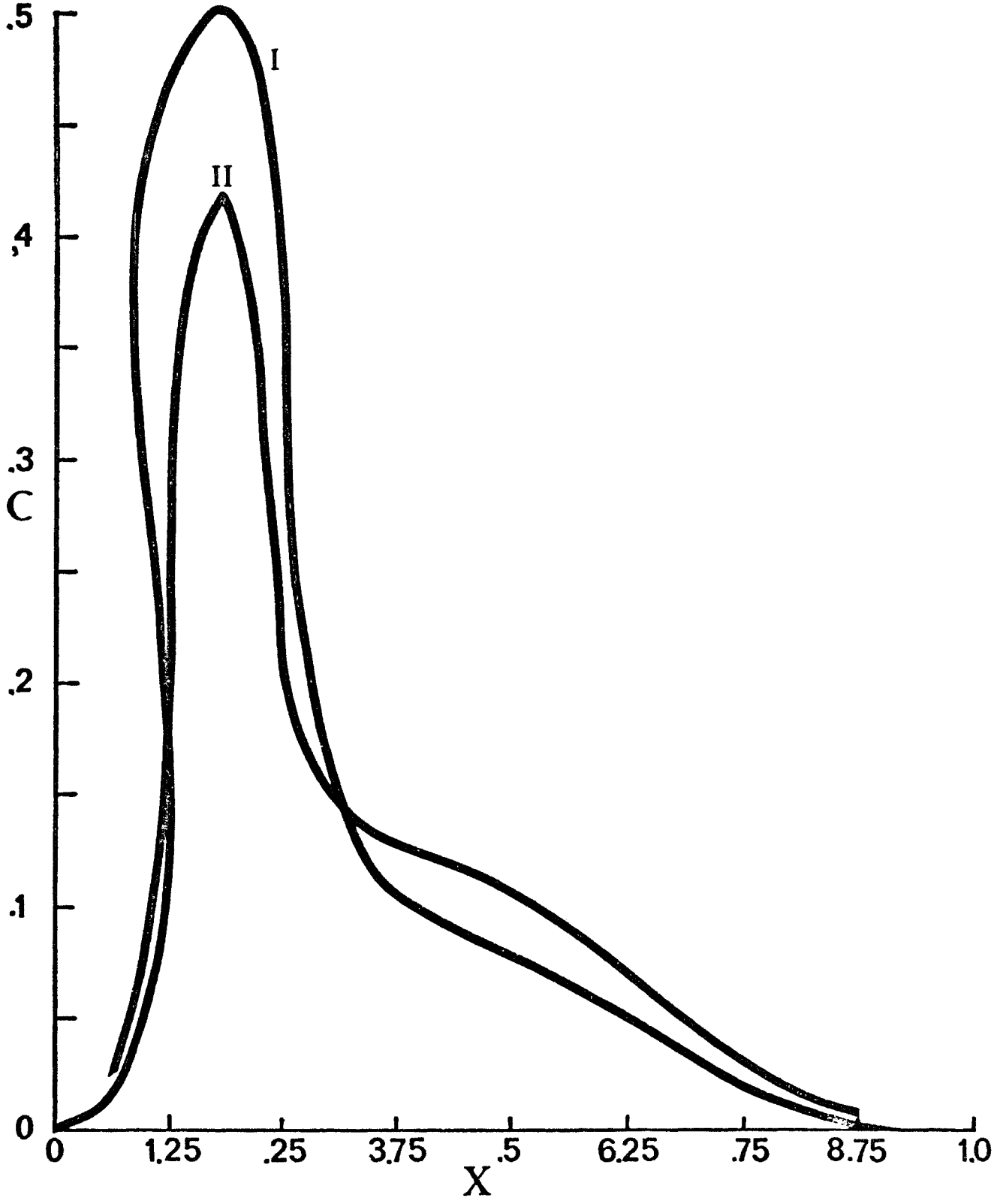

FIGURE 8.1

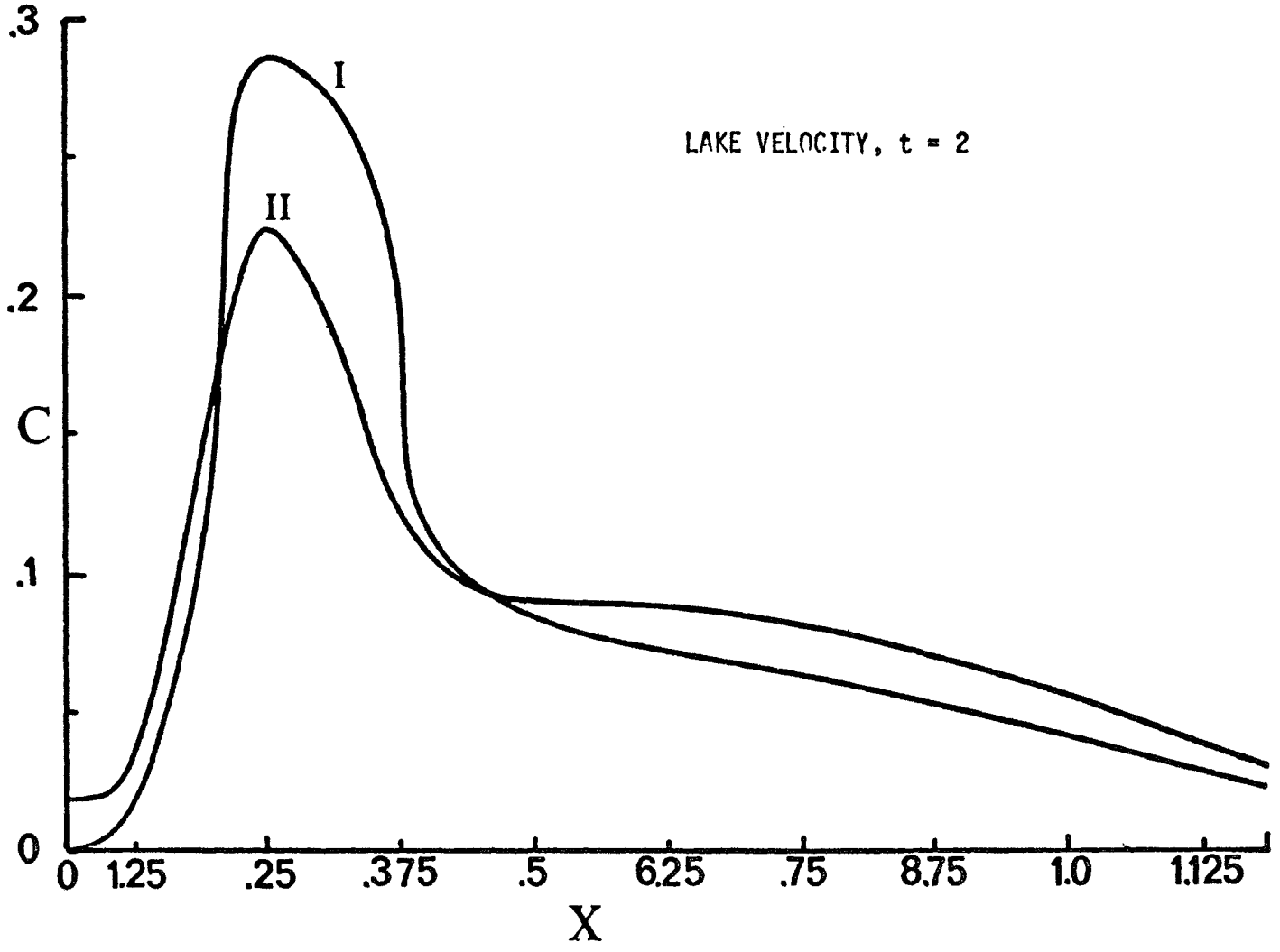

FIGURE 8.2

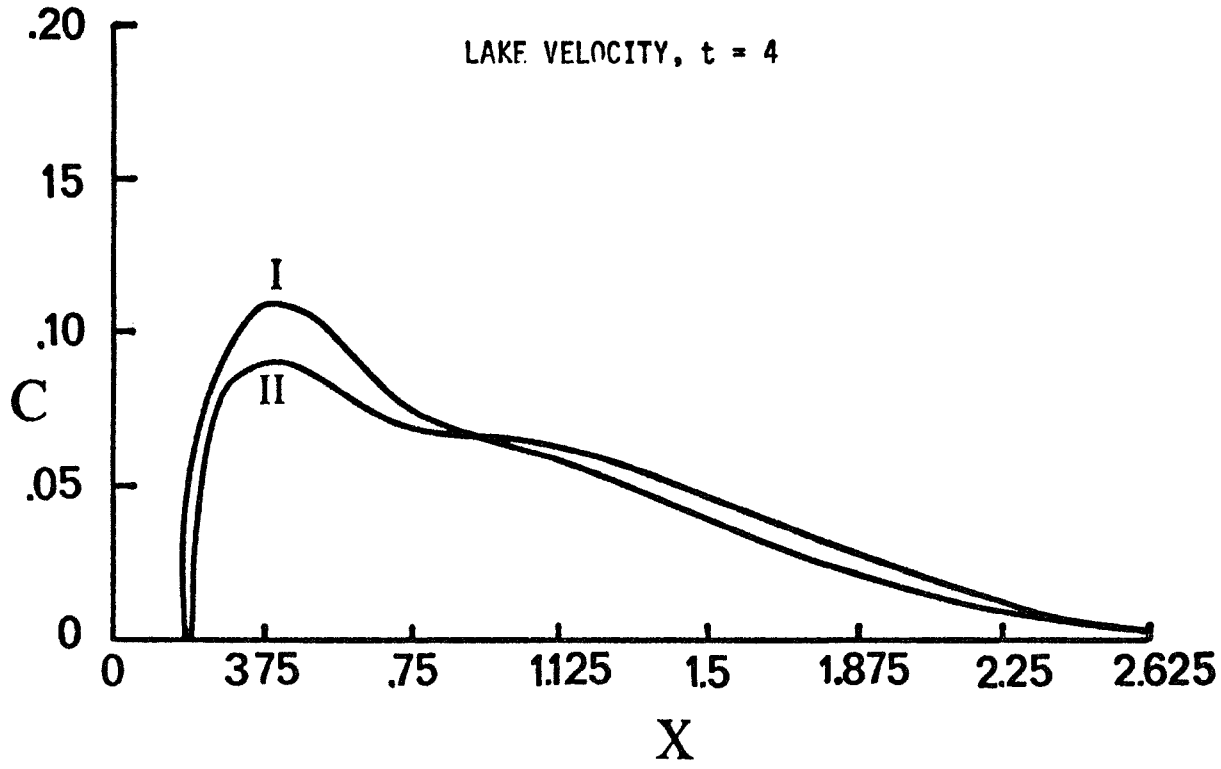
LAKE VELOCITY, t = 4
.20
15
.10
.05
0
C
I
II
0
375
.75
1.125
1.5
1.875
2.25
2.625
X

FIGURE 8.3

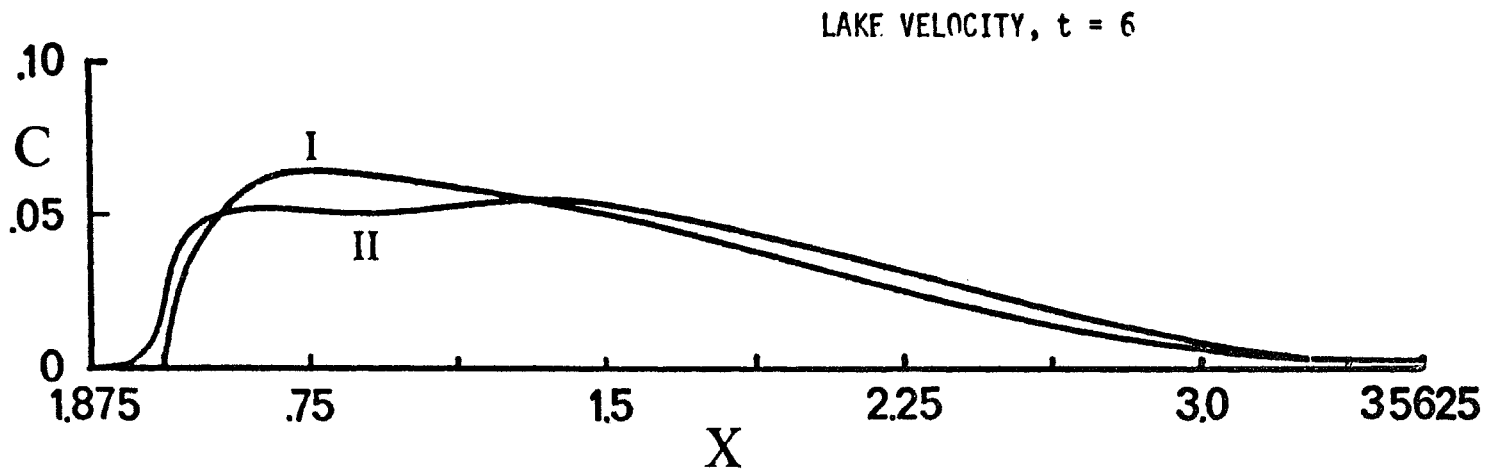

FIGURE 8.4

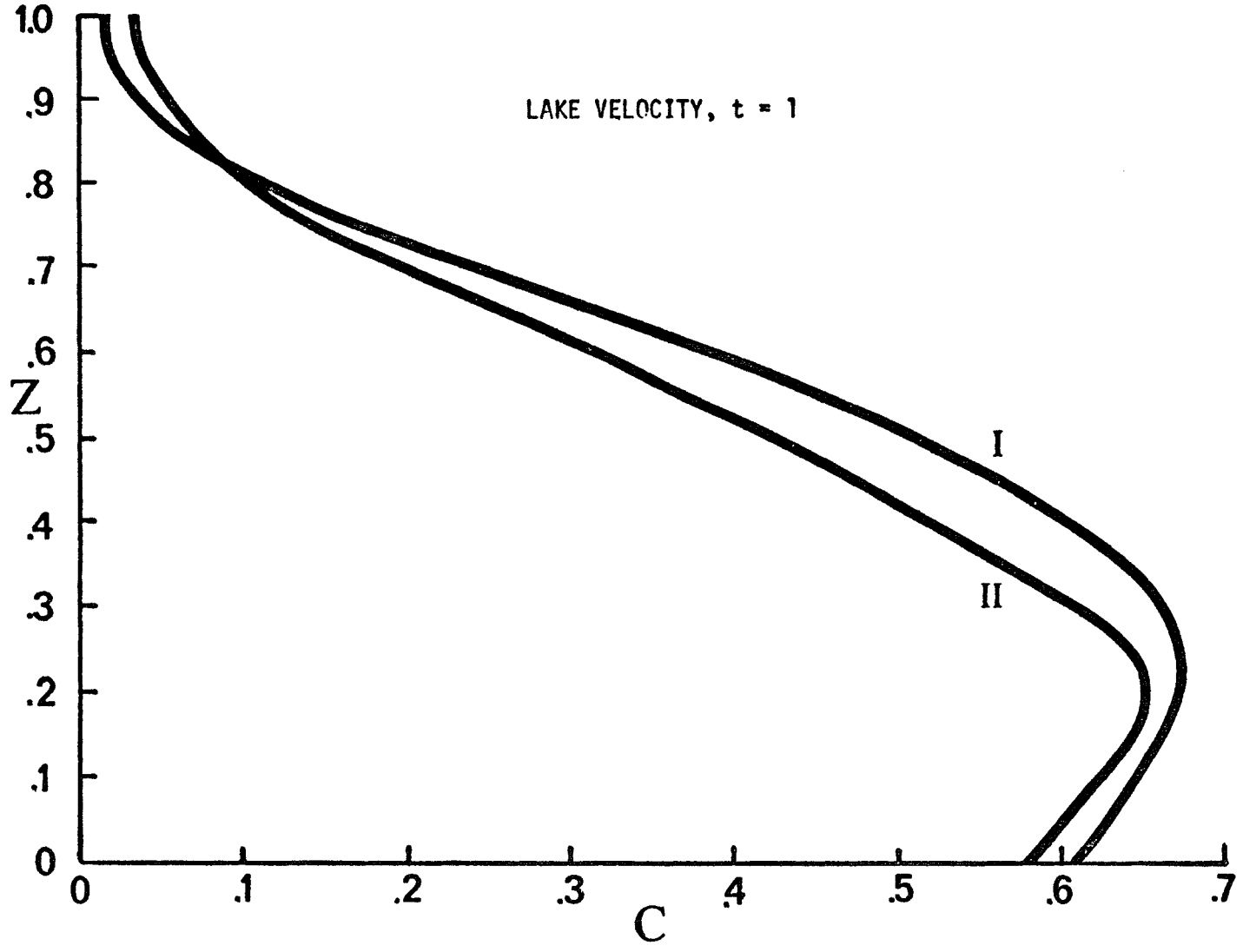

FIGURE 8.5

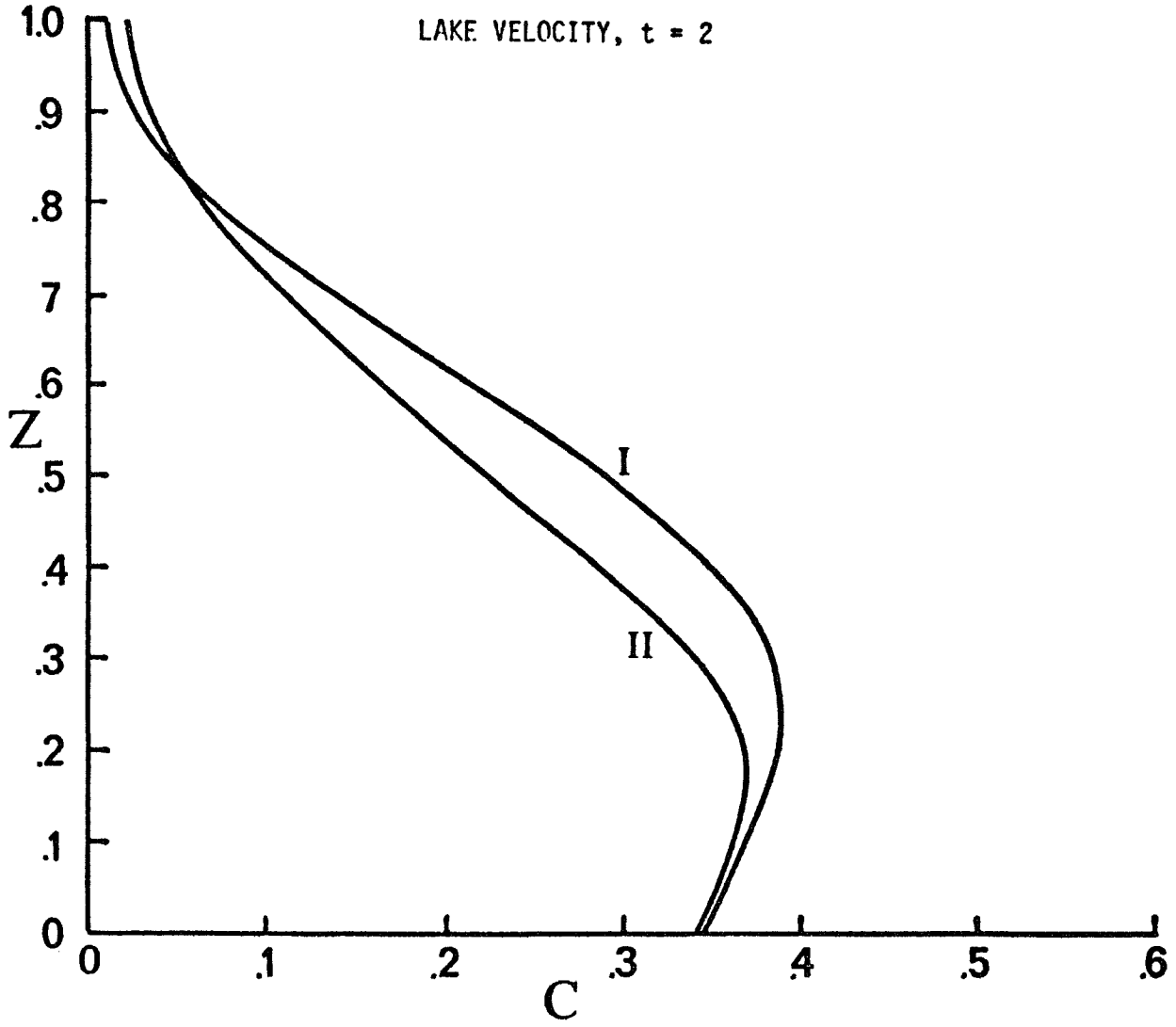

FIGURE 8.6

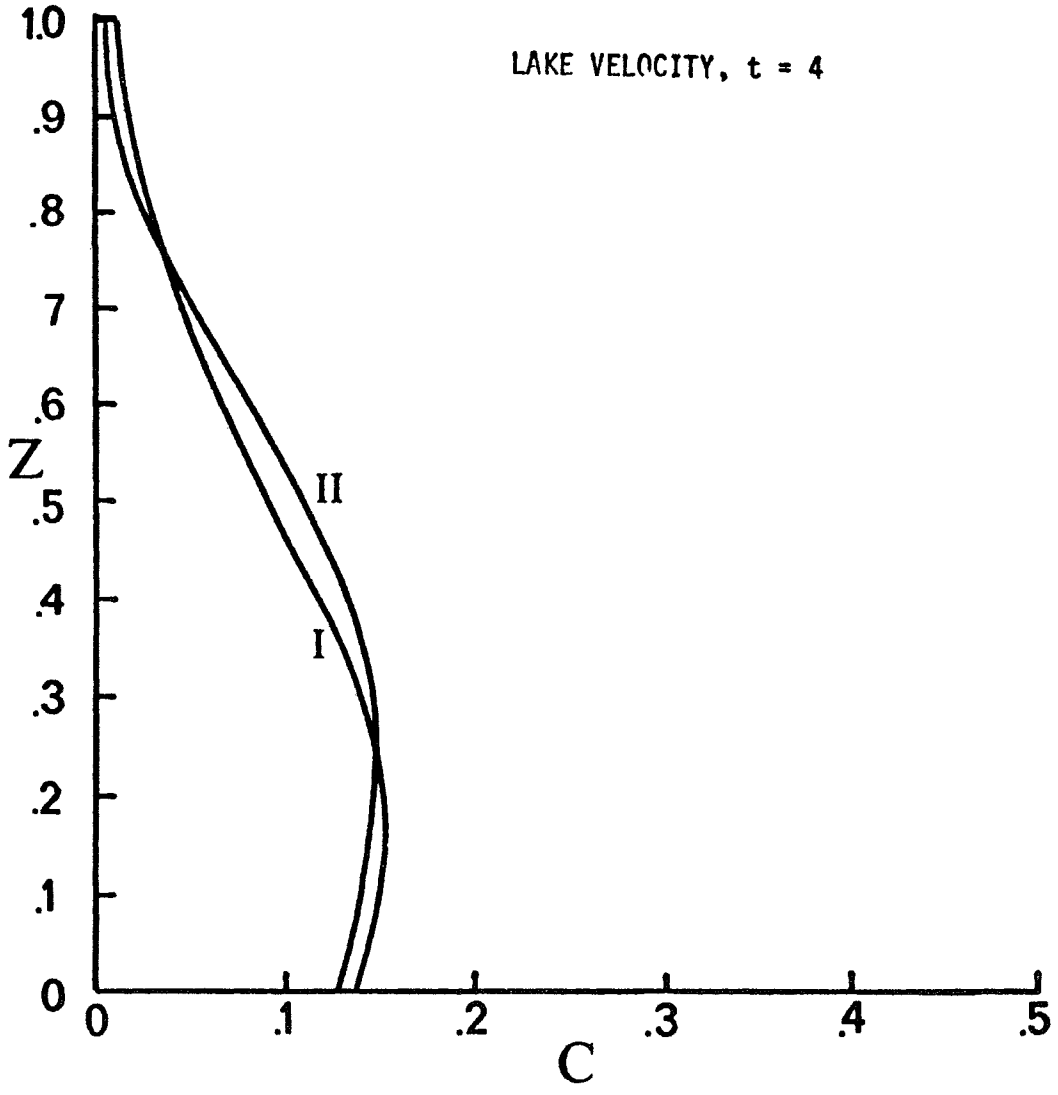

FIGURE 8.7

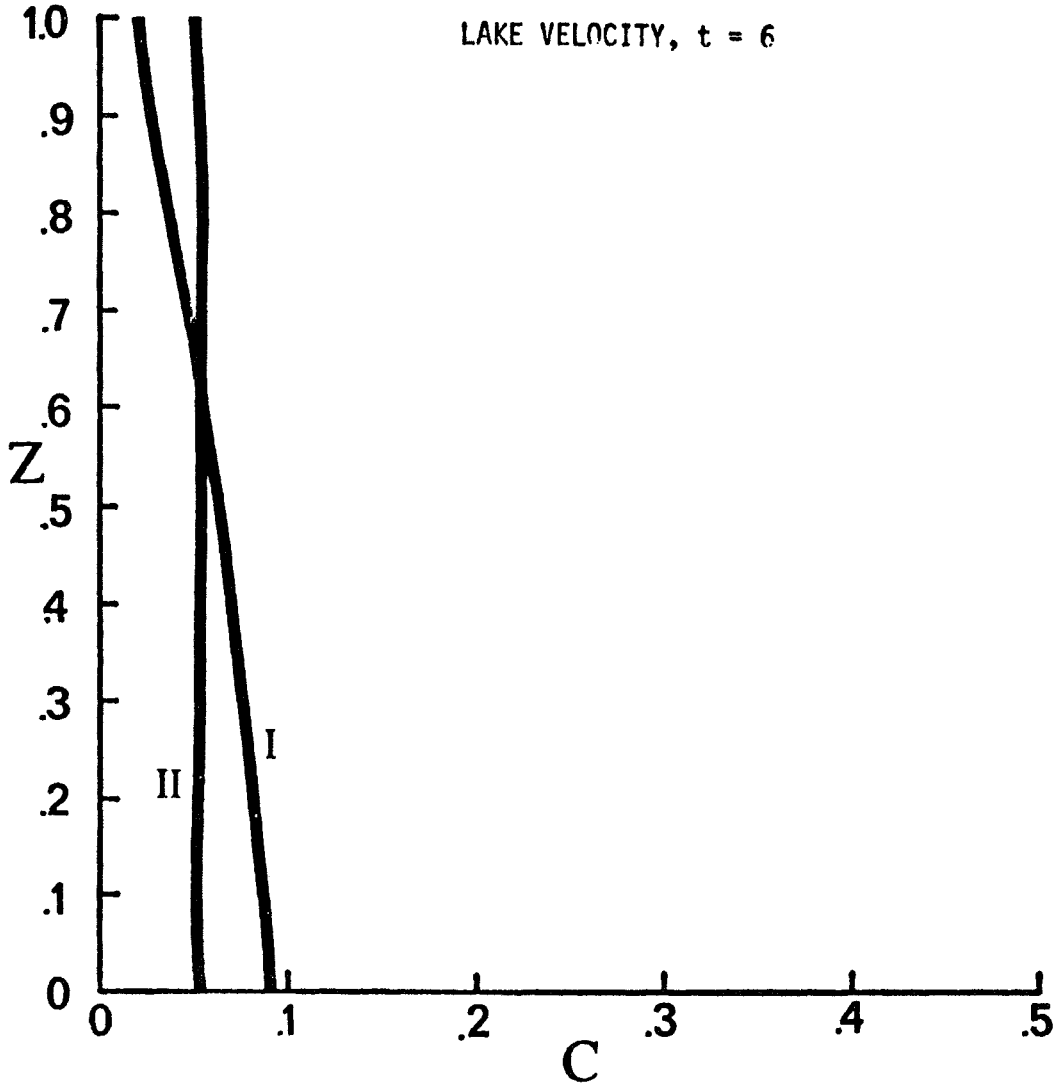

FIGURE 8.8

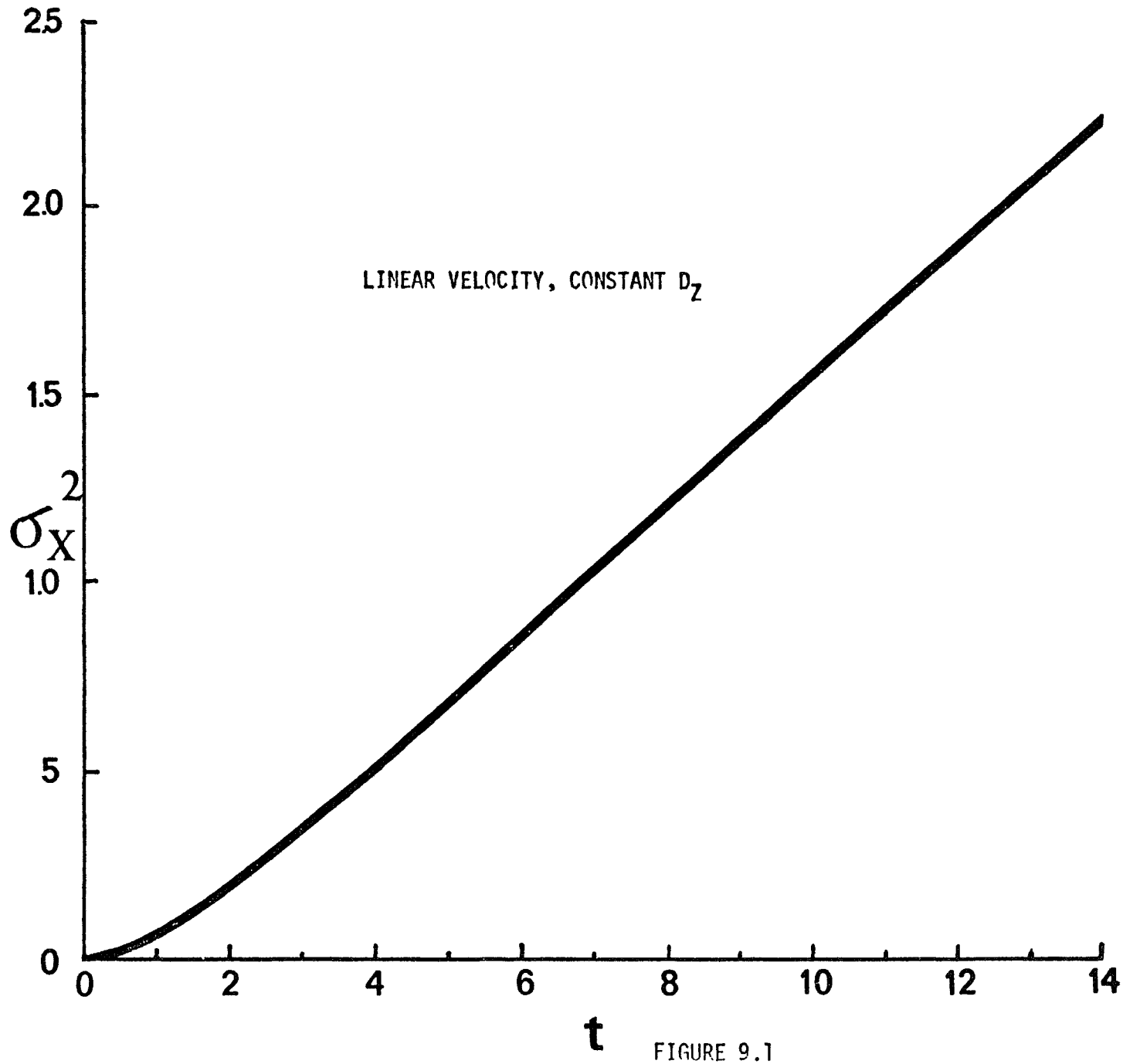
LINEAR VELOCITY, CONSTANT D_Z
2.5
2.0
1.5
σ_X^2
1.0
5
0
0
2
4
6
8
10
12
14
t

FIGURE 9.1

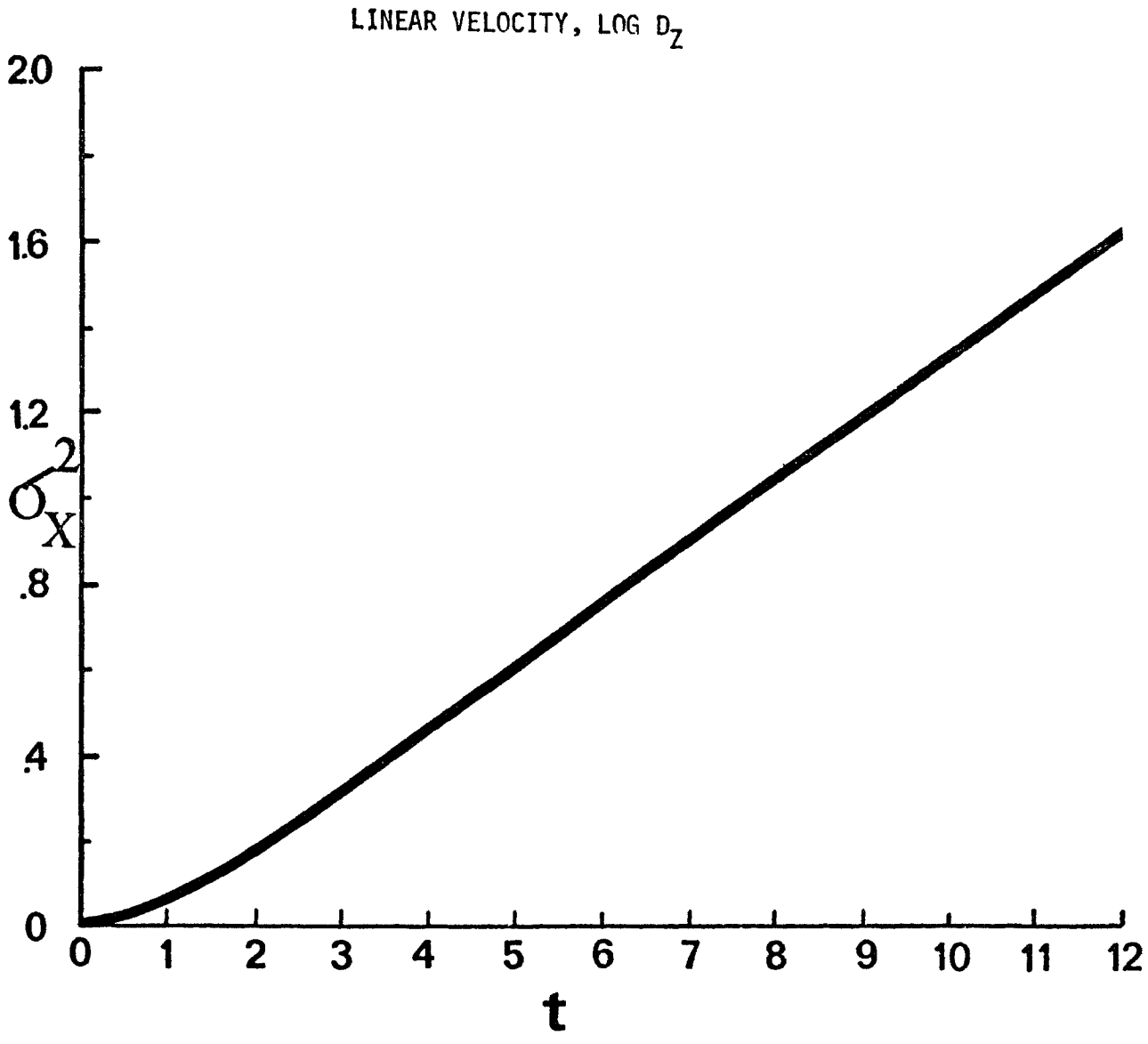
LINEAR VELOCITY, LOG D_Z
2.0
1.6
1.2
σ_X^2
.8
.4
0
0 1 2 3 4 5 6 7 8 9 10 11 12
t

FIGURE 9.2

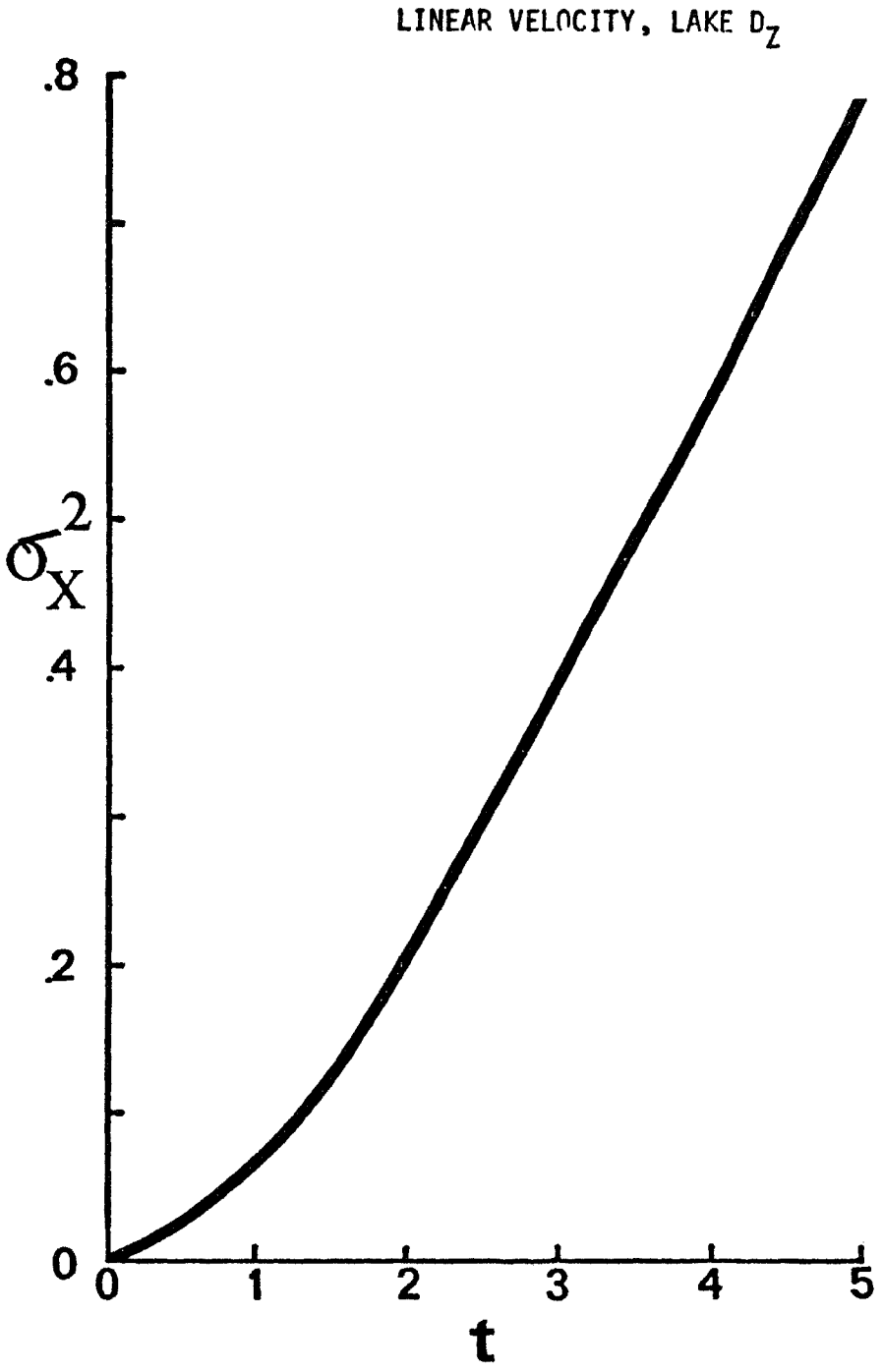

FIGURE 9.3

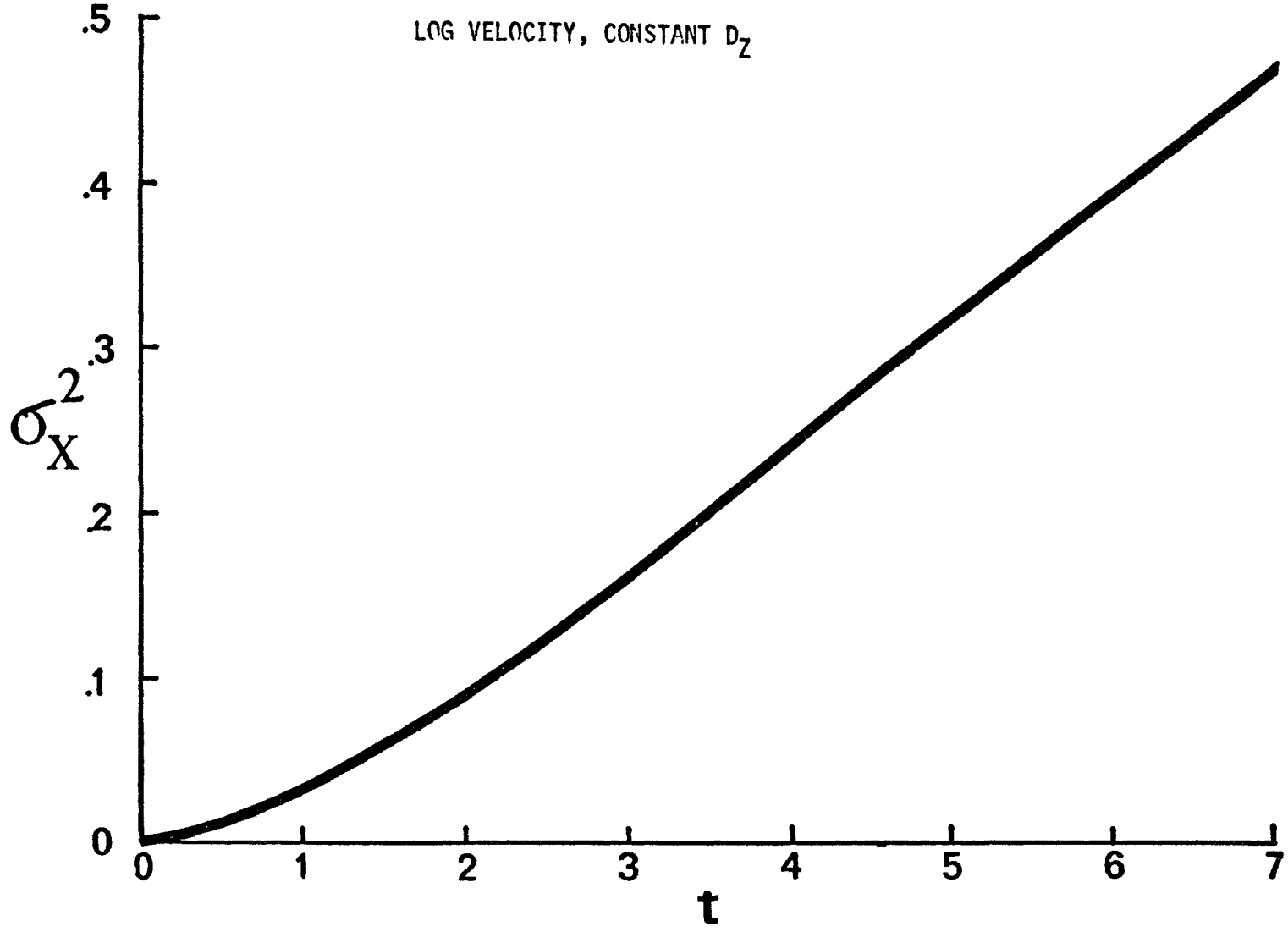

FIGURE 9.4

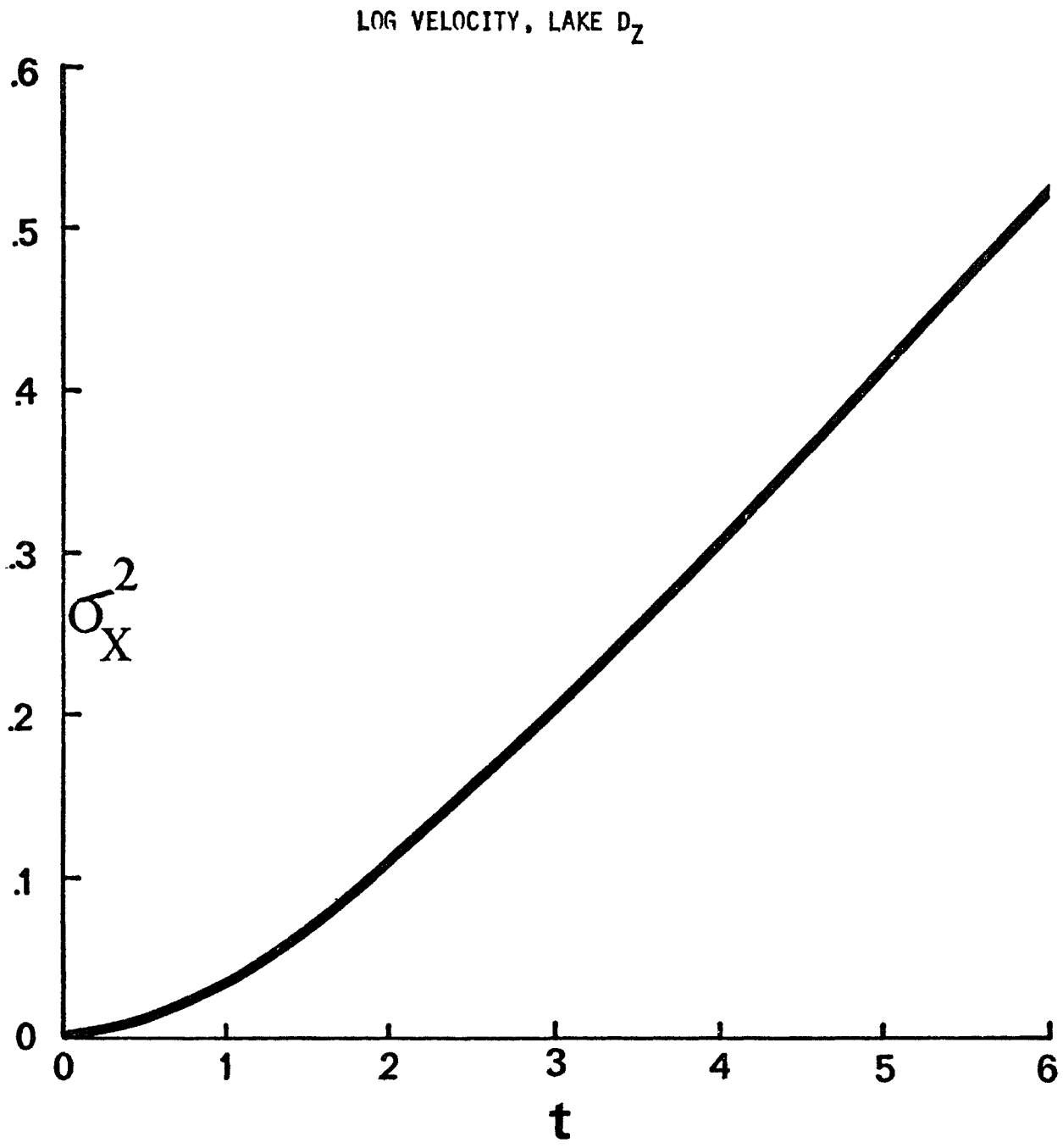

FIGURE 9.5

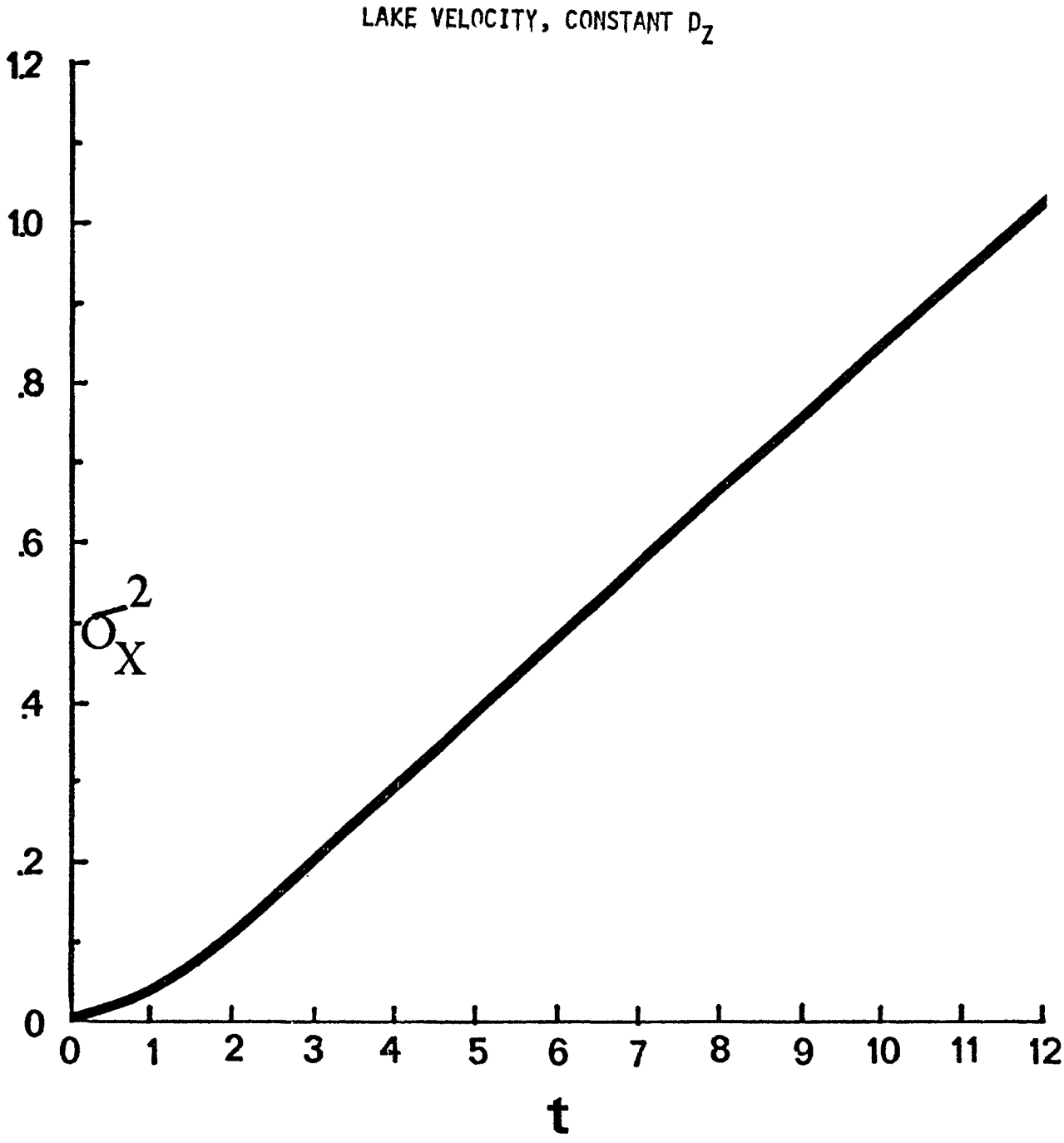
LAKE VELOCITY, CONSTANT D_z
1.2
1.0
.8
.6
.4
.2
0
σ_x^2
0 1 2 3 4 5 6 7 8 9 10 11 12
t

FIGURE 9.6

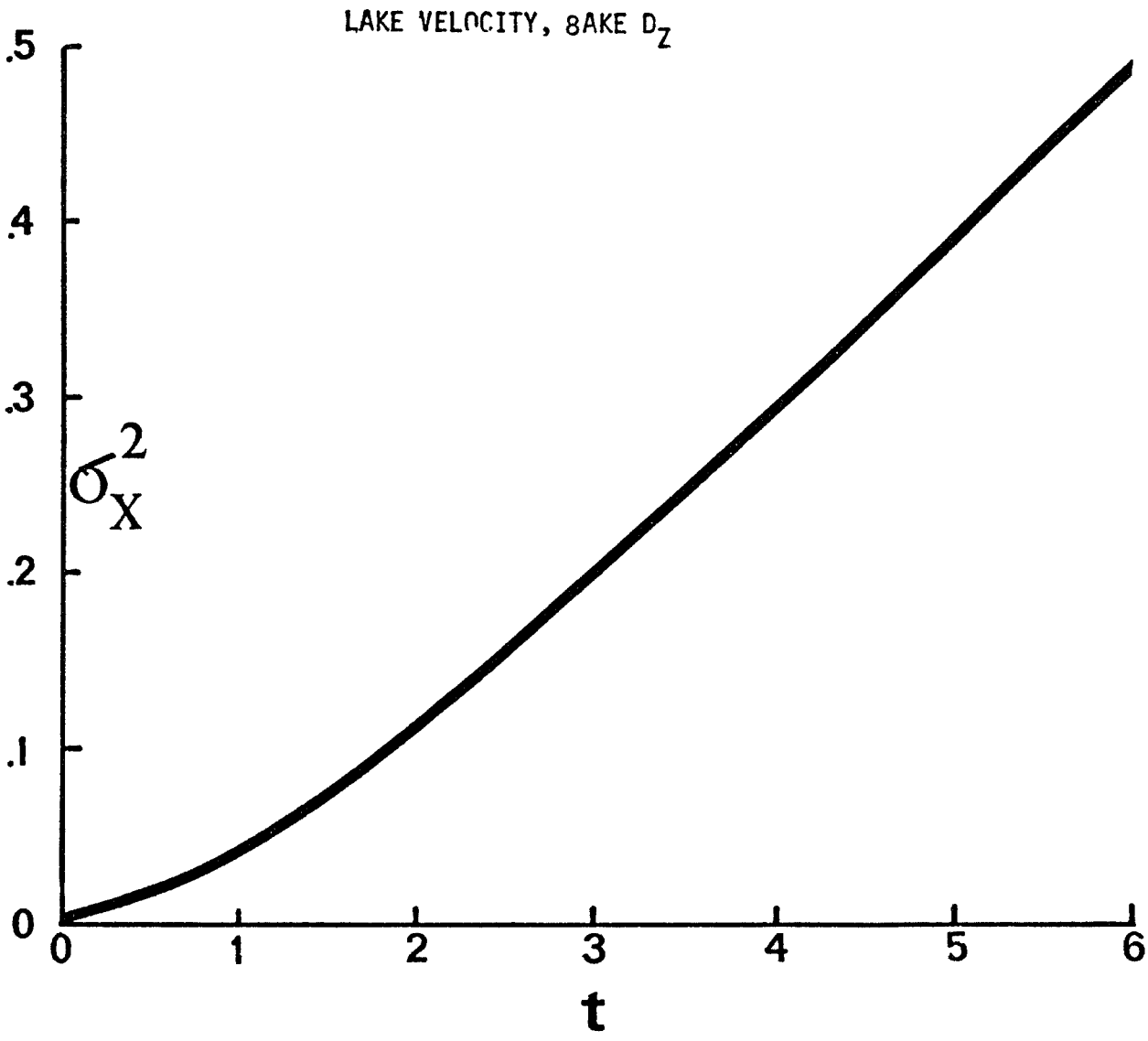

FIGURE 9.7

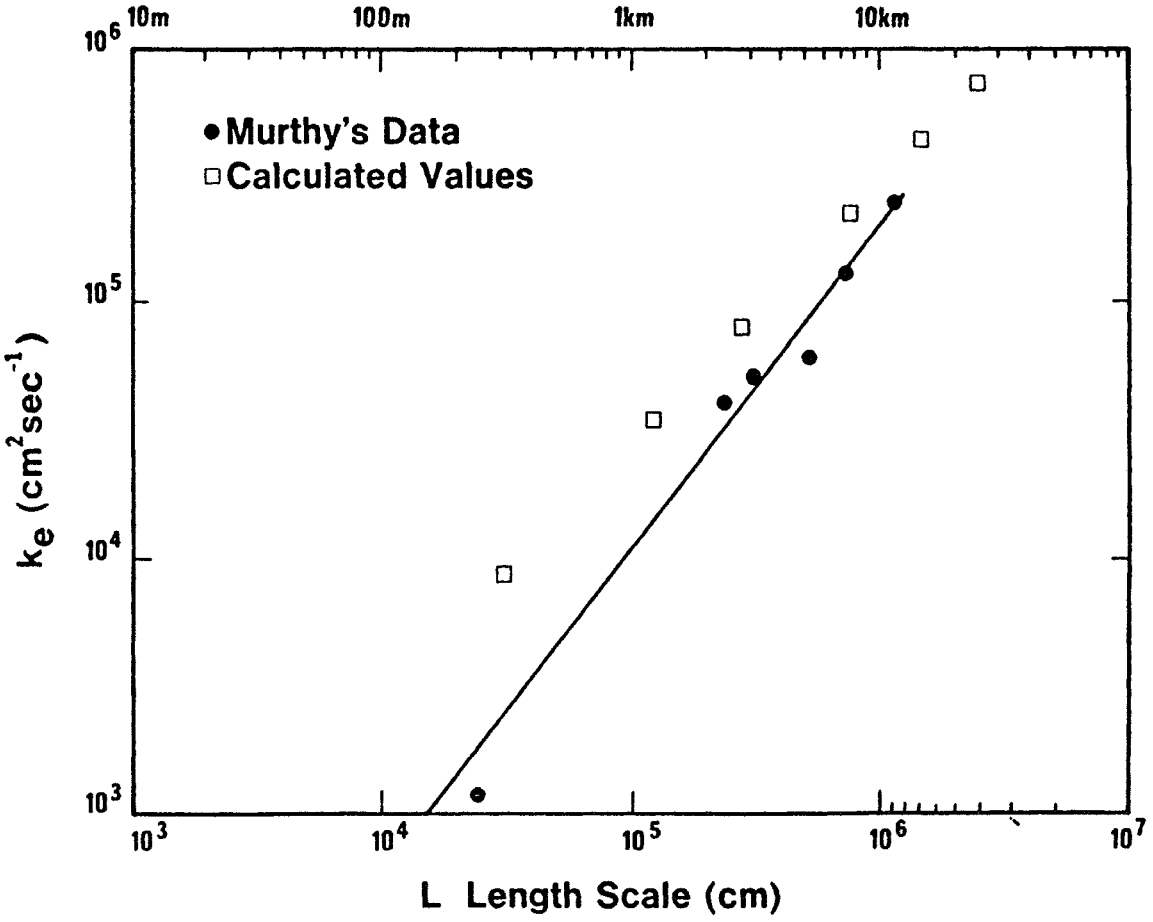
10m
100m
1km
10km
10^6
10^5
10^4
10^3
• Murthy's Data
□ Calculated Values
k_e ($cm^2 sec^{-1}$)
10^3
10^4
10^5
10^6
10^7
L Length Scale (cm)

FIGURE 10.1

BIBLIOGRAPHY

1. Aris, R., "On the Dispersion of a Solute in a Fluid Flowing Through a Tube," Proceedings of the Royal Society of London, Volume 235 (Series A), Page 67 (1956).

2. Bowden, K. F., "Horizontal Mixing in the Sea due to a Shearing Current," Journal of Fluid Mechanics, (1965), Volume 21, part 2, pp. 83-95.

3. Csanady, G. T., "Turbulent Diffusion in the Environment," D. Reidel Publishing Company, Boston (1973).

4. Elder, J. W., "The Dispersion of Marked Fluid in Turbulent Shear Flow," Journal of Fluid Mechanics (1959), Volume 5, part 2, pp. 544-560.

5. Fisher, H. B., "The Mechanics of Dispersion in Natural Streams," Journal of the Hydraulics Division, ASCE, (1968), HY6, pp. 187-216.

6. Fromm, J. E., "A Method for Reducing Dispersion in Convective Difference Scheme," Journal of Computational Physics, (1968), Volume 3, pp. 176-189.

7. Kullenberg, G., "Apparent Horizontal Diffusion in Stratified Vertical Shear Flow," Tellus, 24, #1, pp. 17-27 (1972).

8. Murthy, C. R., "An Experimental Study of Horizontal Diffusion in Lake Ontario," Proceedings of 13th Conference of Great Lakes

Research, (1970), pp. 477-489. Ann Arbor, Michigan: International Association of Great Lakes Research.

9. Natarajan, R., "Numerical Solution to a Two-Dimensional Dispersion Equation," M.S. Thesis, Dept. of Chemical Engineering, The Cleveland State University, 1973.

10. Saffman, P. G., "The Effect of Wind Shear on Horizontal Spread From an Instantaneous Ground Source," Journal of the Royal Meteorological Society, (1962), Volume 88, pp. 382-393.

11. Taylor, G., "Dispersion of Soluble Matter in Solvent Flowing Through a Tube," Proceedings of the Royal Society of London, (1953), Volume A219, pp. 186-203.

12. Thackston, E. L., and Krenkel, P. A., "Longitudinal Mixing in Natural Streams," Journal of the Sanitary Engineering Division, (1967), ASCE, Volume SA5, pp. 67-90.

13. Yotsukura, N., and Fiering, M. B., "Numerical Solution to a Dispersion Equation," Journal of the Hydraulics Division, (1964), ASCE, Volume HY5, pp. 83-103.

APPENDIX

APPENDIX I

ANALYTICAL SOLUTION OF D_x^* FOR THE LINEAR VELOCITY AND THE LOG DIFFUSIVITY PROFILES

The linear velocity profile u = z, the log diffusivity profile,

$$D_z = \frac{1.5}{2.5} z(1-z) \quad \text{for } 0.03 \leq z \leq 0.97$$

$$D_z = 0.0175 \quad \text{for } 0.00 \leq z \leq 0.03 \text{ and } 0.97 \leq z \leq 1.0$$

$$\bar{u} = \int_0^1 u\,dz = \int_0^1 z\,dz = \frac{z^2}{2}\Big|_0^1 = 0.5$$

$\emptyset$ (z) is defined (equation 2.18) as,

$$\emptyset(z) = \int_{z_1}^{z} \frac{dz}{D_z} \int_0^z (\bar{u} - u)\,dz \qquad \text{(A1:1)}$$

Consider the integral

$$\int_0^z (\bar{u} - u)\,dz$$

$$= \int_0^z (0.5 - z)\,dz$$

$$= 0.5\,z\,(1-z)$$

Substituting in equation (A1:1)

$$\emptyset(z) = \int_{z_1}^{z} \frac{0.5z(1-z)}{D_z}\,dz$$

We have to divide this integral into three functions as D_z varies according to three different conditions.

Let us say

$$G(z) = G_1(z) + G_2(z) + G_3(z)$$

where

$$G_1(z) = \frac{0.5z(1-z)}{0.0175} \quad \text{for } 0 \leq z \leq 0.03$$

and

$$G_1(z) = 0 \quad \text{otherwise}$$

$$G_2(z) = \frac{0.5\ z\ (1-z)}{0.6\ z\ (1-z)} = 0.833 \text{ for } 0.03 \leq z \leq 0.97$$

and $G_2(z) = 0$ otherwise

$$G_3(z) = \frac{0.5\ z\ (1-z)}{0.0175} \quad \text{for } 0.97 \leq z \leq 1.0$$

and

$$G_3(z) = 0 \quad \text{otherwise}$$

Now $$\phi(z) = \phi_1(z) + \phi_2(z) + \phi_3(z)$$

where

$$\phi_1(z) = \int_{z_1}^{z} G(z)\, dz \quad \text{for } 0 \leq z \leq 0.03$$

$$\phi_2(z) = \int_{z_1}^{z} G(z)\, dz \quad \text{for } 0.03 \leq z \leq 0.97$$

and

$$\phi_3(z) = \int_{z_1}^{z} G(z)\, dz \quad \text{for } 0.97 \leq z \leq 1.0$$

Lower limit z_1 is unknown and is based on the following condition

z_1 should be such that,

$$\int_0^1 \phi(z)\, dz = 0$$

Let us assume $0.03 < z_1 < 0.97$

then

$$\phi_1(z) = -\int_z^{0.03} G_1(z)\,dz - \int_{0.03}^{z_1} G_2(z)\,dz \qquad (A1:2)$$

$$\phi_2(z) = -\int_z^{z_1} G_2(z)\,dz \qquad (A1:3)$$

The -ve sign is due to the change of limits.

$$\phi_3(z) = \int_{z_1}^{0.97} G_2(z)\,dz + \int_{0.97}^{z} G_3(z)\,dz \qquad (A1:4)$$

Thus,

$$\phi_1(z) = -\int_z^{0.03} \frac{0.5z(1-z)}{0.0175}\,dz - \int_{0.03}^{z_1} 0.833\,dz$$

It can be shown that

$$\phi_1(z) = 0.0124 - 0.833z_1 + 28.6\left(\frac{z^2}{2}-\frac{z^3}{3}\right) \qquad (A1:5)$$

is the solution of the above integral. Similarly equations (A1:3) and (A1:4) give

$$\phi_2(z) = -0.833\,z_1 + 0.833\,z \qquad (A1:6)$$

and

$$\phi_3(z) = -3.9482 - 0.833\,z_1 + 28.6\left(\frac{z^2}{2} - \frac{z^3}{3}\right) \qquad (A1:7)$$

Now, as $\phi(z) = \phi_1(z) + \phi_2(z) + \phi_3(z)$

$$\int_0^1 \phi(z)\,dz = \int_0^{0.03} \phi_1(z)\,dz + \int_{0.03}^{0.97} \phi_2(z)\,dz + \int_{0.97}^{1.0} \phi_3(z)dz = 0 \qquad (A1:8)$$

Each integral in (A1:8) gives

$$\int_0^{0.03} \phi_1(z)\,dz = 0.0004987 - 0.025\,z_1 \qquad (A1:9)$$

$$\int_{0.03}^{0.97} \phi_2(z)\, dz = -0.783\, z_1 + 0.3915 \qquad (A1:10)$$

$$\int_{0.97}^{1.0} \phi_3(z)\, dz = 0.0246 - 0.025\, z_1 \qquad (A1:11)$$

Thus,

$$\int_0^1 \phi(z)\, dz = 0.0004987 - 0.025\, z_1$$

$$- 0.783\, z_1 + 0.3915$$

$$+ 0.0246 - 0.025\, z_1 = 0$$

Solving this equation

$$z_1 = 0.5$$

Substituting value of z_1 in equations (A1:5), (A1:6) and (A1:7), we get

$$\phi_1(z) = 0.4289 + 28.6\left(\frac{z^2}{2} - \frac{z^3}{3}\right)$$

$$\phi_2(z) = -0.4165 + 0.833\, z$$

and

$$\phi_3(z) = -4.3647 + 28.6\left(\frac{z^2}{2} - \frac{z^3}{3}\right)$$

Now

$$D_x^* = \int_0^1 u\phi(z)\, dz = \int_0^1 z\, \phi(z)\, dz$$

Therefore,

$$D_x^* = \int_{0.}^{0.03} z\, \phi_1(z)\, dz + \int_{0.03}^{0.97} z\, \phi_2(z)\, dz + \int_{0.97}^{1.0} z\phi_3(z)\, dz$$

By substituting values of $\phi_1(z)$, $\phi_2(z)$ and $\phi_3(z)$ and solving the above equation,

$$D_x^* = 0.0676$$

APPENDIX II

THE TIME DEPENDENCE OF $\frac{d\sigma x^2}{dt}$

The basic approach is based on that given by Aris (Ref. 1). Starting with equation

$$\frac{\partial C}{\partial t} + u \frac{\partial C}{\partial x} = \frac{\partial}{\partial z} \left[D_z \frac{\partial C}{\partial z} \right] \qquad \text{(A2:1)}$$

the functions Ψ and v are introduced as

$$\frac{\partial C}{\partial t} + u \left[1 + \frac{v}{u} \right] \frac{\partial C}{\partial x} = \overline{D}_z \frac{\partial}{\partial z} \left[\psi \frac{\partial C}{\partial z} \right] \qquad \text{(A2:2)}$$

where u is the average value of u across the layer, v is a measure of the deviation of the local velocity from the average, $\overline{D}_z$ is the average value of D_z across the layer, and $\psi = D_z/\overline{D}_z$. By definition

$$\frac{1}{h} \int_0^h v \, dz = 0 \quad \text{and} \quad \frac{1}{h} \int_0^h \psi \, dz = 1.$$

If a downstream coordinate, $x' = x - ut$, is introduced, (A2:2) becomes

$$\frac{\partial C}{\partial t} + v \left[\frac{\partial C}{\partial x} \right] = \overline{D}_z \frac{\partial}{\partial z} \left[\psi \frac{\partial C}{\partial x} \right] \qquad \text{(A2:3)}$$

Introducing the non-dimensional variables

$$x^* = x/h, \quad z^* = z/h, \quad t^* = t/(h/U_{max}), \quad v^* = v/U_{max},$$

(A2:3) becomes

$$\frac{\partial C}{\partial t^*} + v^* \frac{\partial C}{\partial x^*} = \overline{D}_z^* \frac{\partial}{\partial z^*} \left(\psi \frac{\partial C}{\partial z^*} \right) \qquad \text{(A2:4)}$$

where h is the layer thickness, U_{max} is the maximum absolute difference in all values taken on by v over h, and $\bar{D}_z^* = D_z/ChU_{max}$). The * in equation (A2:4) will be dropped to simplify notation in the remaining development. Now introduce

$$C_o(z) = \int_{-\infty}^{\infty} C(x,z)\, dz$$

where $C_o(z)$ is the solute in the plane at level z. Then (A2:4) becomes

$$\frac{1}{\bar{D}_z} \frac{\partial C_o}{\partial t} = \frac{\partial}{\partial z} \left[\psi \frac{\partial C_o}{\partial z}\right] \qquad \text{(A2:5)}$$

If (A2:5) is solved subject to the boundary conditions

$$\psi \left.\frac{\partial C_o}{\partial z}\right|_{z=0,1} = 0 \qquad \text{(A2:6)}$$

which results from similar conditions on C, the solution is

$$C_o = A_o + \Sigma A_i \phi_i e^{-\alpha_i \bar{D}_z t} \qquad \text{(A2:7)}$$

where α_i and ϕ_i are the eigenvalues and corresponding eigenfunctions of the Strum-Liouville problem resulting from (A2:5) and (A2:6). The A_i are determined by the initial distribution of C_o.

Next introduce into (A2:4)

$$C_1(z) = \int_{-\infty}^{\infty} x\, C(x,z)\, dz$$

where $C_1(z)$ is the first moment of the distribution of C in the x direction. Assuming $C \to 0$ sufficiently rapidly with x, (A2:4) becomes

$$\frac{\partial C_1}{\partial t} = v C_o + \bar{D}_z \frac{\partial}{\partial z} \left(\frac{\partial C_1}{\partial z}\right) \qquad \text{(A2:8)}$$

(A2:8) is to be solved subject to the boundary conditions

$$\psi \left.\frac{\partial C_1}{\partial z}\right|_{z=0,1} = 0$$

which again results from the similar conditions on C. The complimentary function for the homogeneous part of (A2:8) is

$$C_{1C} = B_o + \Sigma B_i \phi_i e^{-\alpha_i \bar{D}_z t} \qquad \text{(A2:9)}$$

A particular integral of (A2:8) of the form

$$C_{1p} = f_0 + \Sigma e^{-\alpha_i \bar{D}_z t} f_i \qquad \text{(A2:10)}$$

is sought. Substituting (A2:7) and (A2:10) into (A2:8) gives

$$\begin{aligned}\Sigma(-\alpha_i \bar{D}_z) e^{-\alpha_i \bar{D}_z t} f_i &= v A_o + v \Sigma A_i \phi_i e^{-\alpha_i \bar{D}_z t} \\ &\quad + \bar{D}_z \frac{d}{dz}\left(\psi \frac{df_o}{dz}\right) \\ &\quad + \bar{D}_z \Sigma e^{-\alpha_i \bar{D}_z t} \frac{d}{dz}\left(\psi \frac{df_i}{dz}\right) \qquad \text{(A2:11)}\end{aligned}$$

The f_i are thus determined by the relations

$$\begin{aligned}\bar{D}_z \frac{d}{dz}\left(\psi \frac{df_o}{dz}\right) &= vA_o \\ \bar{D}_z \frac{d}{dz}\left(\psi \frac{df_i}{dz}\right) + \alpha_i \bar{D}_z f_i &= vA_i\phi_i \qquad \text{(A2:12)}\end{aligned}$$

where the f_i must satisfy

$$\psi \left.\frac{df_i}{dz}\right|_{z=0,1} = 0$$

The solution for C_1 is then

$$C_1 = C_{1C} + C_{1p} \qquad \text{(A2:13)}$$

and the B_i in (A2:9) are determined by the initial condition on C_1.

An equation for $C_2(z) = \int_{-\infty}^{\infty} x^2 C(x,z)\, dx$

can similarly be obtained from (A2:4). The result is

$$\frac{\partial C_2}{\partial t} = 2 vC_1 + \bar{D}_z \frac{\partial}{\partial z} \left(\psi \frac{\partial C_2}{\partial z}\right) \qquad \text{(A2:14)}$$

The first and second moments of the total distribution, M_1 and M_2, can be obtained from C_1 and C_2 by integrating over the layer. Thus,

$$M_i = \int_0^1 \int_{-\infty}^{\infty} x^i C\, dx\, dz = \int_0^1 C_i\, dz \qquad \text{(A2:15)}$$

Thus, for i = 1, (A2:15) gives

$$M_1 = \int_0^1 (B_o + f_o)\, dz + \Sigma\, e^{-\alpha_i \bar{D}_z t} \int_0^1 CB_i \phi_i + f_i)dz \qquad \text{(A2:16)}$$

For i = 2, from (A2:15)

$$\frac{dM_2}{dt} = \int_0^1 \frac{\partial C_2}{\partial t}\, dz$$

$$= \int_0^1 vC_1\, dz$$

$$= \int_0^1 v\,(B_o + f_o)\, dz$$

$$+ \Sigma\; e^{-\alpha_i \bar{D}_z t} \int_0^1 v(B_i \phi_i + f_i)\, dz \qquad \text{(A2:17)}$$

The effective dispersion coefficient in the x direction is given by

$$2\,K_e = \frac{d\Sigma x^2}{dt}$$

$$= \frac{h^2}{(h/U_{max})} \left(\frac{dM_2}{dt^*} - \frac{dM_1^2}{dt^*} \right) \qquad \text{(A2:18)}$$

(A2:16) and (A2:17) in connection with (A2:18), show that $\frac{d\Sigma x^2}{dt}$ approaches a constant value exponentially with exponent $- \alpha_1 D_z^* t$, where α_1 is the smallest eigen value from the solution of (A2:5) and (A2:6). This is the basis for equation $t_1 = \frac{h^2}{\alpha_1 \overline{D}_z}$.

It can be seen in the development that the α_i are independent of the velocity profile. The velocity affects the rate of approach of K_e to a constant only through the integrals in (A2:16) and (A2:17) which are the coefficients of the exponential terms. In this sense, the velocity profile has a secondary effect on the approach to constant K_e in comparison with the vertical diffusivity profile, which directly influences the α_i.

APPENDIX III

NUMERICAL SOLUTION OF A FORMULA GIVEN BY CSANADY

```
      DIMENSICN U(210),AI1(210),D1(210),
     1  Z(210),AI2(210),AAI2(210)
      DZ=0.CC5
      DO 700 K=2,202
      RK=K
      Z(K)=(RK-2.)*DZ
      U(K)=Z(K)
700   CCNTINUE
      DO 800 K=2,202
      D1(K)=0.1
800   CCNTINUE
      UAVG=C.0
      DC 501 K=2,201
501   UAVG=DZ/2.0*(U(K)+U(K+1))+UAVG
      PRINT 145, UAVG
145   FORMAT (6H UAVG=,F15.8)
      AI1(2)=0.C
      DC 503 K=3,202
      AI1(K)=(2*UAVG-(U(K)+U(K-1)))*DZ/2.C+AI1(K-1)
      PRINT 146, K,AI1(K)
146   FORMAT (' AI1(',I3,')=',F15.8)
503   CONTINUE
      Z1=0.0
      Z13=0.0
```

```
      JU=0
504   Z11=Z13
505   DO 506 K=2,202
      IDZ1=ABS(Z(K)-Z1)/DZ+2
      DZ1=Z(K)-Z1
      IF (IDZ1-2) 507,507,506
507   IF (DZ1-0.0) 508,509,506
508   AI1(Z1)=AI1(K)+(AI1(K+1)-AI1(K))/DZ*(Z1-Z(K))
      D1(Z1)=D1(K)+(D1(K+1)-D1(K))/DZ*(Z1-Z(K))
      L=K
      PRINT 155,L
155   FORMAT (3H L=,I3)
      PRINT 151, Z1,AI1(Z1)
151   FORMAT (' AI1(',F15.8,')=',F15.8)
      GO TO 506
509   AI1(Z1)=AI1(K)
      D1(Z1)=D1(K)
      L=K
      PRINT 152,L
152   FORMAT (3H L=,I3)
506   CONTINUE
      DO 510 K=2,202
      IDZ1=ABS(Z(K)-Z1)/DZ+2
      DZ1=Z(K)-Z1
```

```
      IF (DZ1-0.0) 511,512,513
511   S6=0.0
      LZ=L-1
      DO 514 N=K,LZ
      IF (L-K) 551,551,514
514   S6=DZ/2.0*(AI1(N)/D1(N)+AI1(N+1)/D1(N+1))+S6
551   RK=(L-2)*DZ
      AI2(K)=-((Z1-RK)/2.0*(AI1(Z1)/D1(Z1)
     1  +AI1(L)/D1(L))+S6)
      PRINT 153, K,AI2(K)
153   FORMAT (' AI2(',I3,')=',F15.8)
      GO TO 510
512   AI2(K)=0.0
      GO TO 510
513   S7=0.0
      NZ=L+2
      IF (NZ-K) 531,531,530
531   DO 515 I=NZ,K
515   S7=S7+DZ/2.0*(AI1(I)/D1(I)+AI1(I-1)/D1(I-1))
530   SK=(L-1)*DZ
      AI2(K)=S7+(SK-Z1)/2.0*(AI1(Z1)/D1(Z1)
     1  +AI1(L+1)/D1(L+1))
      PRINT 154, K,AI2(K)
154   FORMAT (' AI2(',I3,')=',F15.8)
```

```
510     CCNTINLE
        S2=0.0
        S3=0.0
        DO 516 K=3,201,2
516     S2=S2+AI2(K)
        DO 616 K=4,200,2
616     S3=S3+AI2(K)
        S2=DZ/3.0*(AI2(2)+AI2(202)+4*S2+2*S3)
        IF (ABS(S2)-0.0C1) 517,517,518
518     PRINT 90C,Z1,S2
900     FORMAT (5H 1Z1=,F15.8,/5H 1S2=,F15.8)
        JU=JU+1
        IF (JU-1) 519,519,520
519     Z1=0.34
        Z11=0.0
        S1=S2
        GO TO 505
520     Z12=Z1
        Z13=Z1
        Z1=Z12-(S2/(S2-S1))*(Z12-Z11)
        IF (Z1-0.0) 521,521,522
521     Z1=Z12+0.1
522     IF (Z1-1.0) 532,532,561
561     Z1=Z12+0.1
```

```
      IF (Z12.GT.1.)      GO TO 541
532   S1=S2
      GO TO 504
517   IF (S2-0.00) 518,612,612
612   PRINT 102,S2,Z1
102   FORMAT(4H S2=,F15.8,/4H Z1=,F15.8)
      S4=0.0
      DO 523 K=2,201
523   S4=DZ/2.0*(U(K)*AI2(K)+U(K+1)*AI2(K+1))+S4
      EK=S4
      PRINT 103, EK
103   FORMAT (4H EK=,F15.8)
      GO TO 600
541   PRINT 104, Z1
104   FORMAT (5H ZNC=,F15.8)
600   STOP
      END
```

APPENDIX A3

Criteria for the Use of Vertical Averaging in Environmental Dispersion Models

F.M. GALLOWAY, JR.

The Cleveland State University
Cleveland, Ohio 44115

Vertical averaging, or averaging in a plane perpendicular to the mean flow, in environmental dispersion problems is desirable from the standpoint of efficiency of computer solution. This paper presents a method, based on computer solution of a model transport problem, for estimating when cross-plane averaging is appropriate. The method is applied to four examples representing typical lakes, rivers, estuaries and the atmosphere, respectively. The results are correlated in terms of a characteristic length, velocity and turbulent diffusivity, and two dimensionless parameters that depend on the velocity and vertical diffusivity profiles. It is shown that these parameters vary over a relatively small range for the variety of examples that are considered.

I. Introduction

Dispersion modeling in natural waters is an important aspect of the development of strategies to provide a desired water quality in a given area. Dispersion models are often designed for finite difference solution. The computer time required to obtain a solution increases significantly with each added space dimension. In situations where distance in one or more space directions is small relative to distance in the other directions, the dimensions having the short distances are often eliminated by cross plane averaging. The effect of these averaged out directions is retained in effective dispersion coefficients parallel to the remaining directions. This approach is strictly valid only after an initial period of dispersion has taken place and can lead to serious error when inappropriately applied. The purpose of this paper is to estimate the length of this initial period. A further purpose is to estimate the effective dispersion coefficient which replaces transport in the averaged-out direction. The approach is illustrated by application to flows representing a typical large lake, a river and an estuary, respectively, An example using a typical wind profile is also included for comparison.

II. Background and Problem Formulation

Taylor[1] did pioneering work in the description of dispersion in systems where the space dimensionality can be reduced by averaging in planes or directions perpendicular to the mean flow direction. He investigated theoretically and experimentally the transport of solute by laminar flow in a tube of circular cross-section. He identified two phases of transport. The first, extending from the point of introduction of the solute to some distance downstream, is

characterized by significant cross-plane variations in concentration of solute and an increasing rate of dispersion in the downstream direction of the solute cloud taken as a whole. The second phase begins after a sufficient time so that the cross-plane variations have become small. Taylor showed that the cross-plane averaged concentration in this second regime approaches a Gaussian distribution in the downstream direction. The center of gravity of the cloud moves downstream with the speed of the cross-plane averaged velocity and the further spread of the cloud parallel to the flow can be described by an effective downstream diffusion coefficient acting on the cross-plane averaged concentration. This effective downstream diffusion coefficient depends on the cross-plane shear of the downstream velocity, and the cross-plane diffusion coefficient.

All of the basic concepts for developing criteria for the use of cross-plane averaging in dispersion models are embodied in Taylor's paper. To summarize, he has shown that: (1) cross-plane averaging is a theoretically sound treatment of dispersion problems, provided that the solute cloud has entered the second phase of transport; (2) the effective dispersion coefficient in the second phase is related to cross-plane velocity shear and cross-plane diffusion; and (3) the extent of the first phase of transport (in time and distance) depends on the magnitude of the maximum downstream velocity, the magnitude of the cross-plane diffusion and the dimension(s) of the cross-plane.

Aris[2] generalized Taylor's results to parallel flows where the cross-section, velocity and cross-plane diffusivity profiles, and initial solute concentration distribution are arbitrary. He did this mathematically by deriving and solving equations for the moments of the concentration distribution. Aris' introduction of the moment method has proven very useful in the application of Taylor's concepts to environmental situations.

It is apparent from Taylor's analysis that the determination of when the use of cross-plane averaging becomes appropriate is equivalent to finding the time and distance over which the first phase of transport persists. For practical purposes, this first phase of transport will be defined as extending over the period of significant variation of the effective downstream dispersion coefficient. It will be demonstrated later in the numerical results that by the time this coefficient has reached essentially a constant value, the cross-plane variations in concentration have become well relaxed. Although the approach to true normality of the concentration distribution is much slower, as Aris[2] has pointed out, the error introduced in a computation by taking the definition of the extent of the first phase of transport as given above is not expected to be great for practical purposes.

The determination of the extent of the first phase of transport is approached through the model transport equation for a finite layer

$$\frac{\partial C}{\partial t} + u(z) \frac{\partial C}{\partial x} = \frac{\partial}{\partial z} \left[D_z \frac{\partial C}{\partial z} \right] \tag{1}$$

where C is the concentration of transported material, u(z) is the vertical velocity profile of the x-direction velocity, $D_z(z)$ is the vertical diffusivity profile, x is the downstream coordinate and z is a coordinate in the cross stream direction. (1) is to be solved subject to the initial condition

$$C(x,z,0) = e^{-\frac{(x-.125h)^2}{4ah^2}} \tag{2}$$

and the boundary conditions

$$D_z \left. \frac{\partial C}{\partial z} \right|_{0,h} = 0 \tag{3}$$

where "a" is a parameter and h is the thickness of the layer. By picking "a" small, the initial condition approximates a delta function input. (3) indicates that C is confined within the finite layer.

Using the dimensionless variables

$$x^* = \frac{x}{h}$$

$$z^* = \frac{z}{h}$$

$$u^* = \frac{u}{U_{max}}$$

$$t^* = \frac{t}{h/U_{max}}$$

$$D_z^* = \frac{D_z}{h\ U}$$

where U_{max} is the magnitude of the difference between the maximum and minimum velocities occurring in u(z), then (1) - (3) become

$$\frac{\partial C}{\partial t^*} + u^*(z)\ \frac{\partial C}{\partial x^*} = \frac{\partial}{\partial z^*}\left[D^*_z\ \frac{\partial C}{\partial z^*}\right] \qquad (1a)$$

$$C(x^*, z^*, 0) = e^{-(x^*-.125)^2/4a} \qquad (2a)$$

$$D^*_z \left.\frac{\partial C}{\partial z^*}\right|_{0,1} = 0 \qquad (3a)$$

In applying (1a) - (3a), the direction x is normally picked to maximize the variation in velocity u(z) over the range $0 \leq z \leq h$ if the flow is not parallel across the layer. Diffusion in the x direction is not included since it is usually negligible compared with convection. The evolution of an initial

finite amount of material is studied rather than using a continuous source so that the effective downstream dispersion coefficient may be studied in terms of the growth rate of Σ_{x2}, the x direction variance of C.

The general approach is to solve (1a) for the u(z) and $D_z(z)$ profile of interest in an environmental application. From the solution, C(x,z,t), $\Sigma_x 2$ can be calculated as a function of time. The approach of $\Sigma_x 2$ to a growth rate linear in time reveals the extent of phase I transport. A check of the vertical variation remaining in C(x,z,t) when $\frac{d\Sigma x2}{dt}$ becomes constant then gives some evaluation of the appropriateness of cross-plane averaging using this criterion.

It is shown in Appendix I that, based on (1a), the approach of $\frac{d\Sigma\ x^2}{dt}$ to a constant value is exponential with exponent - $\alpha_1\ \overline{D}_z{}^*t^*$, where α_1 is generally the smallest eigenvalue in a certain Sturm-Liouville problem, and $\overline{D}_z{}^*$ is the mean non-dimensional cross-plane diffusion. α_1 can be estimated from the numerical solution of (1a) - (3a). Dimensional time, t_1, to reach phase II transport thus scales as

$$t_1 = \frac{h^2}{\alpha_1 \overline{D}_z} \tag{4}$$

When phase II is reached, the z direction can be replaced by an effective dispersion coefficient in the x direction, K_x. This, be definition, is

$$K_x = \frac{1}{2} \left. \frac{d\Sigma x2}{dt} \right|_{t \to \infty} \tag{5}$$

and can be evaluated from the solution for C in (1) - (3). A more direct approach is to compute K_x by the method given by Csanady[3],

$$K_x = \frac{1}{h} \int_0^h u(z) \; \phi \; (z) \; dz \tag{6}$$

where

$$\phi\,(z) = \int_{z_1}^{z} \frac{dz}{D_z(z)} \int_0^z (\bar{u} - u)\, dz \tag{7}$$

$\bar{u}$ is the z-averaged velocity and z_1 is chosen to make

$$\int_0^h \phi\,(z)\; dz = 0 \tag{8}$$

If equations (6) - (8) are non-dimensionalized as above, it can be seen that

$$K_x = C_1 \; \frac{h^2 U^2_{max}}{\bar{D}_z} \tag{9}$$

where C_1 is determined from the evaluation of (6) - (8) in dimensionless form with $\bar{D}^*_z = 1$.

Several examples demonstrating the use of equations (1a) - (3a), (4) and (6) - (8) are given in section III. In these examples, equations (1a) - (3a) have been solved numerically. In the finite-difference approximation to (1a), the diffusion term

$$\frac{\partial}{\partial z^*} \left(D_z^* \; \frac{\partial C}{\partial z^*} \right)$$

has been approximated by a central difference approximation. The combined unsteady and convective terms,

$$\frac{\partial C}{\partial t^*} + u^*(z) \; \frac{\partial C}{\partial x^*}$$

have been approximated using a scheme given by Fromm[4,5]. The scheme possesses very low numerical dispersion. Details of the computational scheme are available elsewhere[6]. The evaluation of K_x from equations (6) - (8) is accomplished by a numerical integration of these equations in dimensionless form for given $u(z)$ and $D_z(z)$ profiles. The trapezoidal rule was used to approximate the integrals. The answer for K_x should be the same as that determined more indirectly from the solution of (1a) - (3a). Comparison of K_x obtained by the two methods provides a check on the accuracy of the computational schemes.

Prediction of the extent of phase I transport in environmental applications seems to have been quite limited. Fischer[7,8] has done the most extensive work. In considering flow in rivers and channels he reasoned that the time needed to reach the "diffusive" period, or phase II, would be given by the Lagrangian time scale for the flow. In developing this idea, and using data for flow in channels, he arrived at the criterion

$$t = 1.8 \frac{l^3}{r\, U^*} \tag{10}$$

where l is the distance from maximum surface velocity to the nearest shore point, r is the hydraulic radius and U^* is the friction velocity. One of the criteria used by Fischer to define the beginning of the "diffusive" period was the approach to constancy of $\Sigma_x 2$ which is the criterion used here. Taking $D_z = .23\, dU^*$ for channels and rivers, where d is the local depth, then (10) becomes

$$t = 1.8 \frac{l^2}{r\, D_z/.23d} \tag{11}$$

Using a mean value for D_z and assuming $r = \bar{d}$, then (11) becomes

$$t = .41\, l^2/\bar{D}_z \tag{12}$$

Saffman[9], for atmospheric dispersion beneath an inversion layer, gives

$$t >> \frac{h^2}{2\ \bar{D}_z} \tag{13}$$

as a criterion for phase II transport. (12) and (13) are both in the form of equation (4). While (13) may be a safe prediction in most cases of atmospheric transport, the aim of the approach here is to define α_1, and thus the time of phase I transport, more sharply.

Many more investigations have considered the evaluation of K_x in environmental situations. A sampling of these are Elder[10] for channel flow, Saffman[9] for atmospheric dispersion, Thackston and Krenkel[11] and Fischer[7,8] for dispersion in streams, and Bowden[12] for flow in estuaries and coastal waters. Some of these will be referred to again in section III.

Fiering and Yotsukura[13] solved equation (1a) by a finite-difference technique. However, their numerical scheme was completely different. Moreover, they were interested in finding the shape of the downstream concentration distribution as a function of time. They used only one vertical diffusivity and velocity profile, whereas in this investigation it is the effect of varying D_z and u on α_1 and C_1 which is of interest.

III. Results

A. Lakes

A velocity profile, $u^*(z^*)$, for use in (1a), typical of wind driven currents in a shallow constant depth lake was taken from the results of Gedney[14]. The profile is given in Table 1.

TABLE 1

$u^*(z^*)$ for wind driven currents in a shallow constant depth lake

z^*	$u^*(z^*)$
1.0	.777
.9	.452
.8	.227
.7	-.066
.6	-.111
.5	-.161
.4	-.201
.3	-.223
.2	-.178
.1	-.111
0	0

A constant value of $D_z^* = \overline{D}_z^* = 0.1$ was used.

Figure 1 shows the concentration profile vs x^* at $z^* = .5$ for $t^* = 1,2$ and 6. The spreading out in the x^* direction due to the velocity shear is apparent. Also, the profile is losing its skewness and is gradually approaching a normal distribution. Figure 2 shows concentration vs. z^*, at an x^* where the concentration is a maximum, for $t^* = 1$, 2 and 6. The profile has become quite flat by the time $t^* = 6$. Figure 3 shows Σ^*_{x2} vs t^*. For $t^* \geq 3$, Σ^*_{x2} grows

linearly with t*. Evaluating K^*_x from the dimensionless form of equation (5) and the slope, $\frac{d\Sigma^* x^2}{dt^*}$, from Figure 3 gives $K_x^* = .0527$. The evaluation of K_x^* from the dimensionless form of (6) - (8) gives $K_x^* = .0536$, confirming the accuracy of the computations. The use of these results in modeling pollution dispersion in the western basin of Lake Erie will now be illustrated. Since $t_1^* = 3$ is the approximate transition point from phase I to phase II transport, then $\alpha_1 \overline{D}_z^* = 1/3$ and since $\overline{D}_z^* = .1$ in this case, $\alpha_1 = 3.3$. Galloway[15] found in modeling dispersion in the western basin of Lake Erie that $D_z = 5$ cm^2/sec marked approximately the dividing value for D_z in terms of whether or not a vertically averaged dispersion model yielded results in agreement with a full three-dimensional model. The velocity profile given in Table 1 is typical of the velocity distribution used in the model over much of the western basin. When $D_z = 50$ cm^2/s was used, there was essentially no difference in the answers from the vertically integrated model and the three-dimensional model. When $D_z = .5$ cm^2/s, there were significant differences in the answers from the two models. $D_z = 5$ cm^2/s produced answers that were slightly different in the two cases. Reference quantities for the western basin of Lake Erie are $h = 750$ cm and $U_{max} = 30$ cm/s. For $D_z = 50$, 5 and .5 cm^2/s, the predicted time limits for phase I transport, from Equation (4), are .95, 9.5, and 95 hours, respectively, with corresponding length scales, based on the reference velocity U_{max}, of 1, 10, and 100 km. The western basin dispersion computations[15] were performed using a finite difference grid size in the horizontal directions of 3.2 km. Based on the above predicted limits for phase I transport, it would

therefore be expected that vertical averaging would be a good approximation to the three-dimensional calculations for D_z = 50 cm^2/s, a fair approximation for D_z = 5 cm^2/s and a poor approximation for D_z = .5 cm^2/s. As indicated above, this, in fact, was the case.

The calculated value for K_x from equation (9), corresponding to D_z = 5 cm^2/s, is 6 * 10^5 cm^2/s. This is comparable to the value reported by Murthy[16] for the "horizontal diffusivity" in Lake Ontario for a length scale of 10 km. It bears re-emphasizing, however, that K_x results from vertical shear of the horizontal velocity and is therefore directionally dependent. In vertically averaged dispersion models for large bodies of water it is not, strictly speaking, correct to use a single typical value for the horizontal diffusivity in all directions. Rather, an effective dispersion coefficient should be calculated for each coordinate direction. In a large lake calculation these coefficients will quite likely vary from point to point. Since these variations are automatically included in a three-dimensional calculation by the horizontal convective terms and the vertical diffusion term, it may be more efficient in some cases to use a three-dimensional model even if vertical averaging is appropriate.

B. Rivers

Natural rivers are typically much wider than they are deep. Thus z, in equation (1), is in the direction across the river, and x is downstream distance. It is assumed that there is negligible concentration variation with depth. u(z) is now the vertically averaged velocity profile across the river. $D_z(z)$ is the cross-river diffusivity profile and includes depth variation as a

weighting factor to account for the variable cross-stream transport area. $u(z)$ and $D_z(z)$ were picked to approximate a river studied by Fischer[8]. In dimensionless form, they are

$$u^*(z^*) = 32\,[z^*(1 - z^*)]^{2.5}$$

and

$$D_z^*(z^*) = .251\,[z^*(1-z^*)]^{.5} + .005$$

Thus $\overline{D}_z^* = 0.1$.

Figure 4 shows the approach to normality of the downstream concentration distribution. It should be noted that the x* scale is different for t* = 3.5 and 7.5. Figure 5 indicates that by t* =3.5, cross-river concentration variations have become quite small. Figure 6 shows that by t* = 2, Σ^*_{x2} has approached an approximately linear growth rate. Thus

$$\alpha_1 \overline{D}^*_z = \frac{1}{2}$$

and

$$\alpha_1 = 5$$

Therefore,

$$t_1 = \frac{h^2}{5\,\overline{D}_z} \tag{14}$$

is the prediction for this river. Assuming $l = \frac{h}{2}$ in equation (12), then Fischer's time for phase I transport, based on his measurements, is

$$t_1 = .1\,\frac{h^2}{\overline{D}_z} \tag{15}$$

The factor of two difference between (14) and (15) is considered to be negligible due to the degree of arbitrariness in defining the end of phase I, and also the approximations made in obtaining (15) from (10).

The value of K_x^* from the slope of Figure 6 is .032. This is sufficiently close to the more accurate value of .030 obtained from the dimensionless form of equation(6). If $\overline{D}_z = .23\ u^*\ \overline{d}$, as suggested by Fischer, where u* is the friction velocity and has the typical value of 9.9 cm/s for channel flow, and $\overline{d}$ is the mean depth, then t_1 and K_x can be calculated for various rivers. In Fischer's example, $\overline{d} \simeq 81$ cm, $h \simeq 1800$ cm and $U_{max} \simeq 82$ cm/s. Thus $\overline{D}_z = 184$ cm^2/s.

Then, from equation (9), $K_x = (.030*.1)\ \dfrac{h^2 U_{max}^2}{\overline{D}_z} = 3.6* 10^5\ cm^2/s$

The factor .1 must be included because the value of $K_x^* = .030$ was obtained using $\overline{D}_z^* = .1$ instead of 1. Fischer[8] calculated the value of 2.1×10^5 cm^2/s from the actual profile data. The time for phase I transport, from equation (14), is .98 hr, corresponding to a distance of 2.9 km based on U_{max}.

C. The Atmosphere

The case considered here is for material confined between ground level and some finite height, h, due to the presence of an inversion. z in equation (1) is distance measured above ground level, and x is downwind distance from the point of release of dispersing material. Following an example given by Saffman[9], a power law wind profile was used for u(z), and $D_z(z)$ was determined from the Reynolds analogy. In dimensionless form, they are

$$u^*(z^*) = z^{*.143}$$

and

$$D_z^*(z^*) = .186\ z^{*.857}$$

so that again $\overline{D}_z^* = 0.1$.

Figure 7 shows the gradual approach to normality of the downwind concentration distribution. Note that the x* scale is different for the t* = 4.5 case. Figure 8 shows that the variation of concentration over most of the layer is quite small by t* = 4.5, although a significant variation of concentration is still apparent from z* = 0 to z* = .2. Figure 9 indicates that $\Sigma^*_{x^2}$ has approached a linear growth rate by t* = 4. Thus,

$$\alpha_1 \overline{D}^*_z \simeq \frac{1}{4}$$

and

$$\alpha_1 = 2.5$$

Therefore the time bound on phase I transport in this case is

$$t_1 = \frac{h^2}{2.5\ \overline{D}_z} \tag{16}$$

Thus, Saffman's general criterion given in equation (13)

$$t >> \frac{h^2}{2\ \overline{D}_z} \tag{13}$$

is seen to predict a time which is too large for most practical applications. Of course, the constant in equation (16) depends on the $D_z(z)$ profile, and to a lesser extent on the u(z) profile.

The value of K_x^* from the slope of Figure 9 is .022. This is somewhat higher than the more accurate value of .0145 from the dimensionless form of equation (6). The difference is thought to result from too large a grid size used in the solution of equations (1a) - (3a) for this example, which was more

demanding numerically than the other examples. A significant improvement was noted as the grid in the z direction was halved, but computer limitations prevented a further refinement. Based on $K_x^* = .0145$,

$$K_x = .0145 * .1 * \frac{h^2 U^2_{max}}{\overline{D}_z}$$

$$= .00145 * \frac{h^2 U^2_{max}}{\overline{D}_z}$$

D. Estuaries

A combined logarithmic - parabolic velocity profile is chosen to represent a tidal current. According to Bowden[17], this agrees with some observations of tidal currents. In dimensionless form the velocity profile is

$$u^* = 0, \quad 0 \leq z^* < .01$$

$$u^* = (4.62 + \ln z^* - z^*)/4.40, \quad .01 \leq z^* < .2$$

$$u^* = [5.00 (z^* - \tfrac{1}{2} z^{*2}) + 1.89]/4.40, \quad .2 \leq z^* \leq 1$$

The corresponding vertical diffusivity profile, based on Reynolds analogy, is

$$D^*_z = .556 z^*, \quad 0 \leq z^* < .2$$

$$D^*_z = .111, \quad .2 \leq z^* \leq 1$$

Thus,

$$\overline{D}^*_z = .1 \text{ again.}$$

As in previous examples, Figures 10 and 11 show the developing horizontal and vertical concentration profiles, respectively, and Figure 12 shows Σ^*_{x2} vs t*. The approach of Σ^*_{x2} to a linear growth rate in time is the least sharp of any of the examples. Using Figure 11 in conjunction with Figure 12, t* is estimated to be 5 in order to have reached the end of phase I transport. Even at t* = 5, Figure 11 indicates a variation in concentration from top to bottom by a factor of more than five. Taking t* = 5,

$$\alpha_1 \overline{D}_z^* = \frac{1}{5}$$

and

$$\alpha_1 = 2$$

Therefore,

$$t_1 = \frac{h^2}{2\,\overline{D}_z} \tag{17}$$

From the dimensionless form of equation (6), $K_x^* = .0372$ for $\overline{D}^*_z = .1$, giving

$$K_x = .00372 * \frac{h^2 U^2_{max}}{\overline{D}_z} \tag{18}$$

It should be emphasized that K_x in equation (18) does not take into account tidal oscillations. Using typical values for estuaries of h = 2000 cm and $\overline{D}_z$ = 10 cm^2/s in equation (17) gives t_1 = 56 hr. t_1 thus extends over four 12 hr periods of tidal oscillations. This indicates that methods of calculating K_x for estuaries based on assuming phase II transport is in effect, such as presented by Bowden[12], are not strictly valid for time scales less than about 2 days. For shorter times, the vertical diffusion of material must also be taken into account.

IV. Discussion

In all the examples presented in section III, the approach of K_x to a constant value coincides reasonably well with the approach of C to uniformity in the cross-plane direction. This is in agreement with the predictions of Aris[2] and the development in the Appendix. The use of the criterion, $K_x \rightarrow$ constant, in connection with the solution of the model equations (1) - (3), to mark the beginning of phase II transport was demonstrated to be satisfactory in two ways. First, it was shown to give the correct prediction for the time and length scales beyond which cross-plane averaging was appropriate for dispersion calculations in the western basin of Lake Erie[15]. Second, it corresponded well with dispersion measurements made in a river[8]. The fact that cross-plane concentration differences are largely damped out when K_x is approximately constant justifies calculation of other phenomena, e.g., chemical reactions, based on homogeneity in the cross-plane direction during this stage of transport.

The profiles for $u(z)$ and $D_z(z)$ in the examples of section III are thought to represent a wide range of flows in the environment. Table 2 summarizes the results for these examples.

TABLE 2

	α_1	C_1
Lake	3.3	.00527
River	5	.0030
Atmosphere	2.5	.00145
Estuary	2	.0037

$$t_1 = \frac{h^2}{\alpha_1 \overline{D}_z} \qquad K_x = C_1 \frac{h^2 U^2_{max}}{\overline{D}_z}$$

In estimating t_1 and K_x, α_1 and C_1 are the only parameters that depend on the shape of the profiles for D_z and u. From Table 2, α_1 varies by a factor of only 2.5 over the profiles studied. C_1 varies by less than a factor of 4. (C_1 for estuaries in Table 2 does not take into account current oscillations). Thus t_1 and K_x can be well estimated from these results for a wide range of cases of practical interest. Only for situations where $D_z(z)$ and $u(z)$ are significantly different from any of the examples given would it be expected that α_1 and C_1 would vary greatly from the range in Table 2. The major contribution to the difference in t_1 and K_x from one example to the next is in the variation of h, U_{max} and $\overline{D}_z$.

The fact that U_{max} appears to the second power in the expression for K_x in Table 2 indicates the wide variation to be expected in the effective horizontal dispersion coefficients in the directions parallel and transverse, respectively, to the main flow. Such variation has, of course, been noted in many investigations. Care must be exercised, then, to use the proper effective dispersion coefficient in each horizontal direction when cross-plane averaging is used.

V. Conclusions

The following conclusions can be drawn from the work presented here. (1) The arrival of K_x to a constant value, as determined by the solution of the model given in equations (1) - (3) for suitably defined $u(z)$ and $D_z(z)$, appears to be a practical criterion for the use of cross-plane averaging.

(2) t_1, the time for phase I transport, scales as

$$t_1 = \frac{h^2}{\alpha_1 \overline{D}_z}$$

and K_x, the effective dispersion coefficient, scales as

$$K_x = C_1 \frac{h^2 U^2_{max}}{\overline{D}_z}$$

(3) α_1 varies by a factor of 2.5 and C_1 varies by a factor of less than 4 within the range of D_z and u profiles studied.

(4) α_1, and thus the time for phase I transport, is mainly dependent on $D_z(z)$ and is only weakly affected by u(z) (see Appendix 1).

Acknowledgement

This work was supported by a grant from the U. S. Dept. of the Interior, Office of Water Resources Research, under the Annual Allotment Program to Ohio, grant #A-036-OHIO.

Donation of computer time to this project by The Cleveland State University is sincerely appreciated.

NOTATION

a	parameter defined in equation (2), dimensionless
C	concentration, mass/length^3
C_1	evaluated from dimensionless form of equation (6) with $\bar{D}^*_z = 1$, dimensionless
D_z	vertical diffusivity, length^2/time
d	local river depth, length
h	layer thickness, length
K_x	effective dispersion coefficient in x direction, length^2/time
l	distance from maximum surface velocity to nearest shore point of river, length
r	hydraulic radius, length
t	time
U_{max}	reference velocity taken to be magnitude of the difference between maximum and minimum velocities across the layer, length/time
U^*	friction velocity, length/time
u	velocity in x direction, length/time
x	downstream distance, length
z	cross plane distance, length
α_1	smallest eigenvalue of Sturm-Liouville problem defined in Appendix 1, dimensionless
ϕ	function of z defined by equations (7) and (8), length
Σ_{x2}	x direction variance of C distribution, length^2

SYMBOLS

*	superscript indicating dimensionless quantities, except when used for U*
-	superscript indicating cross plane averaged quantities

REFERENCES

1. Taylor, G., Proc. Roy. Soc. Lond., A219, 186 (1953).

2. Aris, R., Proc. Roy. Soc. Lond., A235, 67 (1956).

3. Csanady, G. T., Turbulent Diffusion in the Environment, D. Reidel Publishing Company, Boston (1973).

4. Fromm, J. E., J. Comp. Phys., 3, 197 (1968).

5. Fromm, J. E., Phys. Fl. Supplement II, 3 (1969).

6. Natarajan, R., Numerical Solution to a Two-Dimensional Dispersion Equation, M.S. Thesis, Dept. of Chemical Engineering, The Cleveland State University, 1973.

7. Fischer, H. B., J. Hyd. Div., ASCE, HY6, 187 (1967).

8. Fischer, H. B., J. Sanit. Eng. Div., ASCE, SA5, 927 (1968).

9. Saffman, P. G., Quart, J. Roy. Meteorol. Soc., 88, 382 (1962).

10. Elder, J. W., J. Fluid Mech., 5, #4, 544 (1959).

11. Thackston, E. L., and Krenkel, P. A., J. Sanit. Eng. Div., ASCE, SA5, 67 (1967).

12. Bowden, K. F., J. Fluid Mech., 21, #2, 83 (1965).

13. Yotsukura, N., and Fiering, M. B., J. Hyd. Div., ASCE, HY5, 83 (1964).

14. Gedney, R. T., NASA TMX-52985, March, 1971.

15. Galloway, F. M., Proc. 16th Conf. Great Lakes Res., Int. Assoc. Great Lakes Res., 1973.

16. Murthy, C. R., Proc. 13th Conf. Great Lakes Res., Int. Assoc. Great Lakes Res., 1970.

Appendix 1

The time dependence of $\frac{d\Sigma_{x2}}{dt}$

The basic approach is based on that given by Aris[2]. Starting with equation (1),

$$\frac{\partial C}{\partial t} + u \frac{\partial C}{\partial x} = \frac{\partial}{\partial z}\left[D_z \frac{\partial C}{\partial z}\right] \tag{A1}$$

the functions ψ and v are introduced as

$$\frac{\partial C}{\partial t} + U\left[1 + \frac{v}{U}\right] \frac{\partial C}{\partial x} = \overline{D}_z \frac{\partial}{\partial z}\left[\psi \frac{\partial C}{\partial z}\right] \tag{A2}$$

where U is the average value of u across the layer, v is a measure of the deviation of the local velocity from the average, $\overline{D}_z$ is the average value of D_z across the layer, and $\Psi = D_z/\overline{D}_z$. By definition,

$$\frac{1}{h}\int_0^h v\,dz = 0 \quad \text{and} \quad \frac{1}{h}\int_0^h \Psi\,dz = 1.$$

If a downstream coordinate, $x' = x - Ut$, is introduced, (A2) becomes

$$\frac{\partial C}{\partial t} + v \frac{\partial C}{\partial x'} = \overline{D}_z \frac{\partial}{\partial z}\left[\Psi \frac{\partial C}{\partial z}\right] \tag{A3}$$

Introducing the non-dimensional variables

$$x^* = x'/h, \quad z^* = z/h, \quad t^* = t/(h/U_{max}), \quad v^* = v/U_{max},$$

(A3) becomes

$$\frac{\partial C}{\partial t^*} + v^* \frac{\partial C}{\partial x^*} = \overline{D}_z^* \frac{\partial}{\partial z^*}\left(\psi \frac{\partial C}{\partial z^*}\right) \tag{A4}$$

where h is the layer thickness, U_{max} is the maximum absolute difference in all

values taken on by v over h, and $\overline{D}_z^* = \overline{D}_z/(h\, U_{max})$. The * in equation (A4) will be dropped to simplify notation in the remaining development. Now introduce

$$C_o(z) = \int_{-\infty}^{\infty} C(x, z)\, dx$$

where $C_o(z)$ is the solute in the plane at level z. Then (A4) becomes

$$\frac{1}{\overline{D}_z} \frac{\partial C_o}{\partial t} = \frac{\partial}{\partial z} \left[\psi \frac{\partial C_o}{\partial z} \right] \tag{A5}$$

If (A5) is solved subject to the boundary conditions

$$\psi \left. \frac{\partial C_o}{\partial z} \right|_{z = 0,1} = 0 \tag{A6}$$

which result from similar conditions on C, the solution is

$$C_o = A_o + \Sigma A_i\, \phi_i\, e^{-\alpha i\, \overline{D}_z\, t} \tag{A7}$$

where α_i and ϕ_i are the eigenvalues and corresponding eigenfunctions of the Sturm-Liouville problem resulting from (A5) and (A6). The A_i are determined by the initial distribution of C_o.

Next introduce into (A4)

$$C_1(z) = \int_{-\infty}^{\infty} x\, C(x,z)\, dx$$

where $C_1(z)$ is the first moment of the distribution of C in the x direction. Assuming $C \to 0$ sufficiently rapidly with x, (A4) becomes

$$\frac{\partial C_1}{\partial t} = v\, C_o + \overline{D}_z \frac{\partial}{\partial z} \left(\frac{\partial C_1}{\partial z} \right) \tag{A8}$$

(A8) is to be solved subject to the boundary conditions

$$\psi \left.\frac{\partial C_1}{\partial z}\right|_{z=0,1} = 0$$

which again results from the similar conditions on C. The complimentary function for the homogeneous part of (A8) is

$$C_{1c} = B_o + \Sigma B_i \phi_i e^{-\alpha_i \bar{D}_z t} \tag{A9}$$

A particular integral of (A8) of the form

$$C_{1p} = f_o + \Sigma e^{-\alpha_i \bar{D}_z t} f_i \tag{A10}$$

is sought. Substituting (A7) and (A10) into (A8) gives

$$\begin{aligned} \Sigma (-\alpha_i \bar{D}_z) e^{-\alpha_i \bar{D}_z t} f_i = {} & v A_o + v \Sigma A_i \phi_i e^{-\alpha_i \bar{D}_z t} \\ & + \bar{D}_z \frac{d}{dz} \left(\psi \frac{df_o}{dz}\right) \\ & + \bar{D}_z \Sigma e^{-\alpha_i \bar{D}_z t} \frac{d}{dz} \left(\psi \frac{df_i}{dz}\right) \end{aligned} \tag{A11}$$

The f_i are thus determined by the relations

$$\bar{D}_z \frac{d}{dz} \left(\psi \frac{df_o}{dz}\right) = v A_o,$$

$$\bar{D}_z \frac{d}{dz} \left(\psi \frac{df_i}{dz}\right) + \alpha_i \bar{D}_z f_i = v A_i \phi_i \tag{A12}$$

where the f_i must satisfy

$$\psi \left.\frac{df_i}{dz}\right|_{z=0,1} = 0$$

The solution for C_1 is then

$$C_1 = C_{1c} + C_{1p} \tag{A13}$$

and the B_i in (A9) are determined by the initial condition on C_1.

An equation for $C_2(z) = \int_{-\infty}^{\infty} x^2 \; C(x,z)\, dx$ can similarly be obtained from (A4). The result is

$$\frac{\partial C_2}{\partial t} = 2 v C_1 + \overline{D}_z \frac{\partial}{\partial z} \left(\psi \frac{\partial C_2}{\partial z}\right) \tag{A14}$$

The first and second moments of the total distribution, M_1 and M_2, can be obtained from C_1 and C_2 by integrating over the layer. Thus,

$$M_i = \int_0^1 \int_{-\infty}^{\infty} x^i \; C \, dx dz$$

$$= \int_0^1 C_i \, dz \tag{A15}$$

Thus, for i = 1, (A15) gives

$$M_1 = \int_0^1 (B_o + f_o)\, dz + \Sigma \, e^{-\alpha_i \overline{D}_z t} \int_0^1 (B_i \phi_i + f_i)\, dz \tag{A16}$$

For i = 2, from (A15)

$$\frac{dM_2}{dt} = \int_0^1 \frac{\partial C_2}{\partial t} \, dz$$

$$= \int_0^1 2\, v\, C_1\, dz$$

$$= \int_0^1 2v\, (B_o + f_o)\, dz + \Sigma e^{-\alpha_i \bar{D}_z t} \int_0^1 2\, v\, (B_i \phi_i + f_i)\, dz \qquad \text{(A17)}$$

The effective dispersion coefficient in the x direction, as defined by equation (5) in the text, is thus given by

$$2K_x = \frac{d\, \Sigma\, x^2}{dt}$$

$$= \frac{h^2}{(h/U_{max})} \left(\frac{dM_2}{dt^*} - \frac{dM_1^2}{dt^*} \right) \qquad \text{(A18)}$$

(A16) and (A17), in connection with (A18), show that $\frac{d\Sigma_x 2}{dt}$ approaches a constant value exponentially with exponent $-\alpha_1 \bar{D}_z^* t^*$, where α_1 is the smallest eigenvalue from the solution of (A5) and (A6). This is the basis for equation (4) in the text.

It can be seen in the development that the α_i are independent of the velocity profile. The velocity affects the rate of approach of K_x to a constant only through the integrals in (A16) and (A17) which are the coefficients of the exponential terms. In this sense, the velocity profile has a secondary effect on the approach to constant K_x in comparison with the vertical diffusivity profile, which directly influences the α_i.

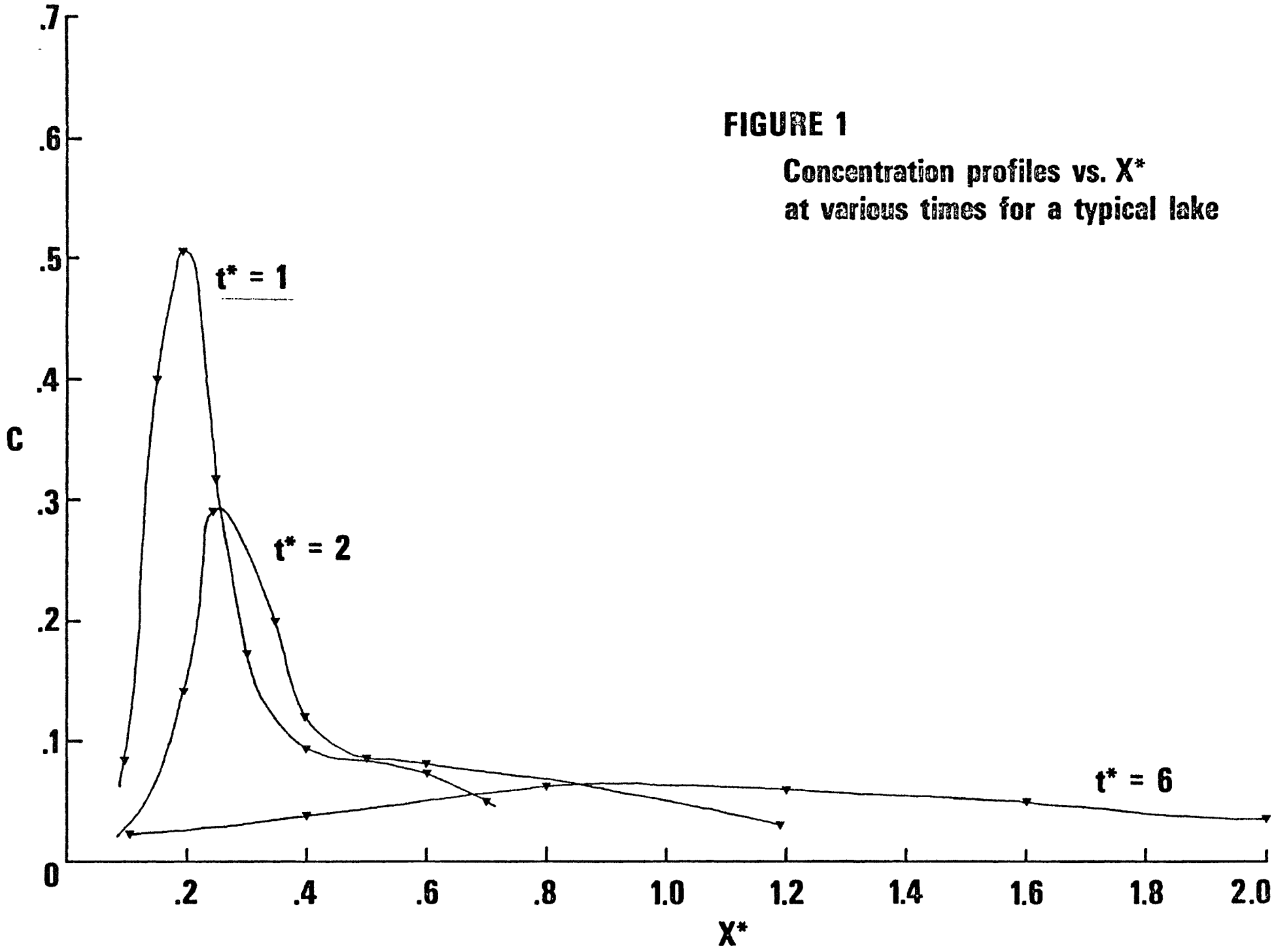

FIGURE 1

Concentration profiles vs. X*
at various times for a typical lake

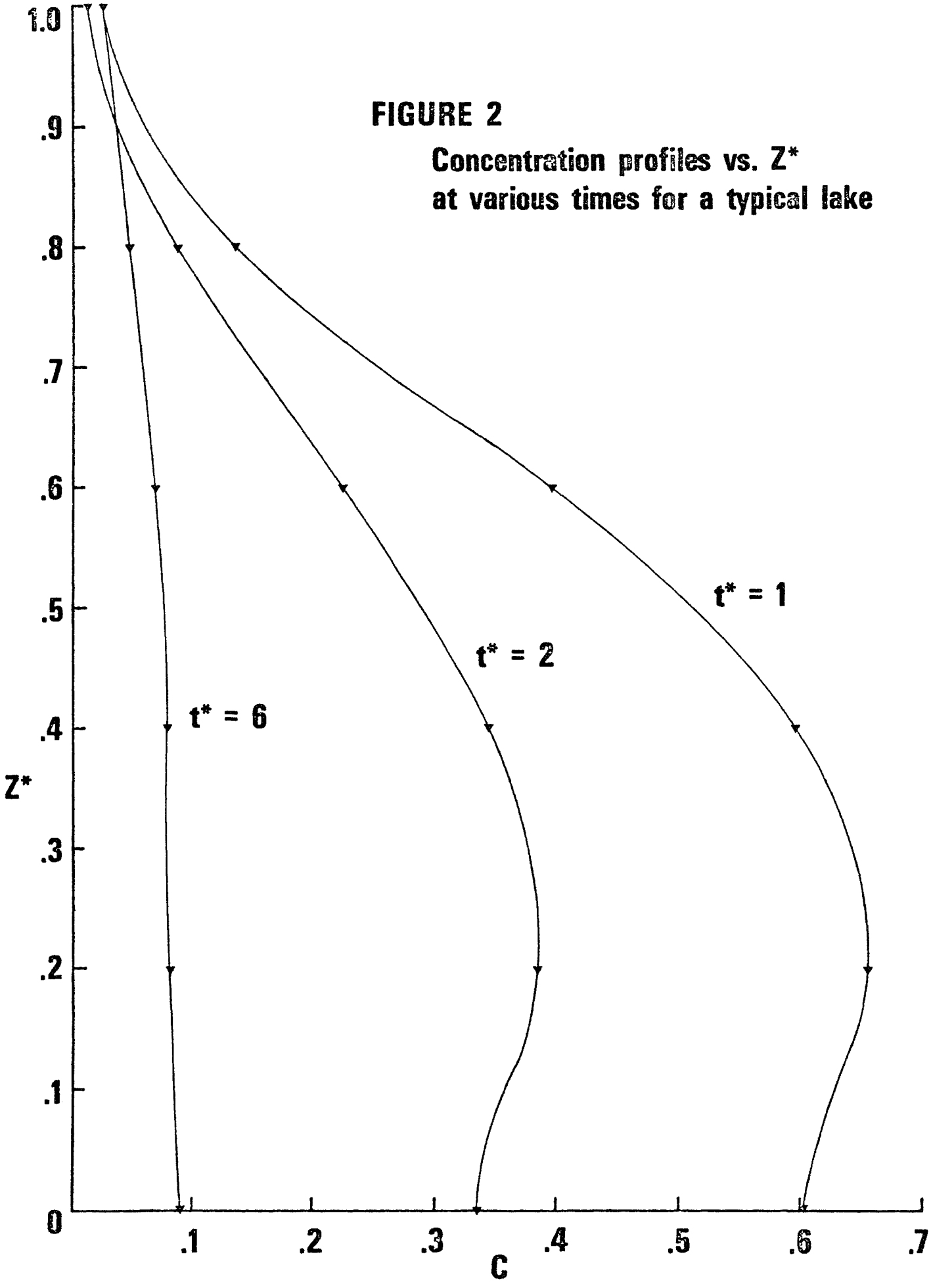

FIGURE 2

Concentration profiles vs. Z*
at various times for a typical lake

FIGURE 3

$\Sigma^* x^2$ vs. t^* for a typical lake

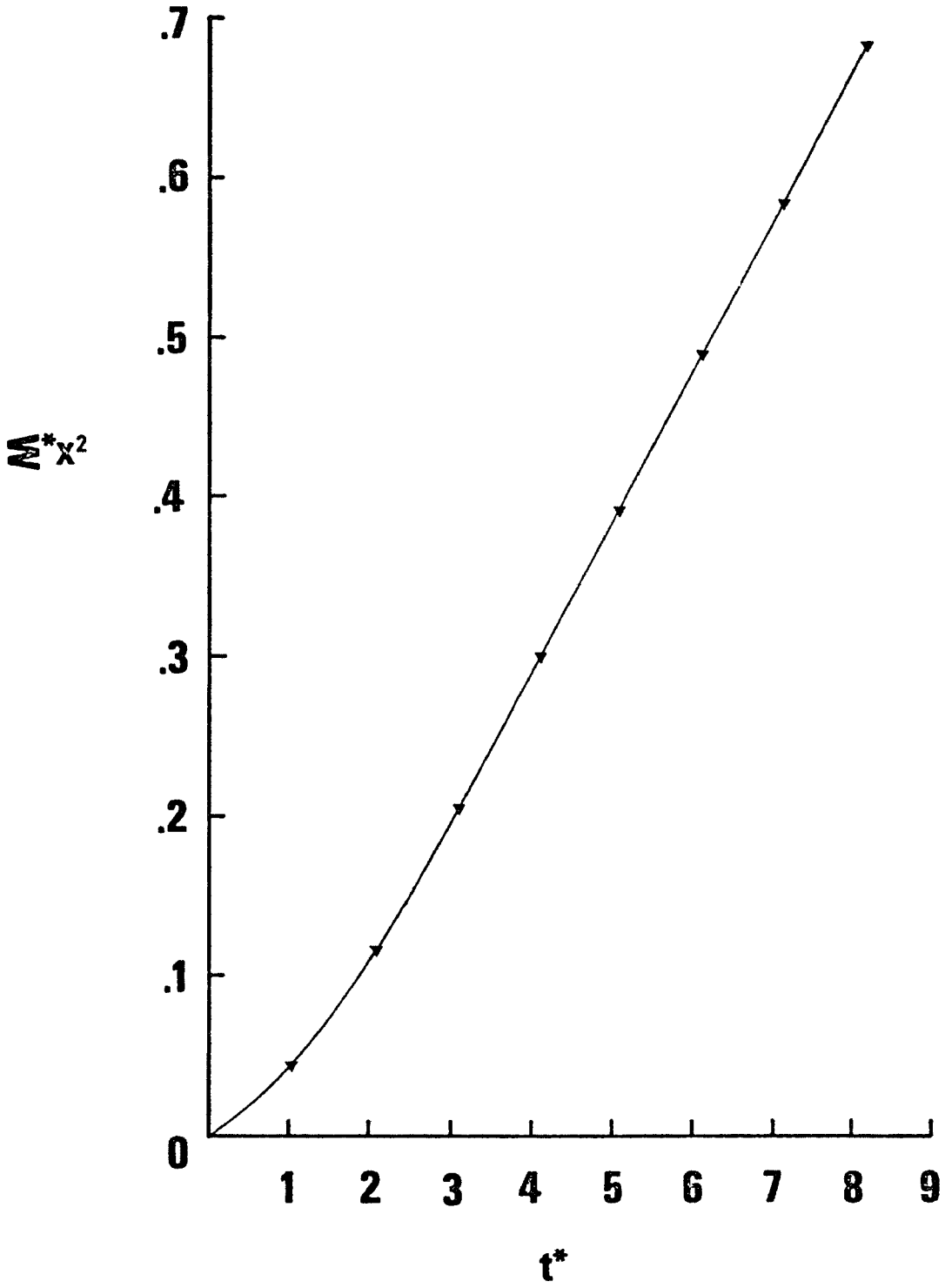

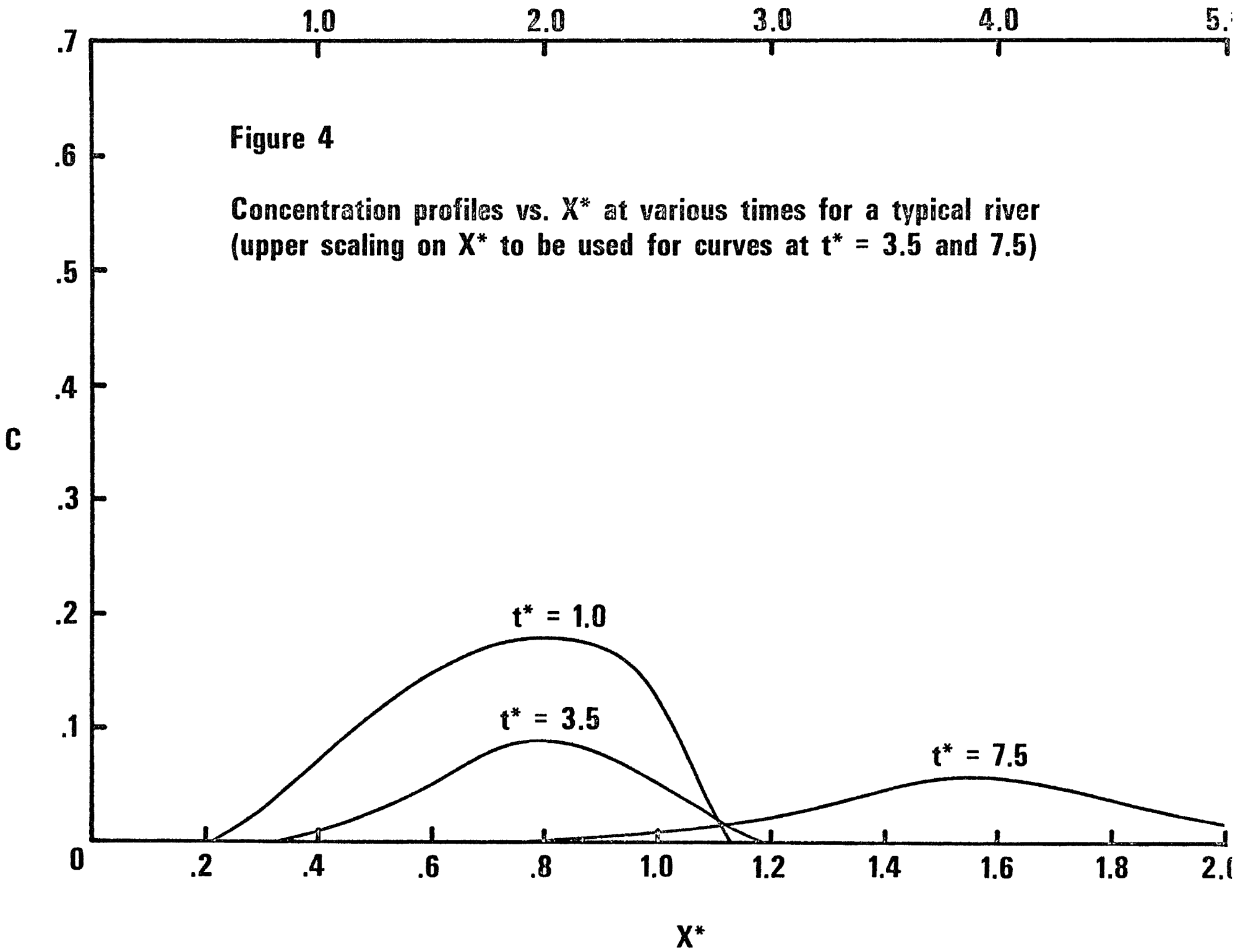

Figure 4

Concentration profiles vs. X* at various times for a typical river (upper scaling on X* to be used for curves at t* = 3.5 and 7.5)

Figure 5

Concentration profiles vs. Z*
at various times for a typical river

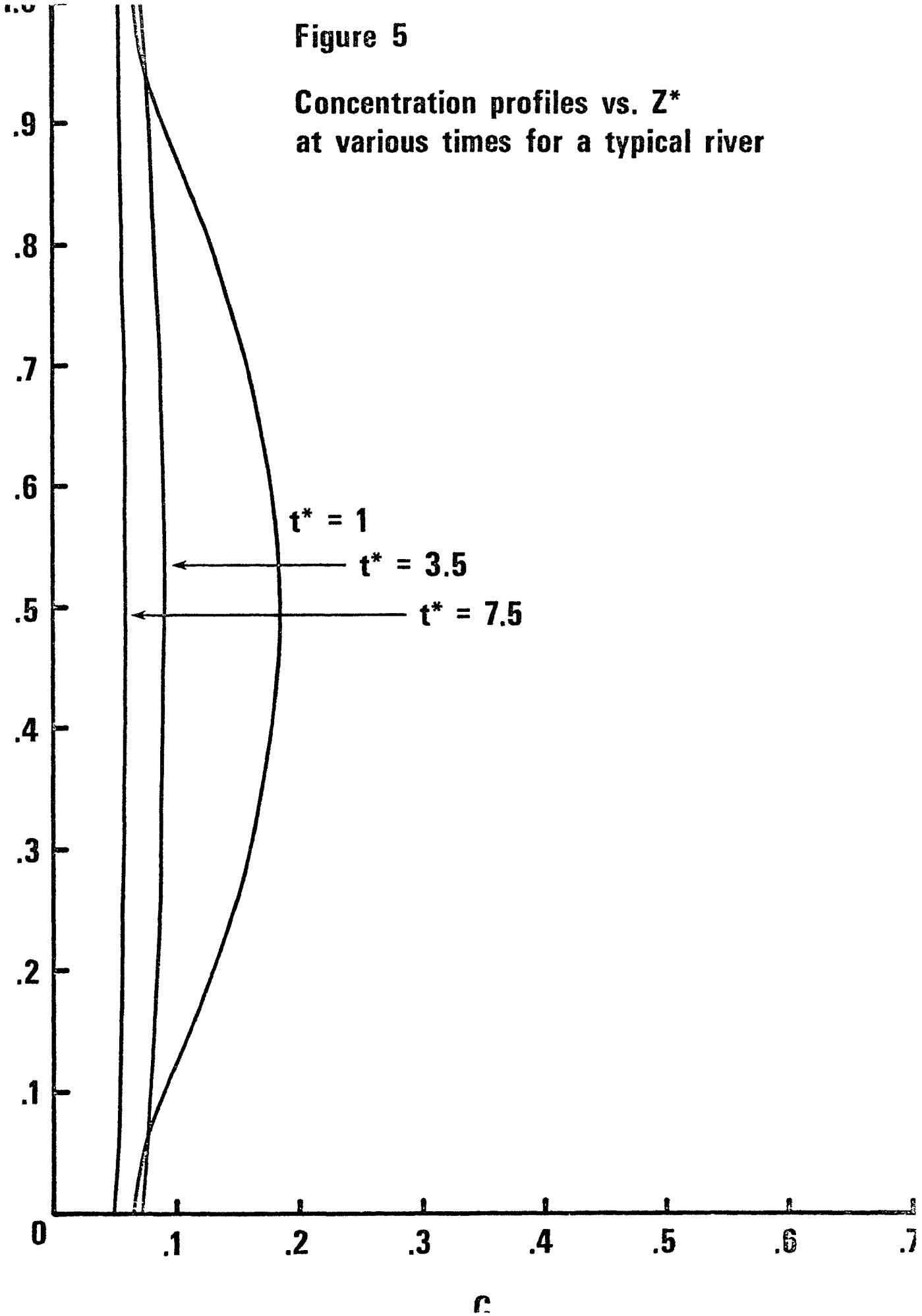

Figure 6

$\Sigma^* X^2$ vs. t^* for a typical river

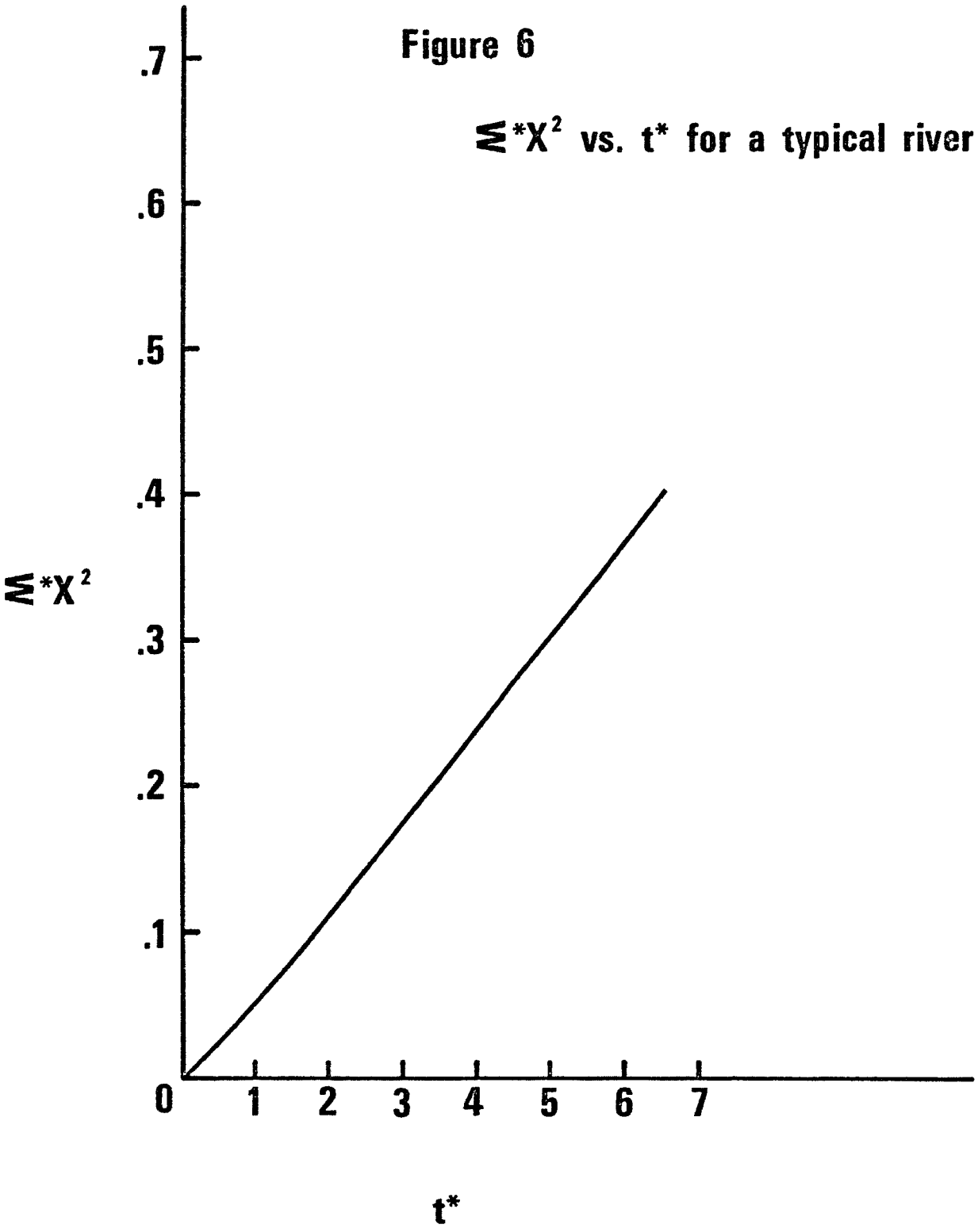

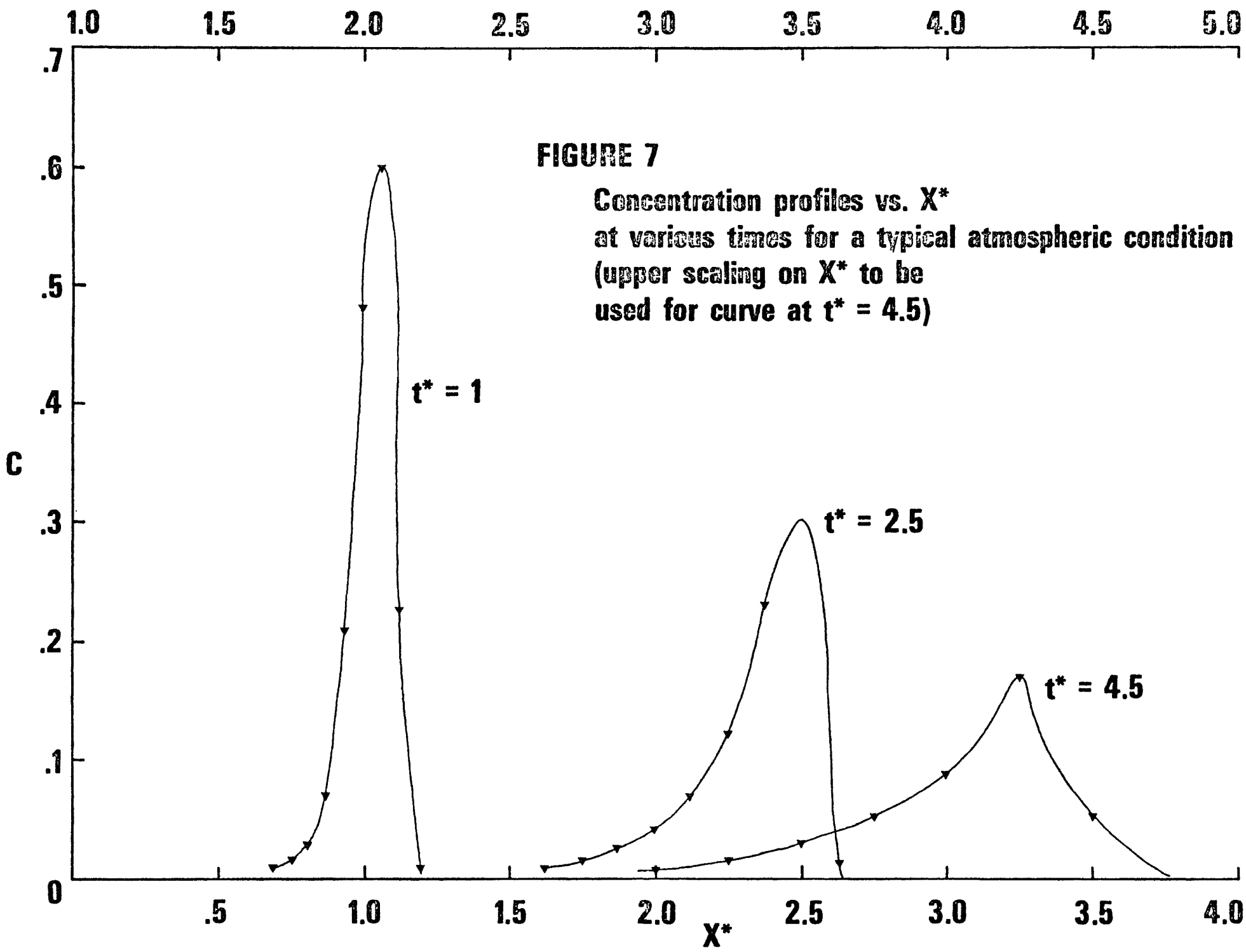

FIGURE 7

Concentration profiles vs. X*
at various times for a typical atmospheric condition
(upper scaling on X* to be
used for curve at t* = 4.5)

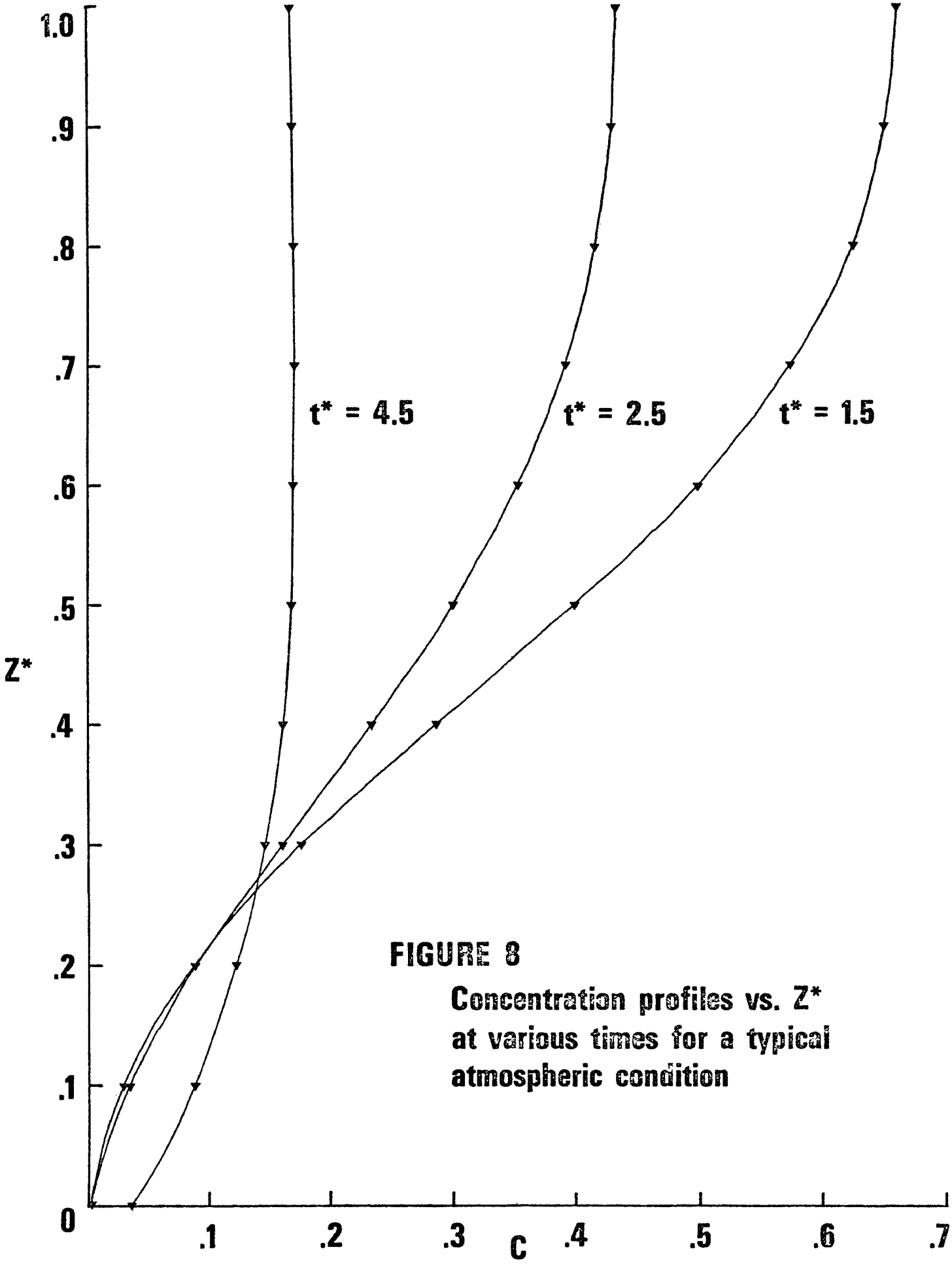

FIGURE 8

Concentration profiles vs. Z* at various times for a typical atmospheric condition

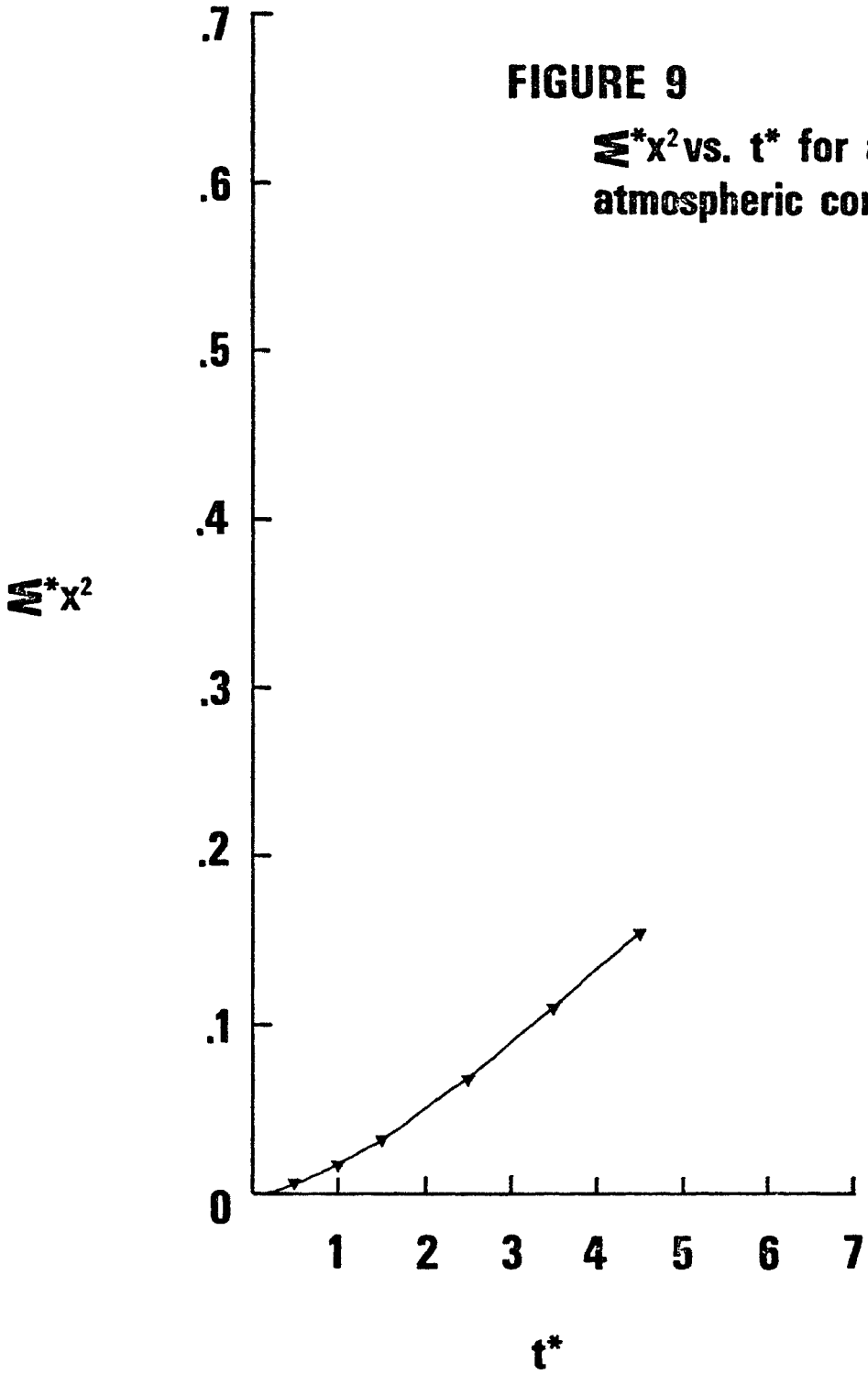

FIGURE 9

$\Sigma^* x^2$ vs. t* for a typical atmospheric condition

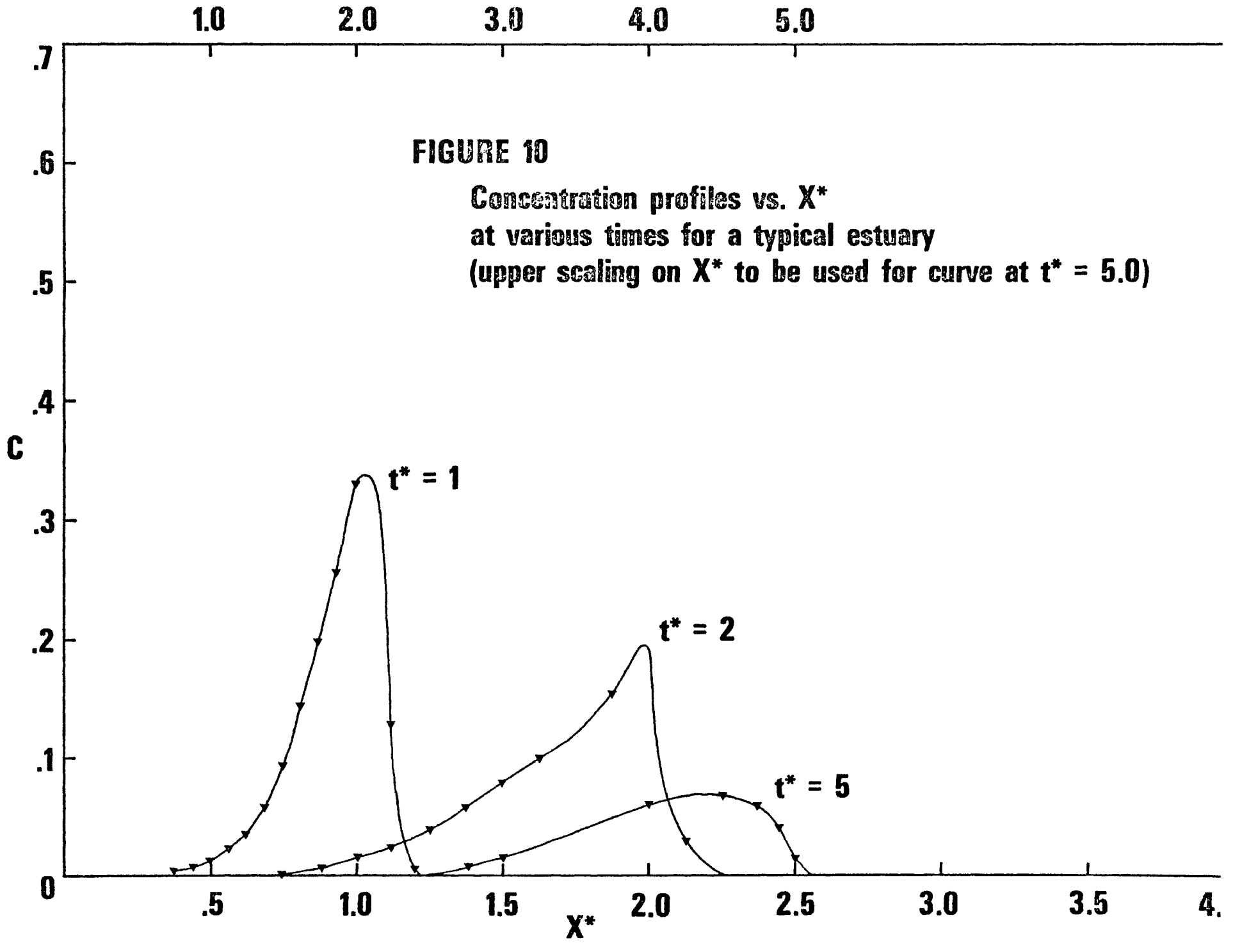

FIGURE 10

Concentration profiles vs. X*
at various times for a typical estuary
(upper scaling on X* to be used for curve at t* = 5.0)

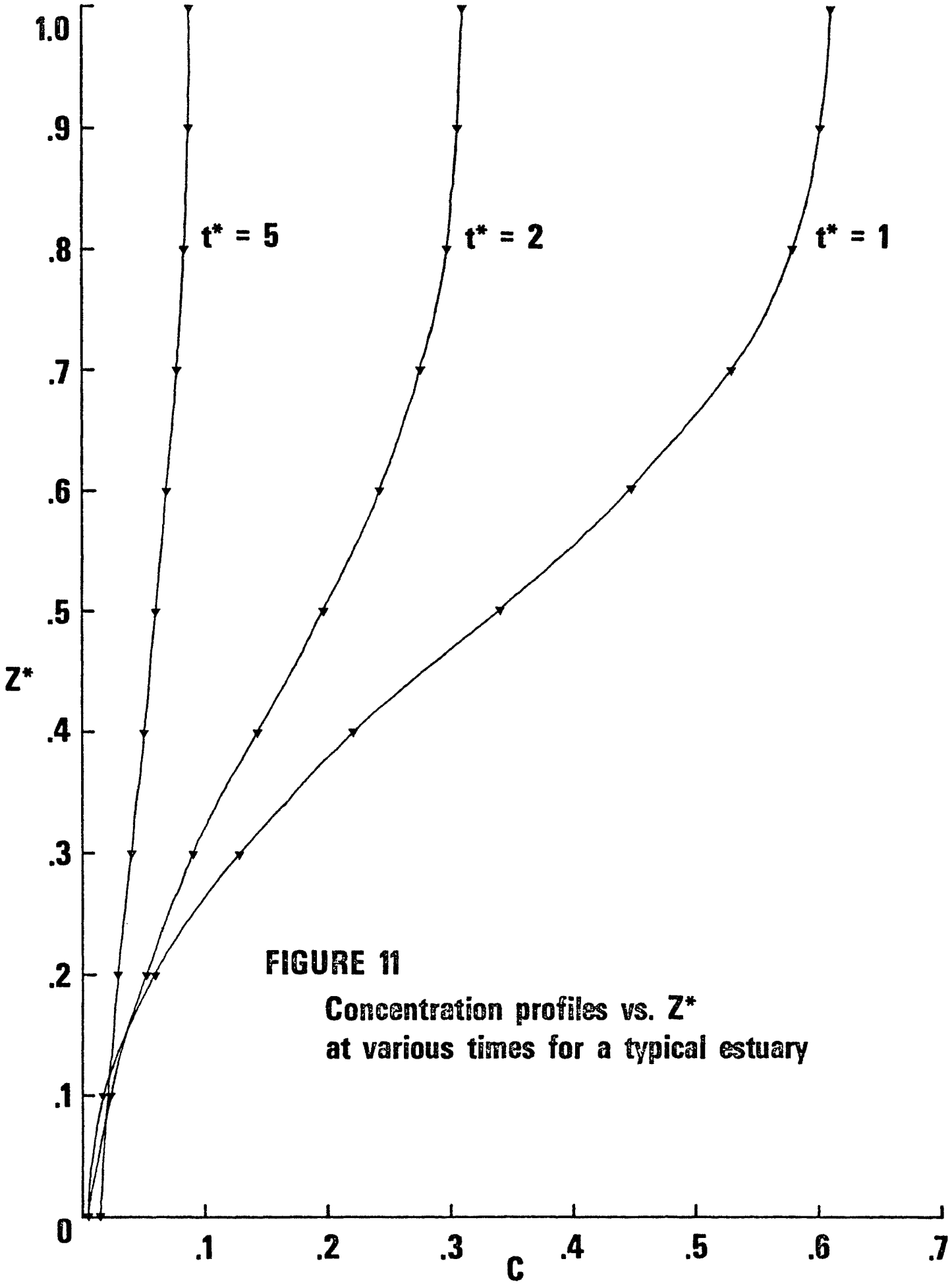

FIGURE 11

Concentration profiles vs. Z*
at various times for a typical estuary

FIGURE 12

$\Sigma^* x^2$ vs. t^* for a typical estuary

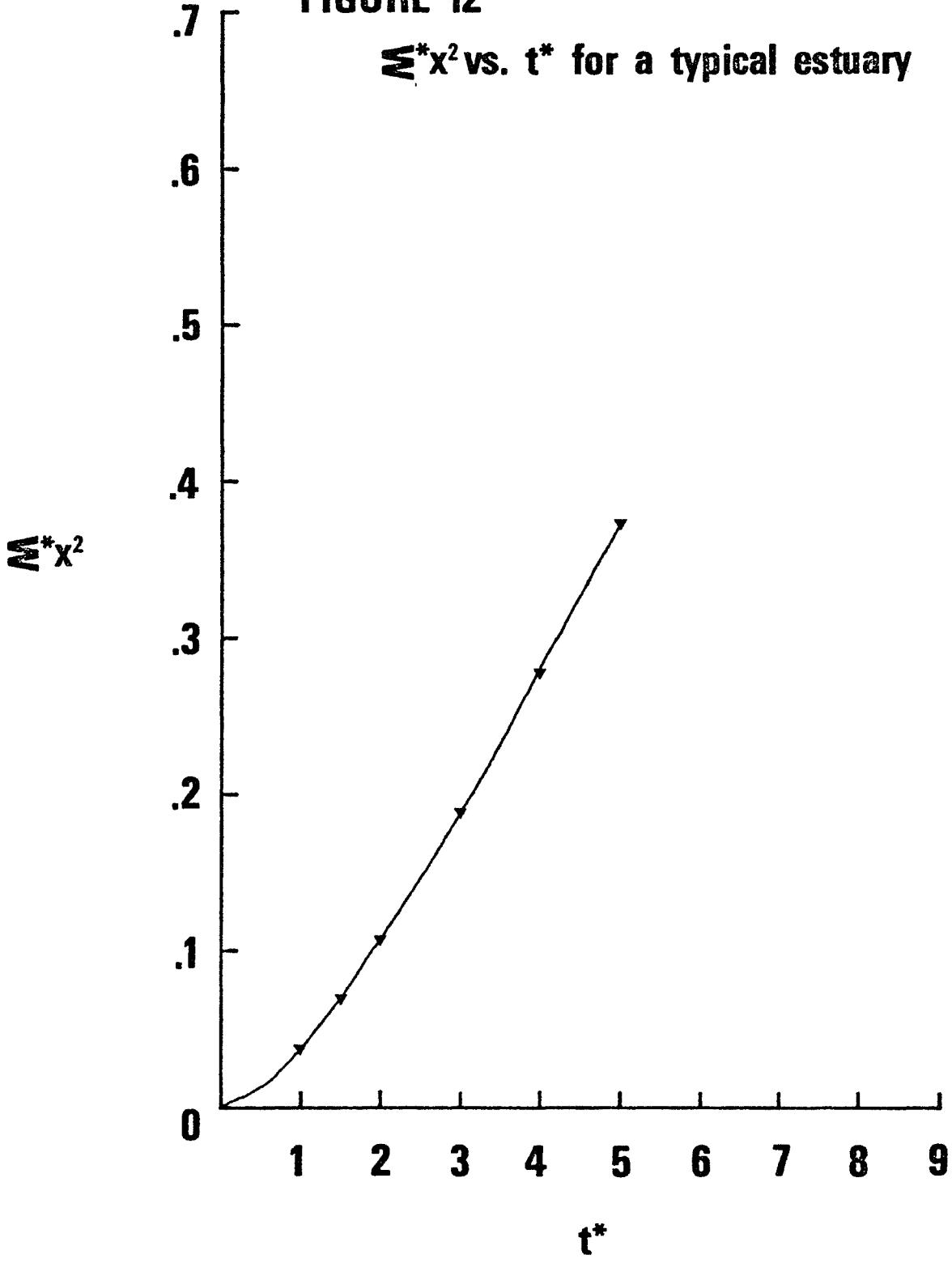

APPENDIX A4

CRITERIA FOR THE USE OF VERTICAL AVERAGING IN GREAT LAKES DISPERSION MODELS

by

F. M. Galloway, Jr.

S. J. Vakil

Department of Chemical Engineering
The Cleveland State University
Cleveland, Ohio 44115

May 1975

ABSTRACT

A basic question in developing a dispersion model is when can vertical averaging be used to reduce the dimensionality of the problem, thus resulting in considerable savings of computer time. A model problem involving horizontal convection and vertical diffusion is solved on the computer to establish criteria for vertical averaging. Different combinations of vertical profiles of velocity and diffusivity were used. The arrival of the horizontal direction variance of the concentration distribution to a linear time dependence was found to be a suitable criterion for the use of vertical averaging.

Effective horizontal dispersion coefficients (K_e), for use after vertical averaging, were computed from the results of the model problem and also from a formula given by Csanady. Both methods gave good agreement for the values of K_e.

It is shown that the time to reach the condition for vertical averaging correlates as $t_1 = h^2/(\alpha_1 \overline{D}_z)$, while $K_e = (C_1 h^2 U^2)/\overline{D}_z$, where h is depth, $\overline{D}_z$ is average vertical diffusivity, U is a characteristic velocity and α_1 and C_1 depend on profiles used. Over the range of profiles studied, α_1 varied by a factor less than 1.5 and C_1 by a factor less than 3.0.

Predicted values of K_e as a function of horizontal length scale are in good agreement with measured horizontal dispersion coefficients from dye release studies in Lake Ontario. The mechanism involving vertical shear of velocity and vertical diffusion may therefore be as important as horizontal turbulence, or more so, in producing horizontal dispersion.

INTRODUCTION

The transport of a dilute, dissolved, conserved pollutant is described by

$$\frac{\partial C}{\partial t} + u \frac{\partial C}{\partial x} + v \frac{\partial C}{\partial y} + w \frac{\partial C}{\partial z} = D_\mu \left(\frac{\partial^2 C}{\partial x^2} + \frac{\partial^2 C}{\partial y^2} + \frac{\partial^2 C}{\partial z^2} \right) \qquad (1)$$

where C is concentration, t is time, x and y are considered to be horizontal space coordinates, z is the vertical space coordinate, u, v and w are velocities in the directions x, y and z, and D_μ is the molecular diffusivity. The finite difference solution of (1) is very costly in terms of computer time due to its three space dimensions. Considering (1) as applied to transport in a large lake, we might try eliminating dependency on z by vertically averaging (1). Thus, the operation

$$\frac{1}{h} \int_0^h [\ (1)\ ]\ dz\ , \qquad \text{where h is local depth produces}$$

$$\frac{\partial \overline{C}}{\partial t} + \overline{u} \frac{\partial \overline{C}}{\partial x} + \overline{v} \frac{\partial \overline{C}}{\partial y} + \overline{u' \frac{\partial C'}{\partial x}} + \overline{v' \frac{\partial C'}{\partial y}}$$

$$= D_\mu \left(\frac{\partial^2 \overline{C}}{\partial x^2} + \frac{\partial^2 \overline{C}}{\partial y^2} \right) \qquad (2)$$

where the over bar denotes a vertically averaged quantity and the prime indicates local deviation from the vertical average. Following the usual approach in turbulent flow problems, we assume

$$\overline{u' \frac{\partial C'}{\partial x}} = -K_{e_x} \frac{\partial^2 \overline{C}}{\partial x^2}$$

with a similar approximation for the y-direction term where K_{e_x} and K_{e_y} are effective horizontal dispersion coefficients. Thus, (2) becomes

$$\frac{\partial \overline{C}}{\partial t} + \overline{u} \frac{\partial \overline{C}}{\partial x} + \overline{v} \frac{\partial \overline{C}}{\partial y} = K_{e_x} \frac{\partial^2 \overline{C}}{\partial y^2} + K_{e_y} \frac{\partial^2 \overline{C}}{\partial y^2} \qquad (3)$$

where the molecular diffusion terms have been dropped since they are negligible. (3) is now a much more efficient equation for computer solution. However, it is only useful in a practical sense if K_{e_x} and K_{e_y} can be determined.

The main concern of this investigation is to predict when time-independent K_e 's can be expected in equation (3), and also to estimate their constant values. The question of when does K_e become time-independent is answered in terms of a criterion for the use of vertical averaging that depends on the interaction of horizontal velocity and D_z. It is also shown how K_e can then be calculated as a function of horizontal velocity and D_z.

The model problem from which the criterion for vertical averaging is obtained is derived from a simplification of equation (1). First it is assumed that x is a local coordinate in the direction of the main flow so that the term "$v \frac{\partial C}{\partial y}$" is negligible compared with "$u \frac{\partial C}{\partial x}$". Ignoring also the molecular diffusion terms, (1) becomes

$$\frac{\partial C}{\partial x} + u\frac{\partial C}{\partial y} + w \frac{\partial C}{\partial z} = 0 \qquad (4)$$

Equation (4) is now operated on with

$\frac{1}{2\ell}\int_{-\ell}^{+\ell}$ [(4)] d z , where 2ℓ is the size of the largest eddies effective in the vertical transport of concentration.

$$\frac{\partial \overline{C}}{\partial t} + \overline{u} \frac{\partial \overline{C}}{\partial x} + \overline{w} \frac{\partial \overline{C}}{\partial z} + \overline{u' \frac{\partial C'}{\partial x}} + \overline{w' \frac{\partial C'}{\partial z}} = 0 \qquad (5)$$

is the result of this operation.

Assuming the terms $\bar{w}\ \frac{\partial \bar{C}}{\partial z}$ and $\overline{u' \frac{\partial C'}{\partial x}}$ to be small, and letting $\overline{w' \frac{\partial C'}{\partial z}} = -\ \frac{\partial}{\partial z}\ (D_z\ \frac{\partial \bar{C}}{\partial z})$, where D_z is a vertical eddy diffusivity which can be a function of depth, produces the model problem from which the results are derived.

Pioneer study of the interaction between horizontal velocity and vertical diffusivity and their combined effect on dispersion was done by Taylor (1953). He illuminated theoretically and experimentally, for a laminar flow in a circular tube, basic concepts involved in the interaction between vertical diffusion and horizontal convection. Two phases of transport were identified. The first, extending from the point of introduction of the solute to some distance downstream, is characterized by significant cross-plane variations in concentration of solute and an increasing rate of dispersion in the downstream direction of the solute cloud taken as a whole. Small variations in crossplane concentration, after a sufficient time, characterizes the second phase. Further spread in this phase can be described mathematically by an effective downstream diffusion coefficient which depends on the cross-plane shear of the downstream velocity, and the cross-plane diffusion coefficient. Thus, he showed that cross-plane averaging is a theoretically sound treatment of dispersion problems, provided that the solute cloud has entered the second phase of transport. This work concerns the detailed calculation of the first phase of transport for the model problem as a means of prediction of the beginning of the second phase. It also predicts the effective downstream diffusion coefficient for the second phase.

Aris (1956) extended Taylor's mathematical analysis to tubes of arbitrary cross-section. Elder (1959) applied Taylor's analysis to obtain the effective horizontal dispersion coefficient for open channel flow. Saffman (1962) extended Taylor's and Aris' concepts to atmospheric dispersion. Thackston and Krenkel (1967) and Fischer (1967) applied the same technique to streams. Bowden (1965) extended the idea to sea for horizontal mixing due to shearing current. Most of this work is very well summarized by Csanady (1973).

The method used here is very similar to the one developed by Natarajan[1]. This work extends Natarajan's investigation to include seven different combinations of velocity and diffusivity profiles.

[1] Natarajan, R., "Numerical Solution to a Two-Dimensional Dispersion Equation" (M.S. Thesis, The Cleveland State University, Cleveland, Ohio, 1973).

METHOD

We will approach the problem by solving the model transport equation described in the introduction,

$$\frac{\partial C}{\partial t} + u(z) \frac{\partial C}{\partial x} = \frac{\partial}{\partial z} \left(D(z) \frac{\partial C}{\partial z}\right) \tag{6}$$

The x-coordinate is in the direction of the mean flow, the z-coordinate is directed vertically upward from the bottom, and C, u and D are defined in terms of the local vertical average indicated in the introduction.

Equation (6) is made dimensionless using the following reference quantities and dimensionless variables:

$H_{ref} = H$ = depth of lake

$C_{ref} = C_{max}$ = maximum concentration occurring in lake

$U_{ref} = U_{max}$ = maximum algebraic difference between maximum and minimum horizontal velocity along a vertical line

$$x^* = \frac{x}{H}$$

$$z^* = \frac{z}{H} \quad (0 \leq z^* \leq 1)$$

$$t^* = \frac{tU_{max}}{H}$$

$$C^* = \frac{C}{C_{max}}$$

$$u^* = \frac{u}{U_{max}}$$

$$D_z^* = \frac{D_z}{U_{max}H}$$

By substitution into equation (6) we obtain:

$$\frac{\partial C^*}{\partial t^*} + u^* \frac{\partial C^*}{\partial x^*} = \frac{\partial}{\partial z^*} \left(D_z^* \frac{\partial C^*}{\partial z^*}\right) \tag{7}$$

The *'s will be omitted henceforth to simplify notation, with the understanding that variables are dimensionless unless stated otherwise.

The initial pollutant concentration is $C = C(x,z,0)$. The boundary conditions are

$$D_z \frac{\partial C}{\partial z} = 0 \text{ at } z = 0 \text{ and } z = 1. \tag{8}$$

A guassian initial distribution is assumed $C(x,z,0) = e^{-[\frac{(x-.125)^2}{4a}]}$. By picking the variance 'a' very small, this initial condition approximates a delta function input.

Equation (8) was solved numerically[2] for various diffusivity and velocity profiles. The results are conveniently described in terms of moments of the C distribution. Let $\overline{C}$ be the vertically averaged concentration at a given x. At any time t, we define the following parameters:

$$\overline{X} = \frac{\int_{\infty}^{\infty} \overline{C}\,(x)\; x\; dx}{\int_{\infty}^{\infty} \overline{C}\,(x)\; dx} \tag{9}$$

$$\sigma_{x^2} = \frac{\int_{\infty}^{\infty} \overline{C}\,(x)\quad (x - \overline{x})^2\; dx}{\int_{-\infty}^{\infty} \overline{C}\,(x)\; dx} \tag{10}$$

[2] Vakil, S. J., "Criteria for the Use of Vertical Averaging in Great Lakes Dispersion Models" (M.S. Thesis, The Cleveland State University, Cleveland, Ohio, 1975).

It can be shown that equation (10) can also be written as

$$\sigma_{x^2} = \frac{\int_{\infty}^{\infty} \overline{C}\ (x)\ x^2\ dx}{\int_{\infty}^{\infty} \overline{C}\ (x)\ dx} - \bar{x}^2 \qquad (11)$$

The longitudinal dispersion coefficient is defined as

$$D^*_x = 1/2 \quad \frac{d\sigma_{x^2}}{dt} \qquad (12)$$

at any time t.

D^*_x represents the spread of pollutant due to the interaction of the vertical variation of horizontal velocity and the vertical diffusion. The integrals in equations (9) to (11) are evaluated by Trapezoidal and Simpson's rule integrations using the C distribution from the numerical solution of equation (7).

The linear velocity profile and the lake velocity profile are discussed by Natarajan[1]. Along with the linear and the lake velocity profiles, we have also considered one more velocity profile which is described by the equation

$$u(z) = 1.0 + 0.217\ \ln (z) \qquad (13)$$

between z = 0.1 and z = 1.0. It is assumed that the velocity profile from z = 0 to z = 0.1 will be linear and follow the equation

$$u(z) = 5z \qquad (14)$$

In this profile, it can be seen that at z = 0, u(z) = 0 and at z = 1, u(z) = 1.0.

Two more vertical diffusivity profiles were taken into consideration besides the constant diffusivity value. These will be referred to as the log diffusivity profile and the lake diffusivity profile. The log diffusivity profile was derived by Reynold's analogy applied to the log velocity profile. The form of the diffusivity profile is

$$D(z) = 0.6\ z\ (1 - z) \tag{15}$$

Equation (15) was slightly modified to prevent D(z) from becoming zero at the boundaries. The lake diffusivity profile is simply a proposed variation of D with depth in an unstratified lake. The form chosen is

$$D(z) = 0.05 + 0.204\ (z - 0.3) \tag{16}$$

between z = 0.3 and 1. D(z) = .05 from z = 0. to 0.3. This profile was used with all three velocity profiles. It should be pointed out that both these diffusivity profiles, when averaged in the z direction, produce $\overline{D}_z = 0.1$.

A second method for calculating D^*_x was derived from the series of equations given in Csanady (1973) for shear-augmented diffusion in a channel. The final equation is

$$D^*_x = \int_0^{1.0} u(z)\ \phi\ (z)\ dz \tag{17}$$

where ϕ (z) can be calculated from D(z) and u(z). Thus, equations (12) and (17) provide two independent methods for computing D^*_x. This gives a means for checking the numerical results.

RESULTS

Results will be presented in turn for each velocity profile with different diffusivity profiles. Mainly, each velocity profile was combined with a constant $D_z = 0.1$ and the lake diffusivity profile. Since all diffusivity profiles give $\bar{D}_z = 0.1$, it will be possible to compare the effect of constant D_z vs. variable D_z when both have the same average value. Only the linear velocity profile was combined with the log diffusivity profile. In all the figures, numerals I, II and III correspond to the constant, the lake and the log diffusivity profiles respectively.

Horizontal Distribution of Concentration for the Linear Velocity Profile

There are three different situations to be considered, the linear profile with constant diffusivity, the log diffusivity profile and the lake diffusivity profile. Concentration at any time is a function of z and x. C values are plotted in the x direction at $z = 0.5$.

Figures 1 and 2 give the concentration distribution for the linear velocity profile at $t = 1$ and 5 respectively. As time progresses, for all the three diffusivity profiles, the skewness starts to smooth out and the concentration distribution approaches a normal distribution.

Vertical Concentration Distribution for the Linear Velocity Profile

Vertical concentration distribution was demonstrated by a series of graphs made of concentration versus z at the x location where maximum concentration occurred at a given time (called x_m). Figures 3 and 4 show the vertical variation in concentration for the linear velocity profile

combined with the constant, log and lake diffusivity profiles at t = 1 and 5 respectively. Examining these figures it is evident that as time progresses the vertical variation in concentration becomes smaller, eventually approaching a straight line in the vertical direction. The most variation in the z direction at time t = 5 is seen for the lake diffusivity profile.

Horizontal Distribution of the Log Velocity Profile

Figure 5 shows the concentration distribution in the x-direction at the final time t = 6. We observe qualitatively the same kind of behavior as for the linear profile. However, there is less spread of the distribution here than for the linear velocity profile.

Vertical Concentration Distribution for the Log Velocity Profile

Figure 6 shows the vertical variation in concentration for the log velocity profile with constant diffusivity and the lake diffusivity profile at time t = 6.

As time progresses variation in the vertical direction decreases and for constant diffusivity it shows practically no variation at t = 6. A little variation in the vertical direction for the lake diffusivity profile persists, however.

Horizontal Distribution of Concentration for the Lake Velocity Profile

Concentration values in the horizontal direction are plotted at different times for constant diffusivity and the lake diffusivity profile. Figure 7 shows the horizontal distribution at time t = 6. Once again as time progresses, for both the diffusivity profiles, the concentration profile is losing its skewness and gradually approaches the normal distribution.

Vertical Concentration Distribution for the Lake Velocity Profile

Figure 8 represents the vertical concentration distribution of the lake velocity profile with constant diffusivity and the lake diffusivity profile at time t = 6. Figure 8 shows that there is still a little variation an the z direction for constant diffusivity, while the lake diffusivity profile gives almost a straight line. This is the reverse of the results for the linear and the log velocity profiles.

D^*_x Values for the Three Velocity Profiles

Figures 9, 10, and 11 show σ_{x^2} versus time for the various velocity and diffusivity profile combinations. According to Aris (1956), for any velocity profile and finite D_z, D^*_x reaches an asymptotic constant value. This value for D^*_x can be calculated from the final constant slope of the curves in Figures 9, 10, and 11 by means of equation (12). These values are given in Table 1.

TABLE 1

D_x^* Values

Diffusivity Profile	Linear Profile	Log Profile	Lake Profile
Constant	0.086	0.039	0.047
Log	0.072	---	---
Lake	0.102	0.054	0.048

D_x^* values were also computed independently by the method summarized by equation (17) as a check of the numerical results. These values are given in Table 2.

TABLE 2

D_x^* Values

Diffusivity Profile	Linear Profile	Log Profile	Lake Profile
Constant	0.083	0.037	0.054
Log	0.069	---	---
Lake	0.100	0.052	0.049

These values of D_x^* for different combinations match sufficiently well with the calculated values of D_x^* given in Table 1 to confirm the numerical methods. The small differences between these two values can probably be accounted for by the numerical error in the solution of equation (7).

It can be shown (see Vakil[2]) that the approach of $\frac{d\sigma_x^2}{dt}$ to a constant value is exponential with exponent $-\alpha_1 \bar{D}_z^* t$, where α_1 is generally the smallest eigenvalue in a certain Sturm-Liouville problem, and $\bar{D}_z^*$ is the mean non-dimensional cross-plane diffusion. Dimensional time, t_1, to reach phase II transport thus scales as

$$t_1 = \frac{H^2}{\alpha_1 \bar{D}_z}$$

where $\bar{D}_z$ in this equation is the mean dimensional diffusivity. When phase II is reached, the z direction can be replaced by an effective dispersion coefficient in the x direction, D_x^*. If equation (17) is non-dimensionalized using $\bar{D}_z^* = 1$, it can be seen that

$$K_e = C_1 \frac{H^2 U_{max}^2}{\bar{D}_z}$$

where C_1 is just .1 D_x^*. The factor .1 is required since D_x^* was calculated with $\bar{D}_z^* = .1$. As the values of D_x^* have been calculated, K_e can be evaluated for each case.

As an example of the evaluation of α_1, consider Figure 9, curve I. This shows that by $t = 4$, σ_{x^2} has approached an approximate linear growth rate. Thus,

$$\alpha_1 \bar{D}_z^* \simeq 1/4$$

and $$\alpha_1 \simeq 2.5 \text{ since } \bar{D}_z^* = 0.1$$

Therefore, $$t_1 = \frac{H^2}{2.5 \bar{D}_z}$$

Values of C_1 and α_1 can be obtained for each combination of velocity and diffusivity profile. Table 3 summarizes these values of C_1 and α_1.

TABLE 3

Velocity Profile	Diffusivity Profile	α_1	C_1
Linear	Constant	2.5	0.0083
Linear	Log	2.5	0.0069
Linear	Lake	2.0	0.0100
Log	Constant	2.0	0.0037
Log	Lake	1.7	0.0052
Lake	Constant	1.7	0.0054
Lake	Lake	2.0	0.0049

DISCUSSION

The examples demonstrate that the vertical variation of concentration and the value obtained for D_x^* can significantly depend upon the combination of velocity and diffusivity profiles. In Table 3, it can be seen that α_1 varies by a factor of 1.5 and C_1 varies by a factor slightly less than 3.0. t_1 and K_e can be estimated from these results for a wide range of cases of practical interest.

For example, it is interesting to compare the values of K_e calculated from these results with values for the horizontal diffusivity obtained by Murthy (1970) from his dye release experiments in Lake Ontario. To do this, a relation between K_e and a horizontal length scale is needed. This is obtained as follows. Start with

$$K_e = C_1 \frac{H^2 U_{max}^2}{\overline{D}_z} \tag{18}$$

and

$$t_1 = \frac{H^2}{\alpha_1 \overline{D}_z} \tag{19}$$

Eliminating H^2 between (18) and (19) gives

$$K_e = C_1 \alpha_1 t_1 U_{max}^2 \tag{20}$$

Equation (20) expresses K_e as a function of time, where the time, t_1, is just long enough to reach phase two type transport for the corresponding H from equation (18) or (19). It is now assumed that (19) is valid for an H that varies continuously with time. Equation (20), therefore, gives the continuous relationship between K_e and time of

diffusion for a case where the depth, H, grows according to (19). The horizontal length scale is

$$L = \int_0^{t_1} U_{max}\, dt \tag{21}$$

where U_{max} will vary with H and, therefore, with time. Thus,

$$L = a_1(t_1)\, U_{max}\, t_1 \tag{22}$$

where U_{max} in (22) is the value at t_1 and $a_1(t_1)$ is a function of order 1. Taking $a_1 = 1$ and eliminating t_1 between (20) and (22) gives

$$K_e = C_1\, \alpha_1\, L\, U_{max} \tag{23}$$

So far in obtaining (23), nothing has been specified concerning either the velocity or vertical diffusivity profiles. If we now assume that the velocity profile varies linearly with depth, then

$$U_{max} = a_2 H \tag{24}$$

where a_2 is the slope of the linear profile. Combining (19), (22), and (24) yields

$$H = \left(\frac{\alpha_1 \bar{D}_z}{a_2}\right)^{1/3} L^{1/3} \tag{25}$$

and combining (23), (24) and (25) yields

$$K_e = C_1\, \alpha_1^{4/3}\, \bar{D}_z^{1/3}\, a_2^{2/3}\, L^{4/3} \tag{26}$$

(26) is the desired relationship between K_e and L for a linear velocity profile and constant vertical diffusivity (thus $\overline{D}_z$ is not a function of depth or time). According to the assumptions made in its derivation, it is intended to be a model for the case where soluble material is introduced near the surface and begins to diffuse vertically as it spreads horizontally as was the case in Murthy's experiments.

In (26), $C_1 = .0083$ and $\alpha_1 = 2.5$ from Table 3, corresponding to the linear velocity profile and constant diffusivity case. The dependence on $\overline{D}_z$ is weak. Typical values of 5 and 10 cm^2/sec produced very similar results for K_e. Dependence on the slope of the velocity profile a_2, is more pronounced. Values for a_2 of 30/900 sec^{-1} and 15/900 sec^{-1} were tried. It is interesting to note that the familiar 4/3 power dependency of K_e on L is produced in this model even though nothing is assumed about horizontal turbulence.

Figure 12 compares K_e for three different combinations of $\overline{D}_z$ and a_2. The results suggest that horizontal spreading due to vertical shear in the horizontal velocity coupled with vertical diffusion is at least as important as that due to horizontal turbulence. The effect of horizontal velocity gradients in elongating dye patches in his experiments was noted by Murthy. It should be emphasized that the lines compared with Murthy's results in Figure 12 were computed using typical values of $\overline{D}_z$ and a_2, and do not necessarily correspond

to the conditions of Murthy's experiments. However, the data are fairly well represented over a range of reasonable values for the parameters. Perhaps even more significant is the 4/3 power dependency which is predicted by the model and which Murthy's data seem to follow.

CONCLUSIONS

The examples using the model problem have shown that vertical variation in concentration becoming relatively small and D_x^* reaching a constant value are well correlated. Thus, the use of D_x^* reaching a constant value is a good criterion for using vertical averaging. D_x^* for use in a vertically averaged model can be predicted by this method.

t_1, the time for phase I transport, scales as

$$t_1 = \frac{H^2}{\alpha_1 \overline{D}_z}$$

and K_e, the effective horizontal dispersion coefficient, scales as

$$K_e = \frac{C_1 H^2 U^2_{max}}{\overline{D}_z}$$

Some situations, such as existence of a thermocline, are not covered by the results given here, since this would represent a vastly different D_z profile from any of the examples. However, in all the cases studied α_1 and C_1 varied within a factor of 1.5 and less than 3.0, respectively. Thus, results obtained here can be used to predict t_1 and K_e for a wide range of reasonable velocity and diffusivity profiles. For velocity and diffusivity profiles that are very different from the ones studied here α_1 and C_1 can be calculated by the method used here and new values of t_1 and K_e can be obtained from the above identities.

It was seen in Figure 12 that K_e, as calculated in this investigation, compares favorably with measured horizontal diffusivities in Lake Ontario. The importance of the vertical shear of the horizontal velocity combined with vertical diffusion on horizontal spreading appears to be at least the same as the effect of horizontal turbulence. More information is necessary to decide the dominating factor.

ACKNOWLEDGMENT

This work was supported by a grant from the U.S. Department of the Interior, Office of Water Resources Research, under the Annual Allotment Program to Ohio, Grant #A-036-OHIO.

REFERENCES

Aris, R. 1956. On the Dispersion of a Solute in a Fluid Flowing Through a Tube. Proceedings of the Royal Society of London (Series A) 235:67.

Bowden, K. F. 1965. Horizontal Mixing in the Sea Due to a Shearing Current. Journal of Fluid Mechanics 21:83.

Csanady, G. T. 1973. Turbulent Diffusion in the Environment. Boston: D. Reidel.

Elder, J. W. 1959. The Dispersion of Marked Fluid in Turbulent Shear Flow. Journal of Fluid Mechanics 5:544.

Fisher, H. B. 1968. The Mechanics of Dispersion in Natural Streams. Journal of the Hydraulics Division, ASCE HY6:187.

Murthy, C. R. 1970. An Experimental Study of Horizontal Diffusion in Lake Ontario. In Proceedings of 13th Conference of Great Lakes Research. pp. 477-489. Ann Arbor, Michigan: International Association of Great Lakes Research.

Saffman, P. G. 1962. The Effect of Wind Shear on Horizontal Spread From an Instantaneous Ground Source. Journal of the Royal Meteorological Society 88:382.

Taylor, G. 1953. Dispersion of Soluble Matter in Solvent Flowing Through a Tube. Proceedings of the Royal Society of London A219:186.

Thackston, E. L., and Krenkel, P. A. 1967. Longitudinal Mixing in Natural Streams. Journal of the Sanitary Engineering Division, ASCE SA5:67.

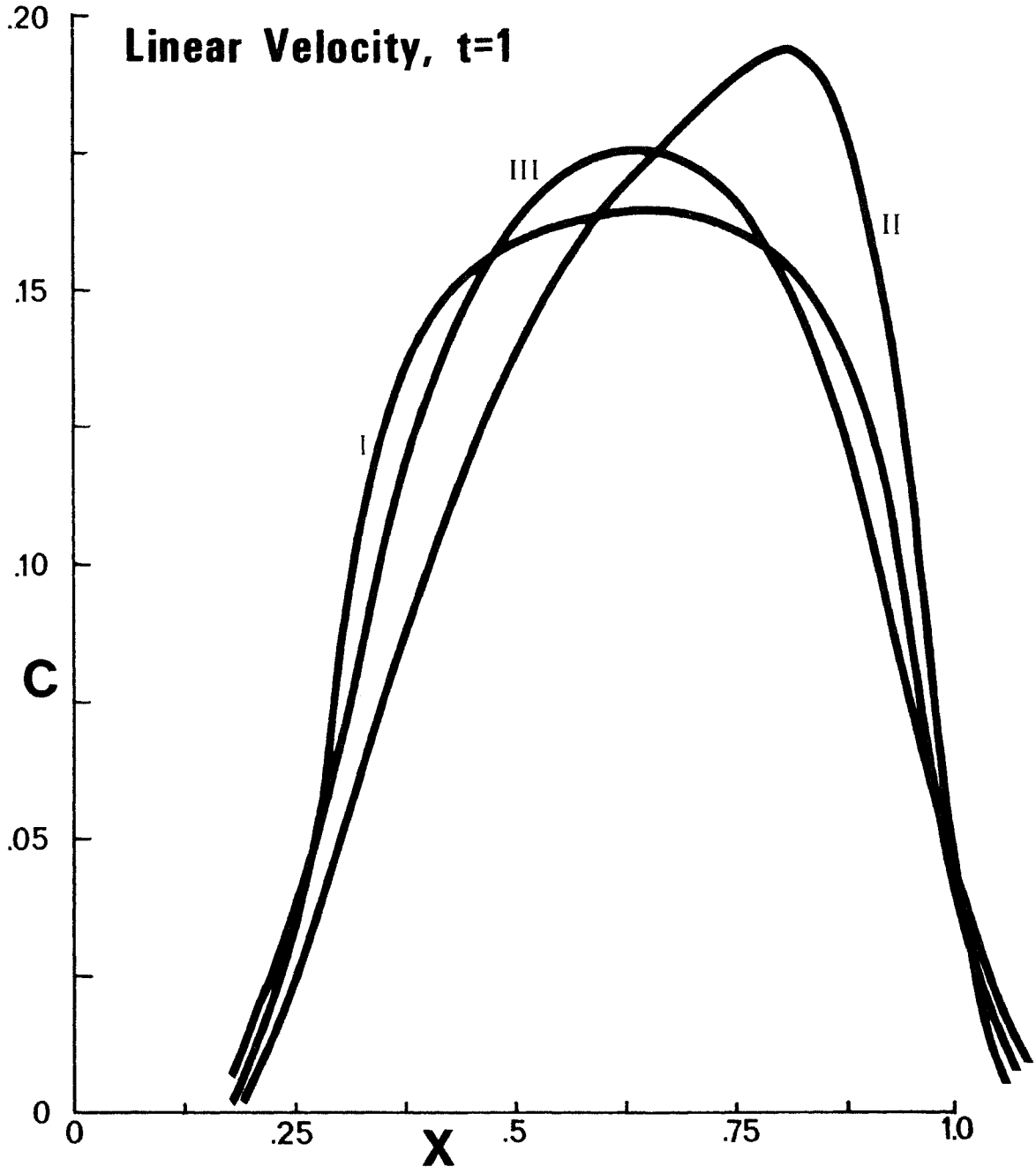

FIGURE 1

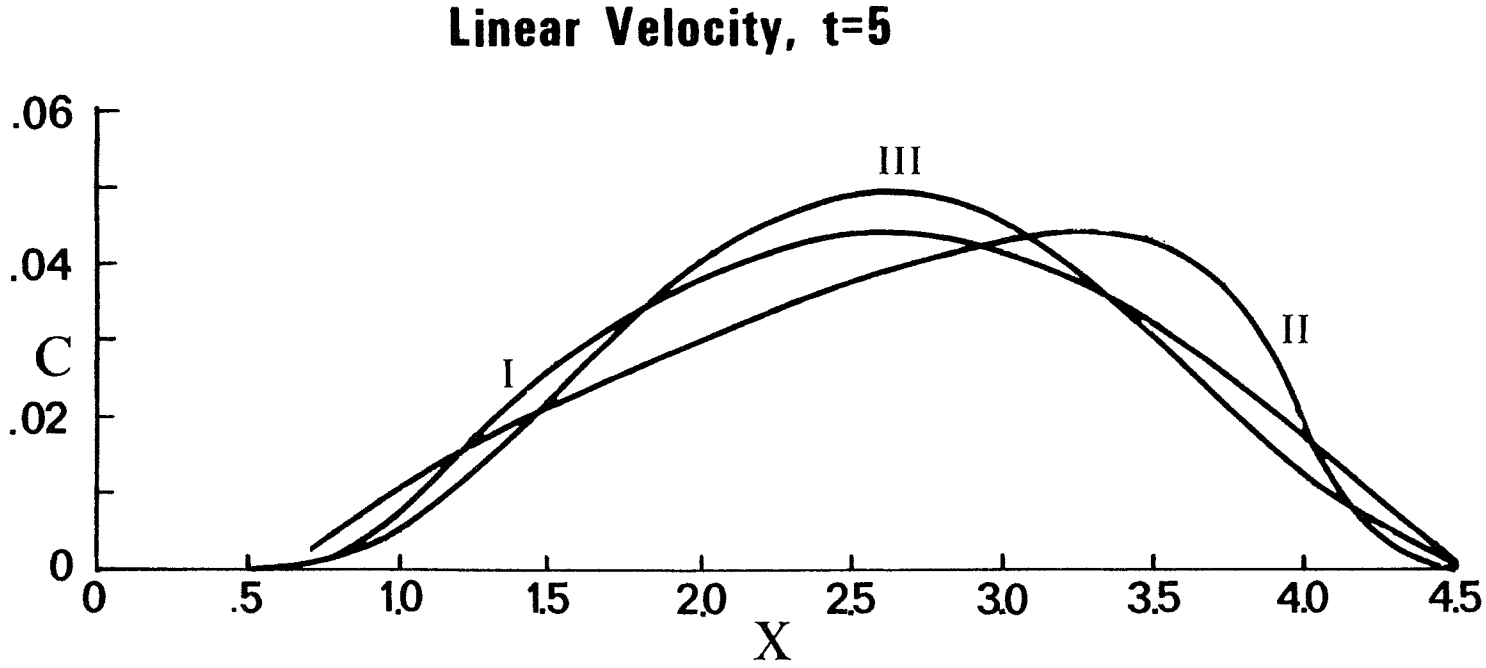

FIGURE 2

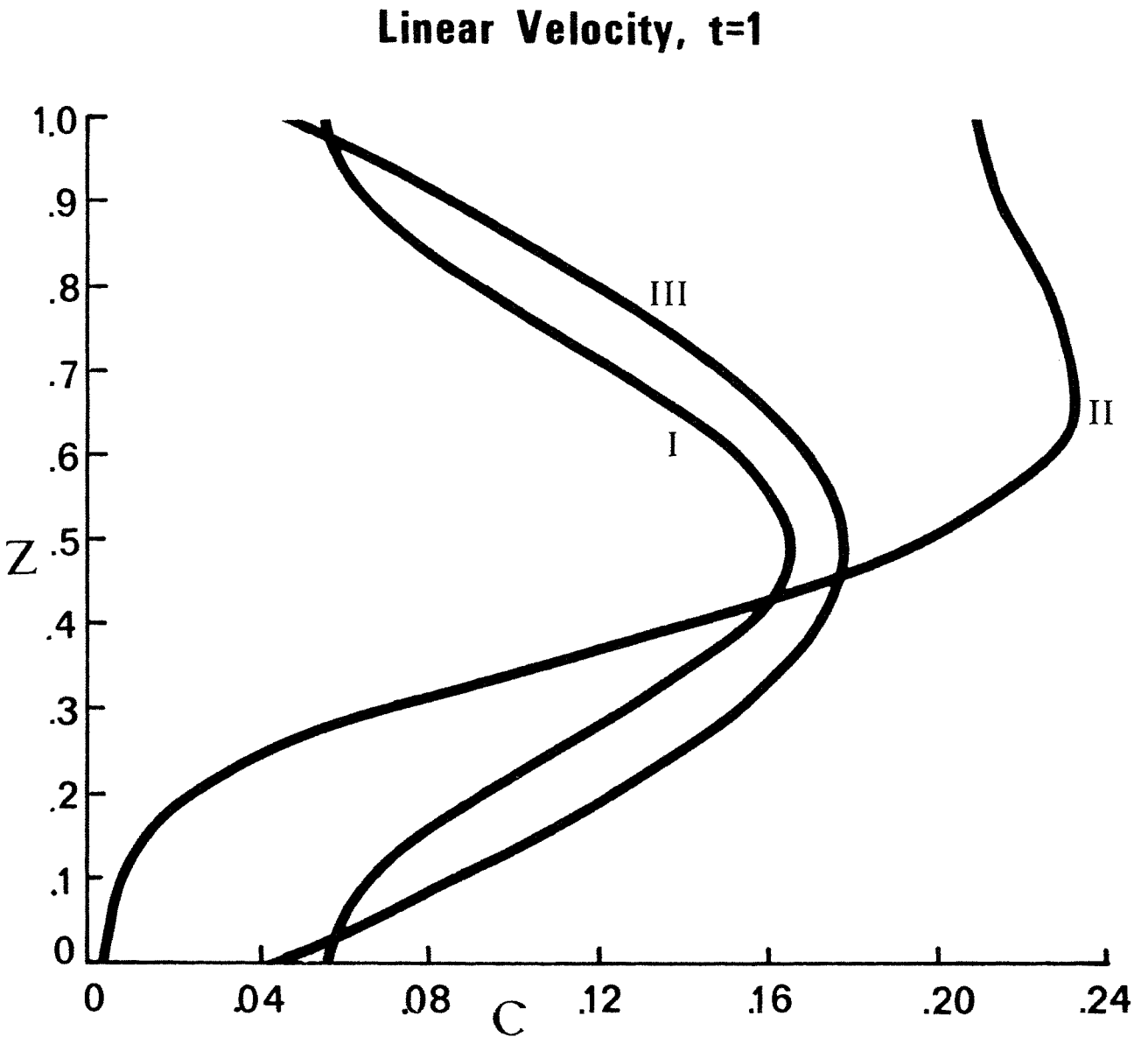

FIGURE 3

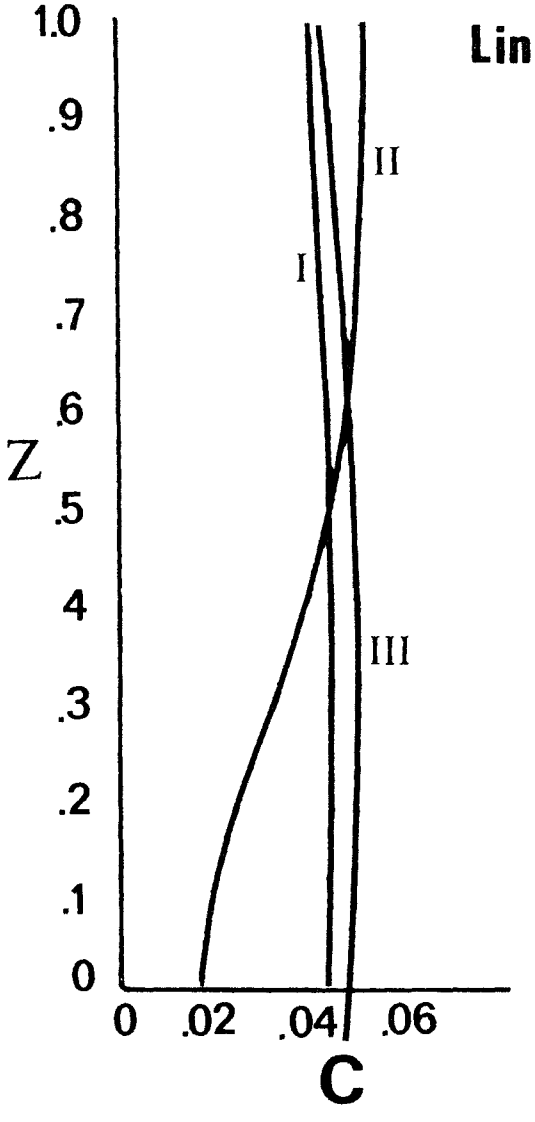

FIGURE 4

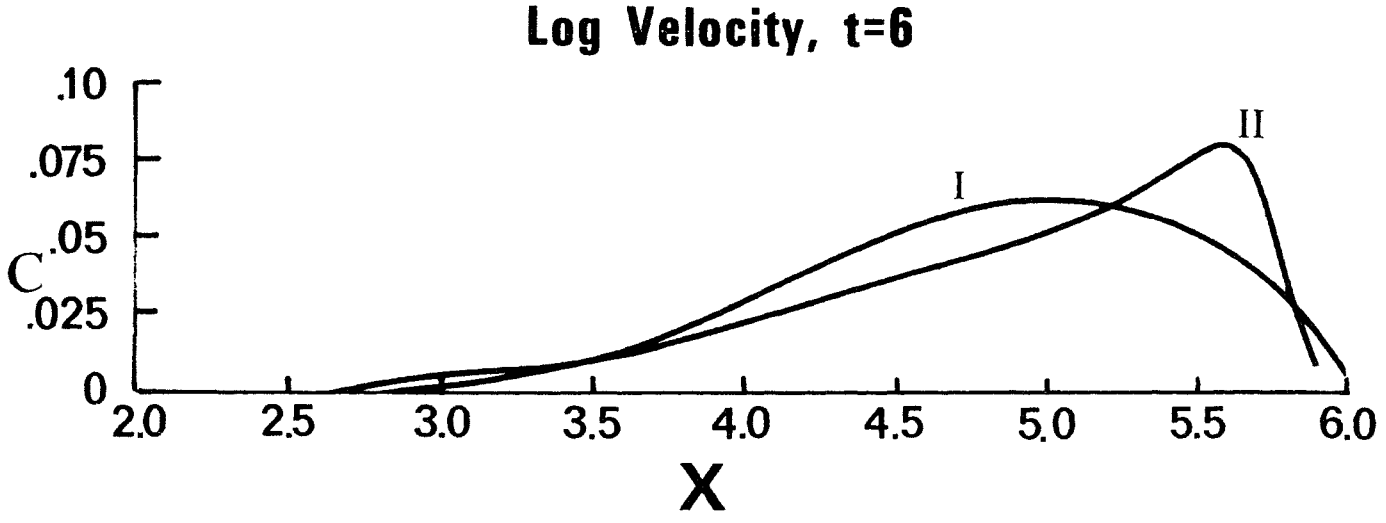

FIGURE 5

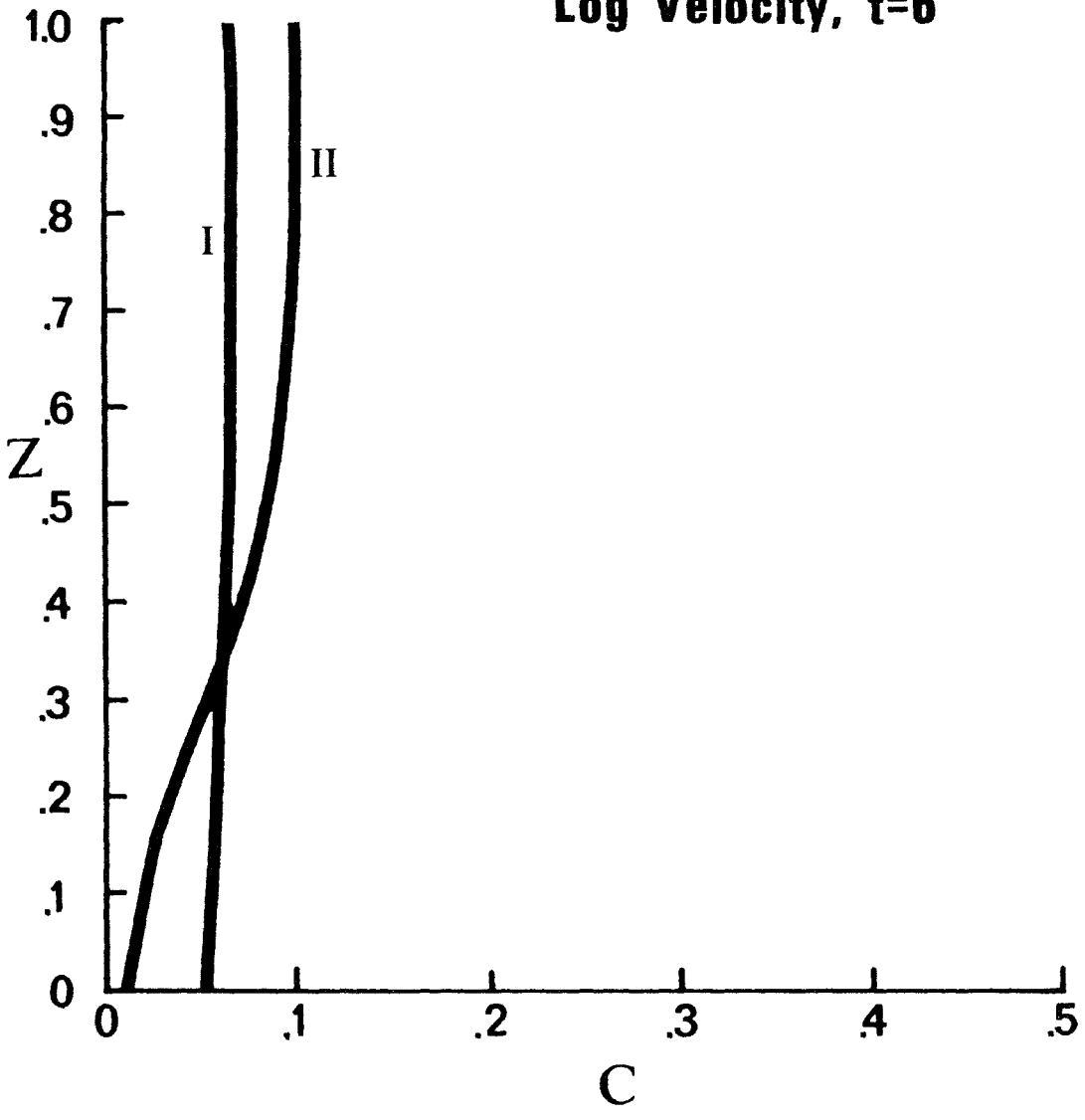

FIGURE 6

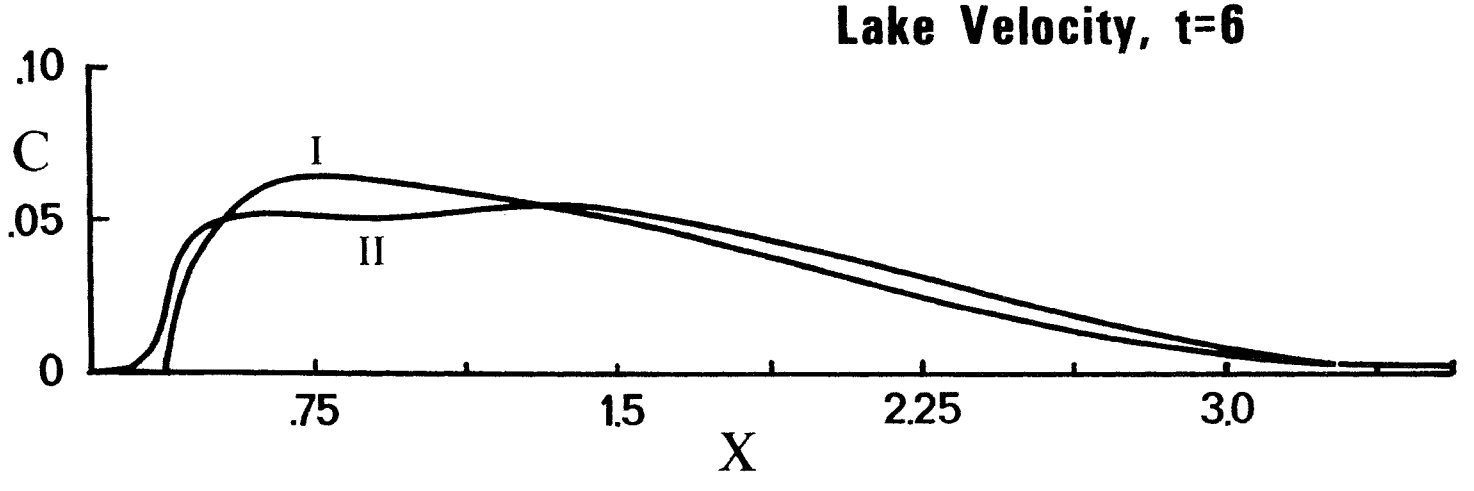

FIGURE 7

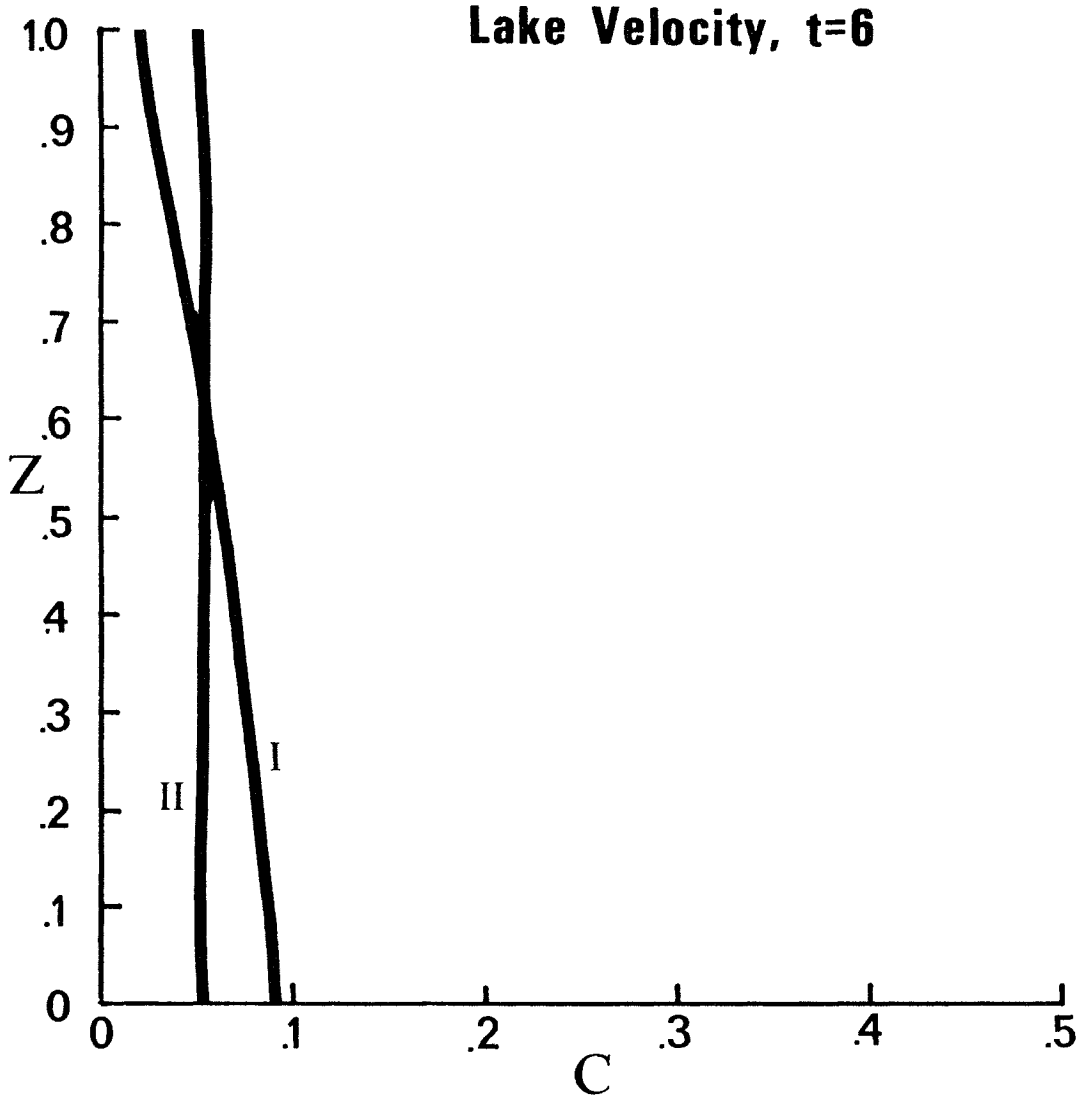

FIGURE 8

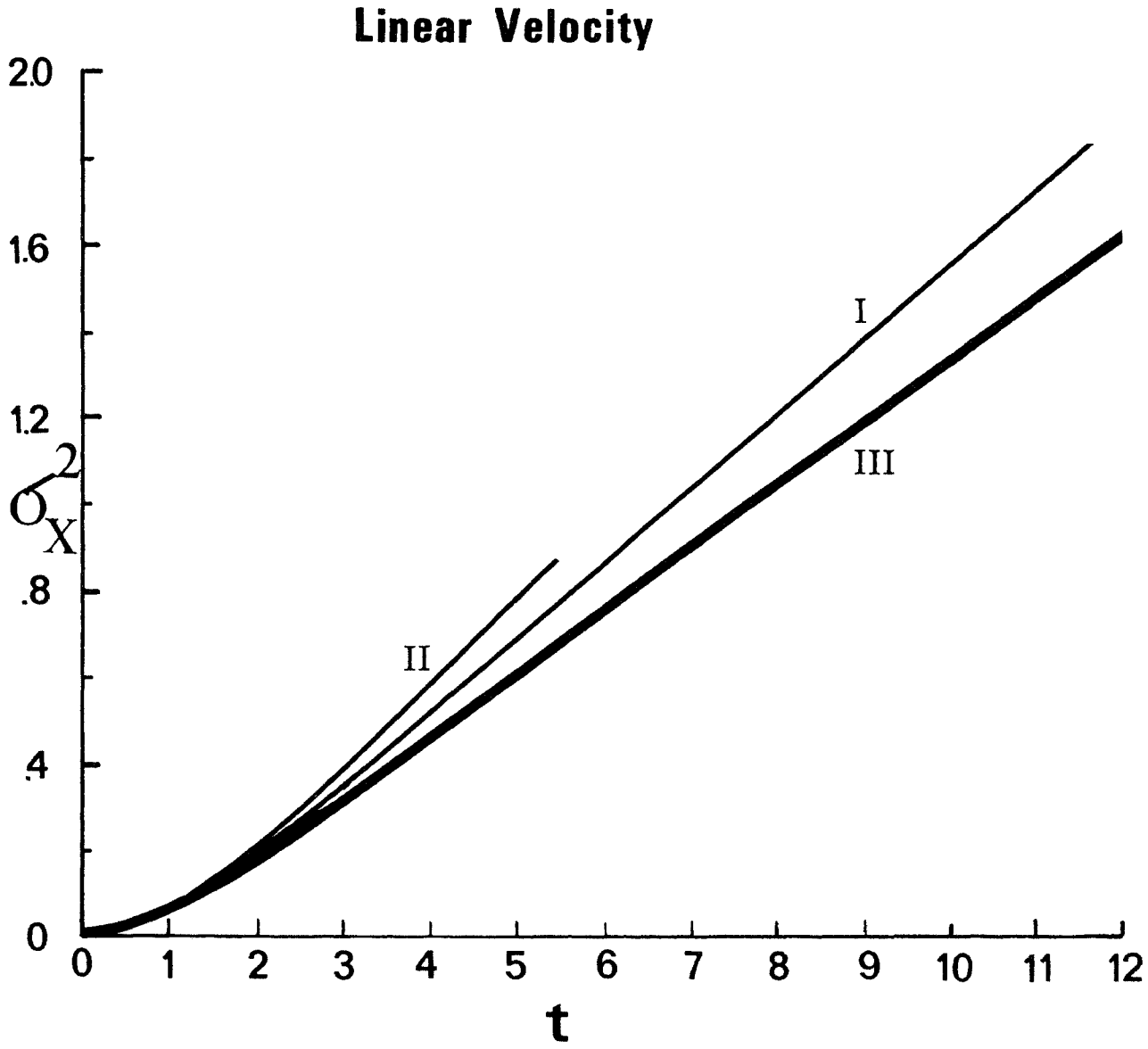
Linear Velocity
2.0
1.6
1.2
σ_X^2
.8
.4
0
I
II
III
0 1 2 3 4 5 6 7 8 9 10 11 12
t

FIGURE 9

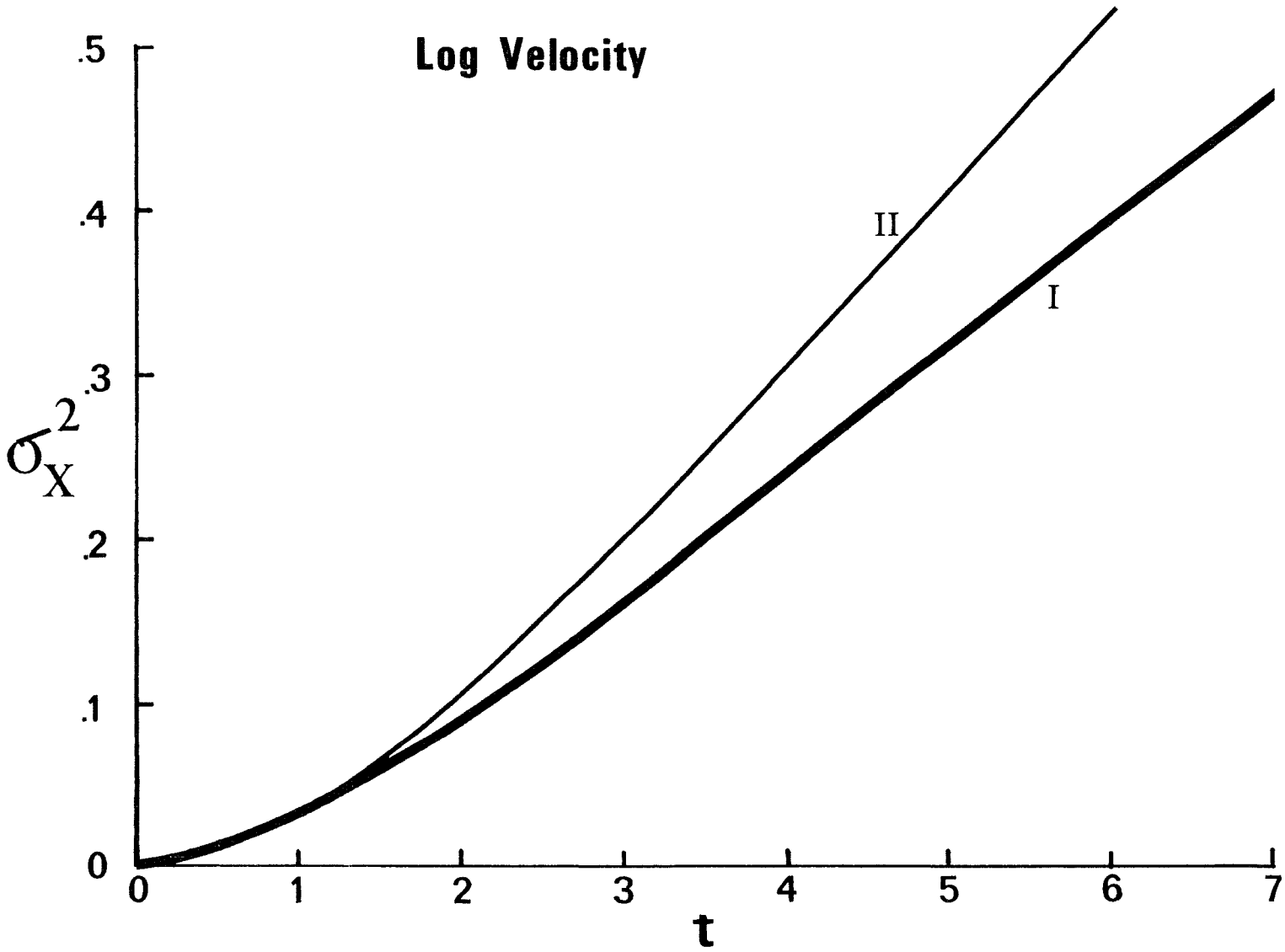

FIGURE 10

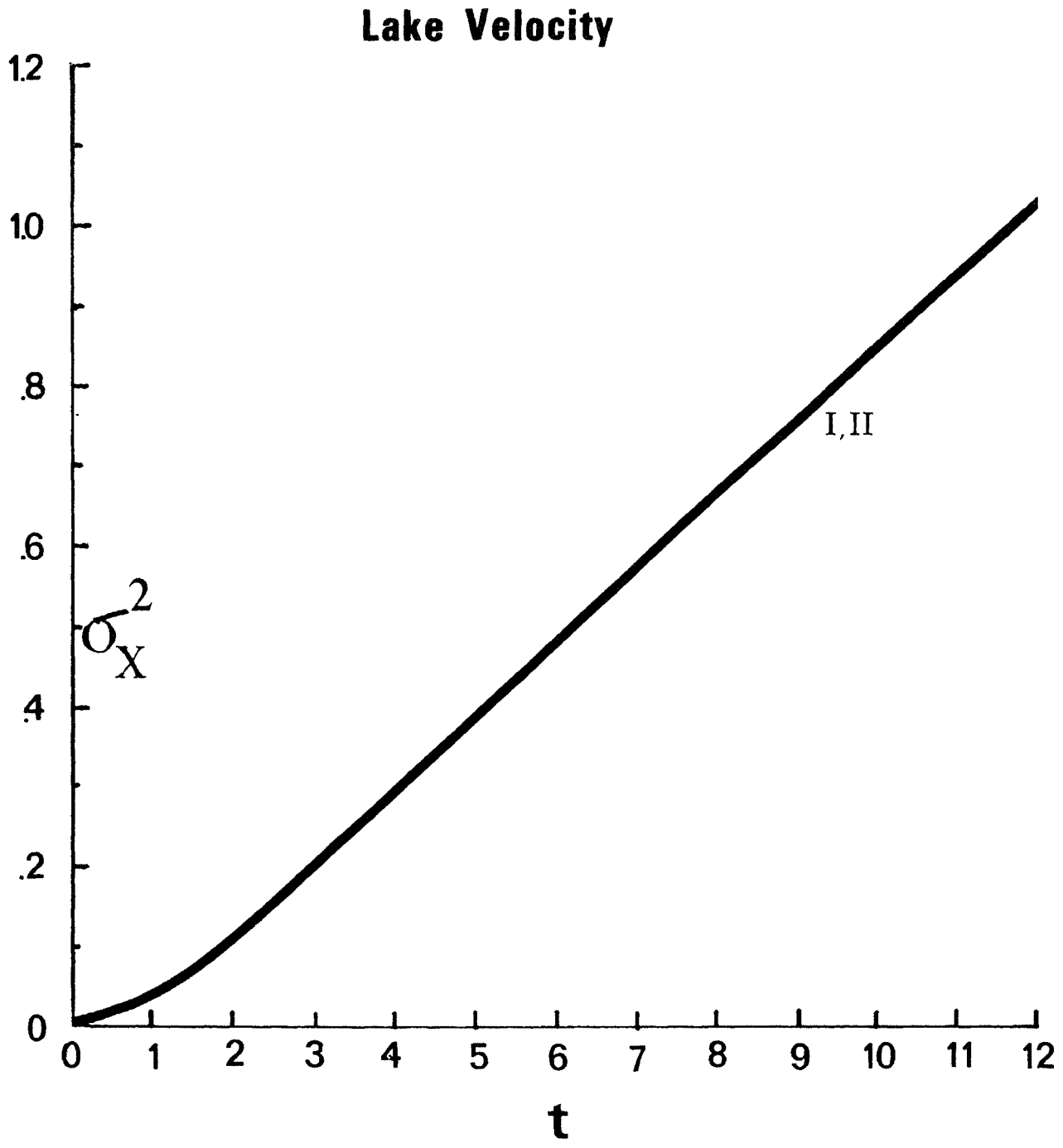

FIGURE 11

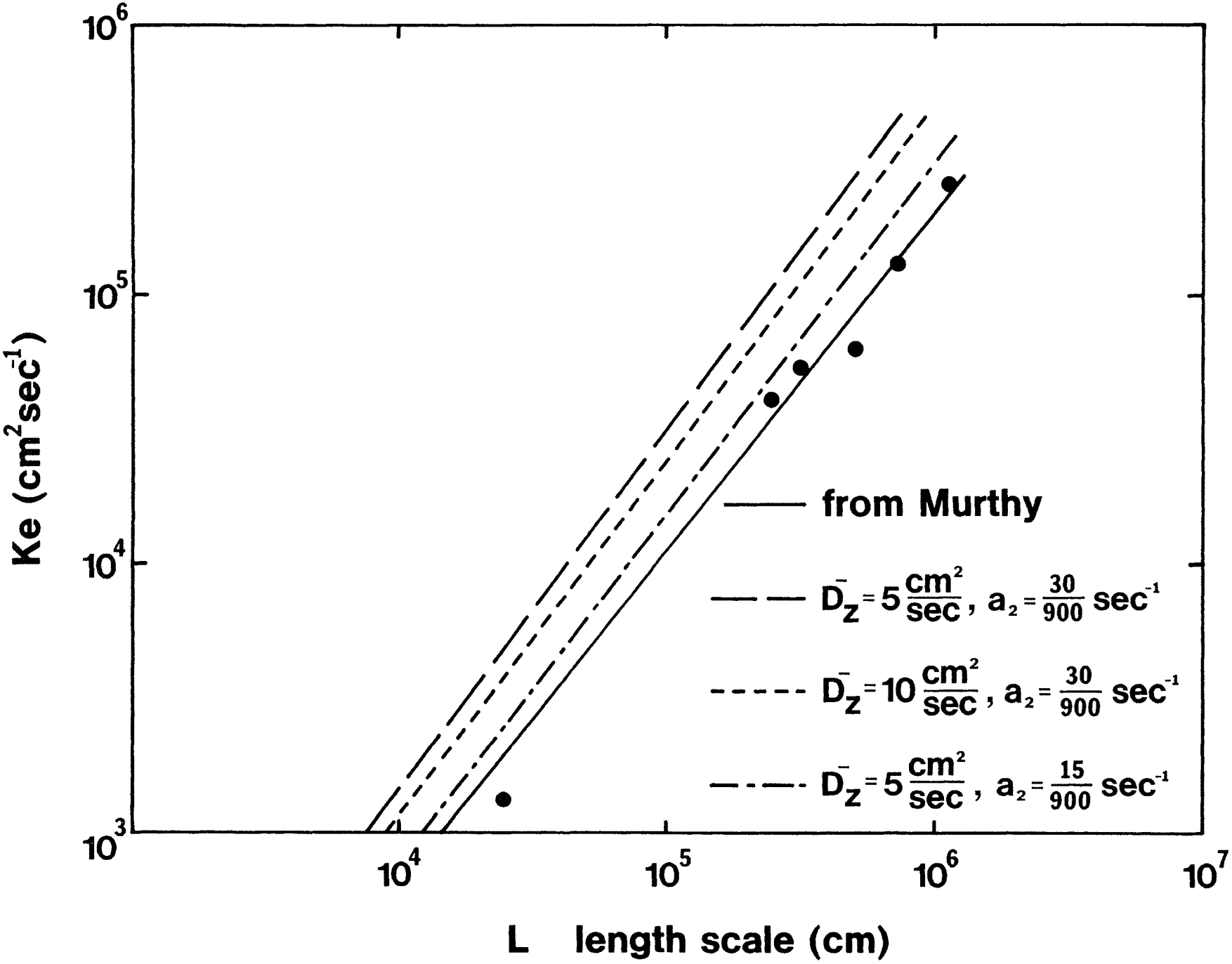
10^6
10^5
10^4
10^3
Ke ($cm^2 sec^{-1}$)
10^4
10^5
10^6
10^7
L length scale (cm)
from Murthy
$\bar{D_z} = 5 \frac{cm^2}{sec}$, $a_2 = \frac{30}{900}$ sec^{-1}
$\bar{D_z} = 10 \frac{cm^2}{sec}$, $a_2 = \frac{30}{900}$ sec^{-1}
$\bar{D_z} = 5 \frac{cm^2}{sec}$, $a_2 = \frac{15}{900}$ sec^{-1}

FIGURE 12